



# Mediastinal Lymphoproliferative Disorders

8

Sergio Pina-Oviedo and Chad D. Strange

## Benign Lymphoproliferative Lesions of the Mediastinum

### Introduction

Benign or reactive lymphoproliferative lesions can occur in the mediastinum as localized disease or as part of a generalized process that may be secondary to multiple etiologies, including inflammatory or infectious processes. Patients may have symptoms or may be asymptomatic. Symptomatic patients present with fever, malaise, chest pain, cough, and/or dyspnea. Most of these lesions manifest as mediastinal lymphadenopathy in the middle or posterior mediastinum that is suspicious for malignancy on imaging. Histopathologic evaluation is ultimately required for diagnosis from tissue obtained via a fine needle aspiration, an imaging-guided core biopsy, a video-assisted thoracoscopy (VATS) biopsy, or an excisional biopsy. In some instances, localized reactive processes may be detected incidentally in a biopsy performed for other reasons, i.e., lung cancer staging, chest pain, etc. The entities described here include sarcoidosis, granulomatous lymphadenitis due to infection or a foreign body-type reaction, Castleman disease, IgG-related disease/sclerosing mediastinitis, and the histiocytic disorders Langerhans cell histiocytosis and Rosai-Dorfman disease. In general, morphologic evaluation and a short panel of ancillary tests (special stains, immunohistochemistry, and/or flow cytometry) are sufficient to arrive to the diagnosis, but in some instances, complementary microbiology and/or serologic studies are required for further interpretation. Likewise, for those systemic processes with mediastinal involvement, it is impor-

tant to correlate with the clinical and radiologic presentation to be able to render a proper pathologic interpretation.

### Sarcoidosis

**General Aspects** There has been controversy as to who should receive credit for the first description of sarcoidosis, reason why the disease received multiple eponyms in the past (Hutchinson-Besnier-Boeck-Schaumann disease). In 1899 Boeck described a patient with “multiple benign *sarkoid* [sic] of the skin” referring to lesions that arose from the underlying connective tissue (Greek “σαρκός,” *sarkos* = flesh). Later in 1914, Schaumann reported few cases of a disease with similar clinical presentation that he called “lymphogranuloma benignum.” Both, Boeck and Schaumann recognized that the disease was not confined to the skin but a systemic disorder that could involve multiple other organs [1].

Sarcoidosis is a rare granulomatous disease that is more prevalent in adults of African descent and affects women more commonly than men. The disease can occur at any age but more frequently affects those between the third to seventh decades of life. The etiology of sarcoidosis remains unknown, and it is hypothesized that the disease represents an exaggerated immune response to an unknown infection or possibly external antigen. Familial predisposition also points to a genetic component of this disorder. Although multiple microorganisms have been suggested as potential underlying factors involved in the development of sarcoidosis, the combination of systemic latent infection with *Propionibacterium acnes* and a defective granulomatous response appear to play a role in the pathogenesis of this disorder [2, 3].

**Clinical Features** Patients may be asymptomatic or present with generalized symptoms, which include fever, weight loss, fatigue, dyspnea, dry cough, lymphadenopathy, arthritis, and sometimes cardiac arrhythmias or a cardiac block. The

S. Pina-Oviedo (✉)  
Department of Pathology, Duke University Medical Center,  
Durham, NC, USA  
e-mail: [Sergio.pinaoviedo@duke.edu](mailto:Sergio.pinaoviedo@duke.edu)

C. D. Strange  
Department of Thoracic Imaging, The University of Texas MD  
Anderson Cancer Center, Houston, TX, USA  
e-mail: [cdstrange@mdanderson.org](mailto:cdstrange@mdanderson.org)

clinical course is long and protracted, but some patients may present with intermittent flares separated by variable periods of waning. Mediastinal disease presents as bilateral hilar lymphadenopathy and pulmonary involvement [4]. Asymptomatic patients are discovered incidentally on chest imaging performed for other reasons.

**Pathology** Lymph nodes involved by sarcoidosis are tan-white to pale yellow with a rubbery or indurated consistency (Fig. 8.1). Microscopically, variable degrees of involvement can be seen with partial or complete effacement of the architecture by numerous granulomas, some of them coalescing, variable number of multinucleated giant cells, and fibrosis (Fig. 8.2). Sarcoid granulomas are non-necrotizing and have a characteristic appearance described as “tight” or “naked” referring to their compact nature made of epithelioid macrophages and the inconspicuous amounts of other inflammatory cells (Fig. 8.3). Although not specific of sarcoidosis, four intracellular structures have been observed within the multinucleated giant cells in this disease, including: (1) asteroid bodies (degenerated or ubiquitinated actin and other proteins), (2) Schaumann bodies (multilaminated structures composed of calcium phosphate, iron, and proteins), (3) calcium oxalate crystals, and (4) “yellow-brown” or Hamazaki-Wesenberg bodies (appear to represent partially degenerated bacteria and lipofuscin material within a phagolysosome) (Fig. 8.4). The uninvolved lymph node shows residual reactive follicles and small lymphocytes. Rare cases of sarcoidosis may be associated with a B-cell lymphoma.

#### **Immunohistochemistry and Other Ancillary Studies** Special stains and correlation with microbiology



**Fig. 8.1** Lymph node involved by sarcoidosis. The surface is tan-white to pale yellow, vaguely nodular and with focal areas of fibrosis

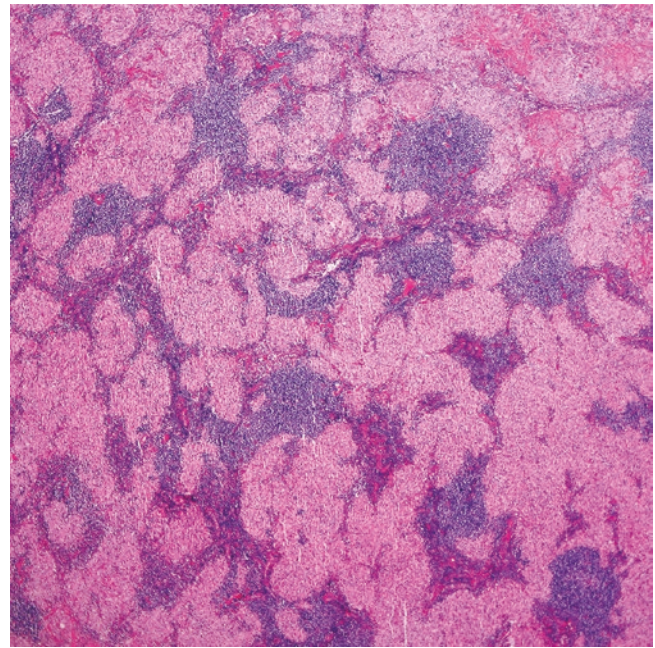


**Fig. 8.2** Numerous granulomas of variable size replacing the lymph node architecture

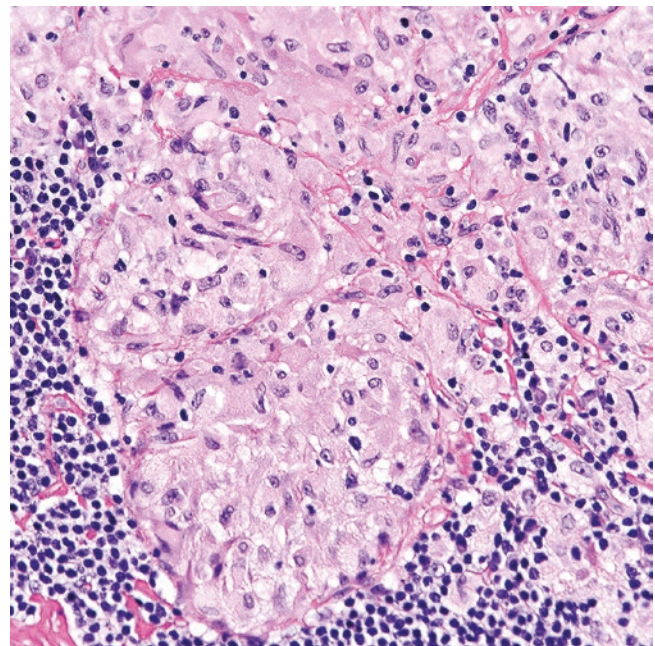


**Fig. 8.3** Sarcoid granulomas are described as “tight” or “naked” without central necrosis or significant inflammation. The surrounding lymphocytes are part of the residual lymph node

studies are mandatory to exclude the possibility of an underlying mycobacterial or fungal infection. Grocott methenamine silver (GMS) stain and acid-fast stains (Fite only) highlight the yellow-brown bodies (Fig. 8.5), but none of the other intracellular structures. Immunohistochemical stains are not required for diagnosis.

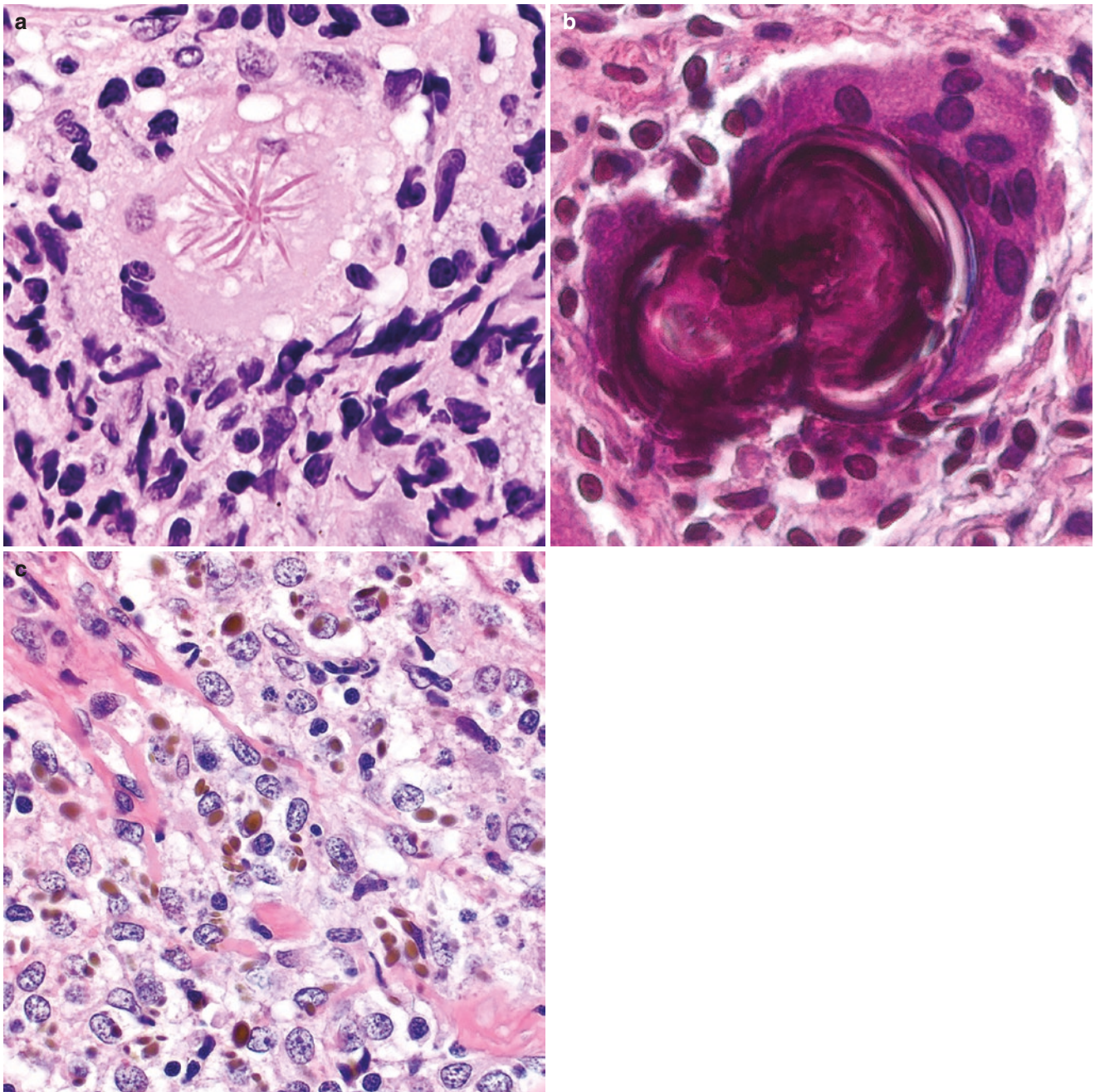


**Fig. 8.4** Inclusions that may be seen in sarcoidosis. (a) Giant asteroid body. (b) Schaumann body. (c) Yellow-brown (Hamazaki-Wesenberg) bodies

**Differential Diagnosis** Sarcoidosis is a diagnosis of exclusion after ruling out an infectious process or another identifiable cause of a systemic granulomatous process, such as an underlying malignancy, the use of certain immunomodulatory medications or a status post-transplant [5]. Special stains, microbiology studies, and/or molecular studies (polymerase chain reaction, PCR) are needed to exclude a possible infection.

Underlying malignancies that have been associated include low-grade B-cell lymphoma and this can be excluded by performing a proper set of lymphoid markers or flow cytometry. Likewise, classic Hodgkin lymphoma and T-cell lymphomas may be accompanied of granulomas, but these are usually necrotizing and not entirely similar as those seen in sarcoidosis. Metastatic carcinomas or germinomas to lymph node may be also accompanied by numerous granulo-

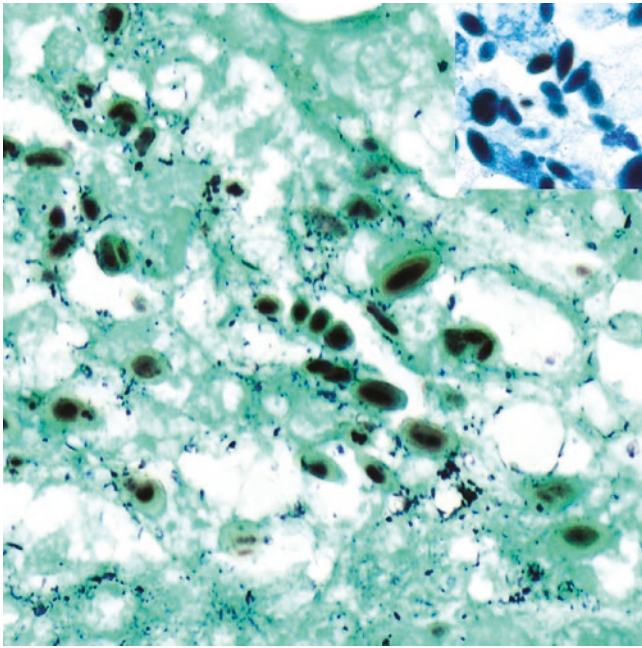


**Fig. 8.5** Yellow-brown (Hamazaki-Wesenberg) bodies are positive for GMS and negative for AFB (inset). Because of their shape and tinctorial properties they should not be confused with yeasts or other microorganisms

mas. Morphology and immunohistochemistry are useful to distinguish between these lesions.

Certain immunomodulatory drugs (TNF-alpha inhibitors), and the novel checkpoint inhibitors (pembrolizumab, etc.) may cause a localized or multiorgan non-infectious granulomatous process that mimics sarcoidosis. A similar phenomenon can be occasionally seen in some patients that are post-transplant. Correlation with clinical history, and the regression of the granulomatous process after removal of a drug, may be helpful to consider these possible etiologies and not sarcoidosis.

### Granulomatous Lymphadenitis Caused by an Infectious Organism or a Known External Substance

**General Aspects** One of the most common causes of mediastinal granulomatous lymphadenitis are infectious organisms or the deposition of foreign material in a lymph node [6]. In both circumstances, the granulomatous process first occurs in the lungs and later spreads to a draining lymph node(s). Two microorganisms that commonly produce granulomatous lymphadenitis in the mediastinum are *Histoplasma capsulatum* and *Mycobacterium tuberculosis*. However, multiple other microorganisms can produce granulomatous lymphadenitis if the infection is systemic. Anthracotic pig-

ment is the most frequent foreign material seen associated with a granulomatous inflammation in hilar lymph nodes, but other less common substances such as talc or silica may be also identified.

**Clinical Presentation** The clinical picture of granulomatous lymphadenitis caused by an infection or foreign body is widely variable. Some patients are asymptomatic and mediastinal lymphadenopathy is only detected for other reasons, i.e., a lung mass. If the process is infectious, symptomatic patients present with fever, productive cough, weight loss, malaise, with or without a pleural effusion. A pneumonic process and mediastinal adenopathy are identified by imaging studies. Immunocompetent individuals may have a prior history of lung infection that remained latent in hilar lymph nodes with the formation of granulomas (Ghon complex in *M. tuberculosis*). Immunosuppressed patients present with severe systemic symptoms and disseminated infection with secondary mediastinal adenopathy. Organisms that can affect mediastinal lymph nodes include *Histoplasma capsulatum*, *Cryptococcus neoformans*, *Aspergillus spp.*, *Candida spp.*, Mucorales (Zygomycetes), *Mycobacterium tuberculosis*, and different types of atypical mycobacteria [7]. Diagnostic laboratory tests vary according to the type of infection and include the identification of the infectious agent either by morphology, special stains, cultures, or by PCR. Patients with mediastinal granulomatous lymphadenitis due to anthracotic pigment are usually asymptomatic and this finding is detected incidentally. Most of these patients are adults and chronic smokers, or individuals who have been exposed to second-hand smoking or live at places with persistent air pollution.

**Pathology** Lymph nodes involved by a granulomatous process are tan-white to pale-pink with rubbery consistency and variable amounts of necrosis. In tuberculosis, there is caseous necrosis. Histologically, granulomatous lymphadenitis is classified into necrotizing or non-necrotizing. The granulomatous process may be focal or diffuse with entire replacement of the lymph node (Fig. 8.6). Fibrosis is usually seen with diffuse involvement. Necrotizing granulomas are more commonly secondary to an infection, while non-necrotizing granulomas are secondary to anthracotic pigment or other foreign materials (Fig. 8.7). Both necrotizing and non-necrotizing granulomas have variable size and shapes (stellate, round, serpiginous, or irregular) and multiple granulomas may coalesce to form large conglomerates. Necrotizing granulomas can be associated with an abscess (suppurative granulomas) (Fig. 8.8) or with acellular central necrosis with calcified structures that mimic yeasts (Figs. 8.9 and 8.10). Eosinophils and plasma cells are variably seen. Mediastinal lymph nodes with extensive

granulomatous inflammation and fibrosclerosis are not uncommonly seen in *Histoplasma* infection. Anthracotic pigment is readily recognized as black granular deposits associated with a granulomatous reaction (Fig. 8.7). Polarized light is required to identify the presence of crystals or other foreign materials that may be the cause of a granulomatous reaction.

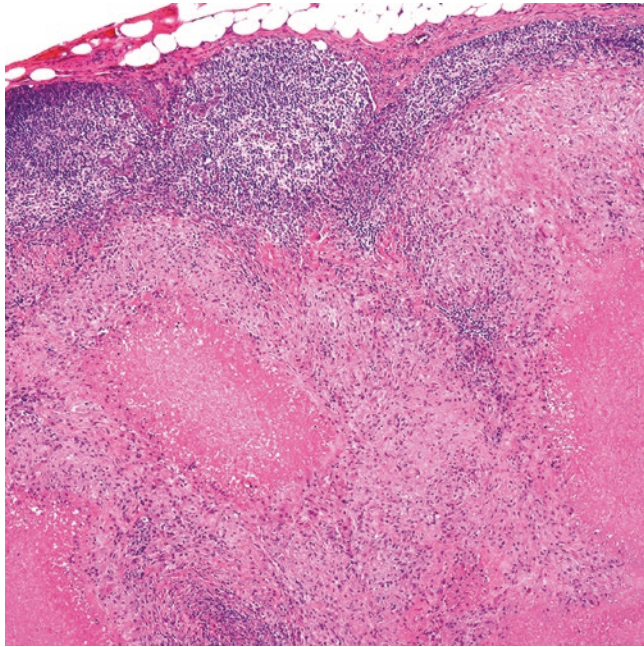


**Fig. 8.6** Necrotizing granulomas almost entirely replacing a mediastinal lymph node. The patient has a history of histoplasmosis

**Immunohistochemistry and Other Ancillary Studies** GMS and/or periodic acid-Schiff (PAS) stains highlight fungal organisms, while acid-fast stains (Ziehl-Neelsen and Fite-Faraco) are useful to highlight mycobacterial organisms (Fig. 8.11). However, acid-fast stains have only intermediate sensitivity and specificity and a high false negative rate of detection. Immunohistochemistry has been suggested as a

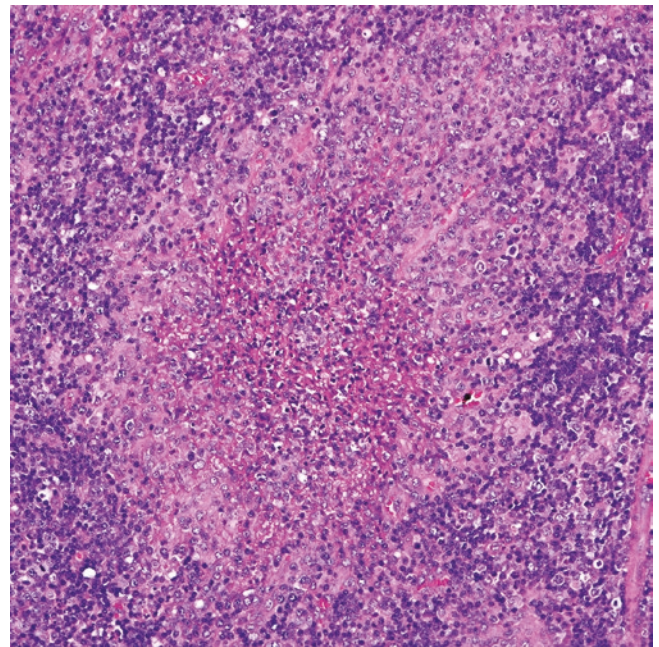


**Fig. 8.8** Lymph node with suppurative granulomas in a case of “cat-scratch disease”

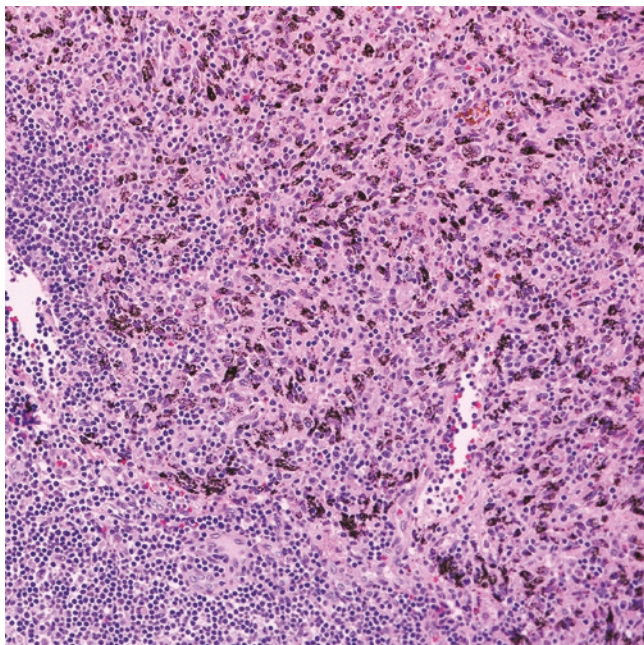


**Fig. 8.7** Mediastinal/hilar lymph node with abundant histiocytes and anthracotic pigment

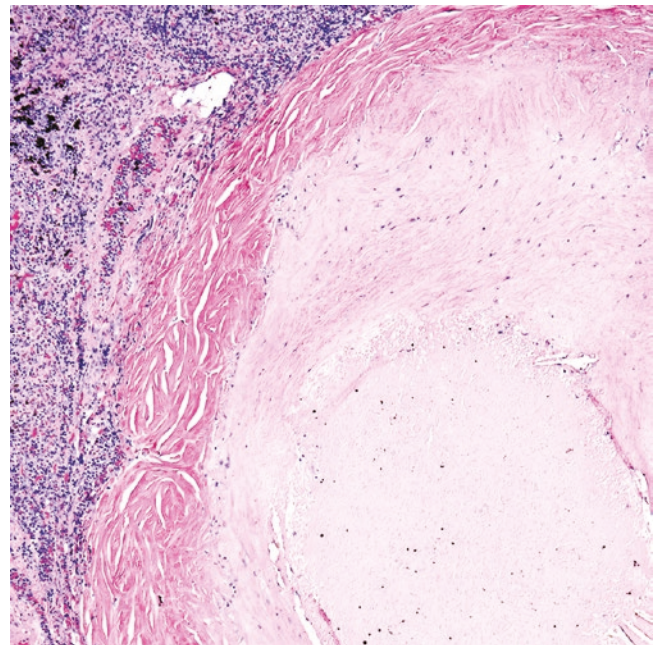


**Fig. 8.9** Mediastinal/hilar lymph node with large hyalinized granuloma with central necrosis

more sensitive and reliable tool for identification of mycobacteria, but these antibodies are not currently available in all laboratories [8]. Although some antibodies against specific fungi are available, these are not needed to establish a diag-

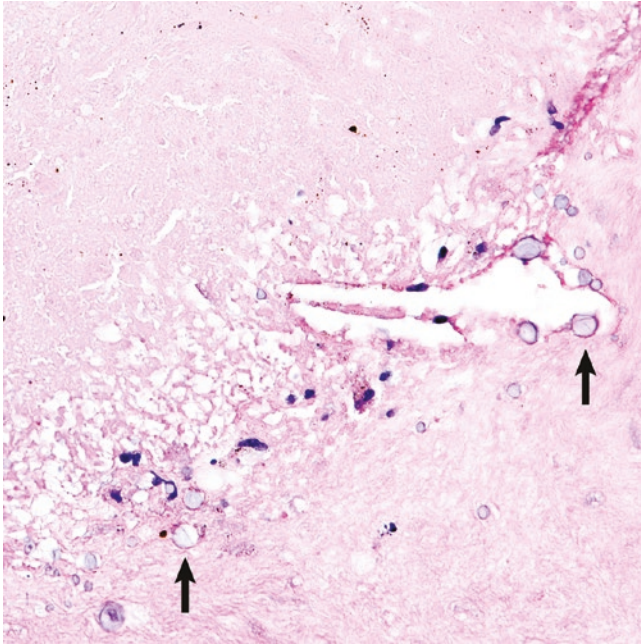


**Fig. 8.10** Mediastinal/hilar lymph node with large hyalinized granuloma with central necrosis. High magnification at the areas of necrosis shows circular pale basophilic structures that resemble yeasts. These structures are refractile and represent mineral condensations and calcifications, not microorganisms. These structures may be positive for GMS

nosis and they should be reserved for specific circumstances such as those when speciation makes a difference for antibiotic therapeutic decisions (i.e., Mucorales vs. *Aspergillus*) and there are no available cultures or material to perform molecular studies. This limited use, however, does not justify the cost of having specific fungi or mycobacteria immunostains as a routine test in a general pathology laboratory. To date, PCR is the best method to identify a pathogen in paraffin-embedded tissues given its high sensitivity and specificity. PCR can detect specific sequences of most organisms (bacteria, fungi, mycobacteria) with highly reliable results. However, pathologists should be aware that PCR may render false negative results when tissue is extensively necrotic due to poor quality of nucleic acids.

**Differential Diagnosis** Special stains, cultures, and/or PCR may be used to identify, support, or exclude a possible infection. Foreign material is readily recognized by careful morphologic review. Similarly, the clinical presentation is helpful to support a possible infection or a concomitant lung process that may be accompanied by hilar lymphadenopathy and may explain the presence of granulomatous lymphadenitis. On the other hand, the presence of granulomatous lymphadenitis is often more nonspecific, and the exclusion of sarcoidosis is mandatory. Sometimes a definitive cause cannot be established and clinical, radiologic, and laboratory correlation is required to exclude infection or any other potential underlying cause of a granulomatous process.

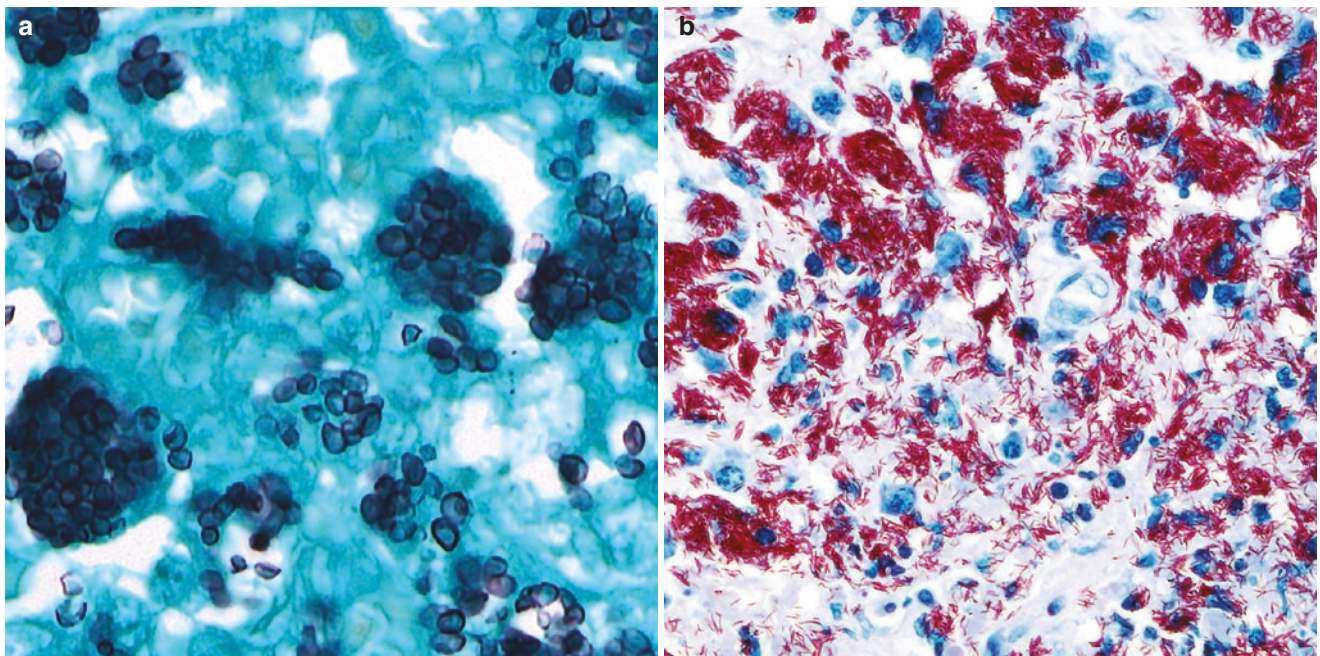


**Fig. 8.11** (a) GMS highlights numerous intracellular yeasts of similar size in a case of *Histoplasma* infection in lymph node. (b) AFB highlights numerous intracellular acid-fast bacilli within histiocytes in a case of disseminated atypical mycobacterial infection

Necrotizing granulomas may contain calcified structures that resemble yeasts and to further complicate the issue, these structures may be positive for GMS. A detailed morphologic evaluation of the location and shapes of these calcified structures is crucial to not overcall a fungal infection. Spherical or laminated structures or their abnormal location in fibrous tissue or encrusted in normal tissue without an associated inflammatory response supports that these are not fungal organisms.

Importantly, granulomatous lymphadenitis may be seen in cases of classic Hodgkin lymphoma, T-cell lymphoma, and metastatic carcinoma or germinoma to a lymph node, and sometimes the granulomatous process may be exuberant enough to obscure the tumor cells. Correlation with the clinical history, a detailed morphologic evaluation and the use of pertaining immunohistochemical markers is required to exclude an underlying malignancy. Table 8.1 lists examples of neoplasms associated with granulomas.

Certain immunomodulatory drugs, i.e., TNF-alpha inhibitors, can cause a systemic noninfectious granulomatous process that may involve mediastinal lymph nodes and a similar phenomenon may be occasionally seen in post-transplant

**Table 8.1** Mediastinal neoplastic processes associated with granulomas

Classic Hodgkin lymphoma
Germinoma (more common in “burned-out” cases)
Metastatic carcinoma, including after chemotherapy
T-cell lymphoma

**Table 8.2** Clinicopathologic features of Castleman disease (CD)

	Unicentric CD	Multicentric CD
Age at presentation	30–40 years	50–60 years (younger if HIV+)
Male to female ratio	1:1	1:1
Clinical features	Asymptomatic Detected incidentally or a mass may cause compression of adjacent organs	Systemic symptoms: malaise, fatigue, fever, weight loss POEMS syndrome (see text) TAFRO syndrome (see text)
Mediastinal lymphadenopathy	Yes	Not unique of this site Systemic disease
Organomegaly	Uncommon	Common
Laboratory abnormalities	Usually none Occasionally normocytic anemia, increase of acute phase reactants, hypergammaglobulinemia	Anemia, thrombocytopenia, hypoalbuminemia, abnormal liver enzymes, and renal function tests If POEMS, endocrine abnormalities and M-protein
Pathology subtype	Hyaline-vascular CD Uncommon plasma cell-rich CD	Plasma cell-rich CD Uncommon hyaline-vascular CD
HIV infection	No	Yes (most cases)
HHV-8 infection	No	Yes (most cases)
Progression to lymphoma	No	May progress to HHV-8+ LBCL
Kaposi sarcoma	No	Yes, in HHV-8+ cases
Progression to FDC sarcoma	Yes, 15–20% with long-standing disease	No
Treatment	Surgical resection, additional radiotherapy if unresectable	Variable, may require chemotherapy and siltuximab (antibody against IL-6)
Outcome	Favorable	Poor without treatment

Abbreviations: *CD* Castleman disease; *FDC*, follicular dendritic cell; *HIV* human immunodeficiency virus; *HHV-8* human herpes virus-8; *POEMS* polyneuropathy, organomegaly, endocrinopathy, M-spike, skin lesions; *TAFRO* thrombocytopenia, anasarca/ascites/microcytic anemia, myelofibrosis, renal dysfunction, organomegaly

patients. Correlation with clinical history is helpful to consider these possibilities. In addition, regression of the granulomatous process after removal of a drug or spontaneous regression of the process may support one of these etiologies.

## Castleman Disease

**General Aspects** In 1956, Dr. Benjamin Castleman (1906–1982) and colleagues described 13 cases of a unique form of localized mediastinal lymph node hyperplasia that clinically, radiologically, and microscopically resembled thymomas [9]. This entity later came to be known as “Castleman disease.” In 1972, Castleman and colleagues described the plasma cell variant of this disease [10]. Castleman disease (CD) is rare condition that predominantly affects lymph nodes and commonly those in the mediastinum. Only rarely the disease affects visceral organs. As we know it today, CD is an “umbrella term” of multiple entities that have a widely variable clinical presentation, pathogenesis, histopathology, risk of malignant progression, and treatment. Clinically, CD can be classified into unicentric or multicentric CD, whereas microscopically, it can be classified into hyaline-vascular or plasma cell-rich CD. Overlapping or mixed cases do exist and this poses a diagnostic challenge as well as a therapeutic problem for clinicians. Ultimately, a diagnosis of CD has to be done along with a proper clinical and radiologic correlation. The clinicopathologic features of Castleman disease are summarized in Table 8.2.

## Hyaline Vascular Castleman Disease

**Clinical Features** This is the most common subtype of CD. The disease affects adults and is exceedingly rare in children. Patients are usually asymptomatic, and the disease is usually discovered incidentally by imaging performed for other reasons. Only when a mediastinal lymph node is large enough to produce compression of mediastinal structures symptoms such as chest pain, cough, or dyspnea may occur. Symptoms tend to develop slowly since hyaline vascular CD has a slow progression. Superior vena cava syndrome is rare.

**Pathology** Grossly, a lymph node affected by hyaline vascular CD is enlarged, with well-demarcated borders and soft consistency. Serial sections show a pink-yellow to orange-red surface with variable fibrosis. At low magnification, there is overall preservation of the lymph node architecture with numerous lymphoid follicles of variable sizes with prominent mantle zones separated by a variably expanded interfollicular region that has a red-pink hue due to increased vascularity (Fig. 8.12). This gives the lymph node a resemblance to spleen. The follicles have atrophic germinal centers with variable number of follicular dendritic cells (FDCs) with atypia or “dysplasia,” and some of them have a large pleomorphic nucleus (Fig. 8.13). The mantle zone lympho-

cytes are arranged in a concentric pattern around the atrophic germinal center, a feature referred to as “onion skinning” (Fig. 8.14). The mantle zones may fuse and surround atrophic germinal centers, a feature called “twinning” (Fig. 8.15). Perifollicular blood vessels show thickened and hyalinized walls and when these vessels penetrate into a follicle they have been referred to as “lollipop” lesions (Fig. 8.16). The interfollicular area shows increased vascularity with variable number of dysplastic dendritic cells and a background of mature lymphocytes, histiocytes, and only few plasma cells (Fig. 8.17). The lymph node capsule and trabeculae may be thickened, and the latter appear as areas of sclerosis that traverse through the parenchyma. Typically, lymphoid follicles are more conspicuous than the interfollicular changes, however, when the interfollicular component expands significantly this has been referred to as stromal-rich hyaline vascular CD. When a dendritic cell proliferation becomes larger and partially overruns the lymph node architecture it has been referred to as a stromal/vascular tumor [11] (Fig. 8.18). In rare instances—and possibly after a long period of time—the proliferation of dysplastic FDCs can progress into a FDC sarcoma. The latter cases may be accompanied by incidental groups of extrathymic thymocytes referred to as indolent T “lymphoblastic” proliferations. The name is a misnomer and has sparked some debate in the past, since these cells are normal immature T-cells and not lymphoblastic lymphoma [12–14].

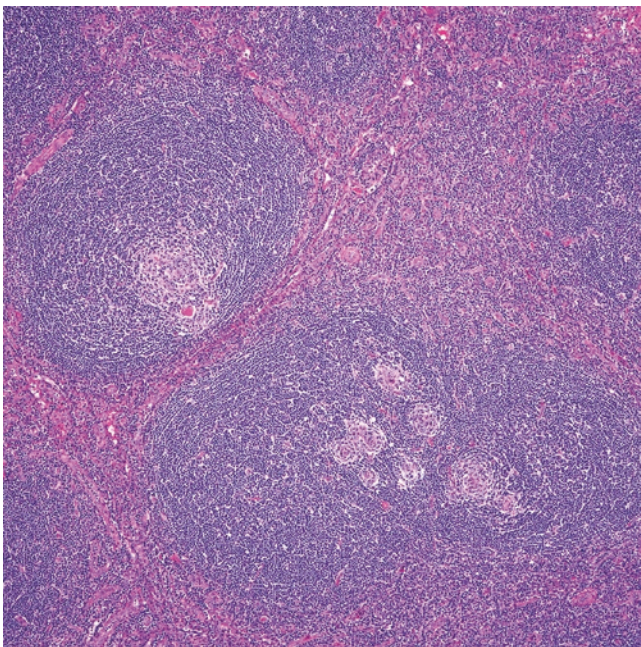


**Fig. 8.12** Hyaline vascular Castleman disease. Follicles with expanded mantle zones with “onion skinning” and atrophic germinal centers. The follicle on the right contains multiple atrophic germinal centers surrounded by one large mantle zone (“twinning”). The interfollicular area is mildly expanded and contains abundant blood vessels

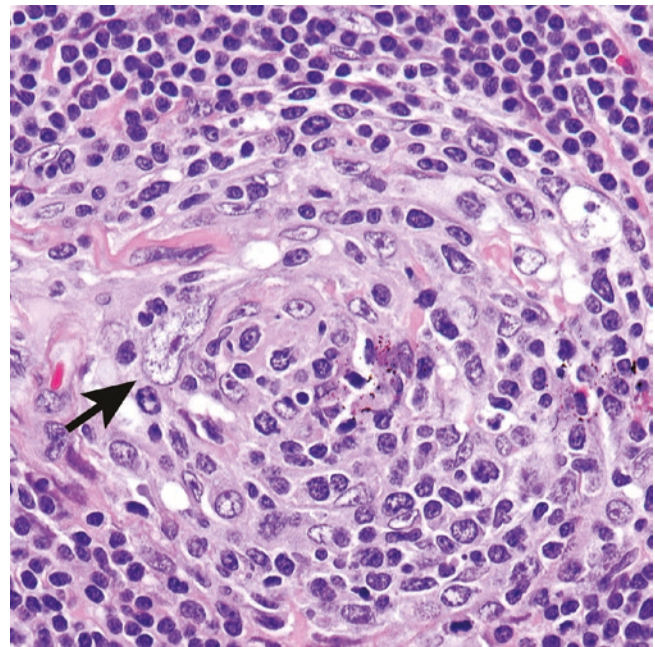


**Fig. 8.13** Atrophic germinal center with a “dysplastic” follicular dendritic cell (arrow)

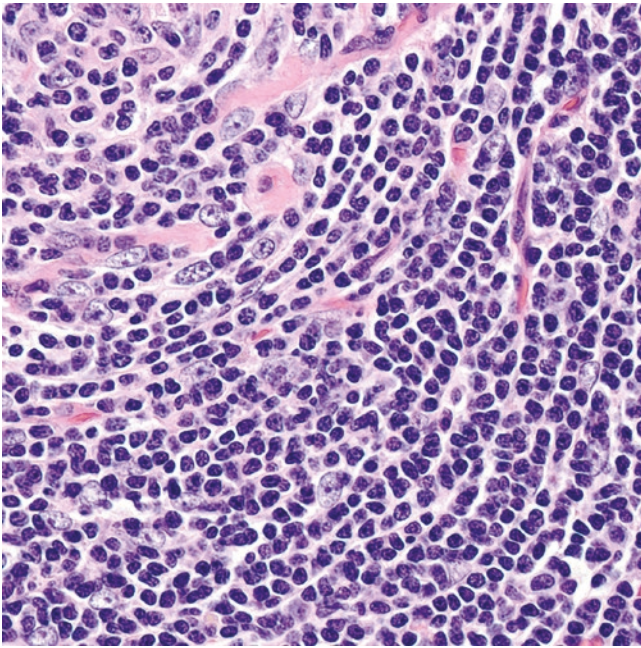


**Fig. 8.14** Mantle zone with lymphocytes arranged in a concentric or multilayered pattern, also known as “onion skinning”

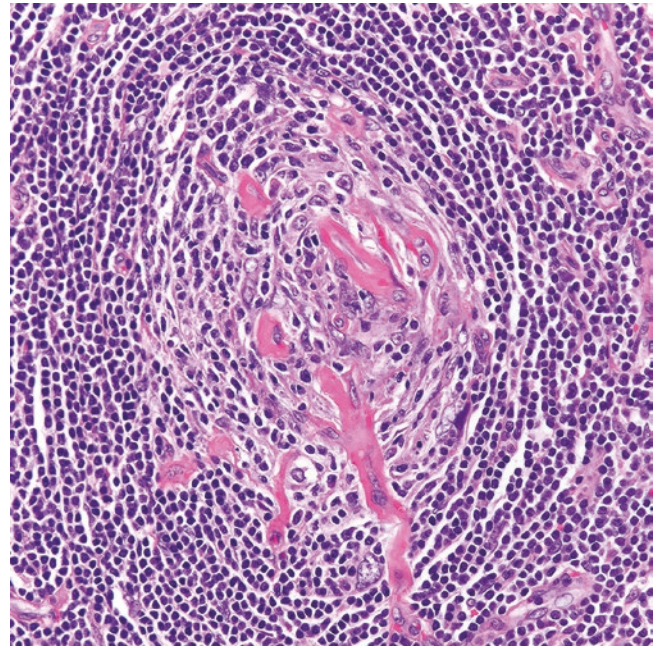


**Fig. 8.16** “Lollipop” lesion. The nurturing vessel is hyalinized and “pierces” into the germinal center forming the stick of the so-called lollipop (center, bottom)

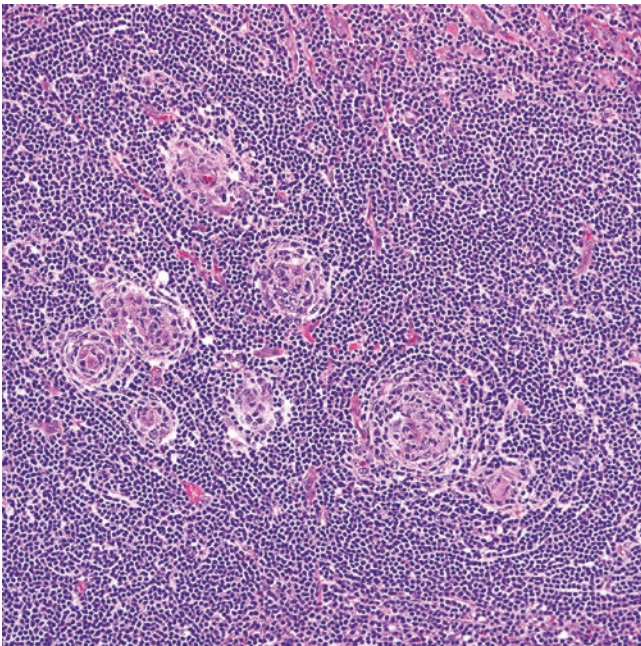


**Fig. 8.15** Follicular “twinning”

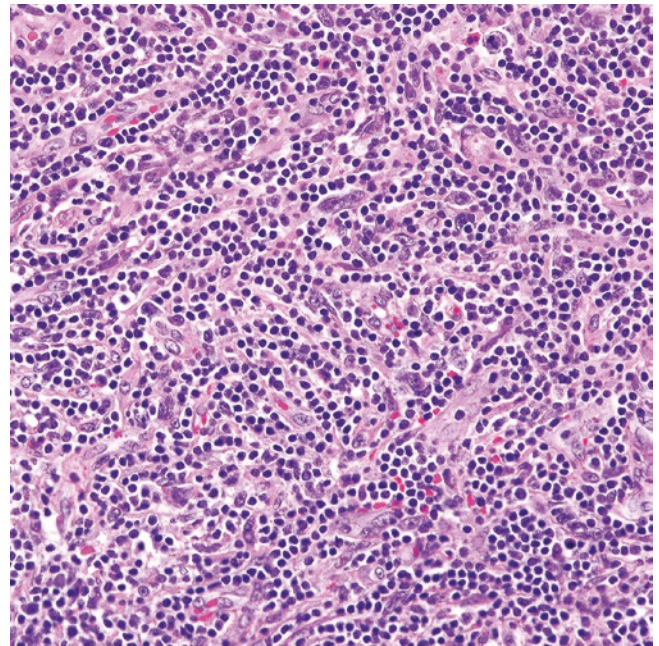


**Fig. 8.17** Interfollicular areas with increased vascularity and few scattered “dysplastic” stromal and dendritic cells

**Immunohistochemistry and Other Ancillary Studies** Immunohistochemistry is not needed to establish a diagnosis of hyaline vascular CD. When immunostains are performed, antibodies for CD3 and CD20 show a reactive pattern with compartmentalization of CD20+ B-cells predominantly within follicles and CD3+ T-cells predominantly in interfollicular

areas. Bcl-2 is positive in T-cells but negative in germinal centers. CD10 and bcl-6 are positive in residual germinal centers. CD21, CD23, and CD35 accentuate the “onion skinning” (Fig. 8.19), the follicular “twinning,” and the presence of atypical FDCs in follicles and few cells interspersed among the interfollicular stroma. The dysplastic FDCs are frequently positive

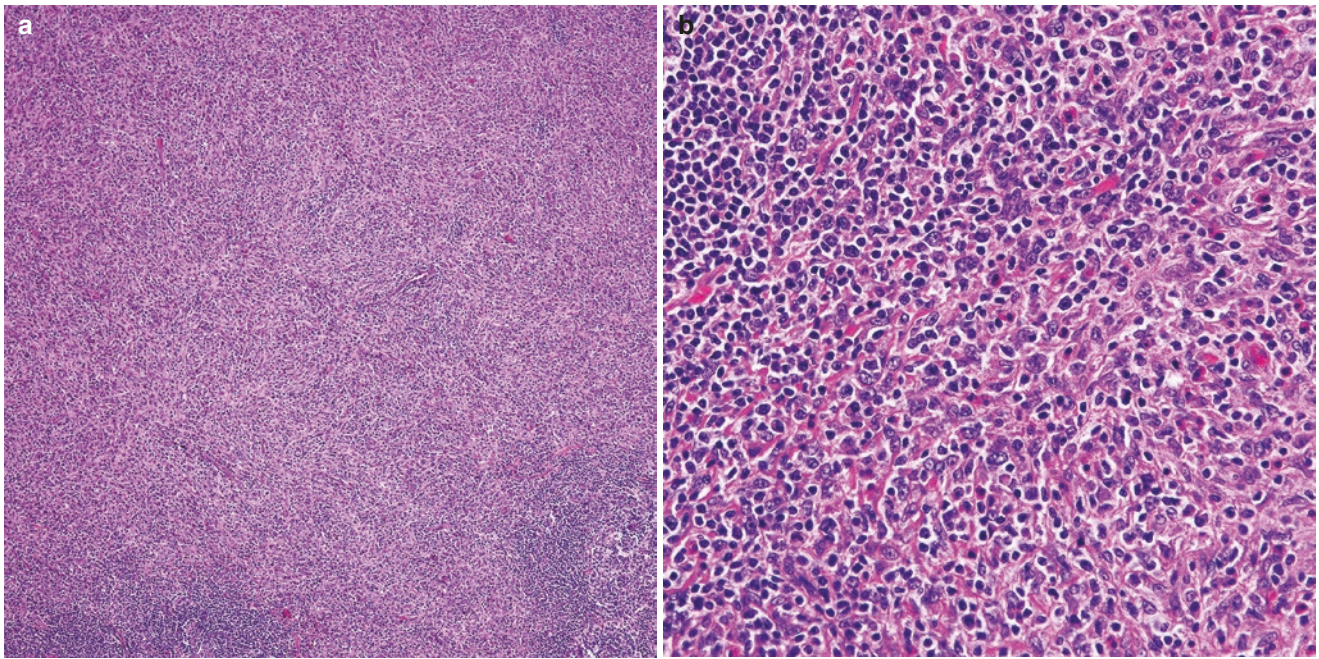


**Fig. 8.18** (a) Stromal proliferation in a case of hyaline vascular Castleman disease. The lymph node was only focally replaced by this process. (b) At higher magnification, the stromal cells and dendritic

cells show bland morphology. This lesion was focally positive for CD34, actin and negative for CD21 (not shown)

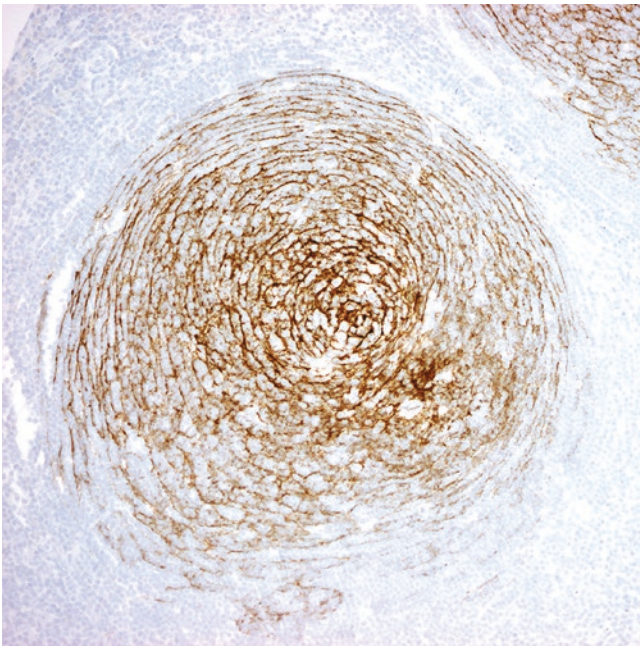


**Fig. 8.19** CD21 immunostain accentuates the concentric or multilayered pattern of the mantle zone or “onion skinning”

for EGFR [15]. The interfollicular stroma is positive for smooth muscle actin (SMA) and vascular markers (ERG, CD31, CD34). The stromal proliferation may show variable labeling for SMA, vascular or FDC markers. If FDC sarcoma is present, the tumor shows expression of >1 FDC markers and/or EGFR (FDC sarcoma is discussed in more detail in the section of mediastinal

neoplasms). HHV-8 and EBER ISH are negative. The “indolent T-lymphoblastic proliferations” are double positive for CD4 and CD8, positive for TdT, CD3, CD1a, CD10, and show a high proliferation index by Ki-67 [12, 13].

**Differential Diagnosis** Although some features between hyaline vascular CD and plasma cell-rich CD overlap morphologically in some cases, both entities can be distinguished by evaluation of the clinical and histopathologic findings.

Hyaline vascular CD should be distinguished from the so-called “CD-like changes” that can be seen in lymph nodes adjacent to a mass and are likely a secondary effect to chronic compression or obstruction of the lymph node drainage. A lymph node with “CD-like changes” is not enlarged and more of an incidental finding in a resection for other reasons. Only one or few features reminiscent of hyaline vascular CD may be seen and these are usually focal (Fig. 8.20). The lack of dysplastic FDCs and the presence of vascular transformation of the sinuses, dilated sinuses, and/or hemosiderin deposition support chronic lymph node compression with CD-like changes and not hyaline vascular CD. The use of the term “CD-like changes” should not be used liberally as this may misguide a treating clinician to think that the patient has CD. Hyaline vascular CD may resemble follicular lymphoma, and the atrophic follicles with “dysplastic” FDCs may be misinterpreted as increased neoplastic centroblasts, a feature of high-grade follicular lymphoma. The presence of other

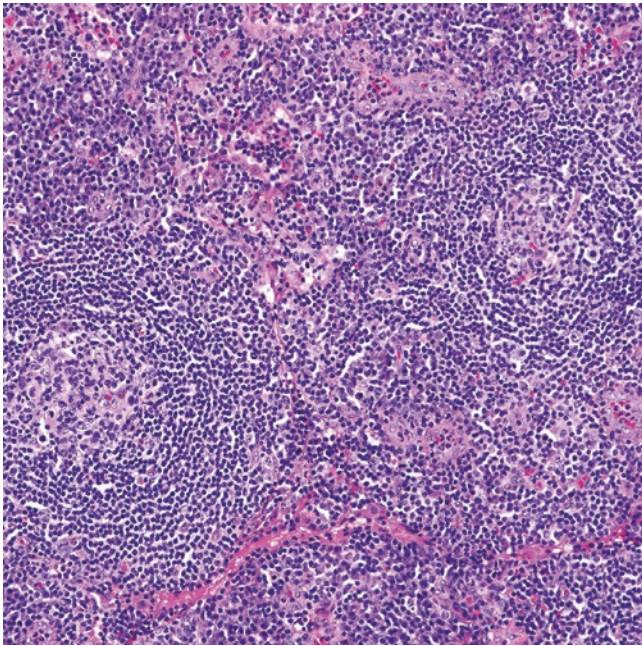


**Fig. 8.20** Castleman disease-like changes. Despite that these follicles have somewhat atrophic germinal centers and increased vascularity, there is no “onion skinning,” “lollipop” lesions, or dysplastic follicular dendritic cells. These changes are nonspecific and may be seen in lymph nodes compressed extrinsically by an adjacent mass

features of hyaline vascular CD as described above, however, should point towards a diagnosis of CD and not lymphoma. Immunohistochemistry for bcl-2 should also be interpreted with caution, since the depleted follicles of hyaline vascular CD are rich in T-cells that are also bcl-2+, and this may suggest that the germinal center is neoplastic. The depletion of B-cells evaluated by CD20 and/or PAX5 immunohistochemistry is helpful to avoid making a wrong interpretation.

Angioimmunoblastic T-cell lymphoma in stages 1 and 2 features increased interfollicular vascularity and can mimic hyaline vascular CD. However, in this T-cell lymphoma there are variable number of atypical lymphoid cells sometimes with clear cytoplasm admixed with histiocytes, plasma cells, and eosinophils. Occasional Reed-Sternberg-like cells may be also seen. Immunohistochemistry and/or flow cytometry are useful to detect aberrant loss or diminished expression of T-cell markers in the neoplastic cells. CD21 demonstrates expanded FDC meshworks extending into interfollicular areas, and EBER ISH is positive in scattered EBV-infected B-cells. None of these features are present in hyaline vascular CD, and also, angioimmunoblastic T-cell lymphoma is an extremely unusual finding as localized disease in the mediastinum. Interfollicular classic Hodgkin lymphoma may also show increased interfollicular vascularity that may suggest hyaline vascular CD. However, the identification of scattered Reed-Sternberg cells that are positive for CD30, weak PAX5, variable CD15, and negative for CD20 and CD45 excludes hyaline vascular CD. The clinical presentation in angioimmu-

**Table 8.3** Differential diagnosis of Castleman disease (CD)

Hyaline vascular CD	Plasma cell-rich CD
“CD-like” changes	Reactive nodal plasmacytosis
Angioimmunoblastic T-cell lymphoma	B-cell lymphomas with plasmacytic differentiation: Marginal zone lymphoma Lymphoplasmacytic lymphoma
Interfollicular classic Hodgkin lymphoma	Plasma cell neoplasm
Follicular lymphoma	IgG4-related lymphadenopathy (multicentric CD-like variant)

noblastic T-cell lymphoma, and classic Hodgkin lymphoma with systemic symptoms, and multifocal lymphadenopathy with or without organomegaly, is completely different from that of hyaline vascular CD. A summary of the differential diagnosis of hyaline vascular CD is shown in Table 8.3.

**Pathogenesis** The etiology and pathogenesis of hyaline vascular CD remains unknown. However, the presence of dysplastic FDCs and interfollicular DCs cells suggests that the disease may be secondary to a lymph node stromal cell pathogenetic process, which may culminate in the progression of FDC sarcoma in some cases. This variant of CD is not associated with increased levels of IgE, interleukin-6, immunosuppression, HIV, and/or HHV-8 infection.

### Plasma Cell-Rich Castleman Disease

**Clinical Features** This is a less common subtype of CD and is almost always symptomatic. Patients not infrequently have underlying immunosuppression secondary to an autoimmune disorder, immune dysregulation, or HIV infection. Systemic symptoms, fatigue, malaise, weight loss, dyspnea, and a cutaneous rash are common as well as the development of multiple lymphadenopathies and organomegaly, hence the term multicentric CD. Some patients may present with generalized edema or an effusion but localized mediastinal disease is not a feature. Patients that are HIV-positive may also develop concurrent Kaposi sarcoma. Laboratory findings include >1 cytopenia(s), and elevated serum levels of C reactive protein, interleukin-6 (IL-6) and vascular endothelial growth factor, as well as hypoalbuminemia and hypergammaglobulinemia. Increased levels of IL-6 and infection with human herpesvirus-8 (HHV-8, formerly Kaposi sarcoma-associated herpesvirus) play an important role in the pathophysiology of multicentric CD. A subset of patients presents with consistently associated symptoms and qualify for the designation of a syndrome, namely, Crow-Fukase or POEMS (Polyneuropathy, Organomegaly, Endocrinopathy, M-spike, and Skin lesions) syndrome, and the Castleman-Kojima or TAFRO (Thrombocytopenia, Anasarca/ascites/anaemia—usually microcytic—myeloFibrosis, Renal dysfunction,

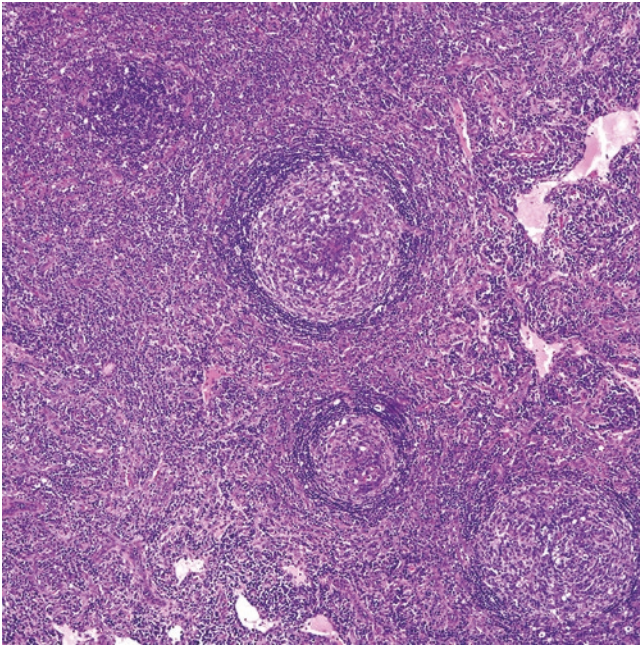


**Fig. 8.21** Plasma cell-rich Castleman disease. Reactive and atrophic follicles with “onion skinning”. The interfollicular area contains numerous plasma cells

and Organomegaly) syndrome [16, 17]. Those cases where no cause is identified after a thorough clinical and laboratory evaluation are designated idiopathic multicentric CD [18].

**Pathology** Grossly, the lymph nodes show a tan-pink surface and soft consistency. Microscopically, there are numerous follicles that show a spectrum from follicular hyperplasia to atrophic follicles similar to those seen in hyaline vascular CD (Fig. 8.21). The germinal centers do not typically contain atypical FDCs and “onion skinning,” follicular “twinning,” and “lollipop” lesions are only variably seen. The mantle zones are variably expanded and may contain scattered intermediate to large cells with eccentric nucleus, fine chromatin, prominent nucleus, and basophilic cytoplasm (the so-called “plasmablasts”) (Fig. 8.22). These cells may be seen in the mantle zone, at the germinal center-mantle zone interphase, and few ones may be seen in interfollicular areas. The latter are variably expanded and show increased vascularity along with numerous mature-appearing plasma cells, hence the name, plasma cell-rich CD (Fig. 8.23). The interfollicular areas

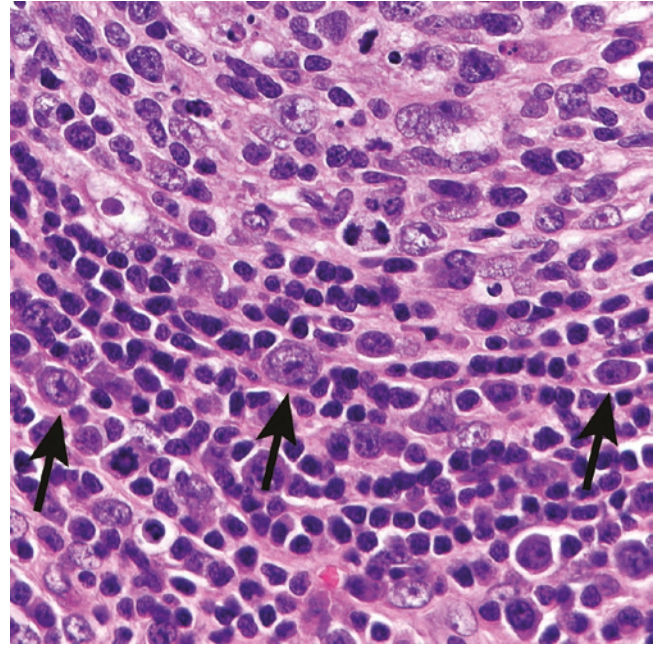


**Fig. 8.22** “Plasmablasts” (arrows) are large cells located at the mantle zone: germinal center interphase. These cells are usually positive for HHV-8

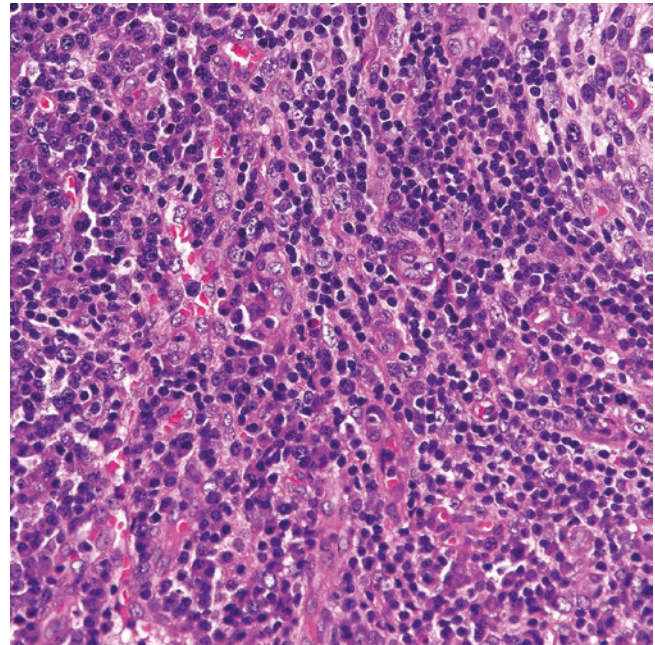


**Fig. 8.23** Interfollicular area with numerous plasma cells and increased vascularity

may also contain few small lymphocytes, histiocytes, and occasional granulocytes. Cases that are accompanied by Kaposi sarcoma (most of the time seated around the lymph node capsule with focal extension into the parenchyma) are virtually diagnostic of HHV-8-associated multicentric CD and are a strong indicator of an underlying HIV infection. In some instances, distinction between plasma cell-rich CD or hyaline vascular CD is difficult and those cases fall in the category of CD with a “mixed pattern.” Clinical and laboratory correlation is mandatory for these cases since rendering a diagnosis of “mixed pattern CD” is not recommended. Basically, the therapeutic approach in this scenario strictly depends on the clinical presentation and the laboratory results rather than the pathologic findings.

**Immunohistochemistry and Other Ancillary Studies** Immunostains for CD3 and CD20 show a reactive pattern with compartmentalization of CD20+ B-cells predominantly within follicles and CD3+ T-cells predominantly in the interfollicular areas. Bcl-2 is positive in T-cells but negative in germinal centers. CD10 and bcl-6 are positive in germinal centers. CD21, CD23, and CD35 accentuate the “onion skinning” and the follicular “twinning” if

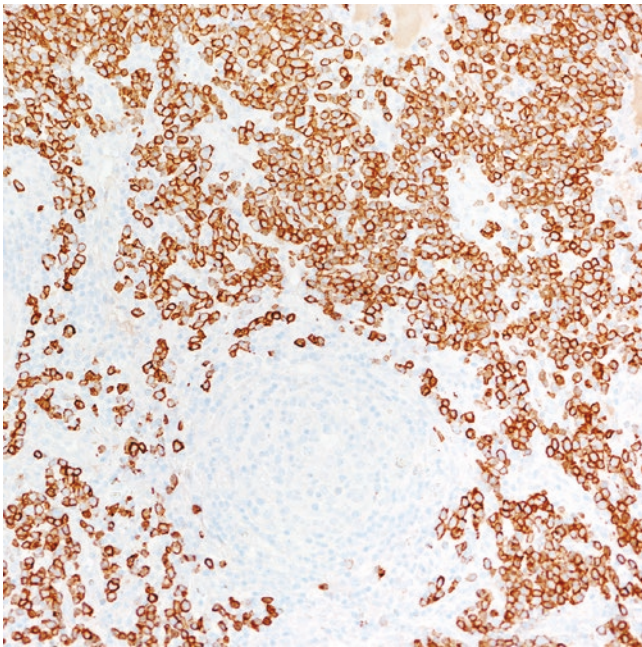


**Fig. 8.24** Plasma cell-rich Castleman disease. CD138 immunohistochemistry highlights numerous plasma cells in between lymphoid follicles

present. The interfollicular plasma cells are positive for CD138, MUM1 and have polytypic light chain expression (Fig. 8.24). HHV-8 immunostain must be performed in all cases of plasma cell-rich CD. When positive, HHV-8 has a nuclear coarse granular pattern in the “plasmablasts” at the mantle zones and in the Kaposi sarcoma, if present (Fig. 8.25). The “plasmablasts” are positive for CD138 and MUM1 and may or may not be positive for CD20. Not uncommonly some of these cells show light chain restriction—usually lambda—, which suggests that these restricted “plasmablasts” are the likely precursors of HHV-8+ large B cell lymphomas that can occur in multicentric CD (Fig. 8.25).

**Differential Diagnosis** Although some features between hyaline vascular CD and plasma cell-rich CD overlap morphologically in some cases, both entities can be distinguished by evaluation of the clinical and histopathologic findings.

Plasma cell-rich CD needs to be distinguished from a plasma cell neoplasm or a B-cell lymphoma with plasmacytic differentiation involving a lymph node. Therefore, immunohistochemistry or ISH is mandatory to confirm polytypic plasma cells in plasma cell-rich CD or monotypic plasma cells in plasma cell neoplasms or B-cell lymphomas. In POEMS syndrome, however, the plasma cells are clonal and produce IgA lambda.

Nodal reactive plasmacytosis also enter the differential diagnosis of plasma cell-rich CD. However, in the former, atrophic follicles, “twinning,” “onion skinning,” “lollipop” lesions, “plasmablasts,” interfollicular increased vascularity, and HHV-8+ cells are not seen. Multiple conditions may produce nodal reactive plasmacytosis, including a persistent localized inflammatory process, an autoimmune disorder (i.e., rheumatoid arthritis), and IgG4-related lymphadenopathy. The clinical presentation and laboratory findings are extremely useful to discern between a reactive condition and plasma cell-rich/multicentric CD. However, that may not be the case of IgG4-related lymphadenopathy, which may present with systemic symptoms and morphologic features reminiscent to multicentric CD (multicentric CD-like pattern) [19]. Therefore, it is also recommended to perform immunohistochemistry for IgG and IgG4 in these cases to exclude this possibility. A summary of the differential diagnosis of hyaline vascular CD is shown in Table 8.3.

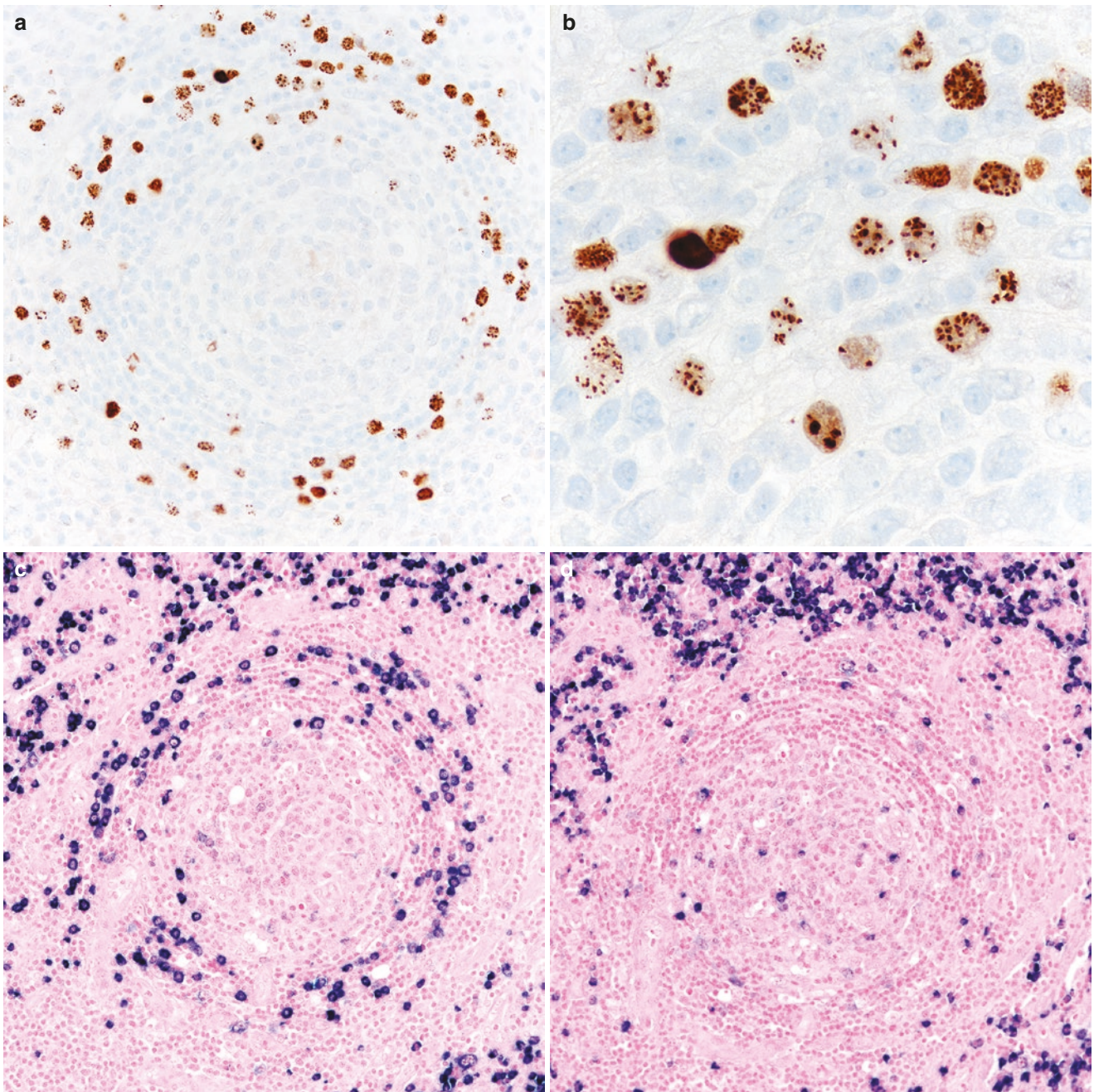


**Fig. 8.25** (a) The location of the “plasmablasts” is better appreciated with the HHV-8 immunostain. (b) Proper HHV-8 immunolabeling includes a coarse to finely granular nuclear pattern. By in situ hybrid-

ization, the “plasmablasts” are positive for (c) lambda (and negative for (d) kappa). The plasma cells at the periphery are polytypic

## Sclerosing Mediastinitis with Emphasis in Mediastinal IgG4-Related Disease

The subject of sclerosing mediastinitis is also presented in the chapter on miscellaneous conditions.

**Introduction** One of the first descriptions of a sclerotic process in the mediastinum with significant clinical manifestations was done by Dozois and colleagues in 1968 where the authors described two patients who showed respiratory compromise secondary to fibrosis of the major bronchi [20]. Since then, the concept of this disease has evolved and the term sclerosing mediastinitis currently encompasses multiple disorders of long-standing onset and variable etiologies that cause mediastinal fibrosis with compromise of regional mediastinal structures. Among the etiologies are: infectious organisms, IgG4-related disease, autoimmune disorders, sarcoidosis, malignant neoplasms, radiation therapy, and drugs, and when no cause is identified the disease is classified as idiopathic [21–29]. Lymphadenopathy, fibroblastic proliferation, and collagen deposition may be the result of a healing infection with *M. tuberculosis* or *H. capsulatum* and this process may progress to mediastinal sclerosis [24, 29]. In IgG4-related disease, sclerosing mediastinitis represents the regional manifestation of systemic disease [22, 30]. Table 8.4 shows the etiologic factors associated with sclerosing mediastinitis.

**Table 8.4** Etiologic factors associated with sclerosing mediastinitis

Infectious: Histoplasmosis, tuberculosis	IgG4-related disease
Sarcoidosis	Radiation
Autoimmune disorders	Medications: methysergide
Neoplastic: primary or metastatic tumors, mast cell activation syndrome?	Idiopathic
<b>Histopathologic stages of sclerosing mediastinitis [29]</b>	
Stage I	Edematous fibromyxoid tissue with mixed inflammation Thin-walled vessels Lack of cellular atypia and necrosis
Stage II	Thick glassy bands of haphazardly arranged collagen Focal interstitial spindle cells, lymphocytes, and plasma cells
Stage III	Dense acellular collagen Scattered lymphoid follicles Occasional areas with dystrophic calcification

**Clinical Features** IgG4-related disease typically affects young adults with no gender predilection. Patients may or may not present with fever, malaise, weight loss, or lymphadenopathy and clinical symptoms vary according to the affected site. Visceral organs, the retroperitoneum, and/or the mediastinum may be involved by this process at variable degrees usually in the form of a mass-forming lesion. In the mediastinum, the clinical symptoms vary depending on the affected site with respiratory distress, cough, hemoptysis, and dyspnea for cases affecting the tracheobronchial tree or the lungs; chest pain and heart conduction problems for those cases occurring in the anterior mediastinum and heart; dysphagia for those involving the esophagus; and superior vena cava syndrome or aortic compression for those affecting the great vessels [20, 22–26, 28–30]. In the case of an infectious process or IgG4-related disease, there may be or may not be associated lymphadenopathy. Laboratory results vary according to the underlying condition causing sclerosing mediastinitis, ranging from positive serologies for those cases with an underlying infection, and elevated levels of serum IgG4 (>135 mg/dL) in those with IgG4-related disease. Anecdotal cases have been associated with the presence of HLA-A2 in peripheral blood typing or with systemic disorders producing mast cell activation [21, 26]. In a subset of cases, sclerosing mediastinitis may represent the residual tumor bed (“burned-out”) classic Hodgkin lymphoma or mediastinal germinoma after treatment with chemotherapy and/or radiotherapy [31]. A small number of patients with plasma cell hyalinizing pulmonary granulomas may also develop sclerosing mediastinitis [32].

The prognosis is variable and depends on the organs affected by sclerosis with worse outcomes for those patients who present with respiratory failure, superior vena cava syndrome, or heart block. Identification of the underlying etiology is crucial in an attempt to minimize the disease progression. Surgical resection and/or stenting of affected blood vessels or affected airways have been used as palliative methods. The importance of recognizing IgG4-related disease as an underlying etiology in sclerosing mediastinitis rests on the excellent response of this disorder to steroids rather than to surgery.

**Pathology** On gross examination, sclerosing mediastinitis is a gray-white mass-forming lesion with rubbery consistency. If adjacent structures are present, they are encased by fibrosis and may be partially to totally obliterated. Microscopically, there is extensive collagen fibrosis of keloidal type and char-

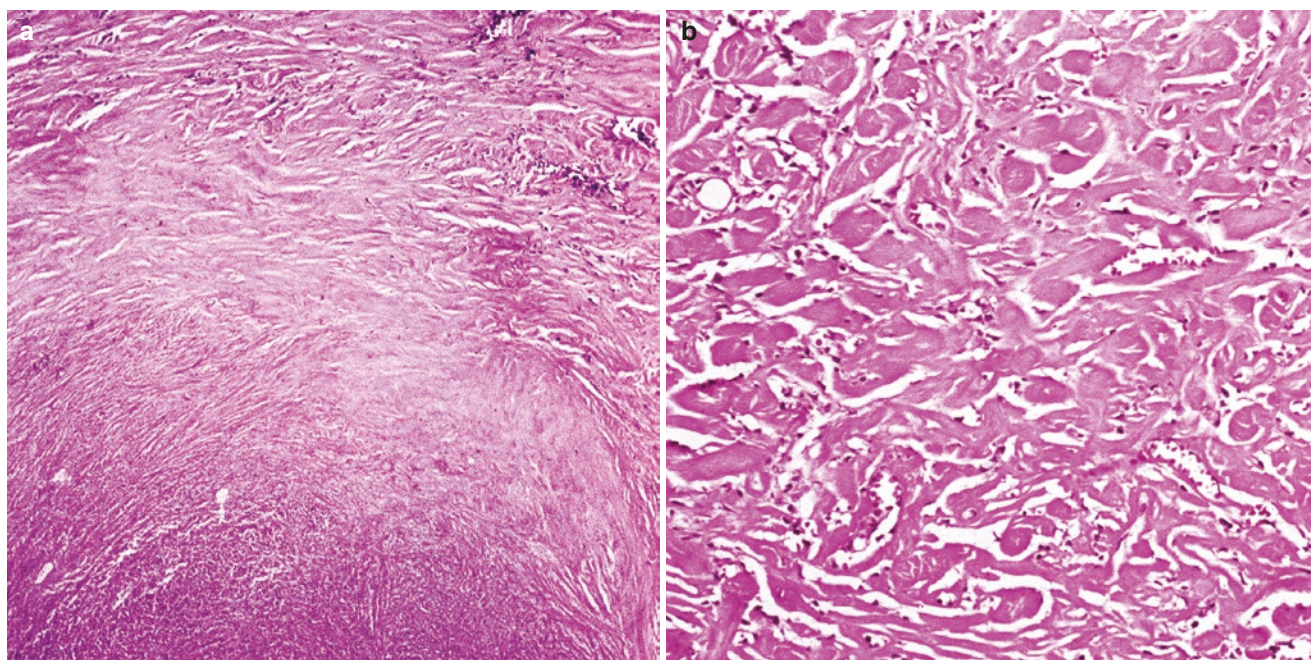


**Fig. 8.26** (a, b) Keloidal-type sclerosis of a lymph node in a case of sclerosing mediastinitis. Only scant cellularity is appreciated

acteristic concentric perivascular arrangement. Cellularity is scant to nearly absent (Fig. 8.26). A lymphoplasmacytic infiltrate may suggest the possibility of IgG4-related disease. Those cases secondary to infection do not have a particular histopathologic feature. The idiopathic form of sclerosing mediastinitis has been divided into three stages (see Table 8.4), including: edematous fibromyxoid tissue with mixed inflammation, thin-walled vessels, no cellular atypia or necrosis (stage I); thick bands of haphazardly arranged collagen with focal interstitial spindle cells, lymphocytes, and plasma cells (stage II); and, dense acellular collagen with scattered lymphoid follicles and occasional foci of dystrophic calcification (stage III) [29, 33]. Since none of these findings is specific, the interpretation of sclerosis in the mediastinum has to be done always in conjunction with the clinical and radiologic findings [29].

**Immunohistochemistry and Other Ancillary Studies** If an infectious etiology is suspected, GMS and/or acid-fast stains are needed to evaluate for fungal or mycobacterial organisms. Given the resemblance of glassy collagen fibrosis with amyloid, sometimes a Congo red stain is needed to rule out amyloidosis. Immunohistochemical stains are of limited use and not needed for diagnosis of sclerosing mediastinitis, but they are required in cases that are suspicious of an underlying IgG4-related disease (Fig. 8.27). According to the consensus criteria for this disease all cases require the detection of an IgG4/IgG ratio of >40%, but no specific number of IgG4+ plasma cells/high power field was defined for scleros-

ing mediastinitis [34]. Lindholm and Moran have proposed a cutoff of >10 IgG4+ plasma cells/high power field to consider this etiology in sclerosing mediastinitis [29].

**Differential Diagnosis** Identification of the underlying cause of sclerosing mediastinitis dictates the potential differential diagnoses. As mentioned above, the histopathologic findings are not specific and clinical, radiological, and laboratory correlations are required to further attempt to determine a cause. If no cause is identified, then the possibility of idiopathic sclerosing mediastinitis should be considered. Immunohistochemical studies may prove useful to evaluate for IgG4-related disease, a possible underlying lymphoma or a burned-out germinoma.

Mediastinal fibromatosis and solitary fibrous tumor may enter the differential diagnosis of stage I sclerosing mediastinitis, particularly in a core biopsy. Immunohistochemical stains for STAT6, CD34, bcl-2, CD99 may be used to exclude solitary fibrous tumor, and evaluation for nuclear beta-catenin may be needed to rule out fibromatosis.

Cases of stage II–III sclerosing mediastinitis may resemble extensive amyloid deposition or amyloidoma. A Congo red stain can be performed to exclude the presence of amyloid.

A common reactive phenomenon occurring around masses is the development of a marked fibro-inflammatory response or the formation of a capsule. Pathologists should be careful not to render a diagnosis of sclerosing mediastinitis in isola-

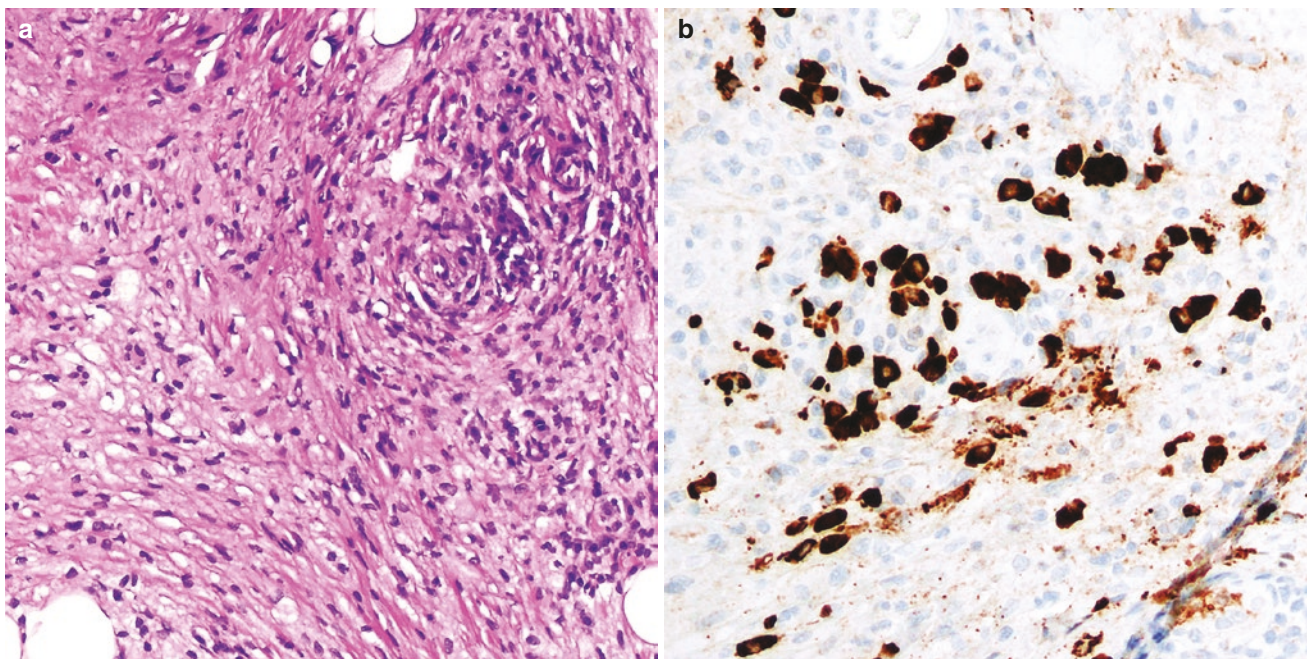


**Fig. 8.27** Sclerosing mediastinitis secondary to IgG4-related disease. (a) Fibrosis with moderate cellularity and perivascular lymphoplasmacytic inflammation (top, right). (b) IgG4 immunostain highlights abundant IgG4+ plasma cells

tion, as a core needle biopsy showing features similar to stage I–II sclerosing mediastinitis could potentially represent fibro-inflammatory tissue or the capsule of a primary mediastinal neoplasm or a metastasis. Clinico-radiologic correlation and discussion of the pathologic findings with the clinical team should be always done in this scenario.

## Langerhans Cells Histiocytosis (LCH)

**Introduction** LCH is a subtype of histiocytic disorder that in the first half of the twentieth century included multiple entities, namely, eosinophilic granuloma or Otani’s tumor (localized form), Hand-Schüller-Christian disease (multiorgan disease), and Abt-Letterer-Siwe disease (systemic form) [35]. It was not until 1953 that L. Lichtenstein—and to some extent S. Otani—hypothesized that these histiocytic proliferations represented different spectrums of the same disease. Lichtenstein coined the term “histiocytosis X” to point that this histiocytosis derived from yet unknown cells [35]. Two decades later, C. Nezelof demonstrated that the cell of origin was a Langerhans cell, and then coined the term Langerhans cell histiocytosis (LCH) [36, 37]. Langerhans cells were described in 1868 by P. Langerhans Jr. using silver impregnations [38] and he first thought that these were neural cells but later suggested that they were related to the “reticuloendothelial” system. In 1961 the electron microscopist M. Birbeck discovered that Langerhans cells contained ultra-

structural cytoplasmic membranous bodies that are known today as Birbeck granules [39].

For several decades it was not known if LCH represented a reactive or a neoplastic process until 1994 when two independent studies using a HUMARA assay demonstrated that a subset of LCH cases were clonal [40, 41]. Another breakthrough came to the field of histiocytoses in 2010 when the *BRAF* V600E mutation was identified in 50–70% of LCH cases by diverse molecular analyses [42, 43]. After those findings, other studies have identified mutations in multiple other genes codifying for proteins involved in the RAS/RAF/MAPK pathway, including *MAP2K1* (10–20% of cases) and single cases with *ARAF1* and *ERBB3* mutations [44–46]. Alternative mechanisms of BRAF activation (*BRAF* fusions) have also been discovered by whole-exome sequencing [47]. All these findings point to a common mechanism of ERK activation as a major player in LCH pathogenesis and support a clonal origin of the disease at least in the majority of cases [42, 44–46, 48–51]. In 2016, the Histiocyte Society reclassified all histiocytic disorders into several subgroups, each one designated by a letter, with LCH included in group “L” for “Langerhans” [49]. This section focuses into the mediastinal involvement by LCH. Pulmonary involvement is discussed in the lung section.

**Clinical Features** The incidence of LCH is five cases/million/year [52]. The disease is more common in children and is slightly more common in males. LCH can present with

localized, multifocal, or systemic involvement and mediastinal involvement is usually seen as part of the last two. The eponyms associated with the different clinical variants (see above) are not used today. Primary mediastinal LCH is extremely rare with most cases reported involving the thymus or a lymph node [53–58]. In the largest series of mediastinal LCH to date, patients presented with respiratory distress, superior vena cava syndrome, cough, and polypnea [54], and some sporadic reports have reported chest wall swelling [55, 57]. LCH may or may not extend to the lungs or produce compression of the trachea or vena cava. In the same mediastinal LCH series mentioned above, all patients had multi-system disease with an overall 5-year survival of 87% and only one death related to LCH [54].

Treatment varies according to the clinical presentation and mediastinal structure involved. Visceral disease is usually treated with surgical resection and/or chemotherapy [54, 59, 60]. Current trials are evaluating the use of vemurafenib (*BRAF* V600E inhibitor) and other inhibitors of the RAS/RAF/MAPK pathway as potential target therapies in this disease [42, 48, 49, 61].

**Pathology** A reference to lymph node and thymic involvement is done here. Lymph nodes tend to have a thickened capsule and dilated sinuses filled with a proliferation of Langerhans cells admixed with variable proportion of eosinophils, macrophages, and multinucleated giant cells [62] (Figs. 8.28 and 8.29). Some cases may contain few admixed

small lymphocytes and/or few plasma cells. Langerhans cells form large collections and have an epithelioid morphology with a reniform nucleus—often with grooves—thin nuclear membranes, vesicular chromatin, inconspicuous nucleolus, and abundant eosinophilic and finely granular cytoplasm (Fig. 8.30). Mitoses and significant atypia are not

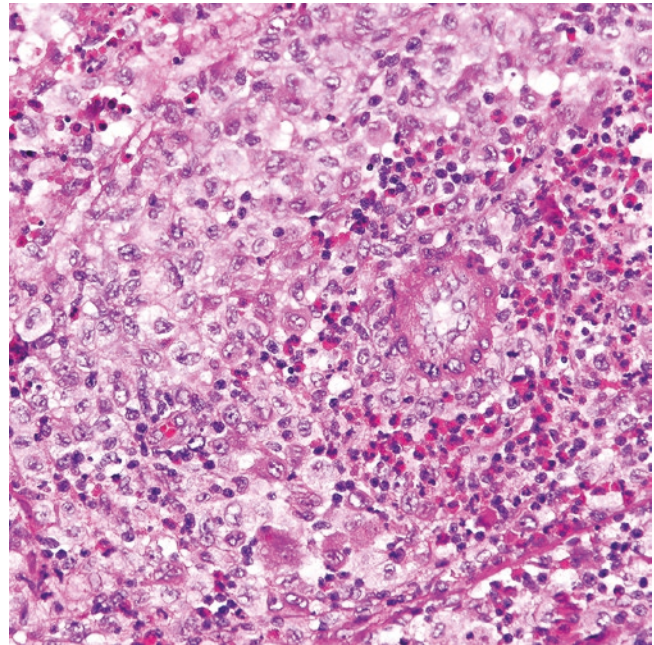


**Fig. 8.29** Langerhans cells have epithelioid morphology and convoluted to reniform nucleus with nuclear grooves. This process is usually accompanied by numerous eosinophils

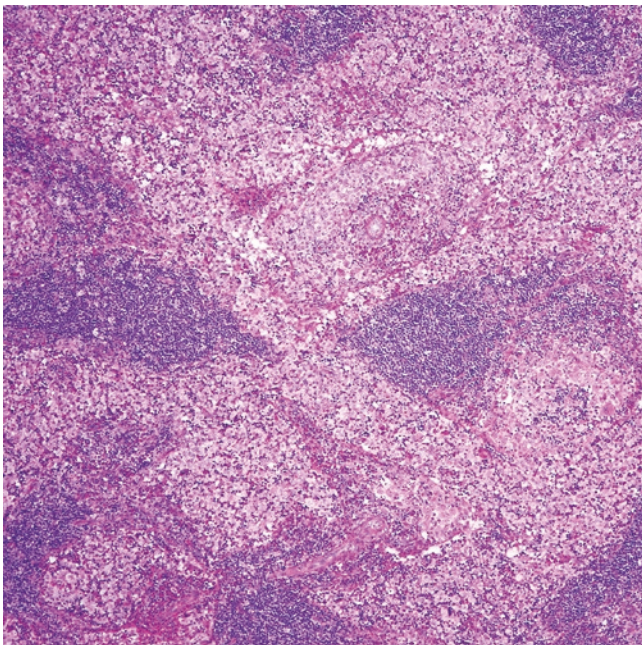


**Fig. 8.28** Sinusoidal distribution in a case of Langerhans cell histiocytosis

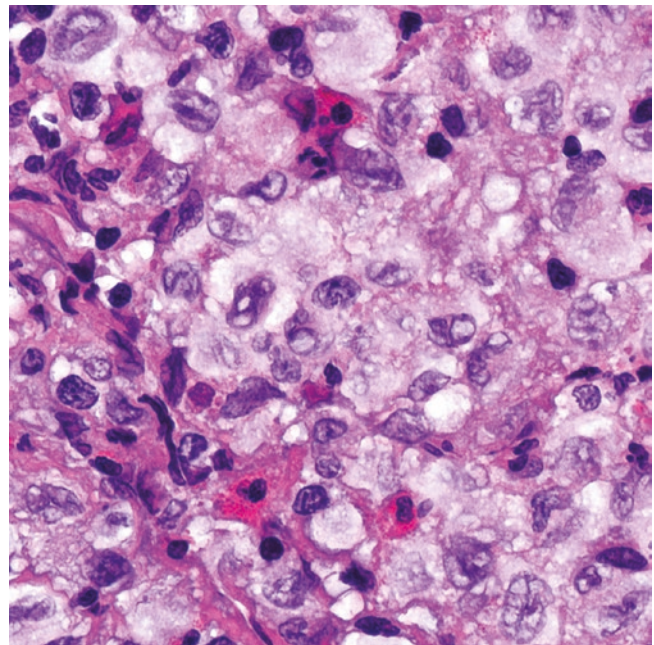


**Fig. 8.30** Langerhans cells show a convoluted to reniform nucleus with nuclear grooves and abundant eosinophilic cytoplasm

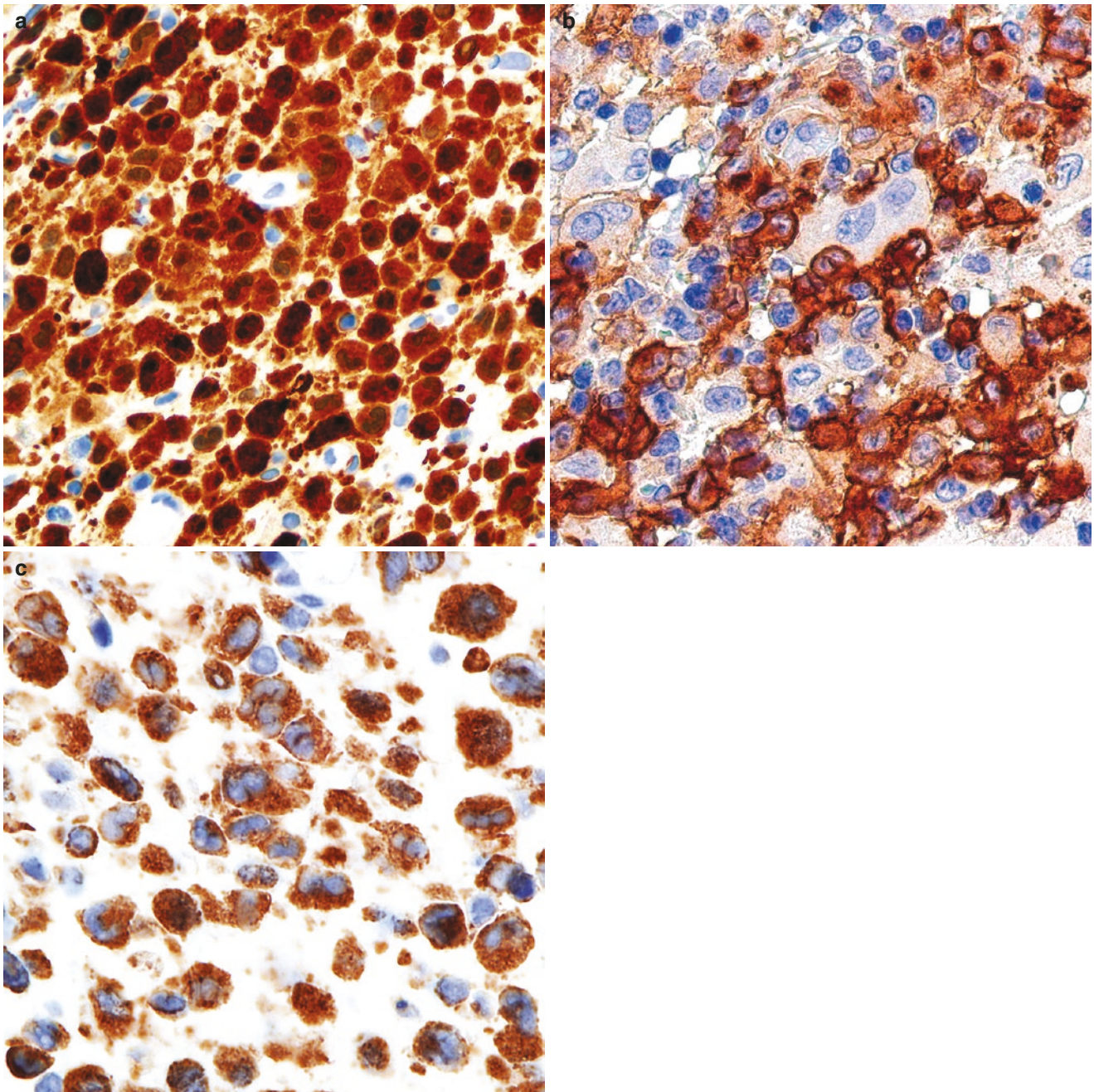


**Fig. 8.31** Langerhans cells histiocytosis are positive for (a) S100, (b) CD1a, and (c) langerin/CD207

a feature. Multiple collections of eosinophils and eosinophilic microabscesses are frequently identified. The uninvolved lymph node shows features of reactive lymphoid hyperplasia. Similar findings are observed in the thymus, with uninvolved thymus showing necrosis, dystrophic calcification, and variable number of cysts.

**Immunohistochemistry and Other Ancillary Studies** Langerhans cells are positive for S100, CD1a,

CD207/langerin, weak CD4, and may show focal CD68 and CD163 (Fig. 8.31). The multinucleated giant cells are usually positive for CD68 and CD163 and not for CD1a suggesting that they are a subtype of macrophages and not of Langerhans cells. LCH is negative for B-cell and T-cell markers, FDC markers, keratin, melanoma markers (SOX10, HMB-45, MART-1), and germ cell tumor markers (OCT3/4, SALL4, beta-hCG). There is a commercially available antibody that detects the mutated BRAF V600E protein (VE-1) that shows cytoplasmic labeling in those cases harboring the

mutation [43, 50] (Fig. 8.32). Table 8.5 summarizes the immunohistochemical profile of histiocytic disorders.

**Differential Diagnosis** Mediastinal LCH should be distinguished from dermatopathic lymphadenopathy, non-Langerhans cell histiocytic disorders, dendritic cell tumors, anaplastic large cell lymphoma, and metastatic melanoma or carcinoma [62].

Dermatopathic lymphadenopathy is a reactive paracortical proliferation of Langerhans cells, interdigitating DCs and histiocytes with variable amounts of melanin pigment that develops in lymph nodes draining from a region with a cutaneous inflammatory process. Although florid cases of dermatopathic lymphadenopathy can mimic LCH, this process is

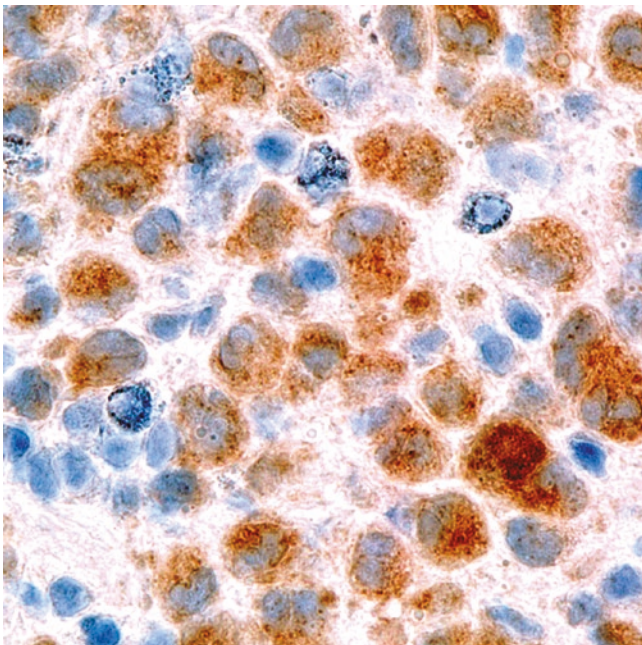


**Fig. 8.32** More than half of cases of Langerhans cell histiocytosis have the *BRAF* V600E mutation that can be detected with the specific *BRAF* VE-1 antibody

unusual in the mediastinum, does not typically expand the sinuses, and it is not accompanied by multinucleated giant cells or eosinophils. The presence of pigment and the identification of other types of interdigitating DCs (S100+/CD1a-) and histiocytes admixed with Langerhans cells militates against LCH. *BRAF* VE-1 is negative [63].

Rosai-Dorfman disease and disseminated juvenile xanthogranuloma may resemble LCH. In Rosai-Dorfman disease there is expansion of sinuses, but these are filled with large macrophages featuring emperipolesis, there are numerous plasma cells and usually no eosinophils. In contrast to Langerhans cells, the histiocytes in Rosai-Dorfman disease are positive for S100, CD68, and CD163 and negative for CD1a and CD207/langerin. The morphology of disseminated juvenile xanthogranuloma involving a lymph node resembles LCH but eosinophils and eosinophilic microabscesses are not seen. In this disease histiocytes differ from LCH since they are positive for CD68, CD163, variable S100 and negative for CD1a and CD207/langerin. Rosai-Dorfman disease and juvenile xanthogranuloma are negative for *BRAF* VE1. Indeterminate dendritic cell tumor is a histiocytic neoplasm that may be morphologically identical to LCH, expresses S100 and CD1a but is negative for langerin. This rare tumor, however, occurs preferentially in the skin and its presentation in the mediastinum would be highly unusual.

Anaplastic large cell lymphoma, and metastatic melanoma and carcinoma with sinusoidal involvement of a lymph node may resemble LCH at low power. However, at higher magnification, the neoplastic cells in all these processes have significant atypia and do not show other features of LCH. Moreover, the immunophenotype is completely different: anaplastic large cell lymphoma is positive for >1 T-cell markers, CD30, and/or ALK, whereas melanoma and carcinoma show expression of melanocytic markers and keratins, respectively.

Epithelioid FDC sarcoma or epithelioid interdigitating DC sarcoma may resemble LCH to a certain extent, however, on close examination these tumors disrupt the lymph node architecture and demonstrate significant atypia and lack of eosinophils. Positivity for >1 FDC markers (CD21, CD23,

**Table 8.5** Immunohistochemical profile of histiocytic disorders

Disease	S100	CD68 and CD163	CD1a	CD207/langerin	<i>BRAF</i> V600E mutation (antibody VE-1)
Langerhans cell histiocytosis	+	-/+	+	+	+ 50–70%
Sinus histiocytosis with massive lymphadenopathy (Rosai-Dorfman disease)	+	+	-	-	-
Erdheim-Chester disease	-/+	+	-	-	+ most cases
Juvenile xanthogranuloma	-/+	+	-	-	-
Indeterminate cell histiocytosis	+	-/+	+	-	-
Sinus histiocytosis (reactive process)	-/+	+	-	-	-

**Table 8.6** Differential diagnosis of Langerhans cell histiocytosis

Dermatopathic lymphadenopathy (pigment, paracortical not sinusoidal)
Other (non-Langerhans cell) nodal histiocytic disorders
– Sinus histiocytosis with massive lymphadenopathy (Rosai-Dorfman disease)
– Indeterminate cell histiocytosis (cutaneous disorder, rare in lymph node)
Metastatic carcinoma or melanoma with sinusoidal pattern
Anaplastic large cell lymphoma
Langerhans cell sarcoma (significant atypia, mitosis, necrosis)
Other dendritic cell neoplasms (significant atypia, mitosis, necrosis)
– Epithelioid follicular dendritic cell sarcoma
– Interdigitating dendritic cell tumor/sarcoma
– Histiocytic sarcoma

CD35) and negative S100, CD1a, and langerin is diagnostic of FDC sarcoma, whereas interdigitating DC sarcoma is positive for S100 but negative for CD1a and langerin. Although rare, these neoplasms can harbor a *BRAF* V600E mutation and therefore, BRAF VE-1 can be potentially detected in a subset of cases. Langerhans cell sarcoma is a neoplasm with an immunophenotype identical to LCH but exhibits overt malignant features, which are not characteristic of LCH. Table 8.6 summarizes the differential diagnosis of LCH.

## Rosai-Dorfman Disease (RDD)

**Introduction** Sinus histiocytosis with massive lymphadenopathy or Rosai-Dorfman disease is a rare histiocytic disorder with peculiar morphologic features. Although sporadic reports of this disease were available since the early 1960s, it was not until 1969 when J. Rosai and R. Dorfman reported four cases of a self-limited nodal histiocytic disorder that they called “massive lymphadenopathy with sinus histiocytosis” [64]. During the late 1970s and mid-1980s, Foucar, Rosai, and Dorfman collected >100 cases of the disease from around the world, created a registry, and presented a detailed clinicopathologic spectrum of the disease, namely, its overall benign behavior and its nodal or extranodal presentation [65–67].

Rosai-Dorfman disease may develop secondary to an abnormal macrophage activation response due to immune dysregulation or possibly a viral infection [68–71]. A small subset of cases can occur in association with IgG4-related disease [72–74]. The disease has been reported in identical twins suggesting an underlying genetic component [75]. In addition, the rare hereditary disorders Faisalabad histiocytosis and the “H” syndrome (hyperpigmentation, hypertricho-

sis, hearing loss, heart anomalies, hepatomegaly, hypogonadism, hyperglycemia, low height, hallux valgus, and hematologic abnormalities) that occur secondary to mutations in the nucleoside transporter *SLC29A3* can show histopathologic features reminiscent of Rosai-Dorfman disease [76, 77]. Recent studies have shown that a subset of cases are negative for *BRAF* mutations but instead harbor mutations in *MAPK1*, another molecule of the RAS/RAF/MAPK pathway, as well as mutations in *KRAS* [78], suggesting that a subset of cases is clonal and may benefit from targeted therapies [79, 80]. The Histiocyte Society classifies the disease in the group “R” for “Rosai-Dorfman” [49].

**Clinical Features** Rosai-Dorfman disease involving the mediastinum is very rare, and it may be a manifestation of localized disease or systemic involvement [81, 82]. The disease can occur at any age and is more common in males. In general, about 60% of cases occur in lymph nodes and the rest affect extranodal sites [83] but the proportion of nodal disease in the mediastinum may be much higher. Symptoms include fever and weight loss, middle or posterior mediastinal lymphadenopathy accompanied or not by cervical lymphadenopathy. Large lymph nodes may produce compression of adjacent structures. Common laboratory abnormalities include polyclonal hypergammaglobulinemia and hemolytic anemia [67, 81, 82]. Most cases are self-limited, but local recurrence may occur [66, 81, 84].

**Pathology** A lymph node involved by Rosai-Dorfman disease usually has a thickened capsule with overall preservation of the architecture with/without follicular hyperplasia and numerous interfollicular and perivascular plasma cells (Fig. 8.33). The characteristic feature of this disease is the marked expansion of all sinuses that are laden with macrophages with central oval nucleus, prominent nucleolus, and voluminous amphophilic cytoplasm filled with variable number of intact lymphocytes, plasma cells, and/or neutrophils. This feature is known as “emperipolesis” (Fig. 8.34), a type of transcytosis, and it is a pathognomonic finding in Rosai-Dorfman disease [85, 86]. Multinucleated cells, necrosis, hemophagocytosis, or increased eosinophils are infrequent. Extranodal involvement has a more challenging histology. At low power, extranodal disease has a “moth-eaten appearance” with variable fibrosis and usually alternating pale and dark areas containing histiocytes and abundant lymphocytes and plasma cells, respectively, that give the tissue the impression of a lymph node. Histiocytes are admixed—and may be obscured—by the inflammatory component. Emperipolesis may not be readily appreciated (Fig. 8.35).

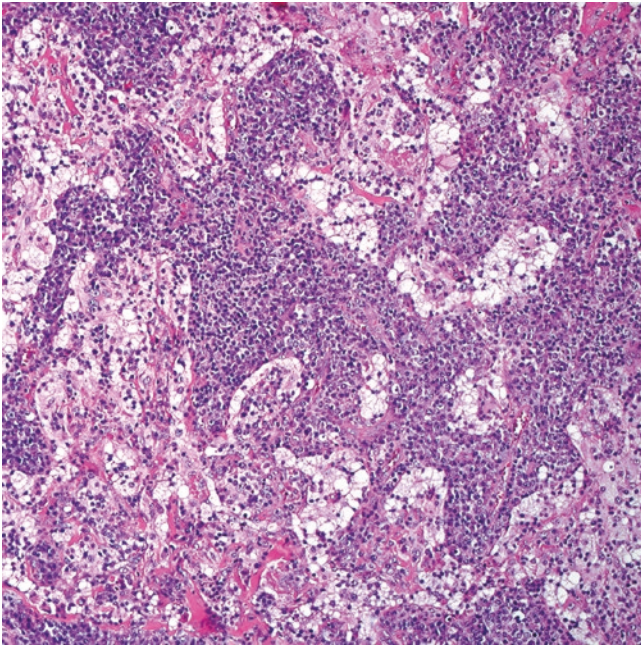


**Fig. 8.33** Nodal Rosai-Dorfman disease or sinus histiocytosis with massive lymphadenopathy. There is dilatation of the sinuses that are filled with histiocytes with clear cytoplasm and inflammatory cells. The medullary cords are laden with numerous mature plasma cells

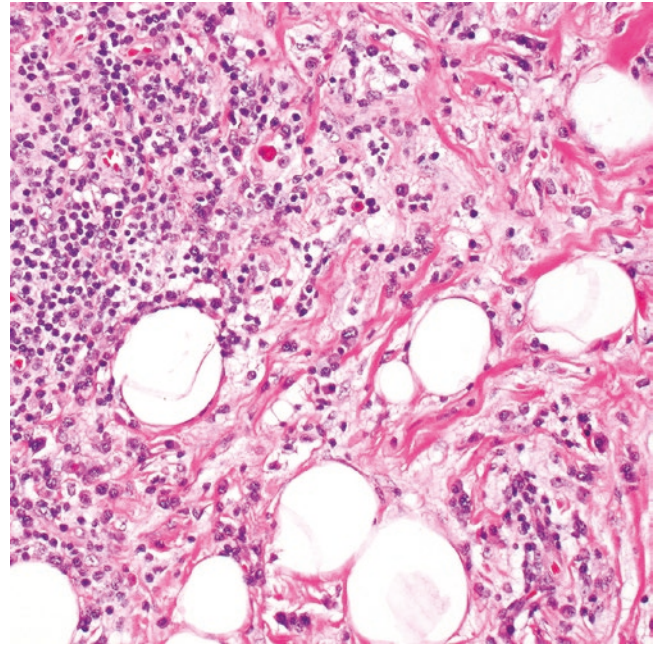


**Fig. 8.35** Extranodal Rosai-Dorfman disease involving mediastinal soft tissue. Macrophages with emperipolesis are not readily appreciated and may be overlooked (top, center). A hint to this lesion is the presence of plasma cells and features reminiscent of fat necrosis, which are actually Rosai-Dorfman histiocytes. Immunohistochemistry for S100 is required to confirm the diagnosis

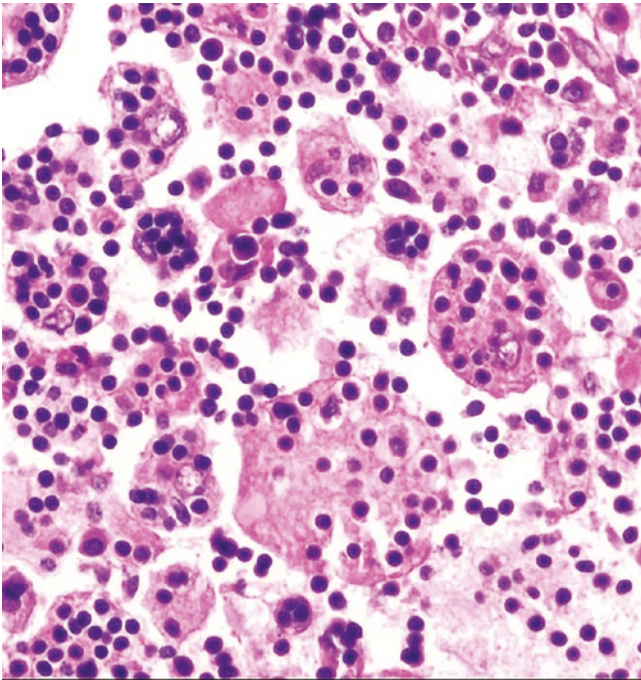


**Fig. 8.34** The macrophages in Rosai-Dorfman disease are enlarged and contain variable number of intact intracytoplasmic lymphocytes and other leukocytes, a phenomenon called “emperipolesis” (a type of transcytosis)

**Immunohistochemistry and Other Ancillary Studies** The macrophages in Rosai-Dorfman disease are weakly positive for CD4, positive for CD68, CD163, and S100, and in some

cases they may also be positive for CD30 [87], whereas they are negative for CD1a, CD207/langerin, BRAF VE-1, ALK, and any B-cell or T-cell marker (Fig. 8.36). S100, CD68, and CD163 tend to highlight the emperipolesis, particularly in extranodal cases. Plasma cells are always polytypic. IgG4+ plasma cell may be increased or not, and when they are increased the possibility of an associated IgG4-related disease should be considered [72–74]. This is true for extranodal cases only but not for nodal disease. Table 8.5 summarizes the immunohistochemical profile of histiocytic disorders.

**Differential Diagnosis** Nodal Rosai-Dorfman disease should be distinguished from reactive nodal sinus histiocytosis, LCH, juvenile xanthogranuloma, Erdheim-Chester disease, and anaplastic large cell lymphoma, and metastatic tumors with prominent sinusoidal distribution.

Nodal sinus histiocytosis is a very common finding in most lymph nodes, including mediastinal ones, but in this condition the sinuses are not as enlarged as in Rosai-Dorfman disease, macrophages do not feature emperipolesis, and plasma cells are not increased. In addition, the macrophages in sinus histiocytosis are negative for S100.

Although LCH may resemble Rosai-Dorfman disease at low magnification, in LCH the histiocytic component is composed mostly of Langerhans cells, multinucleated giant cells,

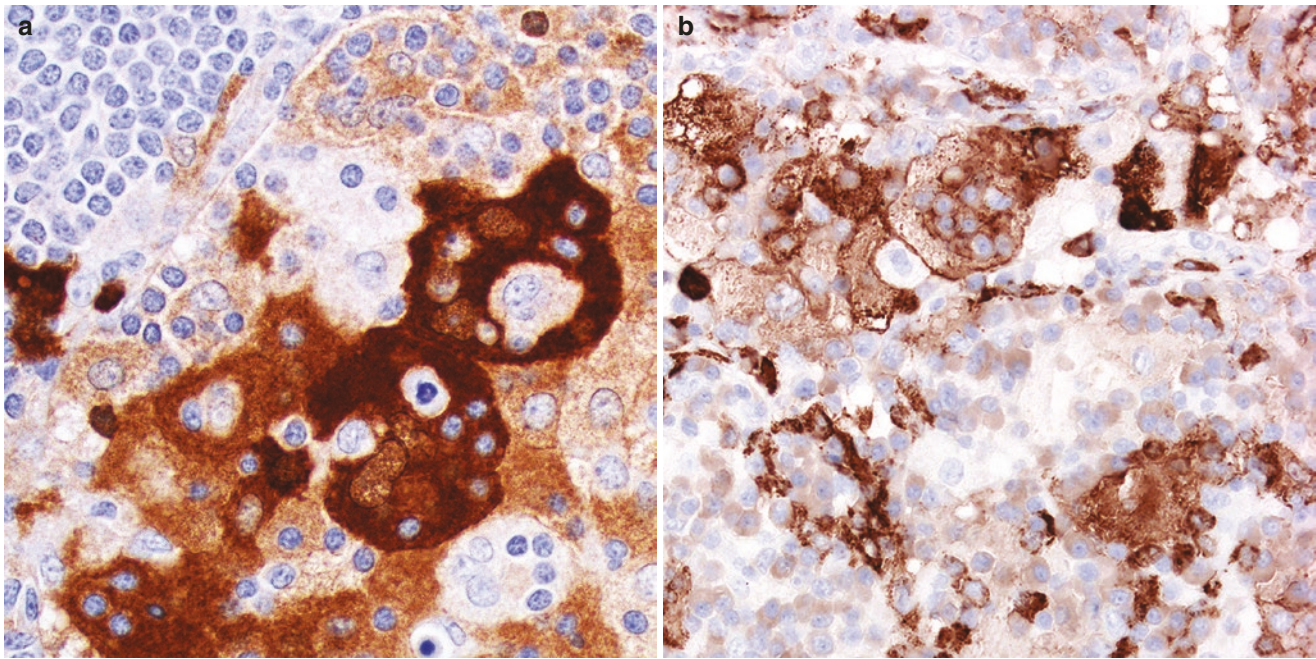


**Fig. 8.36** The macrophages in Rosai-Dorfman disease are positive for (a) S100 and (b) CD68. Both immunostains accentuate intracytoplasmic leukocytes that are negative for these markers

and eosinophils that are not features of Rosai-Dorfman disease. Emperipolesis is not present in LCH and by immunohistochemistry this disease is positive for S100, CD1a, and CD207/langerin with only focal CD68 and CD163, which differs from the findings in Rosai-Dorfman disease. In juvenile xanthogranuloma the macrophages also are not as voluminous or exhibit emperipolesis as seen in Rosai-Dorfman disease, and they are positive for Factor XIIIa with only focal S100. Erdheim-Chester disease is a multiorgan histiocytosis that can affect bone, brain, and perirenal and periaortic soft tissues [49]. These are not the clinical features seen in Rosai-Dorfman disease. Histologically, this process resembles a juvenile xanthogranuloma and some cases harbor a *BRAF* V600E mutation and therefore are positive for the BRAF VE-1 antibody [88]. As mentioned above, BRAF mutations have not been identified in Rosai-Dorfman disease. Pathologists should be aware that some cases of Erdheim-Chester disease may present with identical morphologic features to Rosai-Dorfman disease, and thus, detection of *BRAF* V600E in an otherwise classic case of Rosai-Dorfman disease should raise concern for Erdheim-Chester disease and further evaluation of the patient [89].

Anaplastic large cell lymphoma, and metastatic melanoma and carcinoma with sinusoidal involvement may resemble Rosai-Dorfman disease at low power. However, at higher magnification, the neoplastic cells in all these processes have significant atypia and do not show emperipolesis or increased plasma cells. Moreover, the immunophenotype is completely different: anaplastic large cell lymphoma is positive for >1 T-cell markers, CD30, and/or ALK, whereas melanoma and carcinoma show expression of melanocytic markers and keratins, respectively.

The differential diagnosis of extranodal Rosai-Dorfman disease includes the majority of the disorders described above. Importantly, it should be remembered that Rosai-Dorfman disease in soft tissues may not show obvious emperipolesis, and the diagnosis can be easily missed if not considered. Extranodal infiltration by Rosai-Dorfman disease can mimic fat necrosis, chronic inflammation, an inflammatory pseudotumor, or malakoplakia. Immunohistochemical stains are required to support the presence of S100 and other histiocytic markers to confirm the diagnosis. In addition, immunohistochemistry for IgG4+ is recommended to exclude the possibility of an associated IgG4-related disease. Rosai-Dorfman disease does not contain Michaelis-Goodman bodies as seen in malakoplakia. Table 8.7 summarizes the differential diagnosis of Rosai-Dorfman disease.

**Table 8.7** Differential diagnosis of Rosai-Dorfman disease

#### Nodal

- Florid sinus histiocytosis (common, reactive process)
- Langerhans cell histiocytosis
- Erdheim-Chester disease
- Anaplastic large cell lymphoma
- Other dendritic cell neoplasms with sinusoidal pattern

#### Extranodal

- Fat necrosis and nonspecific chronic inflammation
- IgG4-related disease (minor subset may be associated with Rosai-Dorfman disease)
- Inflammatory pseudotumor
- Erdheim-Chester disease
- Malakoplakia

## Malignant Lymphoproliferative Disorders and Other Hematopoietic Disorders of the Mediastinum

### Introduction

Lymphomas and other hematopoietic disorders comprise about 60% of all malignant neoplasms occurring in the mediastinum, making them the most prevalent malignant tumors at this location [90, 91]. Primary mediastinal involvement is uncommon (5% of cases), whereas secondary involvement from systemic disease is much more frequent (95%) [92, 93]. Non-Hodgkin lymphomas comprise about 65% of all mediastinal lymphomas with the majority of cases being composed of T-lymphoblastic leukemia/lymphoma, diffuse large B-cell lymphoma (DLBCL), and primary mediastinal (thymic) large B-cell lymphoma. On the other hand, mediastinal classic Hodgkin lymphoma (CHL) comprises 35% of all mediastinal lymphomas and most cases are represented by the nodular sclerosis and mixed cellularity subtypes. Other hematopoietic disorders affecting the mediastinum include myeloid sarcoma, but this is an uncommon presentation at this location. FDC sarcoma, although not a hematopoietic-derived neoplasm, is also discussed here since this tumor can arise from mediastinal lymph nodes.

Each one of these entities has a particular clinicoradiologic presentation with variable age of presentation, symptomatology, and location (anterior, middle, or posterior mediastinum), however, certain features remain consistent particularly for those tumors that present with bulky disease (>10 cm), namely, chest pain, dyspnea, cough, superior vena cava syndrome, and pericardial and/or pleural effusions. Importantly, current practice for sampling mediastinal lesions is predominantly performed by interventional radiology in the form of a fine-needle aspiration or a core biopsy, as well as by endobronchial ultrasound, video-assisted thoracoscopic surgery (VATS), or mediastinoscopy. Excisional biopsies and complete resections are less frequent, and this may pose potential problems for diagnostic interpretation with the increase in small or limited specimens. Along with proper morphologic evaluation, the diagnosis of mediastinal hematomatous tumors requires the use of >1 ancillary test(s), including immunohistochemistry, in situ hybridization, and/or flow cytometry, to arrive to a correct diagnosis. In addition, some cases may require cytogenetics, fluorescence in situ hybridization, and/or molecular analysis to identify potential prognostic or predictive factors that may have significance for the use of targeted therapies.

This chapter discusses the mediastinal lymph node and thymic involvement by non-Hodgkin and Hodgkin lymphomas, myeloid sarcoma, and FDC sarcoma. See also Table 8.8. Pulmonary involvement by these hematopoietic tumors is discussed in the lung chapter.

**Table 8.8** Malignant hematopoietic tumors of the mediastinum<sup>a</sup>

<b>Lymphoid</b>
<i>Anterior mediastinum</i>
– Primary mediastinal (thymic) large B-cell lymphoma
– Classic Hodgkin lymphoma, nodular sclerosis
– Mediastinal gray zone lymphoma
– Thymic marginal zone lymphoma of mucosa-associated lymphoid tissue
– T-lymphoblastic leukemia/lymphoma
<i>Middle and posterior mediastinum (may rarely occur in the anterior mediastinum)</i>
– Diffuse large B-cell lymphoma, not otherwise specified (non-thymic)
– Plasmacytoma
– Anaplastic large cell lymphoma
<b>Myeloid</b>
– Myeloid sarcoma

<sup>a</sup>Although follicular dendritic cell sarcoma is included in this chapter, this tumor is not derived from hematopoietic progenitors

## Non-Hodgkin Lymphomas of B-Cell Origin

### Primary Mediastinal (Thymic) Large B-Cell Lymphoma (PM-LBCL)

**Introduction** PM-LBCL represents 3–5% of all DLBCLs and has a particular pathophysiology, clinical presentation, histopathologic findings, and prognosis [94–98]. Before the advent of immunohistochemistry, PM-LBCL and DLBCL were grouped together under various morphologic categories, including those of “mediastinal large cell lymphoma with sclerosis,” “mediastinal sclerotic lymphoma,” and “mediastinal clear cell lymphoma” [99–108]. However, it was not until the advent of immunohistochemistry in the 1980s, and later of cytogenetics and gene expression profiling in the early 2000s that PM-LBCL and DLBCL were shown to have different genetic signatures with PM-LBCL demonstrating features closer to those of CHL and not DLBCL [97, 98].

The putative cell of origin of PM-LBCL is the “asteroid” B-cell found in the thymic medulla around Hassall corpuscles (Fig. 8.37). Normal “asteroid” B-cells are positive for CD20, CD19, CD23, and IgM and negative for CD21, IgA, or IgG [109–112]. CD20 is particularly useful to highlight the star-like shape morphology of these cells, hence their name (Fig. 8.37). “Asteroid” B-cells share certain features with nodal interfollicular B-cells, and they are cells that have undergone somatic hypermutation and have passed through the germinal center reaction [113]. However, their function in the thymus remains only partially understood.

**Clinical Features** PM-LBCL is the second most common primary mediastinal non-Hodgkin lymphoma occurring in the anterior mediastinum after T lymphoblastic lymphoma

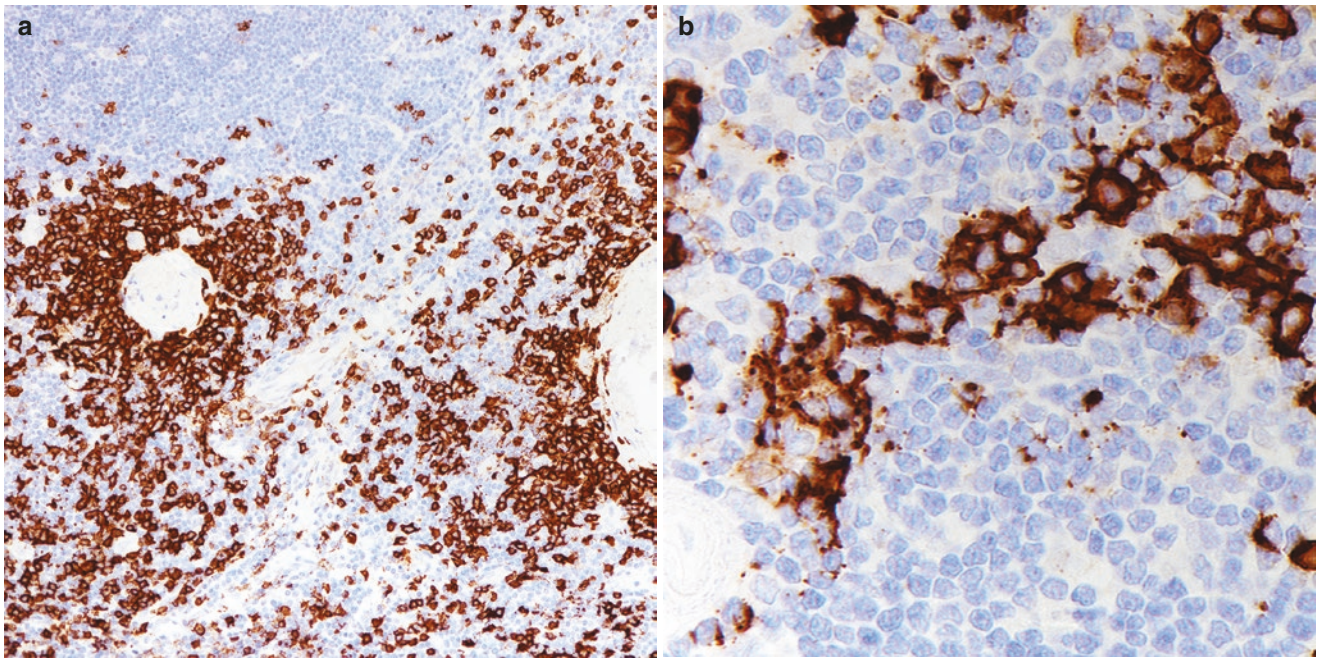


**Fig. 8.37** (a) Asteroid B-cells in the thymic medulla surrounding Hassall corpuscles highlighted by CD20. (b) At higher magnification these cells contain short cytoplasmic processes, hence the name “asteroid” (star-shaped)

[94]. It is more frequent in female than males (male to female ratio 1:2) and usually affects young adults. The tumor presents as an anterior mediastinal mass with or without involvement of adjacent organs producing chest pain, dyspnea, respiratory distress, or superior vena cava syndrome [99–103, 105–107, 114]. Up to 30% of patients may develop a pleural or pericardial effusion. Regional lymphadenopathy is uncommon. Typical sites of spread include immune-privileged organs, namely, the adrenal gland, the testes, and the brain. The current chemotherapy regimen for PM-LBCL is dose-adjusted etoposide, prednisone, vincristine, cyclophosphamide, doxorubicin, and rituximab (DA-EPOCH-R) that has shown a higher event-free survival than the traditional regimen of rituximab, cyclophosphamide, doxorubicin, vincristine, and prednisone (R-CHOP) for DLBCL [115]. Therefore, it is important to distinguish between these two LBCLs.

**Pathology** Gross resections of PM-LBCL are not performed nowadays since the diagnosis is more commonly established in a core needle-biopsy or an incisional biopsy. Gross resections have been described as a tan-white tumor with “fish-flesh” appearance with variable necrosis, and fibrous areas separating the tumor into nodules mimicking nodular sclerosis CHL. Cysts filled with clear fluid may or may not be present as well as a residual rim of thymic tissue around the main mass [116]. On microscopic examination, the thymic gland is widely infiltrated by large cell lymphoma that extends to the surrounding adipose tissue and any adjacent structures. At low magnification, this neoplasm may show diffuse cellular areas, areas with vague nodularity separated by fibrous

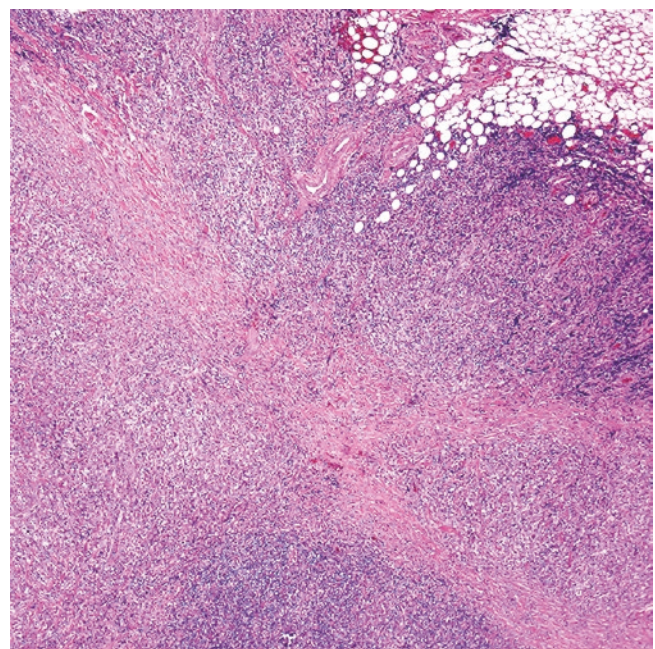


**Fig. 8.38** Primary mediastinal (thymic) large B-cell lymphoma extending to surrounding adipose tissue. There are bands of fibrosis separating the tumor cells into nodules. Courtesy of Daisy Alapat, MD

bands, and areas with sclerosis (Fig. 8.38). Epithelial-lined cysts and residual entrapped Hassall corpuscles are variably seen. At higher magnification, this lymphoma is composed of intermediate to large cells with oval to convoluted and/or multilobated nucleus, and clear to pale eosinophilic cytoplasm. Scattered Reed-Sternberg-like cells may be present but a polymorphic background is not seen. The lymphoma

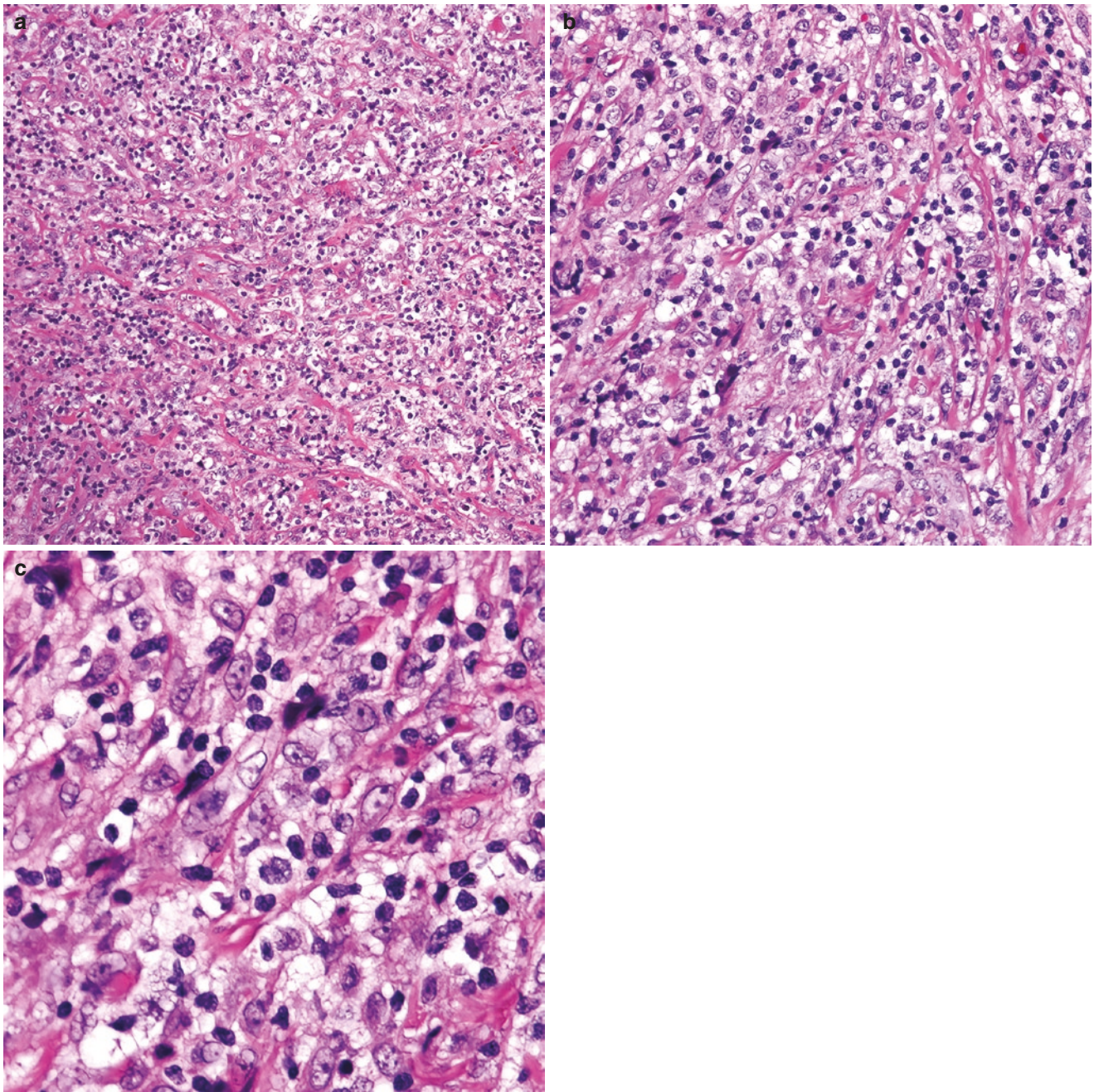


**Fig. 8.39** (a–c) Sheets of large cells with clear cytoplasm separated by delicate fibrosis. If prominent, this feature can be confused with an infiltrating carcinoma. Courtesy of Daisy Alapat, MD

cells can be arranged in solid sheets or separated into smaller clusters by delicate fibrous bands, resembling an infiltrating carcinoma (Fig. 8.39). Frequent mitoses are seen, and necrosis may be focal or extensive. A starry sky pattern is not a feature of this lymphoma. Areas with marked sclerosis are usually paucicellular and with significant crush artifact that does not permit an adequate cytologic evaluation (Fig. 8.40). Rarely, PM-LBCL may show areas that resemble nodular sclerosis CHL raising concern for mediastinal gray zone lymphoma (see corresponding section).

**Immunohistochemistry and Other Ancillary Studies** The lymphoma cells are positive for CD45 and for B-cell markers, namely, CD19, CD20, CD79a, PAX5, OCT2, and BOB.1, and about 80% of cases show a weak and variable labeling with CD30 [117–119] (Figs. 8.41 and 8.42). PM-LBCL “rule of the 70s” refers to the detection of MUM1, CD23, p63, and MAL (myelin and lymphocyte protein) in about 70% of cases [112, 119–122] (Fig. 8.43). Bcl-6 is usually positive, and CD10 and bcl-2 have been reported in up to 30% of cases [95, 118]. CD15 is usually negative, but at least

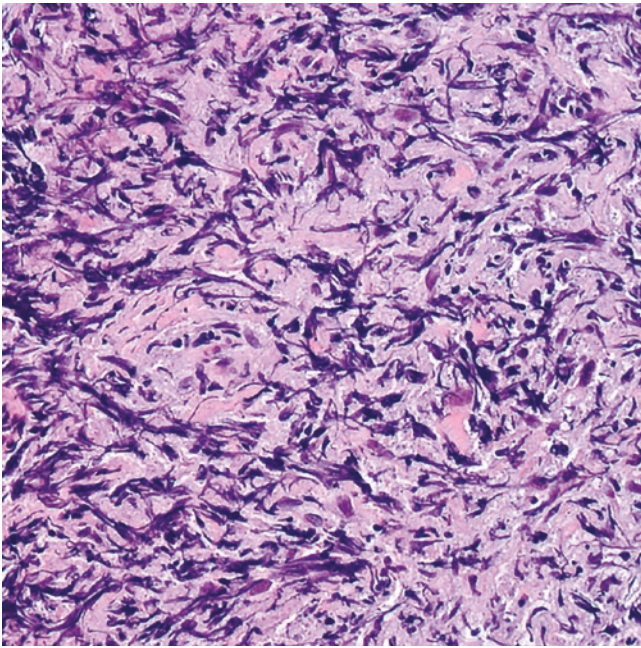


**Fig. 8.40** Marked sclerosis in primary mediastinal (thymic) large B-cell lymphoma. There is marked crush artifact that hinders proper morphologic evaluation

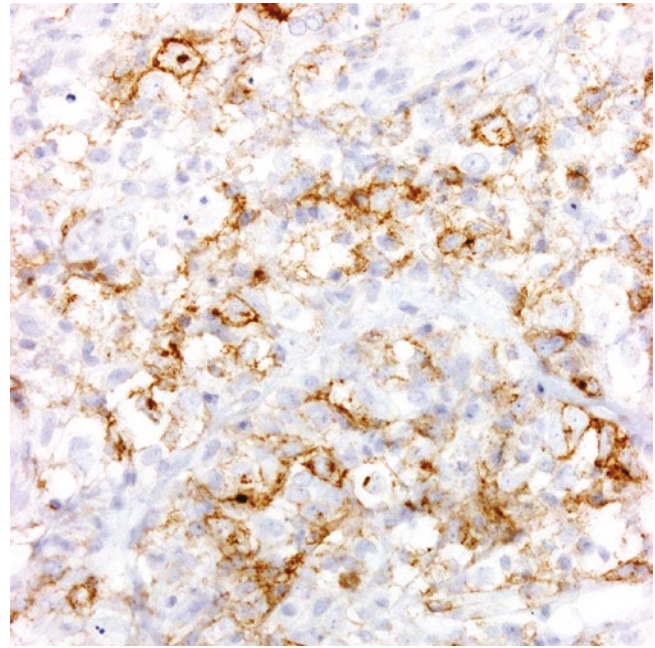


**Fig. 8.42** Primary mediastinal (thymic) large B-cell lymphoma. The CD30 immunostain shows a weak to variable pattern characteristic of this tumor

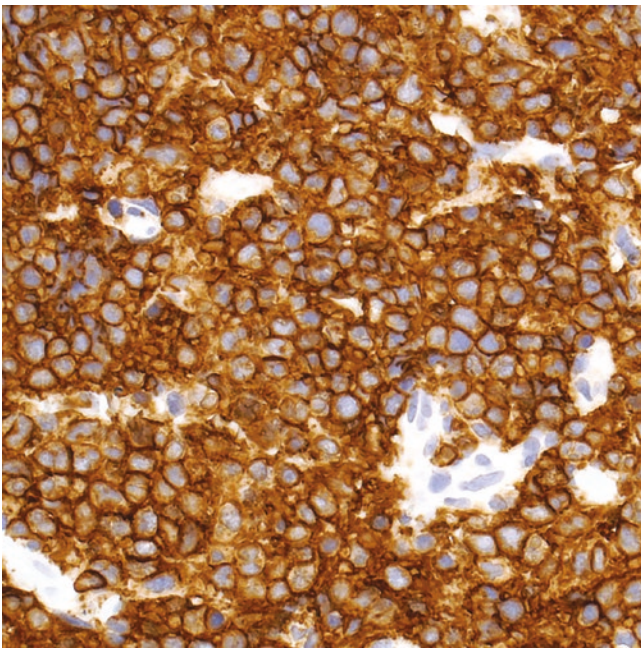


**Fig. 8.41** Primary mediastinal (thymic) large B-cell lymphoma, CD20 immunostain

in one study the authors claimed that this marker was positive in up to 30% of their cases [123] (Fig. 8.43). PM-LBCL is frequently positive for PD-L2 (>60%) but detection of PD-L1 has ranged from 15% to up to 50% [124–126]. PD-L1 and MUM1 have been suggested as potential biomarkers for PM-LBCL but the clinical significance of these findings

requires additional studies [123, 127]. Ki-67 is always high (>30–40%) (Fig. 8.44). PM-LBCL is negative for T-cell markers, TdT, cytokeratins, and melanoma and germ cell tumor markers. Areas of entrapped thymus, residual Hassall corpuscles or cysts lining are highlighted with pancytokeratin. CD3 highlights background T-cells that tend to have perivascular distribution (Fig. 8.45). EBER ISH is negative [95] and only rare cases of PM-LBCL may show scattered EBER positivity after recurrence.

**Differential Diagnosis** The differential diagnosis of PM-LBCL includes other anterior mediastinal hematopoietic and non-hematopoietic tumors, namely, DLBCL, nodular sclerosis CHL, germinoma, atypical thymoma, thymic carcinoma, metastatic amelanotic melanoma, and metastatic carcinoma with clear cell morphology (squamous, renal, other). The clinical, radiologic, and morphologic features are usually sufficient to narrow down the list of possible diagnoses, but confirmation of the diagnosis requires the use of immunohistochemistry. The differential diagnosis of PM-LBCL is summarized in Table 8.9.

Germinoma, atypical thymoma, thymic carcinoma, and metastatic melanoma or carcinoma can be easily ruled out by the lack of hematopoietic and B-cell markers in all these entities. On the other hand, PM-LBCL is negative for cytokeratins, melanoma markers (HMB-45, MART1, tyrosinase, SOX10), and germ cell markers (OCT3/4, SALL4, beta-

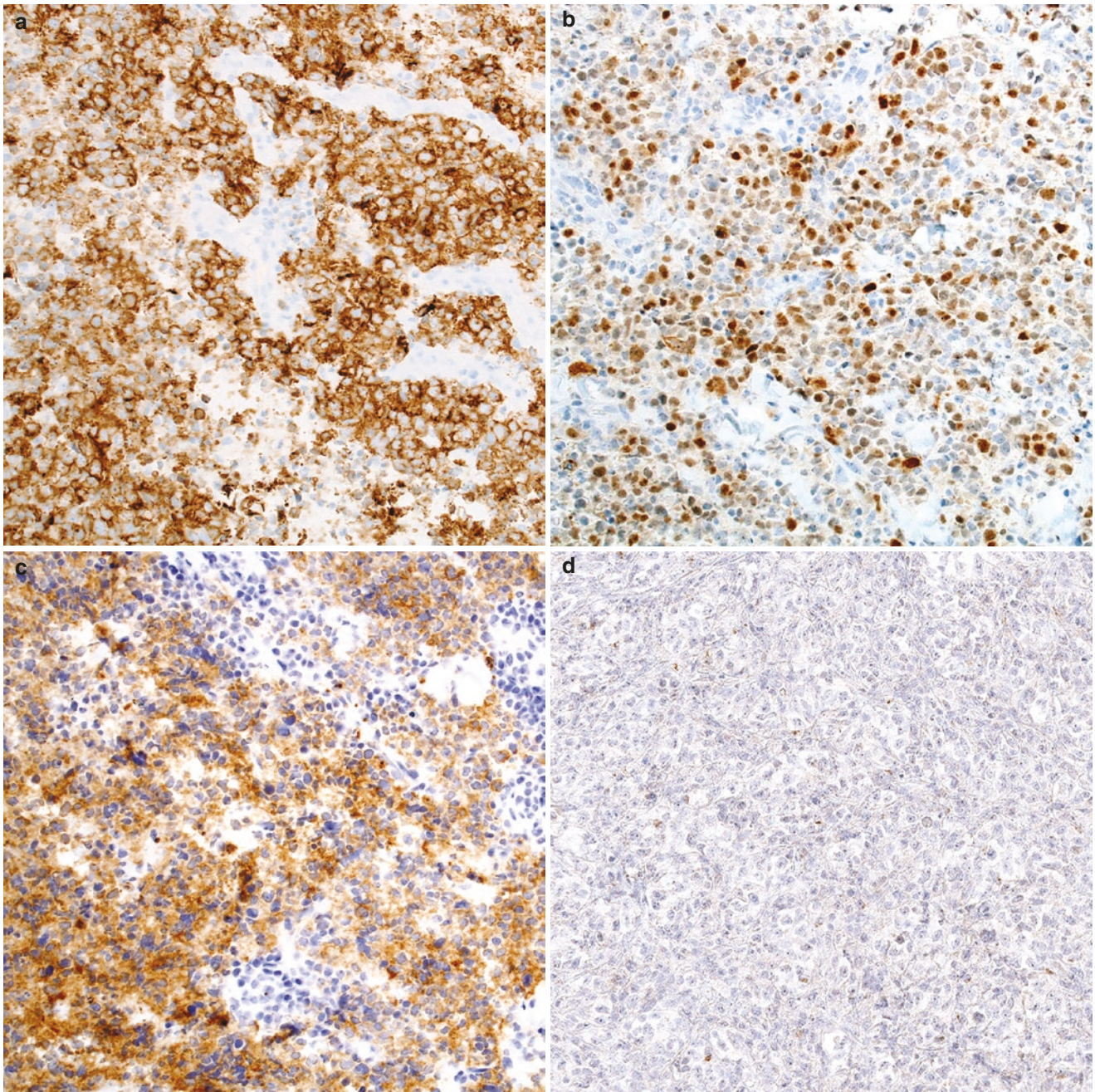


**Fig. 8.43** Primary mediastinal (thymic) large B-cell lymphoma. Immunostains for (a) CD23, (b) MUM1, (c) CD10, and (d) CD15. CD10 is occasionally positive in these cases

hCG). From all germ cell tumors, embryonal carcinoma may pose a difficult distinction from PM-LBCL, since the former is composed of sheets of poorly differentiated cells that are positive for CD30. The use of an additional germ cell marker and a B-cell marker is required to confirm or exclude this possibility. Pathologists should be aware that 70% of PM-LBCLs are positive for p63 in order to avoid rendering a wrong diagnosis of clear cell squamous carcinoma, metastatic clear cell squamous carcinoma, or thymic carcinoma in a core biopsy with fibrosis and infiltrating tumor cells with

clear cytoplasm. Additional evaluation for pan-cytokeratin and B-cell markers easily solves this problem. Similarly, proper interpretation of p63 and keratin in residual thymus and not in the lymphoma cells should be taken into consideration when assessing any anterior mediastinal biopsy.

By morphology PM-LBCL and DLBCL may be similar—if not identical—especially in those cases without clear cells or with marked sclerosis and cytology artifact. The use of B-cell markers or CD45 cannot distinguish between PM-LBCL or DLBCL. In this scenario, the use of CD30,

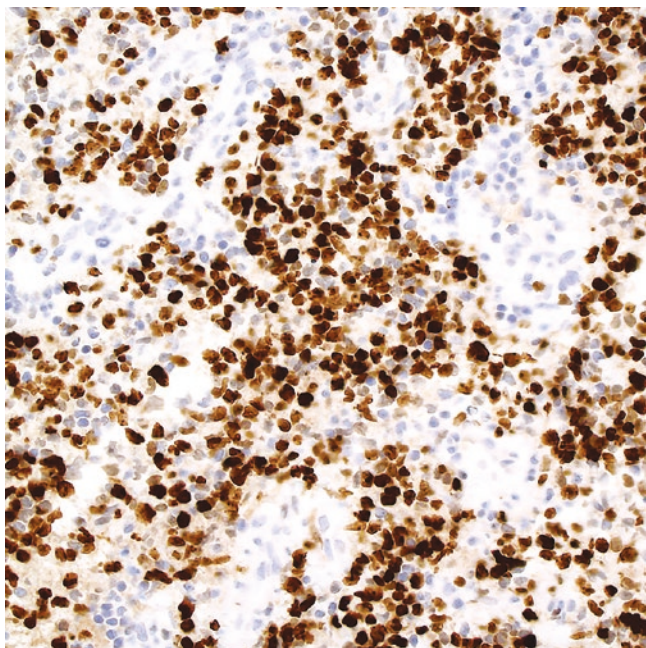


**Fig. 8.44** Primary mediastinal (thymic) large B-cell lymphoma has a high Ki-67 proliferation index

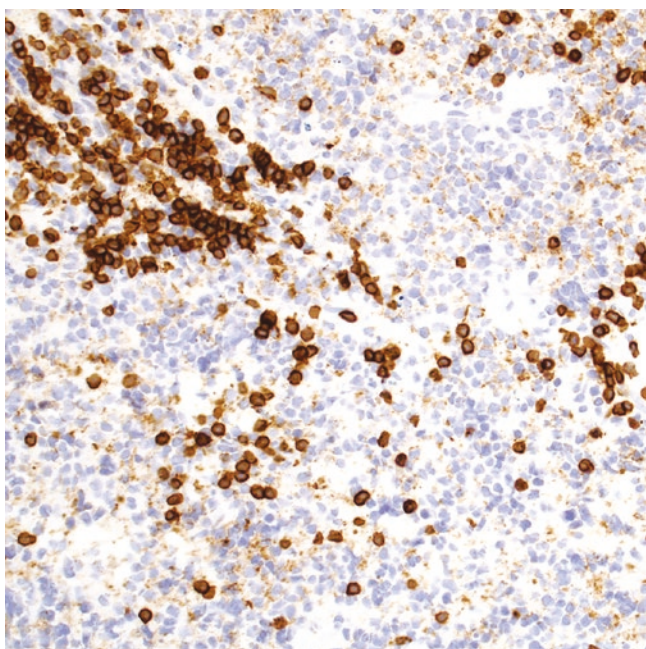


**Fig. 8.45** Primary mediastinal (thymic) large B-cell lymphoma. CD3 immunostain

CD23, MAL, and p63 is extremely useful as these markers are frequently positive in PM-LBCL and not in DLBCL (CD30 is positive in 10–15% of DLBCLs). In a similar fashion, the syncytial variant of nodular sclerosis CHL may resemble PM-LBCL by morphology. In cases with marked cellular distortion and sclerosis, the presence of eosinophils

**Table 8.9** Differential diagnosis of primary mediastinal (thymic) large B-cell lymphoma

<b>Hematopoietic tumors</b>	
Diffuse large B-cell lymphoma, not otherwise specified	
Syncytial variant of nodular sclerosis classic Hodgkin lymphoma	
Mediastinal gray zone lymphoma	
Anaplastic large cell lymphoma	
<b>Non-hematopoietic tumors</b>	
Germinoma	
Metastatic clear cell carcinoma (renal cell, other), metastatic amelanotic melanoma	
Atypical thymoma (WHO B3)	
Thymic carcinoma	

favors CHL over PM-LBCL up to a certain extent, but the diagnosis still requires confirmation by immunohistochemistry. In nodular sclerosis CHL the sheets of Reed-Sternberg cells are diffusely positive for CD30, variable for CD15, weakly positive for PAX5, and negative for B-cell markers and CD45. This immunophenotype does not support PM-LBCL. In difficult cases, the use of an antibody panel for CD79a, BOB.1, and cyclin E has been used to distinguish PM-LBCL from CHL with good results. PM-LBCL is positive for CD79a, and BOB.1, and negative for cyclin E, whereas CHL shows the reverse immunophenotype [119]. In rare instances, a case may show intermediate morphology and intermediate expression of the markers mentioned above that should raise suspicion for the diagnosis of mediastinal gray zone lymphoma (see corresponding section). The main clinicopathologic differences and molecular features of mediastinal large B-cell lymphomas are summarized in Table 8.10.

**Molecular Findings** PM-LBCL is more closely related to CHL than to DLBCL at the genetic level, including the presence of molecular alterations associated with diminished immunogenicity and impaired antigenicity, which might explain in part its thymic primary origin and its preferential spread to immune-privileged organs [128]. Diminished immunogenicity occurs due to alterations in the JAK-STAT signaling at multiple levels, including 1) amplification of 9p24 and gain of function/overexpression of JAK2, PD-L1, and PD-L2; 2) constitutive activation of *STAT6*; and 3) deletion/inactivation of *SOCS1* and *PTPNI*, which are negative regulators of the JAK-STAT pathway [128–130]. Rearrangements/mutations of the Class II Major Histocompatibility Complex Transactivator (*CIITA*) gene located in chromosome 16p13 produce downregulation of HLA class II molecules that are associated with the development of impaired antigenicity. A similar consequence may result from microdeletions of CD58/LFA3 [128, 131, 132]. All these types of molecular alterations allow PM-LBCL cells to escape recognition by the immune system. Another pathway affected in PM-LBCL is the NF- $\kappa$ B signaling.

**Table 8.10** Differential diagnosis of mediastinal large B-cell lymphomas

Lymphoma	Primary mediastinal (thymic) large B-cell lymphoma	Diffuse large B-cell lymphoma (DLBCL), not otherwise specified	Mediastinal gray zone lymphoma (BCL, unclassifiable, with features intermediate between DLBCL and classic Hodgkin lymphoma)
Age and gender predilection	Young adults Male to female ratio 1:2	Older adults, but can occur at all ages Male to female ratio 1:1	Young adults Male to female ratio 2:1
Mediastinal location	Anterior	Middle and posterior > anterior	Anterior
Morphology	Sheets of large cells, clear cytoplasm, variable fibrosis	Sheets of large cells, variable fibrosis, usually no clear cells	“LBCL-like”: Sheets of large cells, may or may not have clear cells, variable fibrosis, and/or Reed-Sternberg-like cells
Immunohistochemistry	Positive: CD20 PAX5 (strong) CD45 CD30 (variable, weak, 80–90%) CD23 (70%) MUM1 (70%) p63 (70%) MAL (70%) PD-L1 (15–50%) PD-L2 (60%) Negative: Usually CD15, bcl-6 and CD10	Positive: CD20 PAX5 (strong) CD45 CD30 (10–15%) CD10 (if GCB) bcl-6 (if GCB) MUM1 (if non-GCB) Negative: CD15 p63 MAL CD23	Immunophenotype: CD30 (variable) CD15 (variable) CD45 (variable or negative) CD20 (variable or negative) PAX5 and other B-cell markers (variable or negative) MUM1 (variable or negative) CD23? MAL?
Molecular alterations	– Amplification 9p24 (JAK2, PD-L1 and PD-L2) with activation of JAK-STAT signaling – <i>CIITA</i> rearrangements with downregulation of HLA class II – No <i>MYC</i> , <i>BCL2</i> , and/or <i>BCL6</i> gene rearrangements	– <i>MYC</i> , <i>BCL2</i> , and/or <i>BCL6</i> gene rearrangements likely with same frequency as in systemic DLBCL – GCB: expression of <i>BCL6</i> and <i>EZH2</i> – Non-GCB: alterations in <i>MYD88</i> , <i>CD79B</i>	– No specific alterations – Similar to primary mediastinal (thymic) large B-cell lymphoma and classic Hodgkin lymphoma Amplification 9p24 (JAK2, PD-L1 and PD-L2) with activation of JAK-STAT signaling – <i>CIITA</i> rearrangements with downregulation of HLA class II molecules

Mutations in this pathway facilitate the survival and proliferation of the lymphoma cells as seen with mutations of *TNFAIP3* and *NFKBIE* (which codify for A20 and I $\kappa$ B $\epsilon$ , respectively) both potent negative regulators of the NF- $\kappa$ B signaling [133, 134]. *BCL6* mutations are frequent in PM-LBCL [117] but rearrangements in *BCL6*, *BCL2*, and/or *MYC* are extremely uncommon [135]. In addition, PM-LBCL lacks *IgV(H)* gene crippling mutations as seen in other B-cell lymphomas.

## Mediastinal Diffuse Large B-Cell Lymphoma (DLBCL)

**Introduction** Mediastinal DLBCL, not otherwise specified (DLBCL, NOS; here referred as to DLBCL) appears to be slightly more common than PM-LBCL, comprising about 5–9% of DLBCL cases) [91, 99]. However, the true incidence of this lymphoma affecting the mediastinum is difficult to estimate since very few studies have focused exclusively on DLBCL. Before the advent of immunohistochemistry, DLBCL

and PM-LBCL were grouped together under various morphologic categories, including those of “mediastinal large cell lymphoma with sclerosis,” “mediastinal sclerotic lymphoma,” and “mediastinal clear cell lymphoma” [99–108]. It was not until the advent of immunohistochemistry in the 1980s, and later of cytogenetics and gene expression profiling in the early 2000s that DLBCL and PM-LBCL were shown to have different genetic signatures [97, 98]. Mediastinal DLBCL can arise in any lymph node from the anterior, middle, or posterior mediastinum, whereas primary thymic disease is exceedingly rare.

**Clinical Features** Mediastinal DLBCL can occur at any age, but in general, it is more common in older individuals and it does not appear to have a gender predilection. DLBCL can develop at any nodal or extranodal site in the mediastinum and the clinical symptoms vary according to the site and extent of involvement. Anterior and middle mediastinal disease may present with chest pain, cough, dyspnea, or superior vena cava syndrome. Posterior mediastinal involvement may present with upper back pain, dysphagia or a pathologic fracture of a thoracic vertebral bone. Systemic B-symptoms are common. Pleural or pericardial effusion may or may not be present.

**Pathology** Large resections of mediastinal DLBCL are becoming less frequent and sampling is mostly accomplished via a thoracoscopic biopsy or an imaging-guided needle biopsy. Gross resection of an involved lymph node or extranodal tissue typically has a “fish-flesh” appearance and variable necrosis. On microscopic examination, mediastinal DLBCL is identical to any large cell lymphoma at other site, composed of sheets of large lymphoid cells and with infiltration into adjacent structures (Fig. 8.46). The morphology of the lymphoma cells is predominantly centroblastic, with oval to round nucleus with fine chromatin, >2 juxtannuclear nucleoli, and scant to moderate amount of basophilic cytoplasm (Fig. 8.47). Scattered cells with immunoblastic or anaplastic features and Reed-Sternberg-like cells may or may not be present. Cases with pleomorphic morphology have been further classified into sarcomatoid, anaplastic carcinoma-like, and lymphocyte depleted CHL-like DLBCL [136]. Mitoses and apoptotic bodies are frequent (Fig. 8.47), and some cases may feature a “starry-sky” pattern. Necrosis is variably seen. Mediastinal DLBCL may be accompanied by sclerosis that may cause marked cellular distortion or spindling of the lymphoma cells (Fig. 8.48).

**Immunohistochemistry and Other Ancillary Studies** The information presented here refers to DLBCL in general. The lymphoma cells are positive for CD45 and for B-cell markers, namely, CD19, CD20, CD79a, PAX5, OCT2, and BOB.1, and are negative for CD15 and for T-cell markers (Fig. 8.49).

CD30 is positive in 10–15% of cases (based on information from DLBCL at other sites), and the frequency of CD30 may be higher in anaplastic DLBCL (Fig. 8.50). Today, it is standard practice to determine the “cell of origin” of a DLBCL using an algorithm or a classifier, among which the one pro-

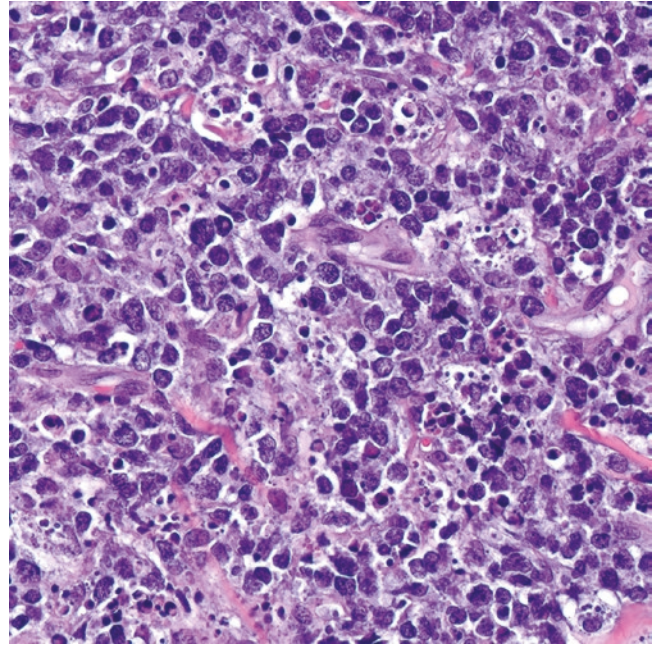


**Fig. 8.47** Mediastinal diffuse large B-cell lymphoma (non-thymic) with abundant tingible body macrophages. If prominent, this feature gives the impression of a “starry-sky”

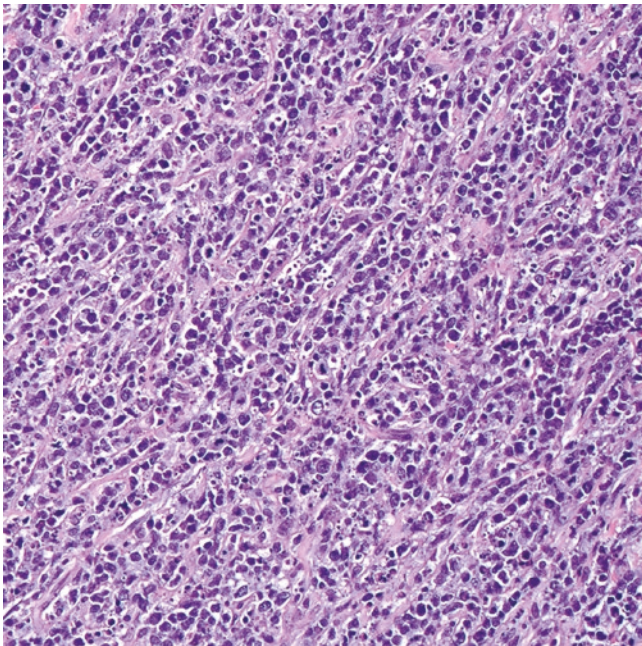


**Fig. 8.46** Mediastinal diffuse large B-cell lymphoma (non-thymic). Sheets of large lymphoma cells with abundant apoptotic bodies and scattered mitoses

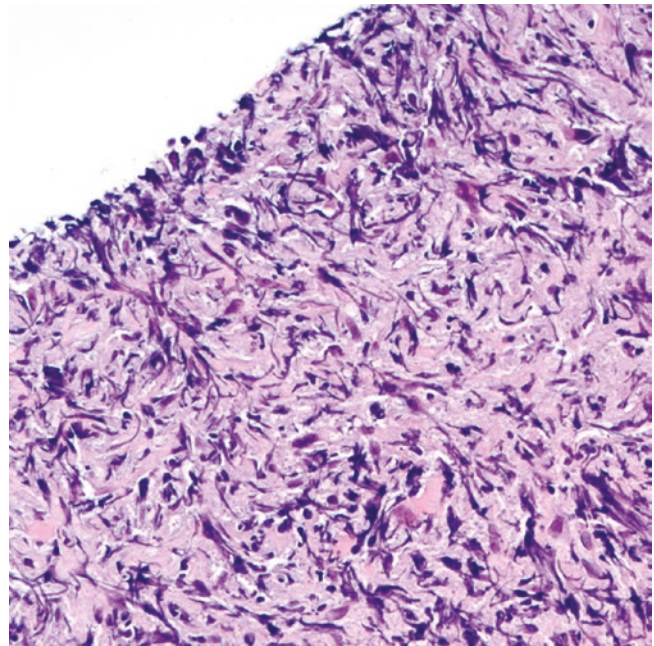


**Fig. 8.48** Marked sclerosis in a core biopsy of mediastinal diffuse large B-cell lymphoma. There is marked crush artifact that hinders proper morphologic evaluation

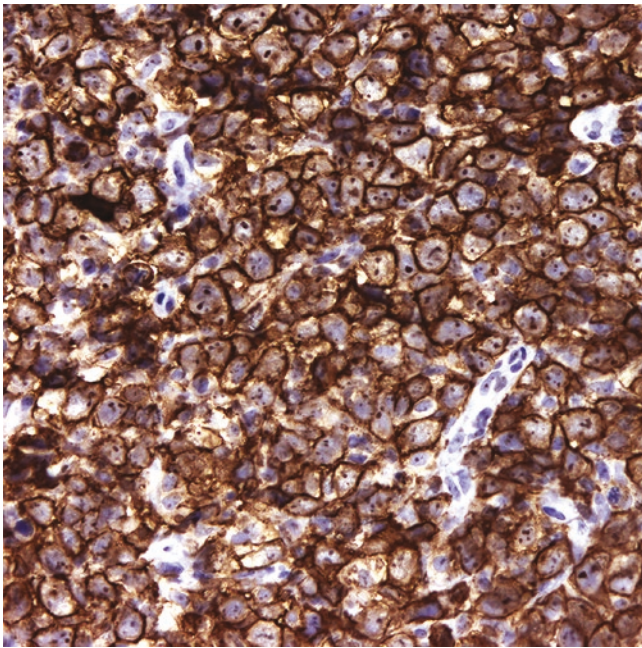


**Fig. 8.49** Mediastinal diffuse large B-cell lymphoma, CD20 immunostain

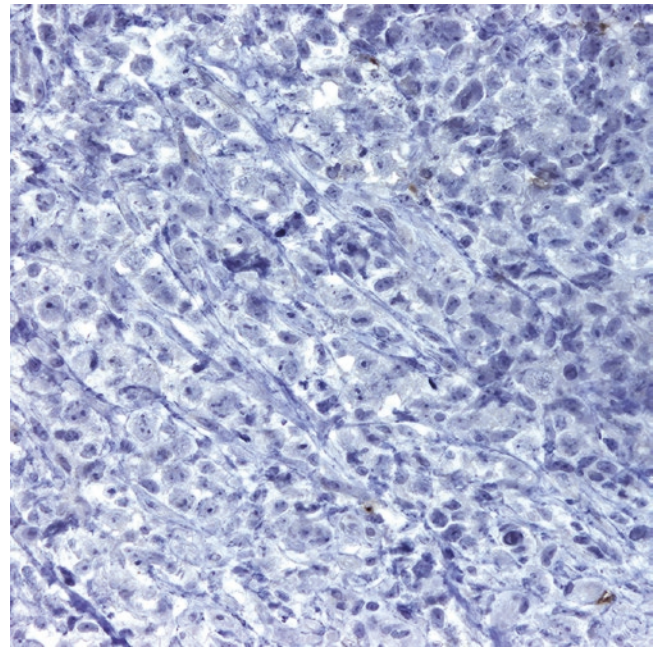


**Fig. 8.50** Mediastinal diffuse large B-cell lymphoma, negative CD30 immunostain

posed by Hans and colleagues is widely used [137]. This algorithm takes into consideration the expression of CD10, bcl-6, and MUM1 to either define DLBCL into germinal center B-cell (GCB)-like (CD10+, bcl-6+/-, MUM1-) or non-GCB/activated B-cell-like (CD10-, bcl-6+/-, MUM1+). The cut-off for all these markers is >30% of lymphoma cells (Fig. 8.51). Non-GCB/ABC-like DLBCL has worse prognosis and a higher frequency of extranodal involvement. In addition, standard of practice also includes assessment of the status of bcl-2 and c-myc by immunohistochemistry (>50% and >40% of tumor cells cutoff, respectively). DLBCLs that are positive for both markers are referred to as “double expressors” and this appears to confer a bad prognosis regardless of the cell of origin (Fig. 8.52). The Ki-67 proliferation index is always elevated (>30%) but usually not higher than 90% (Fig. 8.53). When Ki-67 is >90–95%, it should suggest the possibility of a “high-grade” DLBCL. EBER ISH is negative and cases that are EBV+ should be classified as EBV+ DLBCL, a specific category of DLBCL.

**Differential Diagnosis** Mediastinal DLBCL should be distinguished from other mediastinal hematopoietic and non-hematopoietic tumors. In the anterior mediastinum, PM-LBCL, the syncytial variant of nodular sclerosis CHL, germinoma, atypical thymoma, thymic carcinoma, and metastatic amelanotic melanoma and carcinoma enter the differential diagnosis. In the middle or posterior mediastinum, DLBCL should be distinguished from other large cell lymphomas, metastatic amelanotic melanoma, and carcinoma.

The clinical and radiologic presentation along with morphology help to narrow down the differential diagnosis but ultimately a diagnosis requires the use of an appropriate panel of immunohistochemical markers.

Germinoma, atypical thymoma, thymic carcinoma, and metastatic melanoma or carcinoma can be easily ruled out by the lack of hematopoietic and B-cell markers. On the other hand, DLBCL is negative for cytokeratins, melanoma markers (HMB-45, MART1, tyrosinase, SOX10), and germ cell markers (OCT3/4, SALL4, beta-hCG).

By morphology alone, DLBCL and PM-LBCL may be similar—if not identical—especially in those cases without clear cells or with marked sclerosis and cytology artefact. The use of B-cell markers or CD45 cannot distinguish between DLBCL and PM-LBCL. In this scenario, the use of CD30, CD23, MAL, and p63 is extremely useful as these markers are frequently positive in PM-LBCL and not in DLBCL. In a similar fashion, the syncytial variant of nodular sclerosis CHL may resemble DLBCL by morphology. In cases with marked cellular distortion and sclerosis, the presence of eosinophils suggests CHL and not DLBCL, but the diagnosis still requires confirmation by immunohistochemistry. In nodular sclerosis CHL the sheets of Reed-Sternberg cells are diffusely positive for CD30, variable for CD15, weakly positive for PAX5, and negative for B-cell markers and CD45. This immunophenotype does not support DLBCL. Rarely, mediastinal gray zone lymphoma may show “LBCL-like” morphology but the immunophenotype is closer to CHL than to DLBCL (see corresponding section). See also Table 8.10.

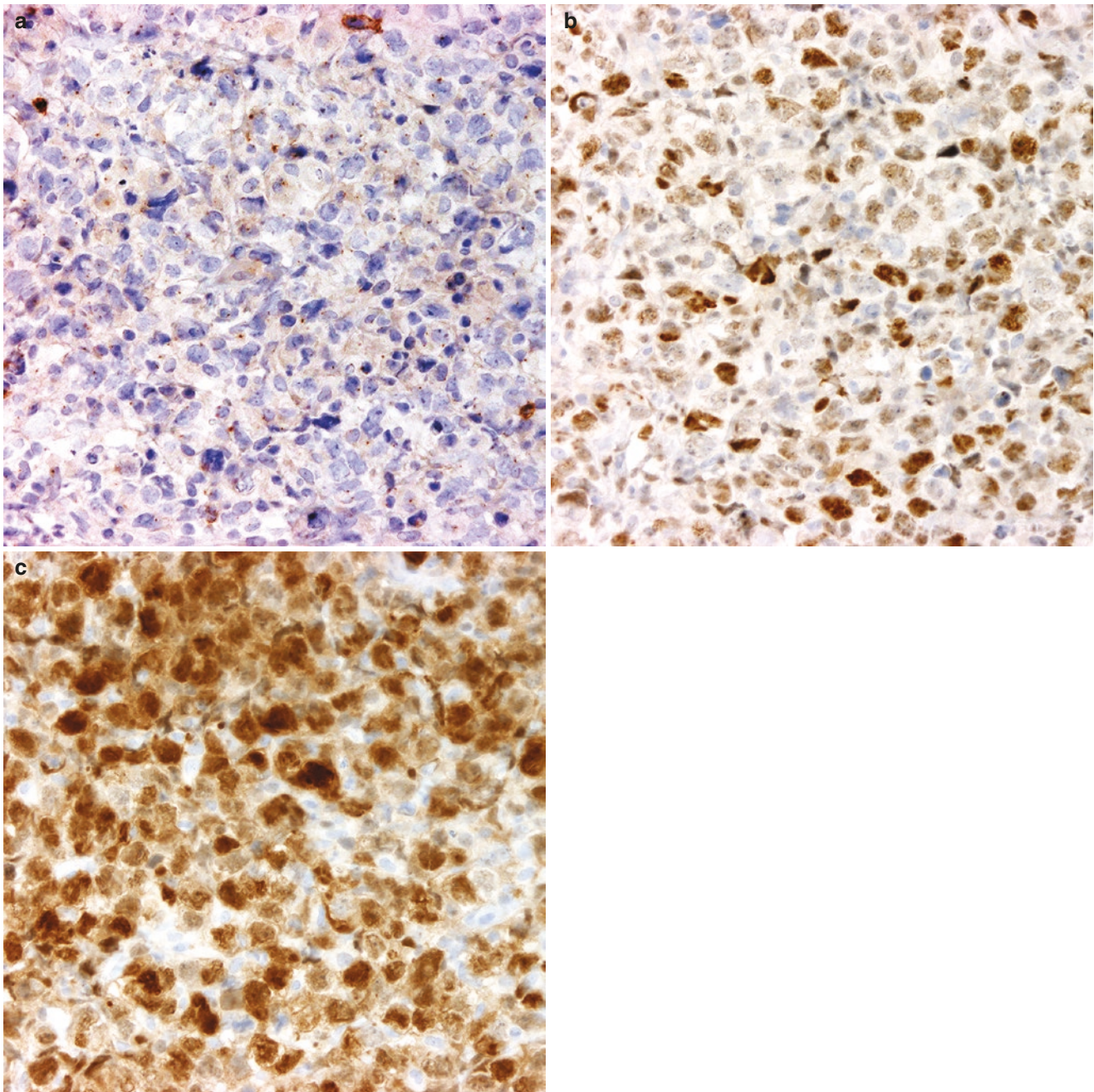


**Fig. 8.51** Mediastinal diffuse large B-cell lymphoma of non-germinal center or activated B-cell type. (a) CD10 is negative. (b) bcl-6 is positive. (c) MUM1 is positive

Apart from metastatic carcinoma or melanoma, the differential diagnosis of DLBCL in the middle or posterior mediastinum includes large cell lymphomas of B- and T-cell origin, including Burkitt lymphoma, plasmablastic lymphoma, anaplastic large cell lymphoma, and peripheral T-cell lymphoma, NOS. A proper set of immunohistochemical markers is helpful to distinguish between these disorders. Burkitt lymphoma only rarely occurs in the mediastinum and is usually extranodal. The lymphoma cells are of intermediate size and the tumor typically exhibits a starry sky pattern. By immunohistochemistry, Burkitt lymphoma is positive for

CD10, negative for bcl-2, and has a Ki-67 index of >90–95%. In some instances, the distinction between Burkitt lymphoma and high-grade DLBCL is challenging, and FISH evaluation becomes the only method to support the diagnosis. Plasmablastic lymphoma has an immunophenotype closer to that of a plasma cell neoplasm, positive for MUM1 and CD138, with consistent expression of EBER and negative or weak expression of CD20 and/or PAX5. This tumor usually develops in immunosuppressed individuals. DLBCL is negative for T-cell markers, which readily excludes the diagnosis of T-cell lymphoma.

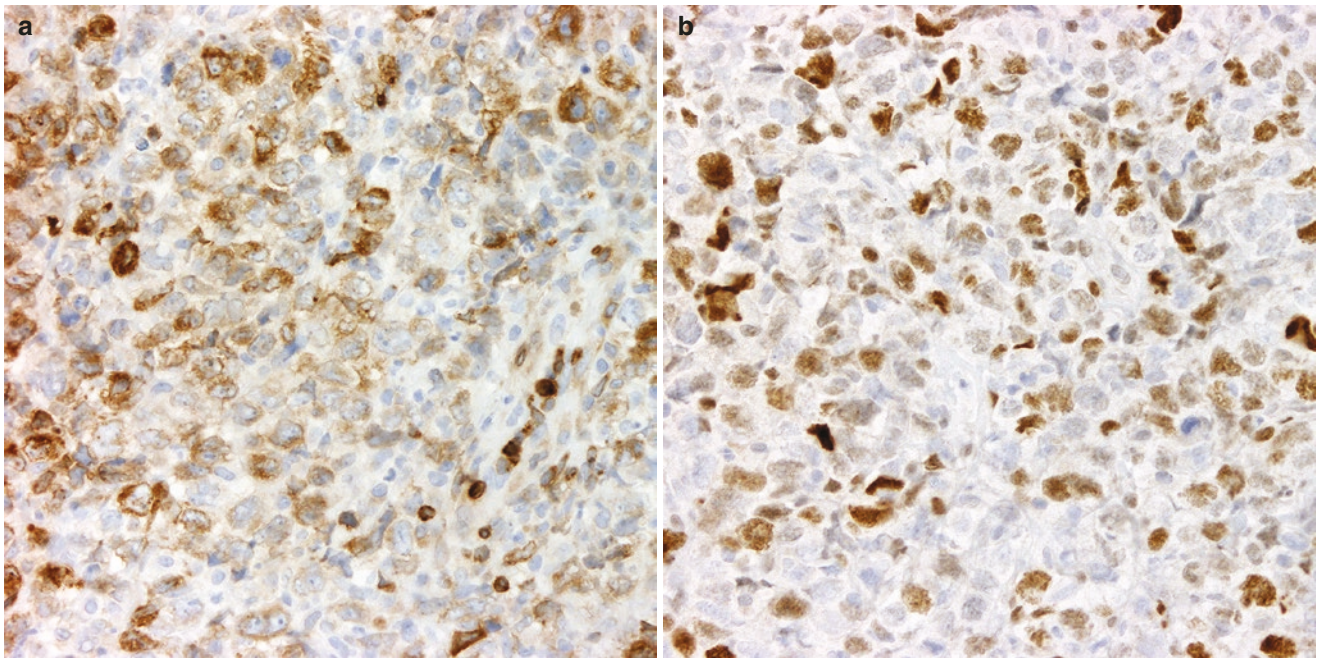


**Fig. 8.52** Mediastinal diffuse large B-cell lymphoma. (a) bcl-2 and (b) c-myc immunostains are positive. Cases with both of these markers positive are referred to as “double expressors”, but these findings do not necessarily correlate with the status of *BCL2* or *MYC* gene rearrangements

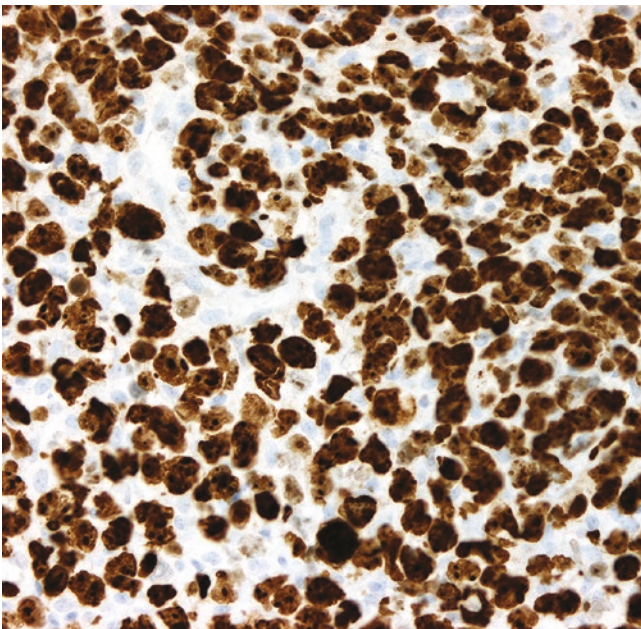


**Fig. 8.53** Mediastinal diffuse large B-cell lymphoma. High Ki-67 proliferation index

**Molecular Findings** A full description of all the findings present in DLBCL are out of the scope of this chapter. Mediastinal DLBCL is likely to harbor similar alterations as those cases outside the mediastinum, however, no studies are available for cases confined to the mediastinum. DLBCL most common alteration includes rearrangement of *BCL6* (~30%), followed by that of *BCL2* (~20%) and *MYC* (~10%). Cases that show *MYC*, *BCL2*, and/or *BCL6* gene rearrangements, also known as “double-hit” or “triple-hit” lymphomas, have a very bad prognosis [138], but the frequency of these cases in the mediastinum is uncertain. Detection of *MYC* and *BCL2* rearrangements by FISH (“double hit” DLBCL) is not interchangeable with “double expressor” DLBCL. In fact, there is a poor correlation between the FISH findings and immunohistochemical results for these two markers. The novel LymphGen classification stratifies DLBCL into subgroups based on molecular abnormalities identified by depth genomic analysis. Using this classification, GCB-like DLBCLs commonly express *BCL6* and *EZH2* genes and demonstrate alterations in PIK3 signaling, cell migration, and immune cell interactions, whereas non-GCB/ABC-like DLBCLs harbor alterations in chronic B-cell receptor signaling (*MYD88*, *CD79B*) and activation of the NF- $\kappa$ B signaling [139].

## **B-Cell Lymphoma, Unclassifiable, with Features Intermediate Between Diffuse Large B-Cell Lymphoma and Classic Hodgkin Lymphoma/Mediastinal Gray Zone Lymphoma (M-GZL)**

**Introduction** Some of the first reports of unusual lymphoma cases with intermediate morphologic and immunophenotypic features between DLBCL and CHL were done around 2005 [140, 141]. However, it was not until 2008 when this entity was incorporated as a provisional entity into the World Health Organization (WHO) classification of hematopoietic and lymphoid tumors with the following definition: a B-cell lymphoma demonstrating overlapping clinical, morphological, and/or immunophenotypic features between CHL and DLBCL, especially PM-LBCL [142]. In the most recent WHO classification from 2017, the definition of M-GZL has been refined to say that “CHL and DLBCL refer especially to nodular sclerosis CHL and PM-LBCL” [143]. As per the WHO, composite lymphomas with separate areas of PM-LBCL or DLBCL and CHL, and cases of CHL that recur as PM-LBCL should not be included in this category [143, 144]. The incidence of M-GZL is unknown, but overall, this is an extremely rare disease [145]. Its incidence is directly related to the confidence of a pathologist to make this diagnosis, and this subjectivity in interpretation appears to be a consequence of the lack of consistent diagnostic features. The existence of an anterior mediastinal lymphoma with intermediate features between PM-LBCL and CHL suggests a common origin and/or shared pathogenesis of these two lymphoproliferative disorders.

**Clinical Features** Clinically, M-GZL cannot be distinguished from CHL or PM-LBCL, with the only difference being that M-GZL is more common in men rather than women. Some studies have shown that M-GZL may be more aggressive than CHL and it appears that M-GZL has a better response to dose-intensive chemotherapy regimens [145–148].

**Pathology** There are no gross features that distinguish this tumor apart from PM-LBCL or CHL. Microscopically, the tumor can resemble PM-LBCL, CHL, or have a combined morphology, reminiscent of DLBCL with Reed-Sternberg-like cells, T-cell/histiocyte-rich LBCL, the syncytial variant of nodular sclerosis CHL, or anaplastic large cell lymphoma. Sclerosis may or may not be identified (Figs. 8.54 and 8.55).

**Immunohistochemistry and Other Ancillary Studies** Immunohistochemistry must be performed in order to suspect the diagnosis of M-GZL. Three possible scenarios of the presentation of M-GZL include [149]:

1. In about 65% of cases: Morphology of CHL (“CHL-like” GZL) with an immunophenotype of DLBCL or PM-LBCL. The HRS cells are positive for CD45, strongly positive for >1 B-cell marker, with variable or negative CD30 and/or CD15 (Fig. 8.54).
2. In about 30% of cases: morphology of PM-LBCL or DLBCL (“LBCL-like” GZL) with the immunophenotype of CHL. The lymphoma cells are positive for CD30 and CD15, variable or negative for CD45, >1 variable or negative B-cell marker, and variable or negative for MUM1 (Fig. 8.55).
3. In about 5% of cases: Morphology and immunohistochemistry overlap or do not fit in the above scenarios. This group allows for extreme variability and a subjective interpretation.

**Differential Diagnosis** As the name implies, M-GZL needs to be distinguished from PM-LBCL, DLBCL, and CHL but this can be challenging, particularly in a core biopsy (see Table 8.10). Moreover, the same list of differential diagnoses for PM-LBCL and CHL should be excluded before attempting to make this diagnosis (see corresponding sections). An immunohistochemistry-based scoring method has been proposed as a potential reproducible tool to favor a diagnosis of M-GZL over CHL or DLBCL [150]. CD20, CD45, MUM1, PAX5, OCT2, BOB.1, and EBER are given a positive or negative numeric value and the sum of all points is calculated. A positive value is in favor of CHL whereas a negative one favors DLBCL. A neutral value (0 or closer to zero) supports M-GZL [150].

Cases of nodular sclerosis CHL that relapse as a tumor with features closer to PM-LBCL should not be called M-GZL [143]. A multi-institutional study from 2017 with a centralized pathology review by expert hematopathologists showed that close to 40% of diagnosed M-GZLs (26/68 cases) were reclassified mostly as nodular sclerosis CHL grade 1 and 2, confirming the lack of consistent diagnostic features for this uncommon tumor [151]. It is strongly recommended to consult a case of possible M-GZL with a hematopathologist.

**Molecular Findings** M-GZL and PM-LBCL share similar genetic and molecular alterations, namely, abnormalities in 9p24 (the locus of *JAK2* and *PDCD1LG2* genes) and rearrangement of 16p13 (the locus of *CIITA*). Other abnormalities include gains of 8q24 (*MYC*) and amplification of 2p16 (*REL/BCL11A*) [96, 143].

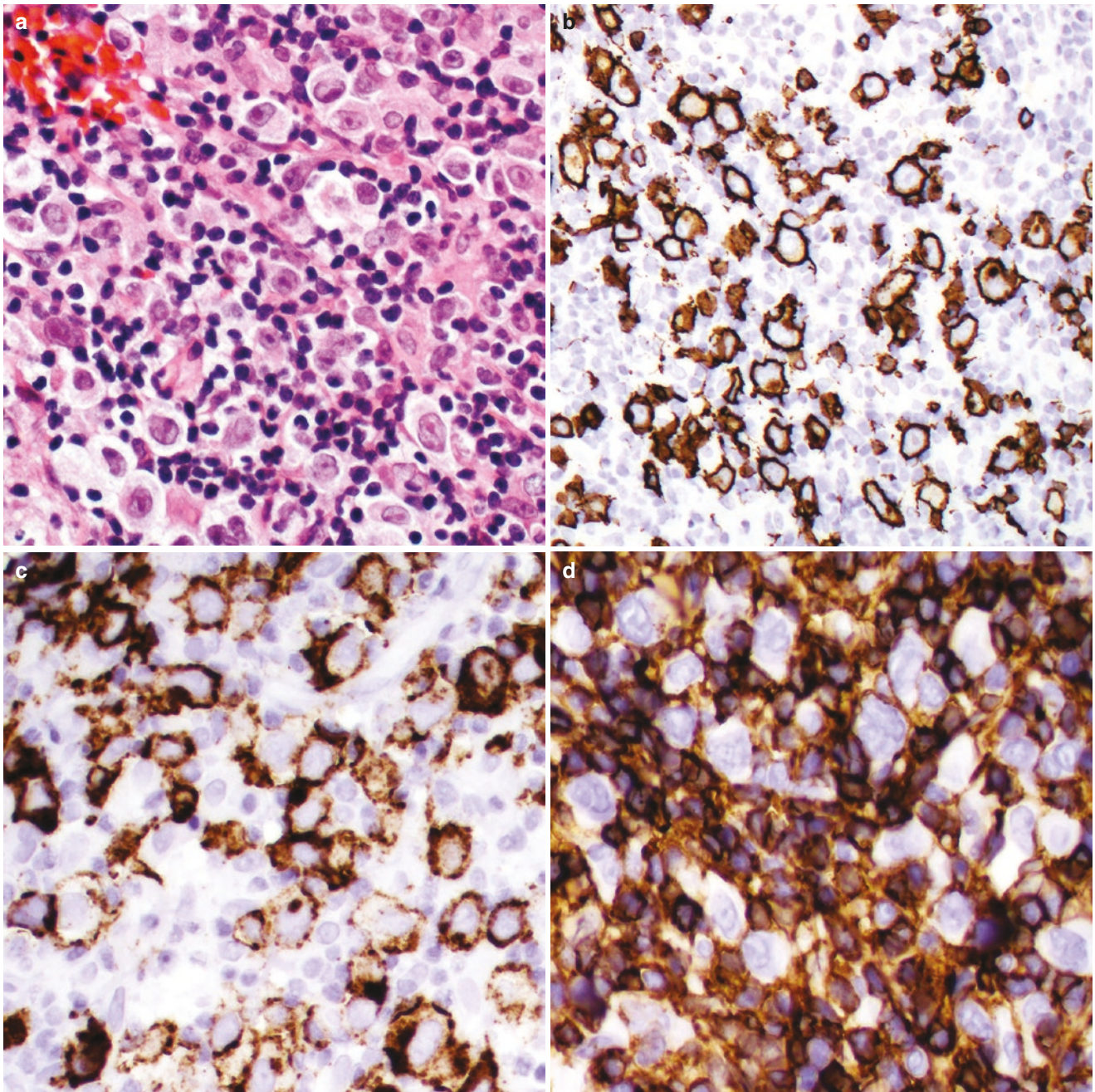


**Fig. 8.54** Mediastinal gray zone lymphoma, “classic Hodgkin lymphoma-like” variant. (a) Scattered large atypical lymphoid cells within an inflammatory background. The large lymphoma cells are

positive for (b) CD20, (c) CD30, and (d) CD45. PAX5 was strong and CD15 was variable (not shown)

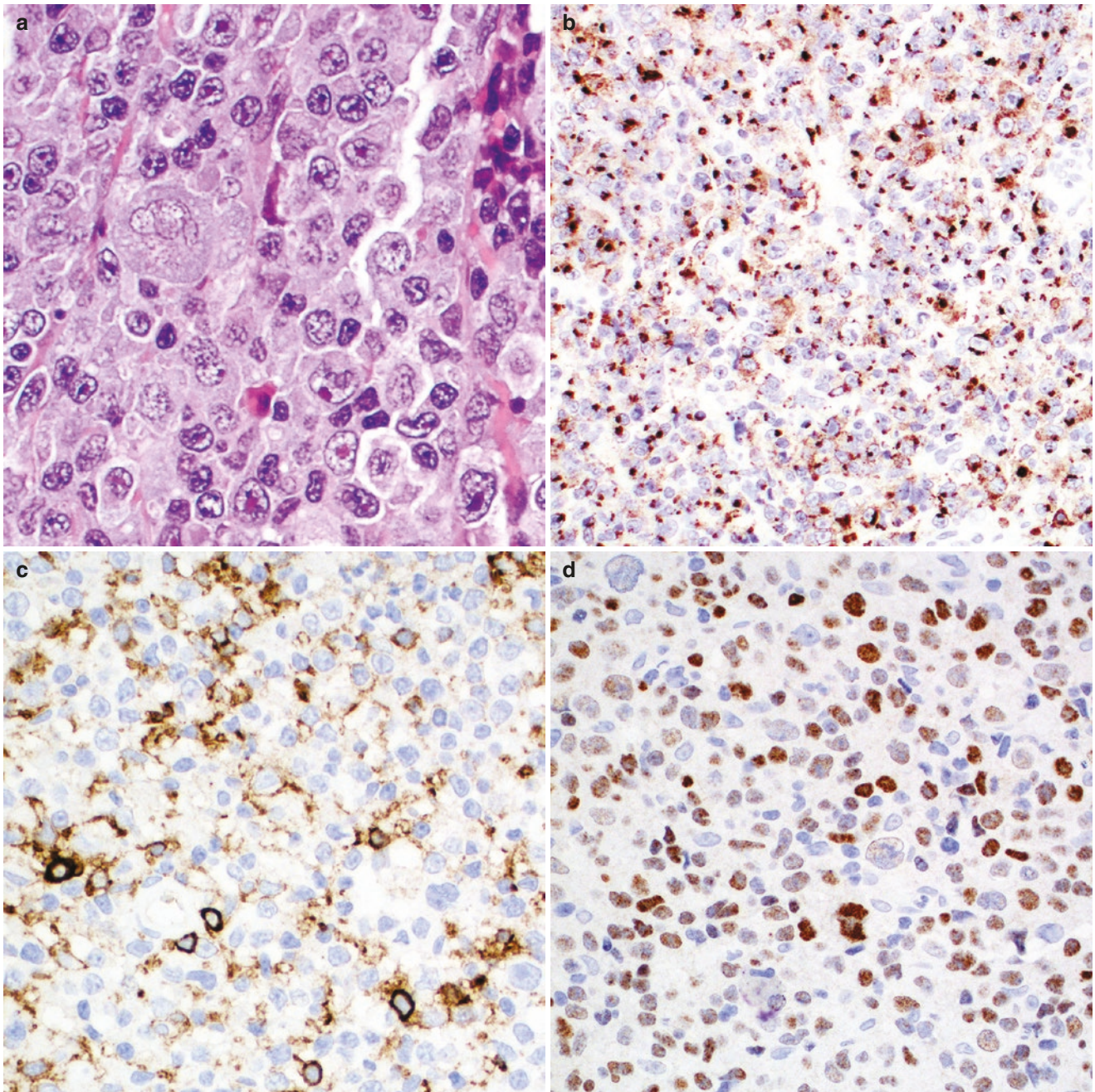


**Fig. 8.55** Mediastinal gray zone lymphoma, “diffuse large cell lymphoma-like” variant. (a) Sheets of large lymphoma cells with scattered Reed-Sternberg-like cells. The majority of these cells are positive

for (b) CD15, (c) weakly positive to negative for CD45, and positive for (d) OCT2. These cells were strongly positive for CD20 and weak to negative for CD30 (not shown)

## Thymic Marginal Zone Lymphoma of the Mucosa-Associated Lymphoid Tissue (Thymic MALT Lymphoma)

**Introduction** Marginal zone lymphoma of the mucosa-associated lymphoid tissue (MZL or MALT lymphoma) was originally described in 1983 by P. Isaacson and D. Wright as a low-grade lymphoma that involved the gastrointestinal tract [152]. The term MALT was coined due to its morphologic resemblance to “normal” MALT, namely, Peyer patches and the Waldeyer ring. Since then, MALT lymphoma has been recognized in several other organs, including the thymus, but involvement of this organ is very rare. The description of thymic MALT lymphoma was done in 1990 by P. Isaacson and colleagues [153] and 2 years later by Takagi and colleagues [154]. They described a thymic lymphoma that showed a striking resemblance to myoepithelial sialadenitis.

It is uncertain if thymic MALT lymphoma originates from “asteroid” B-cells or marginal zone B-cells that populate the thymus after a persistent and long-standing inflammatory process. In 2012, A. Weissferdt and C. Moran described an unusual subtype of thymic hyperplasia with lymphoepithelial sialadenitis (LESA)-like features and hypothesized that this could represent the precursor lesion of thymic MALT lymphoma [155]. This idea is concordant with the original theory suggested by Isaacson in his first description of the disease. Importantly, a recent study has found that LESA-like thymic hyperplasia has a strong association with thymic MALT lymphoma and non-myasthenic autoimmune disorders adding weight to the hypothesis rendered by prior authors [156]. Up to date, no particular infectious agent has been associated with thymic MALT lymphoma.

**Clinical Features** The median age of presentation is 63 years, with a male to female ratio of 1:1. Thymic MALT lymphoma was considered a disease mostly occurring in Asia, but in recent years it has also been identified in Western countries [157–161]. Most patients have a history of Sjögren syndrome and less commonly of rheumatoid arthritis [157–164]. The clinical presentation ranges from no symptoms to fever, malaise, or chest pain. The disease is usually discovered incidentally in asymptomatic individuals. Superior vena cava syndrome is uncommon. Laboratory abnormalities include polyclonal hypergammaglobulinemia or serum IgA paraprotein [160]. Thymic involvement by MALT lymphoma may precede, occur concomitantly, or develop after a diagnosis of MALT lymphoma elsewhere [153, 157, 165–167]. The prognosis of thymic MALT lymphoma is excellent. Complete surgical resection is curative at least for those cases confined to the thymus. Good outcomes have also been observed in cases where low-dose chemotherapy has been used [162, 168].

**Pathology** Large resections of anterior mediastinal lesions are becoming less frequent and sampling is mostly accomplished via a thoracoscopic biopsy or an imaging-guided needle biopsy. On total resections, thymic MALT lymphoma has been described as a tan-white and often multicystic mass. The cysts may be empty or filled with serous fluid. A rim of residual thymus may or may not be identified at the periphery of the tumor. On microscopic examination, MALT lymphoma can present as a monotonous infiltrate almost entirely replacing the thymus (Figs. 8.56 and 8.57) or sometimes can give the impression of a reactive process due to the presence of reactive lymphoid follicles. MALT lymphoma is mostly composed of small lymphocytes, centrocyte-like cells, monocytoid cells, and variable proportion of mature plasma cells (Figs. 8.58 and 8.59). Scattered large lymphoid cells with immunoblastic or centroblastic features are also seen. When present, reactive lymphoid follicles tend to have conspicuous marginal zones with monocytoid cells encroaching into or “colonizing” the germinal centers. Residual thymic epithelium, epithelial-lined cysts, and Hassall corpuscles are commonly infiltrated by lymphoma cells forming lymphoepithelial lesions (Fig. 8.60). Some cysts contain eosinophilic proteinaceous debris, foamy macrophages, hemosiderin, cholesterol clefts, and cholesterol granulomas [153, 154, 160, 161]. Sclerosis is uncommon. Some cases of MALT lymphoma may show extensive plasmacytic differentiation as well as increased large cells; however, large cell transformation is very rare [158]. Concomitant crystal-

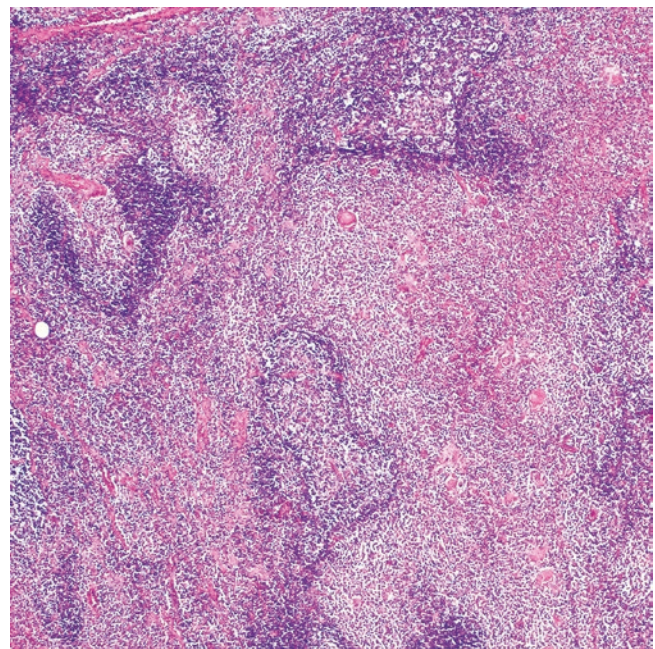


**Fig. 8.56** Thymic marginal zone lymphoma (thymic MALT lymphoma). A diffuse lymphoid process replaces the thymus. Occasional residual distorted lymphoid follicles and Hassall corpuscles are seen. Courtesy of Roberto N. Miranda, MD

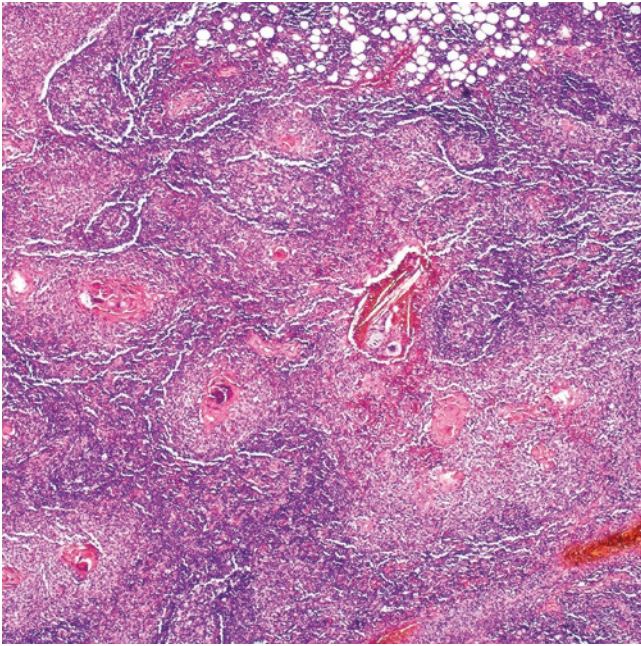


**Fig. 8.57** Thymic MALT lymphoma. Diffuse replacement of the thymus with extension into adjacent fat. Some residual Hassall corpuscles and cysts filled with blood, cholesterol clefts, and giant cells are seen. Courtesy of Roberto N. Miranda, MD

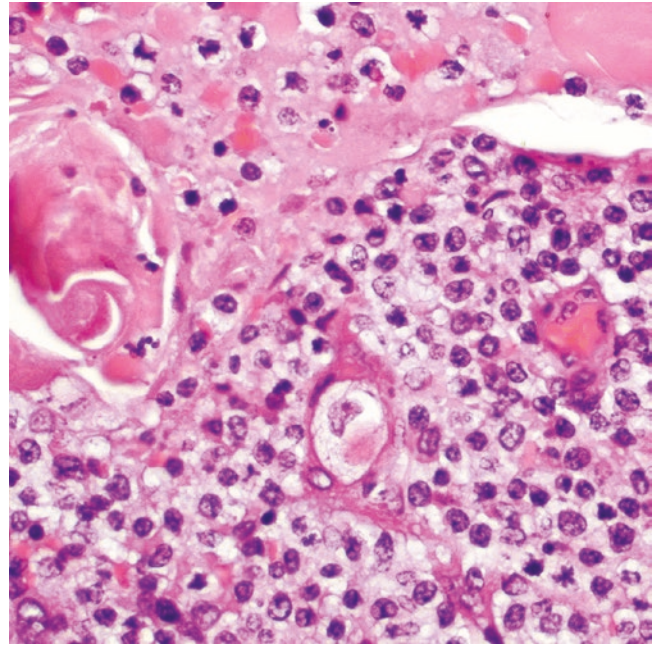


**Fig. 8.59** Thymic MALT lymphoma. Monocytoid lymphocytes around a Hassall corpuscle and a cystic space filled with proteinaceous debris

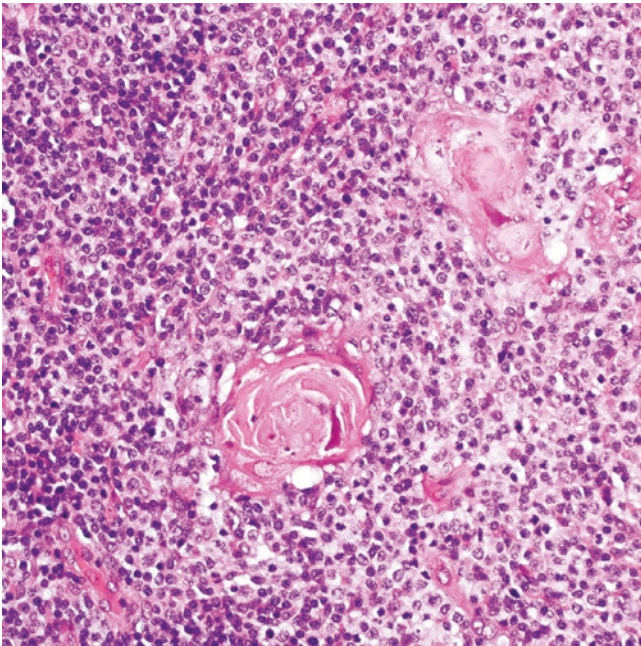


**Fig. 8.58** Thymic MALT lymphoma. The lymphoma cells infiltrate into Hassall corpuscles

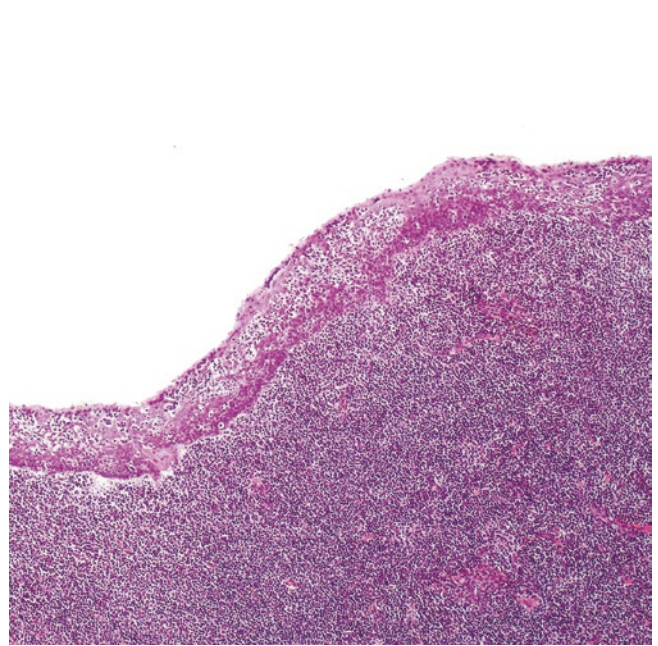


**Fig. 8.60** Epithelial cyst with lymphoepithelial lesions in thymic MALT lymphoma

storing histiocytosis has been reported in sporadic cases [163, 169]. In a recent study, a subset of thymic MALT lymphomas showed residual thymus with features of (LESA)-like thymic hyperplasia [156].

**Immunohistochemistry and Other Ancillary Studies** MALT lymphoma is a CD5-/CD10- B-cell lymphoma (CD20+/PAX5+), with primary thymic cases usually showing IgA positivity (Fig. 8.61). The neoplastic B-cells coexpress bcl-2 and in some cases also CD43 (Fig. 8.62). The lymphoma cells are negative for T-cell markers, CD23, bcl-6, LMO2, LEF1, and cyclin D1 (Fig. 8.63). Plasma cells are positive for CD138 and MUM1 and light chain restriction may or may not be identified, which is usually seen in cases with extensive plasmacytic differentiation. Residual germinal centers are positive for CD10, bcl-6, and the FDC markers CD21, CD23, and/or CD35 are useful to highlight disrupted FDC meshworks of “colonized” follicles (Fig. 8.64). CD20 highlights lymphoepithelial lesions while pan-cytokeratin decorates residual disrupted thymic epithelium, cysts linings, and entrapped Hassall corpuscles (Fig. 8.65). MALT lymphoma has a low Ki-67 proliferation index (<30%) with a high Ki-67 only seen in residual reactive germinal centers. If flow cytometry is performed, there is a population of CD5-/CD10- monotypic B-cells.

**Differential Diagnosis** Thymic MALT lymphoma should be distinguished from reactive inflammatory processes (thymic lymphoid hyperplasia, multilocular thymic cyst, and LESA-like thymic hyperplasia) and other small B-cell lymphomas involving thymus (small lymphocytic lymphoma,

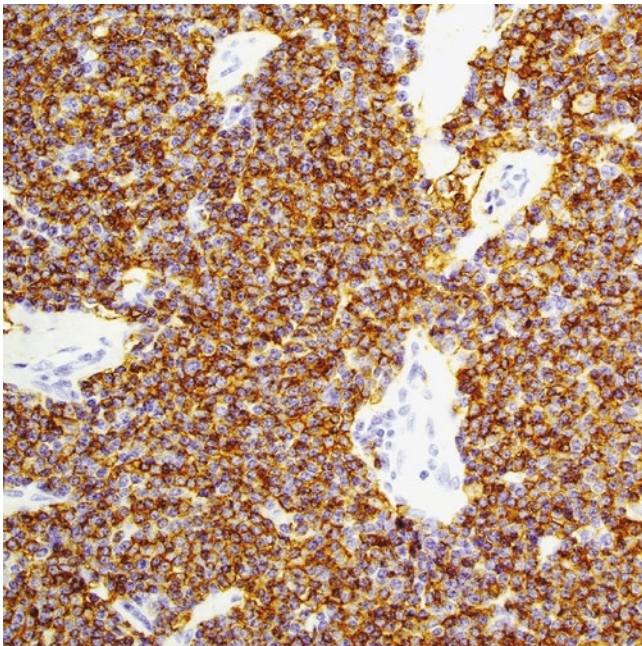


**Fig. 8.61** Thymic MALT lymphoma. Immunohistochemistry for CD20

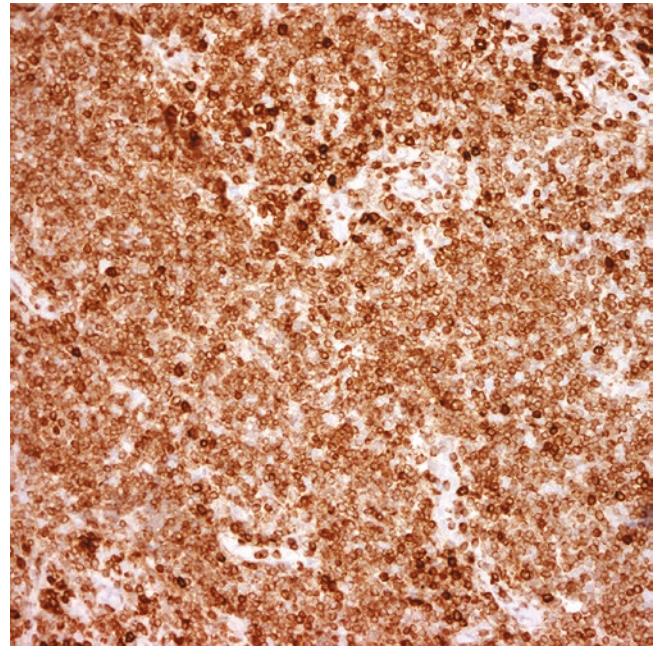


**Fig. 8.62** Thymic MALT lymphoma. Immunohistochemistry for bcl-2 shows aberrant expression of this marker in B-cells. The few scattered brightly positive bcl-2 lymphocytes are T-cells

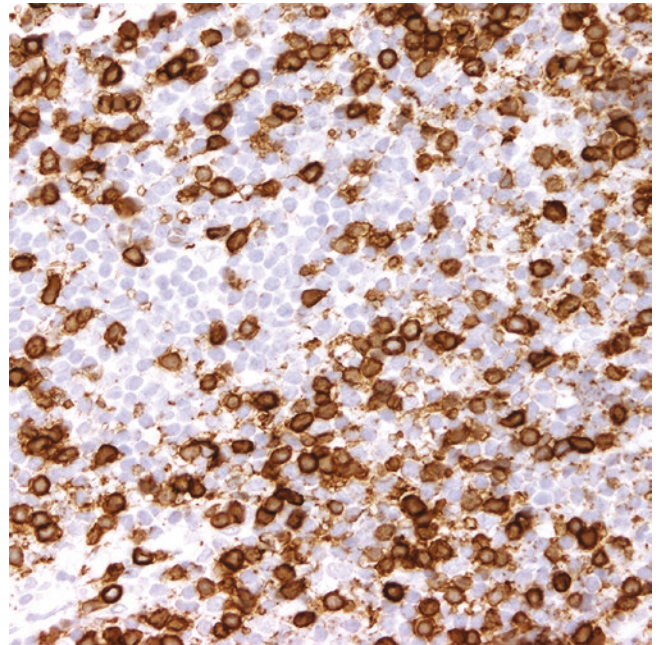


**Fig. 8.63** Thymic MALT lymphoma. Immunohistochemistry for CD3, negative in the lymphoma cells

follicular lymphoma, mantle cell lymphoma, lymphoplasmacytic lymphoma, and plasmacytoma). In a complete resection the diagnosis of MALT lymphoma is usually straightforward, and immunohistochemistry is only needed to confirm the immunophenotype; however, this may not be the case in a core biopsy where distinction from a reactive

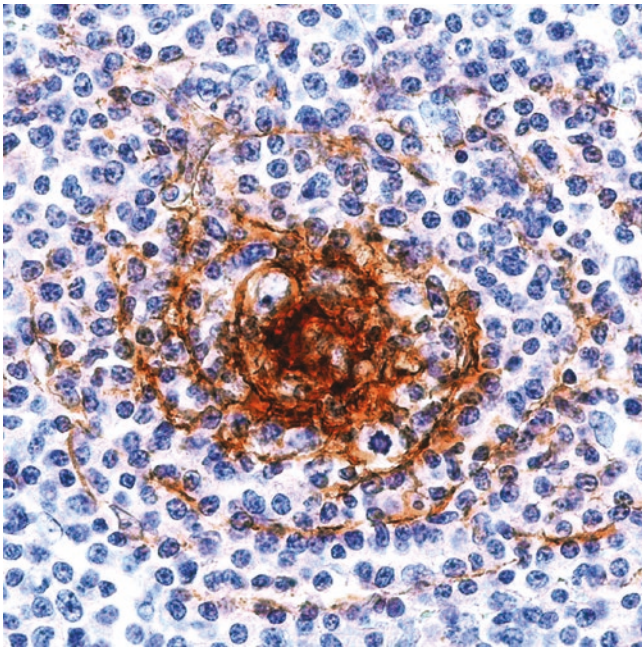


**Fig. 8.64** Thymic MALT lymphoma. Immunohistochemistry for CD21 highlights a residual distorted follicular dendritic cell meshwork

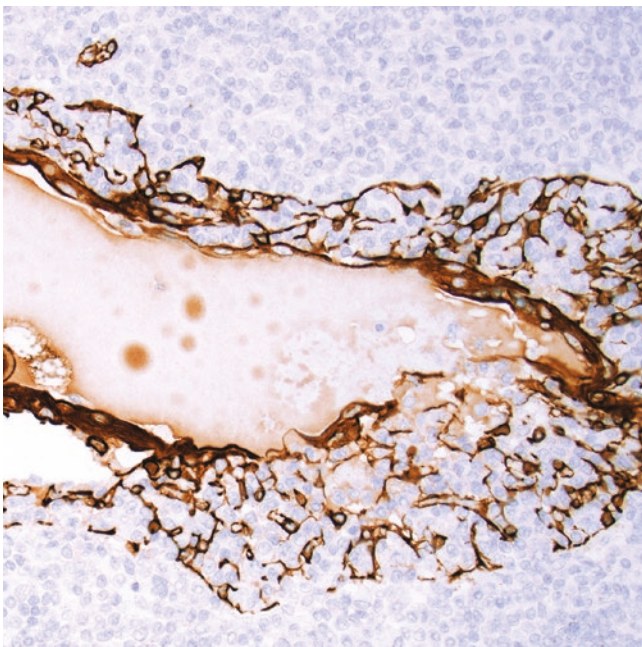


**Fig. 8.65** Thymic MALT lymphoma. Immunohistochemistry for pan-cytokeratin highlights epithelial-lined cysts and residual epithelial structures (lymphoepithelial lesions)

lymphoid process vs. another low-grade B-cell lymphoma may be more challenging. Flow cytometry is very useful in this last scenario, if available. Similarly, *IGH* gene rearrangement may be used to support a clonal process, but this result should never be interpreted without knowledge of the clinical context and the morphologic findings.

Reactive thymic lymphoid hyperplasia, multilocular thymic cyst, and LESA-like thymic hyperplasia distort but do not typically replace the thymic architecture. In the first two conditions, multiple reactive lymphoid follicles are seen, and there are no expanded marginal zones, “colonized” follicles, monocytoid cells, or lymphoepithelial lesions. In thymic hyperplasia with LESA-like features, there is proliferation of thymic epithelium and Hassall corpuscles, a feature that contrasts with the replacement of these structures in thymic MALT lymphoma [155]. In addition, immunohistochemical stains in all these conditions show normal compartmentalization of B-cells in lymphoid follicles and of T-cells in interfollicular areas and a T-cell predominance. No co-expression of *bcl-2* or *CD43* is seen in B-cells. Plasma cells are always polytypic. Keratin highlights attenuated epithelium and Hassall corpuscles but no disrupted epithelial structures.

Thymic involvement by any of the other small B-cell lymphomas is exceedingly rare in the thymus and the first consideration for a small B-cell lymphoma at this location should always be MALT lymphoma until proven otherwise. Morphological and immunohistochemical features and/or flow cytometry (monotypic B-cells) are helpful to confirm a diagnosis of small B-cell lymphoma. MALT lymphoma is a *CD5*<sup>-</sup>/*CD10*<sup>-</sup> B-cell lymphoma that is also negative for *bcl-6*, *LEF1*, *LMO2*, and *cyclin D1*. In contrast, small lymphocytic lymphoma is positive for *CD5*, *CD23*, *LEF1* and negative for *cyclin D1*; mantle cell lymphoma is positive for *CD5*, *cyclin D1* and usually negative for *CD23*; and follicular lymphoma is positive for *CD10* and *bcl-6*. MALT lymphoma with abundant “colonized” follicles may resemble follicular lymphoma but the immunophenotype is different to the one just mentioned. In challenging cases, detection of *t(14;18)* by FISH confirms follicular lymphoma. Lymphoplasmacytic lymphoma may pose a more challenging distinction from MALT lymphoma as this tumor is also *CD5*<sup>-</sup>/*CD10*<sup>-</sup>; however, the former shows striking morphologic differences with MALT lymphoma such as the lack of reactive or “colonized” follicles, lymphoepithelial lesions, and monocytoid cells. *MYD88 L265P* is a common mutation detected in lymphoplasmacytic lymphoma and this may be of use to support the diagnosis. Mediastinal plasmacytoma may mimic MALT lymphoma with extensive plasmacytic differentiation, but the former is exceedingly rare in the thymus. The presence of small lymphocytes, monocytoid cells, and reactive lymphoid follicles in addition to clonal plasma cells should point to the diagnosis of MALT lymphoma and not plasmacytoma. The differential diagnosis of thymic MALT lymphoma is summarized in Table 8.11.

**Molecular Findings** Thymic MALT lymphomas do not carry any of the translocations seen in other extranodal MALT lymphomas [170–172]. Trisomy 3 or gain of chromosome 18 have

**Table 8.11** Differential diagnosis of primary thymic marginal zone lymphoma of the mucosa-associated lymphoid tissue (MALT lymphoma, CD5-/CD10-)

Reactive conditions
Thymic lymphoid hyperplasia
Multilocular thymic cyst
Lymphoepithelial sialoadenitis (LESA)-like thymic hyperplasia (possible precursor lesion of thymic MALT lymphoma)
Neoplastic conditions (thymic involvement extremely uncommon)
Chronic lymphocytic leukemia/small lymphocytic lymphoma (CD5+, CD23+, cyclin D1-)
Mantle cell lymphoma (CD5+, CD23-/+, cyclin D1+)
Follicular lymphoma (CD10+, bcl6+)
Lymphoplasmacytic lymphoma (CD5-/CD10-, >90% of cases MYD88 L265P)
Plasmacytoma (with cases of MALT lymphoma with extensive plasmacytic differentiation)

been found in some cases [157, 167, 170–174]. Clonal *IGH* with a bias toward V(H)3–23 and V(H)3–30 have been identified in cases of thymic MALT lymphoma [175], which suggests that specific antigens play a role in its pathogenesis. One study has reported frequent methylation of the tumor suppressor genes *DAPK1*, *CDH1*, *TIMP3*, and *p14(ARF)* [176].

## Mediastinal Plasmacytoma

**Introduction** Primary mediastinal extramedullary plasmacytoma is very rare, with some cases preceding plasma cell myeloma for few months or even years [177–183]. Primary osseous plasmacytoma is not discussed here.

**Clinical Features** Mediastinal plasmacytoma affects adults (age range, 40–80 years). Clinical symptoms described include chest pain, back pain, and dyspnea [177–183]. Sporadic cases may present with a pleural effusion or primary hyperparathyroidism [178]. Plasmacytoma has been reported in all mediastinal compartments without a particular preferential location. Laboratory studies may or may not detect a serum M-protein at diagnosis [177–183].

**Pathology** Gross descriptions of mediastinal plasmacytoma are not available given its rarity. Microscopically, the tumor is composed of sheets of mature-appearing plasma cells that efface the involved tissue (Fig. 8.66). Scattered plasma cells with prominent nucleolus or few pleomorphic forms may or may not be present. Cytoplasmic spherical eosinophilic deposits of immunoglobulin (Russell bodies) or intranuclear eosinophilic immunoglobulin inclusions (Dutcher bodies) are

variably seen. Mitoses may be observed but apoptotic bodies are uncommon, unless the tumor exhibits high-grade features. The latter include significant pleomorphic forms or a blastic morphology. In some instances, plasmacytoma can show a nested or organoid arrangement similar to that of neuroendocrine carcinomas (Fig. 8.67). A sclerotic background may or

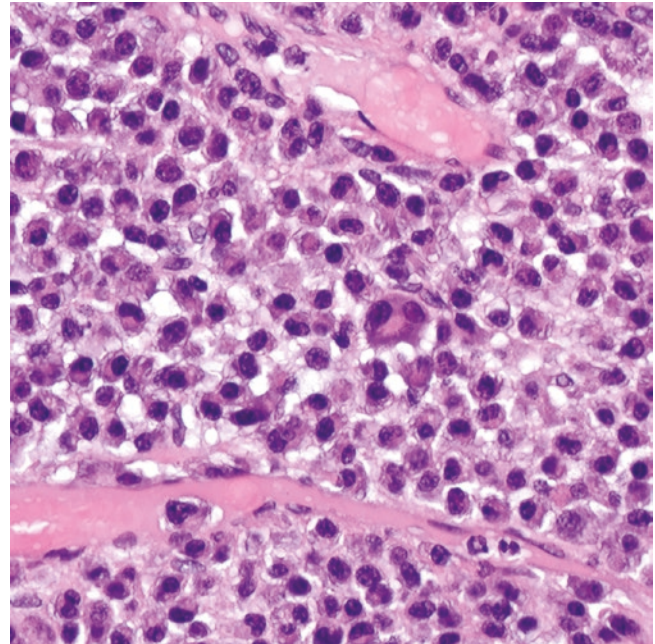


**Fig. 8.66** Posterior mediastinal plasmacytoma. Sheets of mature-appearing plasma cells with occasional binucleated form with prominent nucleoli

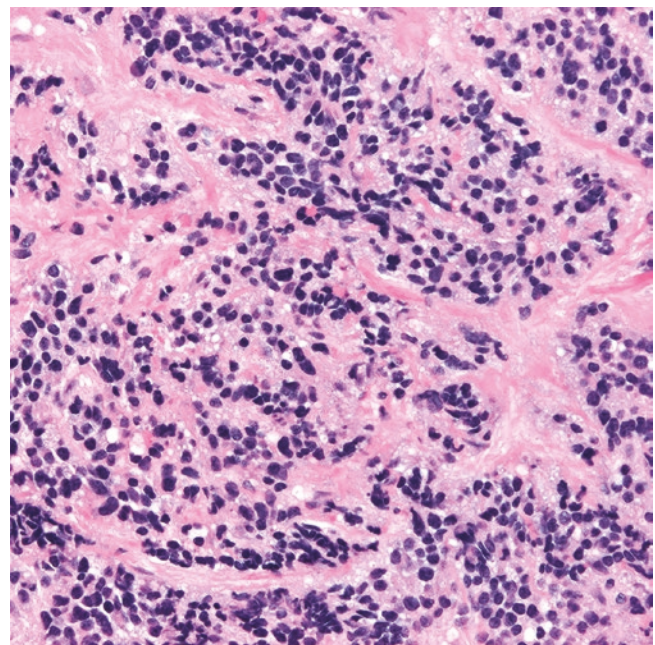


**Fig. 8.67** Mediastinal plasmacytoma with a nested or organoid pattern reminiscent of a neuroendocrine carcinoma

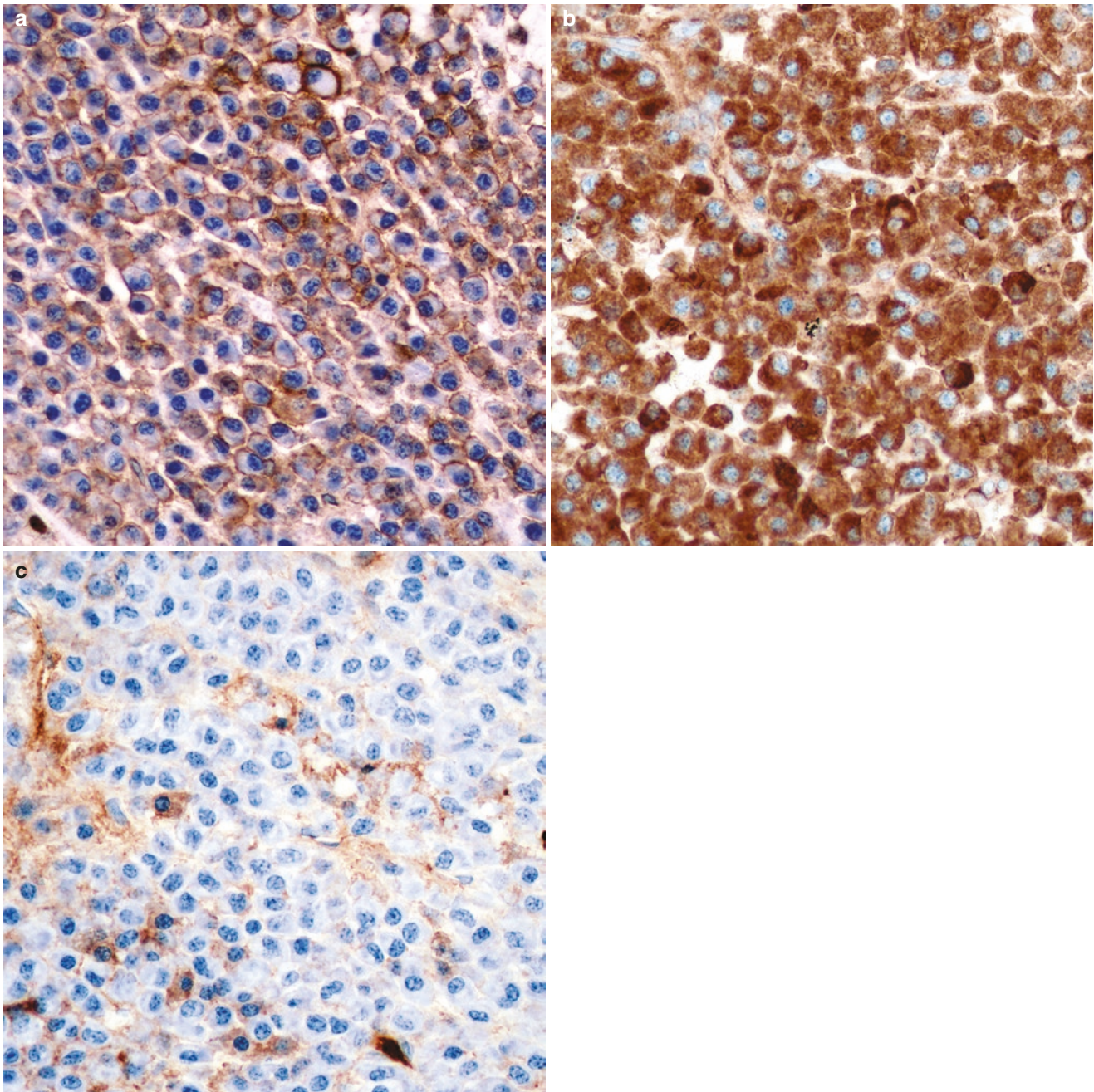


**Fig. 8.68** Mediastinal plasmacytoma, immunohistochemistry is positive for (a) CD138 and (b) kappa light chain, and negative for (c) lambda light chain

may not be present, and some cases may be accompanied by amyloid deposits. Nodal involvement may be partial or diffuse.

**Immunohistochemistry and Other Ancillary Studies** Neoplastic plasma cells are positive for CD138, CD79a, and MUM1, restricted for either kappa or lambda light chain, and frequently show aberrant CD117 and/or CD56, whereas they are weakly positive or negative for CD20, PAX5,

and CD45 (Fig. 8.68). They are negative for T-cell markers, keratins, melanoma markers, or neuroendocrine markers. Rare cases of plasmacytoma may show focal expression of T-cell markers as well as focal paranuclear dot expression of keratin (usually CAM5.2). EBER ISH is negative. Flow cytometry is extremely useful for diagnosis. Plasma cells can be assessed for the presence of a monotypic light chain and the expression of bright CD38 and CD138, CD56, and CD117. With this method, diminished expression or loss of CD19, CD45, CD27, and CD81 supports an aberrant plasma cell immunophenotype.

**Differential Diagnosis** Tumors mainly composed of mature-appearing plasma cells need to be distinguished from chronic lymphoplasmacytic inflammation, IgG4-related disease, and plasma cell-rich Castleman disease. All these processes show polytypic plasma cells that excludes plasmacytoma. In addition, there is lack of aberrant CD117 and/or CD56. The clinical presentation of a solitary mass is also different from the symptoms seen in IgG4-related disease, and plasma cell-rich Castleman disease (see corresponding sections). Mediastinal plasmacytoma may mimic MALT lymphoma with extensive plasmacytic differentiation. The presence of small lymphocytes, monocytoid cells, and reactive lymphoid follicles in addition to clonal plasma cells should point to the diagnosis of MALT lymphoma and not plasmacytoma.

A mediastinal plasmacytoma with intermediate or high-grade features needs to be distinguished from carcinoma, melanoma, neuroendocrine carcinoma, parathyroid carcinoma, or medullary thyroid carcinoma involving the mediastinum. Detection of CD138 or MUM1 is not sufficient to diagnose plasmacytoma, since carcinomas are also positive for CD138, and melanoma is positive for MUM1. The addition of keratins, melanoma markers, neuroendocrine markers, parathyroid hormone, and kappa and lambda light chains may be required to confirm or exclude plasmacytoma. Expression of CD56 in a tumor that has nested or organoid arrangement should not be diagnosed as a neuroendocrine carcinoma until positivity for keratins and neuroendocrine markers is confirmed, since plasmacytoma can also show these two characteristics. The differential diagnosis of mediastinal plasmacytoma is summarized in Table 8.12.

**Molecular Findings** Mediastinal plasmacytoma most likely exhibits the same molecular alterations as extramedullary plasmacytomas at other sites or as plasma cell myeloma. In a study of 38 extramedullary plasmacytomas, chromosomal gains were the most common cytogenetic abnormality (82%), followed by loss of 13q (40%) [184]. In addition,

about 40% of cases showed *IGH* breaks, 16% harbor the t(4;14), but no t(11;14), t(14;16), t(8;14), or *MALT1*, *BCL6*, or *FOXP1* rearrangements were detected. Based on these findings, this study concluded that extramedullary plasmacytoma and plasma cell myeloma were closely related at the cytogenetic level, with some differences in the distribution of *IGH* translocation partners [184]. However, specific data for primary mediastinal plasmacytoma is lacking.

## Non-Hodgkin Lymphomas of T-Cell Origin

### T-Lymphoblastic Leukemia/Lymphoma (T-ALL/ LBL)

**Introduction** T-lymphoblastic leukemia/lymphoma (T-ALL/T-LBL) is the most common non-Hodgkin lymphoma arising in the anterior mediastinum (>80% of cases) [93, 185–188]. In older classification schemes (Rappaport-Kiel, Lukes-Collins), LBL was designated “malignant lymphoma, lymphoblastic type” and “convoluted” or “non-convoluted” LBL [116, 189–191]. With the advent of histochemical and immunohistochemical methods during the 1970s and 1980s, it was discovered that LBLs expressed the enzyme terminal deoxynucleotidyl transferase (TdT) and there were cases of both B- and T-cell lineage [191–195]. T-ALL/LBL recapitulates any of the stages of the T-cell maturation and capacitation process in the thymus and presents more frequently as lymphoma, namely, an anterior mediastinal mass (~85%) rather than as leukemia (~15%), in contrast to its B counterpart that rarely affects the mediastinum and has a common leukemic presentation. Cytogenetic and molecular analysis have shown recurrent translocations in the *TCR* genes located in chromosomes 7 and 14 that appear to have relevance for prognosis.

**Clinical Features** T-ALL/LBL occurs frequently in children and young adults (25% and 20% of cases, respectively) and only few cases occur in older individuals. The male to female ratio is 2:1. Although the disease presents in about 85% of cases as an anterior mediastinal mass, there may be or may not be concurrent involvement of the peripheral blood and bone marrow in up to 15% of cases, reason why the term T-ALL/LBL is recommended [94, 116, 195, 196]. The clinical presentation depends on the type of involvement: predominantly lymphoblastic vs. predominantly leukemic or combined. Most patients present with leukocytosis with circulating blasts (by WHO criterion >25% of WBC count), moderate cytopenias, and hepatosplenomegaly. Once a diagnosis of T-ALL is established, staging demonstrates the pres-

**Table 8.12** Differential diagnosis of mediastinal plasmacytoma

<b>Low-grade (well-differentiated) plasma cell neoplasm</b>
Inflammatory or reactive with polytypic plasmacytosis
IgG4-related disease
Marginal zone lymphoma of mucosa-associated lymphoid tissue (MALT lymphoma) with extensive plasmacytic differentiation
Ectopic parathyroid adenoma
Metastatic parathyroid carcinoma
Metastatic medullary thyroid carcinoma
<b>High-grade (poorly differentiated) plasma cell neoplasm</b>
Primary or metastatic poorly differentiated carcinoma, including neuroendocrine carcinoma
Metastatic amelanotic melanoma

ence of an anterior mediastinal mass on imaging. In contrast, other patients present with symptoms of superior vena cava syndrome, chest pain, and/or respiratory distress and an anterior mediastinal mass is discovered on imaging. These patients may or may not have peripheral blood and/or bone marrow involvement. For those patients without a leukemic presentation, the diagnosis is established in a core biopsy from the anterior mediastinal mass. Laboratory abnormalities include  $>1$  cytopenia and elevated lactate dehydrogenase.

In general, the prognosis of T-LBL is considered good in children, intermediate in young adults, and poor in older adults. In all groups, detection of anemia, bulky mediastinal disease, superior vena cava syndrome, pleural or pericardial effusions, bone marrow, and/or central nervous system involvement correlate with bad prognosis, whereas anemia alone is an important predictive factor in adults [197, 198]. Aggressive therapy with hyper-CVAD (cyclophosphamide, vincristine, adriamycin, dexamethasone plus additional methotrexate, and cytarabine) shows a good prognosis in children, intermediate prognosis in young adults, but poor outcomes for older individuals who may not be candidates for high-dose chemotherapy.

**Pathology** Large resections of anterior mediastinal lesions are becoming less frequent and sampling is mostly accomplished via a thoracoscopic biopsy or an imaging-guided needle biopsy. Grossly, T-LBL consists of a large tan-white mass with “fish-flesh” appearance, variable necrosis, and wide infiltration into adjacent structures

(Fig. 8.69). Microscopically, the tumor consists of sheets of small to intermediate monotonous cells with high nuclear-to-cytoplasmic ratio, oval to cleaved nucleus with finely speckled chromatin, and inconspicuous nucleolus (Fig. 8.70). There are abundant mitoses and apoptotic bodies and not uncommonly some areas may feature a starry-sky pattern. Necrosis is variable. When the tumor involves the thymus, there may be areas of fibrosis and residual thymic epithelium and/or Hassall corpuscles



**Fig. 8.69** T-lymphoblastic leukemia/lymphoma. Autopsy specimen of a young male that died suddenly and was found to have a large anterior mediastinal mass (shown here) and generalized lymphadenopathy. The thymus, adipose tissue, and attached pleura are diffusely involved by a tan-white to pale pink fleshy mass. Histopathology confirmed the diagnosis of T-lymphoblastic leukemia/lymphoma. Courtesy of Anna Tart, MD

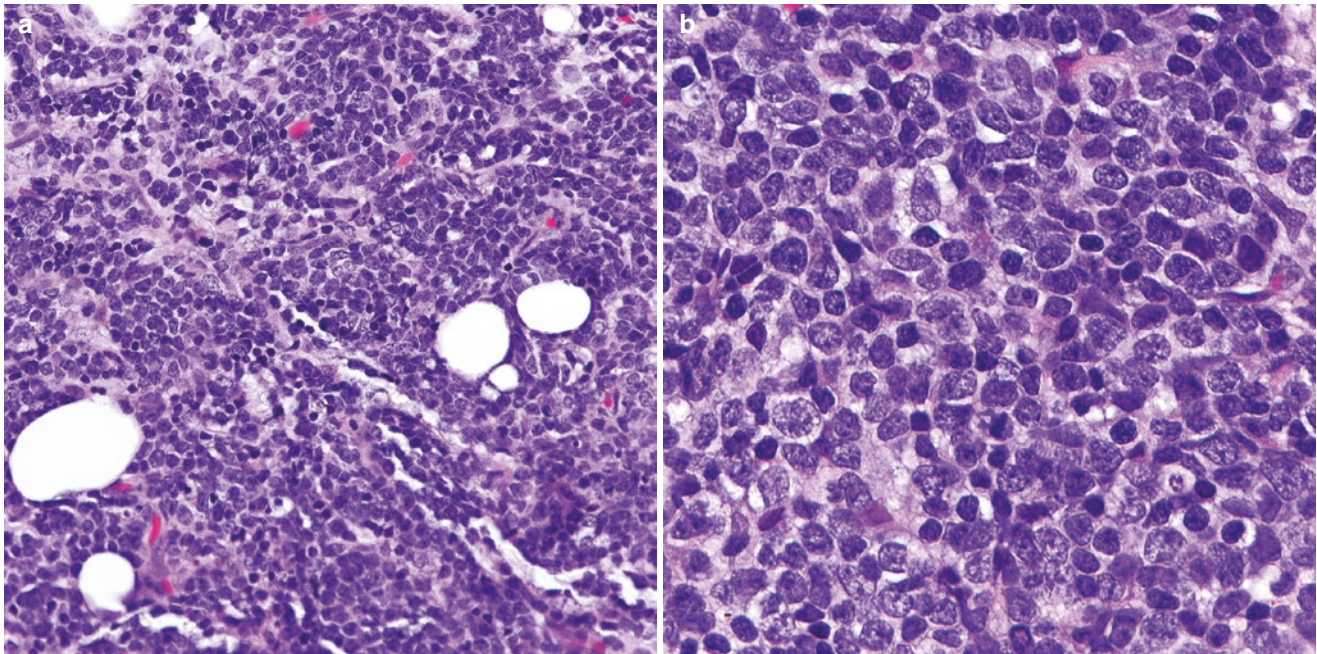


**Fig. 8.70** T-lymphoblastic leukemia/lymphoma. (a, b) Sheets of cells with high nuclear to cytoplasmic ratio and intermediate size replace adipose tissue in this biopsy from an anterior mediastinal mass

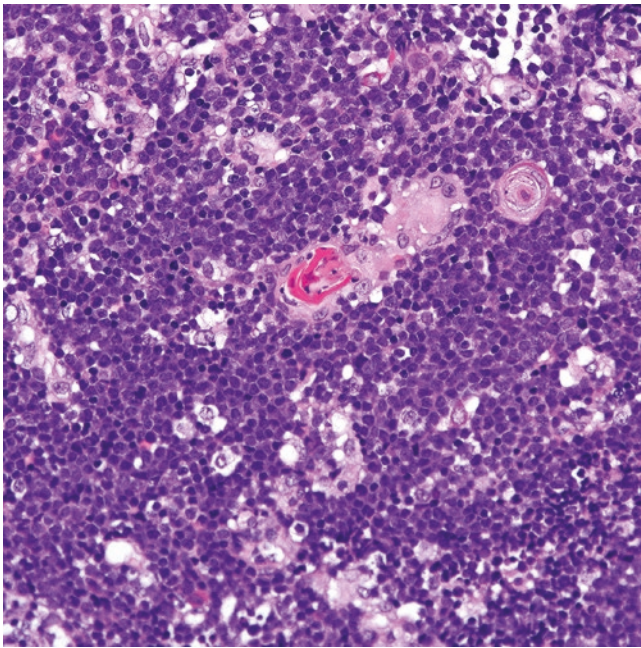


**Fig. 8.71** T-lymphoblastic leukemia/lymphoma infiltrating thymus. Residual Hassall corpuscles are seen (center)

(Fig. 8.71). Nodal involvement may be partial or diffuse, with partial involvement showing lymphoblasts in a paracortical distribution. Occasionally, T-ALL/LBL may demonstrate a pseudo-follicular pattern [199]. If a significant number of eosinophils or eosinophilic precursors are seen admixed with the lymphoblasts, the possibility of T-ALL/LBL arising in the setting of myeloid/lymphoid neoplasm with rearrangement of the *FGFR1* gene (8p11) should be considered [200–203]. On touch prep, needle-aspiration, pleural fluid, peripheral blood, or bone marrow aspirate smears, the lymphoblasts show anisocytosis with small, intermediate and large blasts, with round, cleaved or convoluted nucleus, small nucleolus, and scant to moderate amount of cytoplasm (Fig. 8.72). Cytoplasmic vacuoles are not common unless the patient has received prior treatment. Coarse cytoplasmic granules are seen in up to 10% of cases but Auer rods are not seen.

**Immunohistochemistry and Other Ancillary Studies** T-ALL/LBL recapitulates a particular stage of the T-cell maturation or capacitation that occurs in the thymus, namely, a pro T, pre T, cortical T, or medullary T-cell. These stages of maturation are best appreciated by flow cytometry.

- Pro T: weak CD45+, CD34+, CD117+, CD10+, CD7+, CD2-/-, CD5-/-, cytoplasmic CD3-/-, TdT+, CD1a-, surface CD3-, CD4-, and CD8- (double negative)
- Pre T: weak CD45+, CD34+/-, CD117+/-, CD2+/-, CD5+/-, CD10+/-, cytoplasmic CD3+/-, TdT+, CD4-/-, and CD8-/- (usually double negative), CD1a-/-, surface CD3-

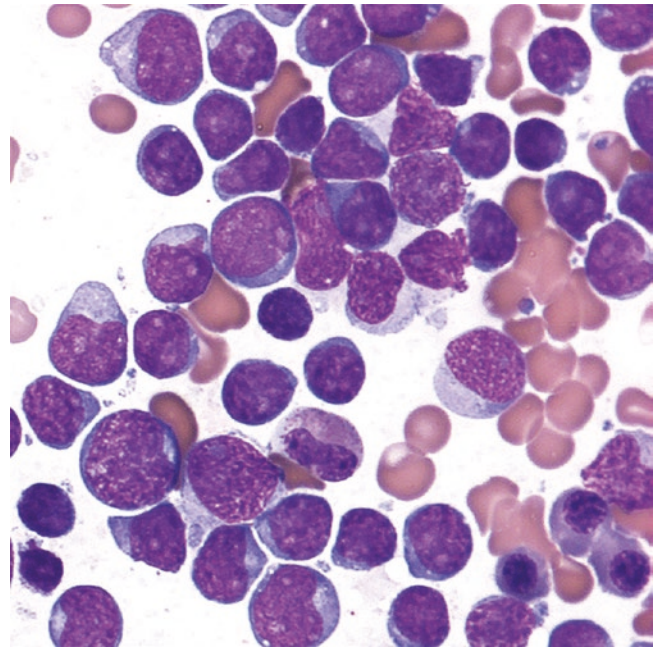


**Fig. 8.72** T-lymphoblastic leukemia/lymphoma. Bone marrow aspirate smear, Wright stain. T lymphoblasts have high nuclear to cytoplasmic ratio, fine chromatin, and variable nucleolus. Blasts are small, intermediate, and large (anisocytosis of blasts) with variable amount of cytoplasm

- Cortical T: variable CD45+, CD7+, CD2+, CD5+, cytoplasmic CD3+, CD1a+, surface CD3+/-, CD4+, and CD8+ (double positive), TdT+, CD10-, CD34-, CD117-
- Medullary T: CD45+, CD7+, CD2+, CD5+, cytoplasmic and surface CD3+, CD4+ or CD8+ (single positive), TdT-, CD10-, CD1a-, CD34-, CD117-

T-ALL/LBL can partially recapitulate any of these stages along with the presence of aberrancies in >1 marker. However, in some cases there may not be a significant difference from the normal maturation pattern. The majority of cases of T-ALL/LBL are TCR-A/B. Aberrant markers, such as CD13, CD33, and cytoplasmic CD79a may be seen in 10–30% of cases. CD19 and MPO are negative. A subtype of this neoplasm with an immunophenotype closer to the “pro T” stage (cytoplasmic CD3, weak CD5, >1 stem cell-associated markers CD34, CD117, HLA-DR, and/or myeloid-associated markers CD13, CD33, CD11b; negative CD1a and CD8) is known as “early T precursor ALL.” This particular variant has a genetic profile closer to acute myeloid leukemia and worse prognosis when compared to the rest of cases of T-ALL/LBL [204]. On paraffin-embedded tissue, T-LBL exhibits variable expression of TdT, CD1a, CD2, CD3, CD5, CD7, CD4 and CD8 (usually double positive), CD10, CD34, CD45, CD99, and CD117 (Figs. 8.73 and 8.74). CD79a may be focally positive in some cases, whereas PAX5, CD20, and MPO are negative. *c-myc* expression is seen in 30% of cases [205] and Ki-67 is high (>90%).

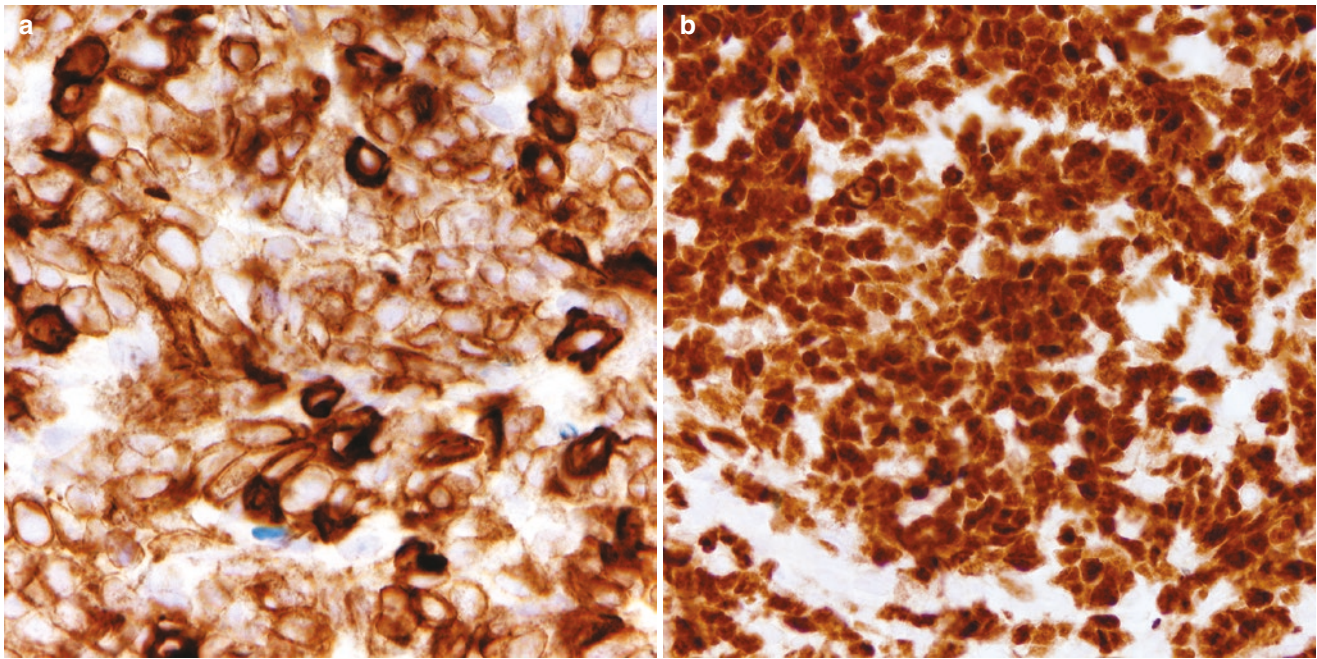


**Fig. 8.73** T-lymphoblastic leukemia/lymphoma. By immunohistochemistry, the blasts are positive for (a) CD3 (variable intensity) and (b) TdT

Cytokeratins, E-cadherin, p63, and/or p40 highlight residual entrapped thymic epithelium, if present (Fig. 8.75).

**Differential Diagnosis** When a mass is present in the anterior mediastinum, T-ALL/LBL should be distinguished from true thymic hyperplasia, thymic lymphoid hyperplasia, or lymphocyte-rich thymoma (WHO B1). On the other hand, small blue round cells tumors from hematopoietic and non-hematopoietic origin should be included in the differential diagnosis of T-ALL/LBL involving lymph nodes of the middle and posterior mediastinum.

Thymic hyperplasia or lymphocyte-rich thymoma usually do not pose a diagnostic problem in a large resection, but the distinction from T-ALL/LBL may be challenging in a core needle biopsy. This is particularly important since the treatment for thymic hyperplasia or lymphocyte-rich thymoma includes surgical resection, whereas T-ALL/LBL is treated with high-dose chemotherapy [206]. In thymic lymphoid hyperplasia, the architecture of the thymus is preserved, usually with cysts of variable size, and a brisk chronic inflammatory infiltrate with abundant reactive lymphoid follicles. Immunohistochemical stains are not usually needed, but the chronic inflammatory infiltrate shows a predominance of T-cells with a mature phenotype (CD10<sup>-</sup>, CD34<sup>-</sup>, TdT<sup>-</sup>, CD4<sup>></sup>CD8) and the reactive follicles are composed of B-cells. The germinal centers are positive for CD10, bcl-6, and negative for bcl-2. True thymic hyperplasia consists of normal thymus without proper involution for age. In this case, the thymus shows normal histology without any abnormal cyto-architectural features. Lymphocyte-rich thymoma grows as

large lobules separated by fibrosis, and there is preservation of the thymic organotypic features, namely, medullary differentiation and perivascular spaces with lymphocytes. Areas with predominant epithelial component may be seen (thymoma AB, B2, or B3), which are not features of T-ALL/LBL. By immunohistochemistry, the lymphoid component is double positive for CD4 and CD8, TdT<sup>+</sup>, CD34<sup>-</sup>, CD10<sup>-</sup>, with a high Ki-67, which shows some overlap with T-ALL/LBL, however, the morphology described above does not support LBL. Pan-cytokeratin, E-cadherin, p63, and/or p40 are extremely useful to highlight thymic epithelial structures in thymic hyperplasia and a prominent network of thymic epithelial cells in thymomas (Fig. 8.76). Rarely, thymomas can be negative for certain keratin, but these cases tend to show “monstrous cells” and do not resemble T-ALL/LBL [207]. The presence of abundant mitoses, apoptotic bodies, a starry sky pattern, and extensive infiltration to perithymic fat supports T-ALL/LBL and not thymic hyperplasia or lymphocyte-rich thymoma. Flow cytometry may prove useful to distinguish between T-ALL/LBL and normal thymocytes, but it is crucial to be aware that some cases of T-ALL/LBL may not feature significant aberrancies—or may be admixed with residual normal thymocytes—and this can pose a real problem for diagnosis by this method. It is recommended to not interpret flow cytometry performed in tissue from an anterior mediastinal mass without correlation with the corresponding morphology [206, 208–210].

Detection of an aberrant immature T-cell population by immunohistochemistry and/or flow cytometry in a mediastinal lymph node is not normal and in this situation the diagnosis of T-ALL/LBL is straightforward, particularly if the lymph

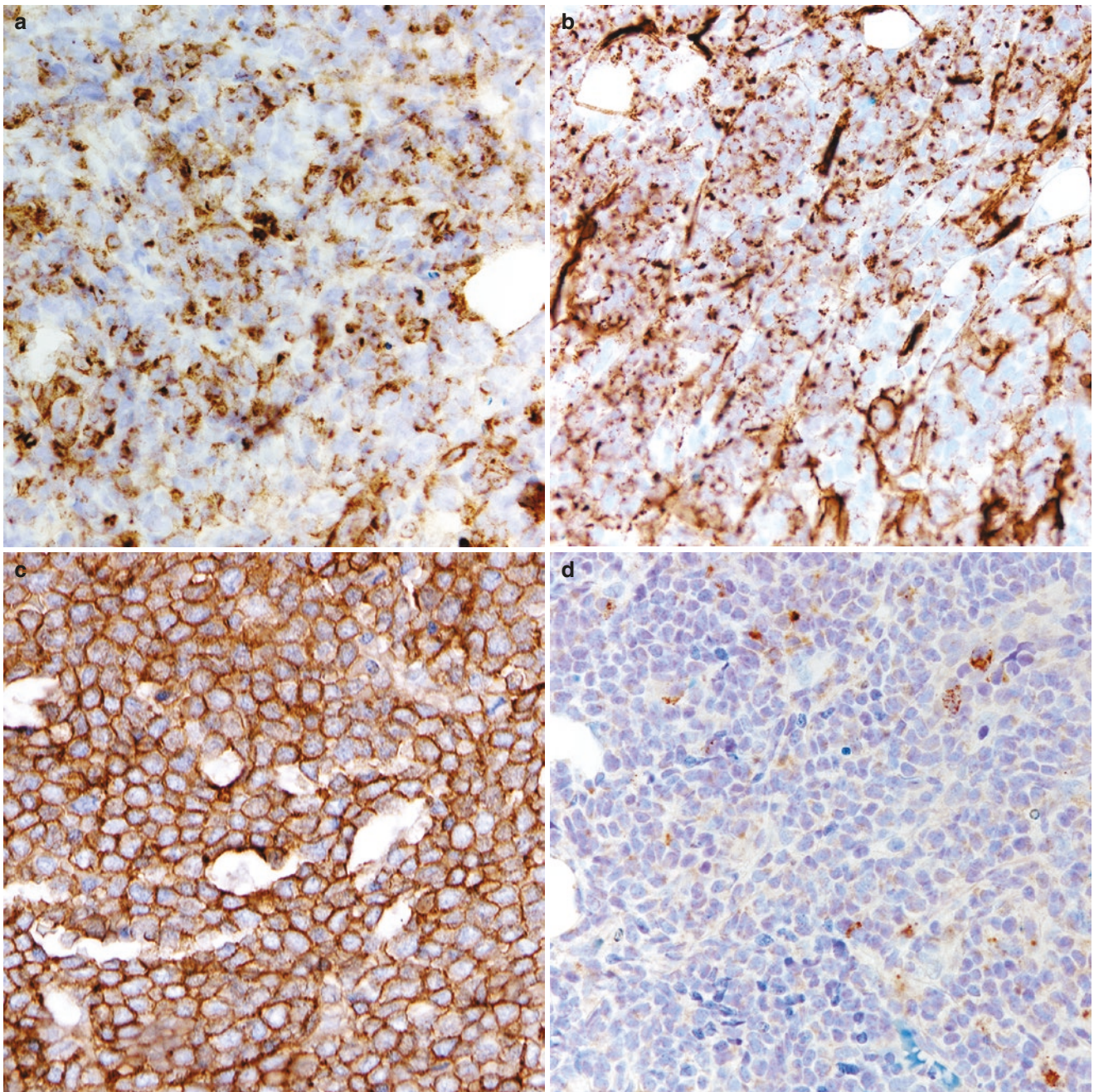


**Fig. 8.74** T-lymphoblasts are positive for (a) CD10 (variable), (b) CD34, and (c) CD99, and are negative for (d) myeloperoxidase

node shows significant or complete replacement of the architecture. The differential diagnosis in this context includes nodal involvement by angioimmunoblastic T-cell lymphoma, peripheral T-cell lymphoma, NOS, and T prolymphocytic leukemia. However, T-cell lymphomas are uncommon in children and do not typically involve mediastinal lymph nodes unless they there is widespread disease, which will be most probably already known at the time of mediastinal involvement. Although the immunophenotype of angioimmunoblastic T-cell lymphoma overlaps with T-ALL/LBL (CD3+, CD4+, CD10+), morphologically this T-cell lymphoma differs significantly from T-ALL/LBL by the presence of a poly-

morphic infiltrate with variable number of clear atypical cells, eosinophils, plasma cells, histiocytes, and prominent vascular proliferation. Peripheral T-cell lymphoma, NOS, can be easily distinguished from T-ALL/LBL also by morphology and by the lack of CD34, CD117, CD10, or TdT as well as by common loss of CD7, a marker that is only rarely absent in T-ALL/LBL. Nodal involvement by T prolymphocytic leukemia may resemble T-ALL/LBL morphologically (small monotonous immature-appearing lymphoid cells) and it may also feature some overlap by immunohistochemistry (double positive for CD4 and CD8), however, this neoplasm is positive for TCL1 and negative for TdT, CD34, and CD1a.

Other hematopoietic tumors that enter the differential diagnosis of T-ALL/LBL are B-ALL/LBL, blastoid mantle cell lymphoma, Burkitt lymphoma, and myeloid sarcoma. None of these neoplasms presents as an anterior mediastinal mass, however, they may present as mediastinal lymphadenopathy. B-ALL/LBL, mantle cell lymphoma, and Burkitt lymphoma are B-cell lymphomas and are easily distinguished

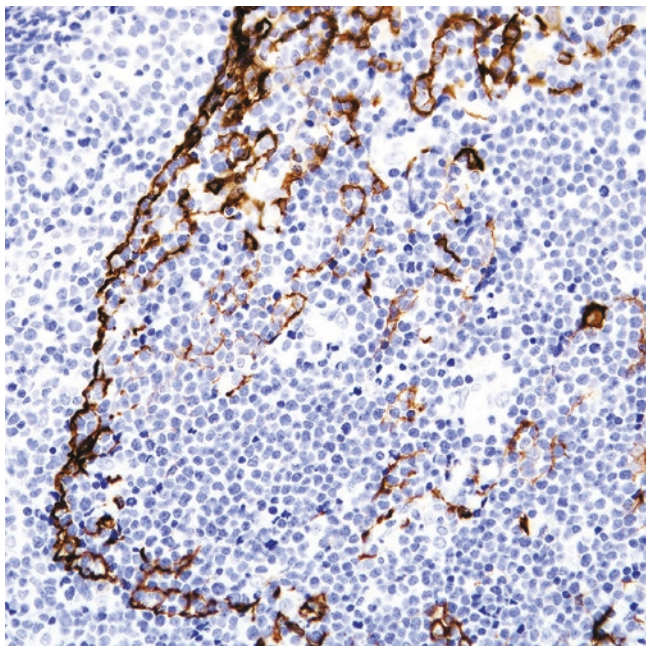


**Fig. 8.75** Disrupted thymic epithelium highlighted by the pan-cytokeratin immunostain in T-lymphoblastic leukemia/lymphoma

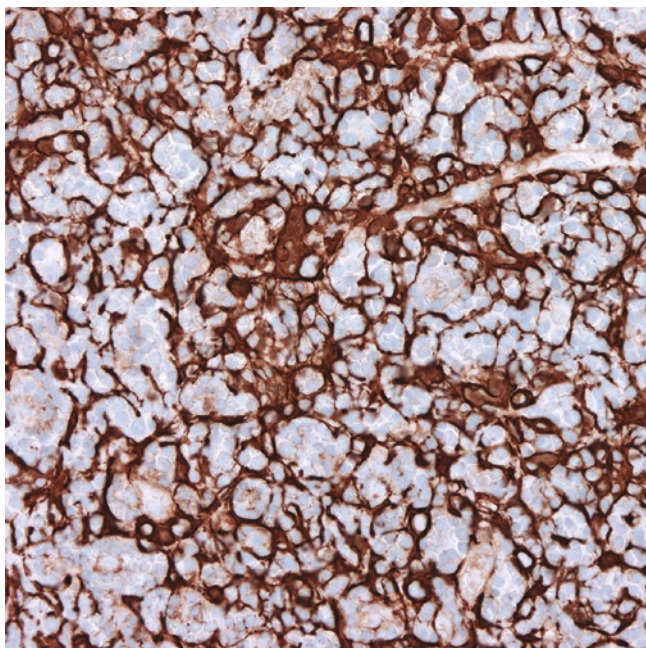


**Fig. 8.76** Lymphocyte-rich thymoma (WHO B1) with preservation of the epithelial architecture and showing a reticular ("lace-like") pattern, highlighted by pan-cytokeratin

**Table 8.13** Differential diagnosis of T-lymphoblastic leukemia/lymphoma

Needle core biopsy of an anterior mediastinal mass
<i>Hematopoietic or thymic-related</i>
True thymic hyperplasia, thymic lymphoid hyperplasia
Lymphocyte-rich thymoma (WHO B1)
B-cell lymphoma with high-grade or blastoid morphology:
B-lymphoblastic leukemia/lymphoma, blastoid mantle cell lymphoma, Burkitt lymphoma, high-grade diffuse large B-cell lymphoma
Mature T-cell lymphoma: T-cell lymphomas with T-follicular helper phenotype (CD4+, CD10+), peripheral T-cell lymphoma, NOS, T-prolymphocytic leukemia/lymphoma
<i>Non-hematopoietic or thymic-related</i>
Depending on the age of presentation, practically any small blue round cell tumor primary or metastatic to this region (see text)

from T-ALL/LBL after demonstration of B-cell differentiation. Myeloid sarcoma may mimic LBL morphologically and both tumors can express CD13, CD33, CD34, CD117, and TdT. Nevertheless, expression of MPO excludes T-ALL/LBL whereas expression of CD3 with/without additional T-cell markers excludes myeloid sarcoma.

Non-hematopoietic tumors that should be distinguished from T-ALL/LBL include primary or metastatic small blue round tumors to the mediastinum that vary on incidence depending on the age of presentation. In the pediatric population, tumors that should be considered include Ewing sarcoma, neuroblastoma, and embryonal rhabdomyosarcoma, whereas tumors that need to be considered in adults and the elderly include poorly differentiated carcinoma, small cell carcinoma, and neuroendocrine thymic carcinoma [205, 211]. All these tumors do not express hematopoietic antigens and can be readily distinguished from T-ALL/LBL with a proper set of immunohistochemical markers, namely, keratin, synaptophysin, chromogranin, FLI1, TTF1, desmin, and myogenin. A special consideration is NUT carcinoma that can present at any age and express CD34, which may lead to an erroneous interpretation of LBL. The differential diagnosis of T-ALL/LBL is summarized in Table 8.13.

**Molecular Findings** No specific molecular studies are available regarding mediastinal T-LBL and the following information refers to T-ALL/T-LBL in general. About 50% of T-ALL/LBLs show a normal karyotype whereas the rest demonstrate multiple cytogenetic abnormalities. Chromosomal alterations described in this disease include pseudodiploidy, deletions, and structural abnormalities involving 9q34 and t(9;17)(q34;q22–23). The latter appears to be more specific for T-LBL than for T-ALL [212]. Loss of heterozygosity of 9p has been associated with male gender and a tendency for favorable event-free survival [213]. T-ALL/LBL also harbors translocations involving the *TCR* genes (14q11.2 [*TCR alpha/delta*]; 7q35 [*TCR beta*]; 7p14 [*TCR gamma*]) with multiple partner genes [185, 186, 199]. These *TCR* gene-associated translocations have been divided into four groups, which include rearrangement with: (1) *TAL*

or *LMO2* genes; (2) *TLX1* (10q24) found in 7% of childhood and 30% of adult cases and associated with favorable prognosis; (3) *TLX3* (5q35) found in 20% of childhood and 15% adult cases, and (4) *HOXA* gene [199, 214, 215]. Other set of mutations that are frequently detected in T-ALL/LBL (50–60% of cases) are activating mutations of *NOTCH1* and *FBXW7*, which confer a favorable prognosis and open an opportunity for targeted therapies [185, 186, 199, 214].

## Anaplastic Large Cell Lymphoma (ALCL)

**Introduction** Before the advent of immunohistochemistry, ALCL was first recognized as “histiocytic lymphoma.” In 1985, Stein and cols. discovered that this tumor was a subtype of T-cell lymphoma that expressed CD30 or Ki-1, hence the term “Ki-1 antigen-positive LCL” [216]. Later in the mid-1990s it was discovered that a subset of ALCLs harbor rearrangements of the anaplastic lymphoma kinase-1 (ALK-1), a molecule that has been pivotal in the understanding of tumorigenesis and cancer molecular biology [217–220]. Mediastinal ALCL is very rare [103, 221–224].

**Clinical Features** Reported cases of mediastinal ALCL have been described in children or young adults. Patients may be asymptomatic and a mediastinal mass is discovered incidentally for other reasons, while other patients may present with chest pain, dyspnea, or systemic symptoms [103, 221, 224]. In the pediatric population, ALCL is not infrequently the underlying etiology of the systemic inflammatory process known as hemophagocytic lymphohistiocytosis (HLH) [222]. In general, ALK+ ALCL has better prognosis than ALK-negative ALCL.

**Pathology** Grossly, ALCL has been described as a tan-white homogeneous mass with variable necrosis. Nodal involvement is usually the rule whereas extranodal disease is uncommon. On microscopic examination, ALCL is composed of sheets of large cells with ample eosinophilic or amphophilic cytoplasm with variable numbers of cells showing horseshoe-shaped nuclei (“hallmark” cells), ring-like nuclei (“doughnut” cells), Reed-Sternberg-like cells, and pleomorphic and multinucleated forms (Fig. 8.77). Nuclear features also include a vesicular chromatin and variable prominent nucleolus. Mitotic figures and areas of necrosis are common. Partial lymph node involvement may occur in the form of sinusoidal involvement, mimicking DLBCL or metastatic carcinoma or melanoma. Fibrosis is uncommon unless ALCL shows a “Hodgkin-like” pattern (mimicking nodular sclerosis CHL). There are several morphologic variants of ALCL, namely, a sarcomatoid, a lympho-histiocytic, a

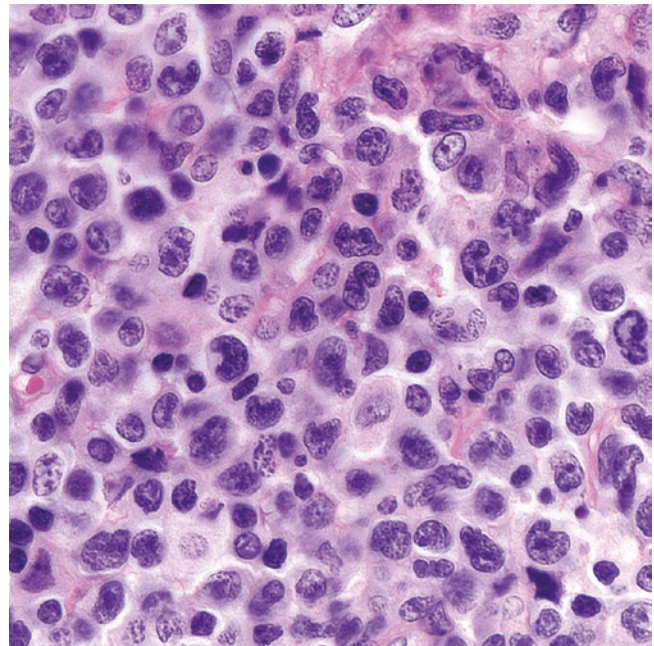


**Fig. 8.77** Anaplastic large cell lymphoma. Sheets of large pleomorphic lymphoma cells, some with horseshoe-shaped nucleus, or so-called “hallmark” cells

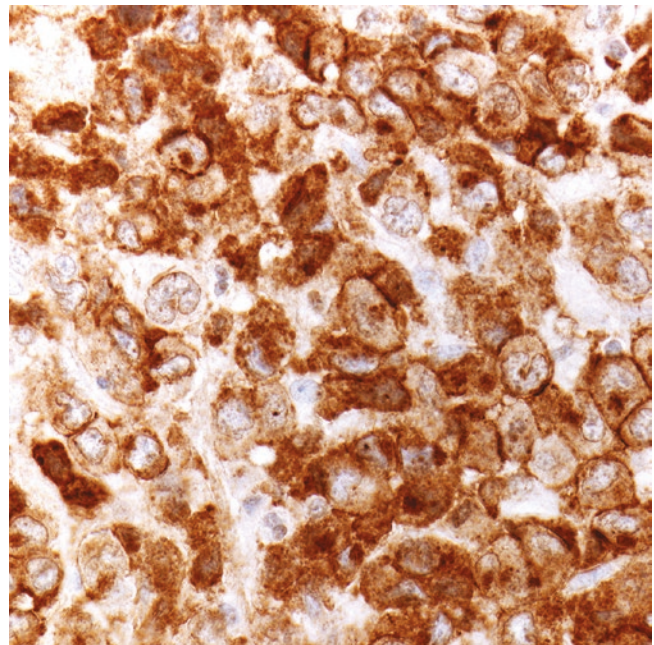


**Fig. 8.78** Anaplastic large cell lymphoma, CD30 immunostain

neutrophil-rich, an eosinophil-rich, and a small cell variant that may pose diagnostic difficulties if this entity is not considered.

**Immunohistochemistry and Other Ancillary Studies** By definition, ALCL is strongly and diffusely positive for CD30, which decorates the neoplastic cells in the membrane and in the Golgi zone (paranuclear dot) (Fig. 8.78). The tumor cells

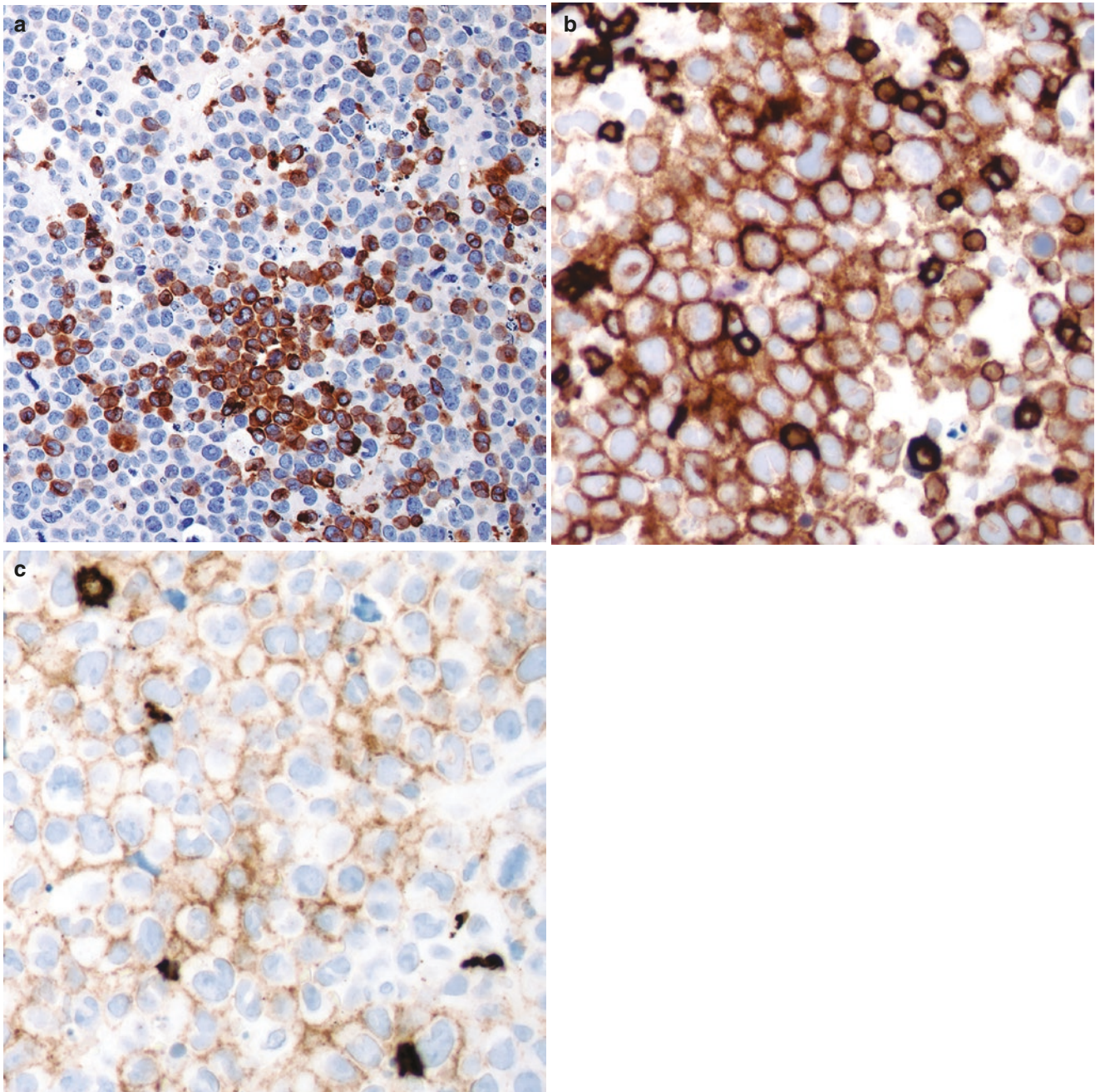


**Fig. 8.79** Anaplastic large cell lymphoma. Immunohistochemistry for (a) CD3 (only positive in few tumor cells), (b) CD5, and (c) CD8 (weak labeling)

are also commonly positive for CD43 and MUM1. For not well-understood reasons, this T-cell lymphoma shows paradoxical expression of CD4 and cytotoxic markers (TIA-1, granzyme B, and/or perforin). CD45, CD2, CD3, CD5, CD7, and CD8, EMA, and clusterin are variably present (Fig. 8.79). B-cell markers, CD15, and EBV ISH are negative. A subset of ALCLs is positive for ALK and this is the basis to separate this tumor into ALK+ or ALK-negative [225]. Normally, the ALK protein is silenced in adult tissues, which makes this immunostain highly sensitive and specific for ALK detection. The subcellular localization of ALK in tumor cells,

namely, nucleus and cytoplasm (Fig. 8.80), diffusely cytoplasmic, and coarse cytoplasmic granules, is an excellent surrogate of the underlying translocation partner with the *ALK* gene (see Molecular findings).

**Differential Diagnosis** In the mediastinum, ALCL should be distinguished from hematopoietic neoplasms, such as anaplastic DLBCL, the syncytial variant of nodular sclerosis CHL, and peripheral T-cell lymphoma, NOS, with large cells, as well as from non-hematopoietic tumors, such as

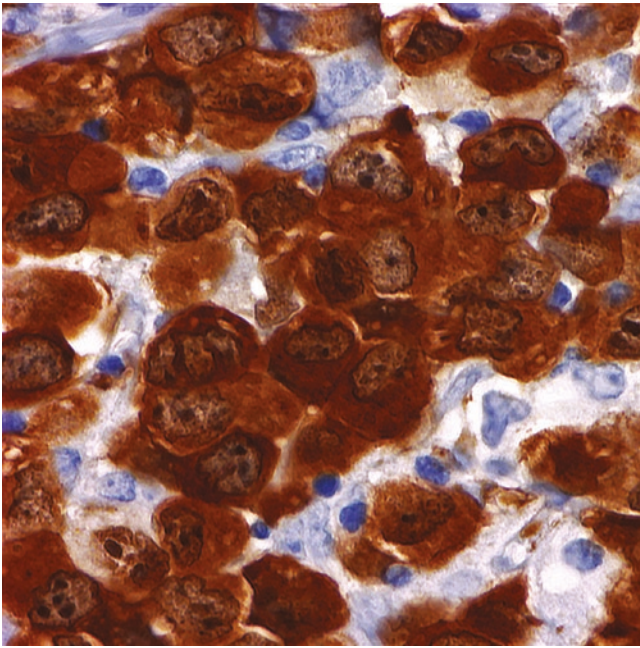


**Fig. 8.80** ALK positive anaplastic large cell lymphoma. Nuclear and cytoplasmic positivity is a surrogate for the presence of t(2;5)(*ALK-NPM*), the most common translocation detected in this T-cell lymphoma

metastatic carcinoma, melanoma, germ cell tumor, or a rhabdoid tumor. A proper panel of immunohistochemical stains is sufficient to distinguish between all these entities. Anaplastic DLBCL is positive for B-cell markers, which excludes ALCL, and the syncytial variant of nodular sclerosis CHL is positive for PAX5 (weak), variable CD15 and EBER, and positive CD30, while negative for T-cell antigens and ALK. ALCL with a “Hodgkin-like pattern” can be distinguished from nodular sclerosis CHL by the expression of >1 T-cell antigens and negative CD15 and PAX5 in the Reed-Sternberg-like cells. Peripheral T-cell lymphoma, NOS, with large cells may show an identical morphology to ALCL, and only the expression of CD30 and/or ALK is useful to distinguish between them. A large T-cell lymphoma with negative or focal CD30 should not be classified as ALCL, whereas a case positive for CD30 and negative for ALK is usually difficult to distinguish from ALK-negative ALCL. In this context, prior clinical history of systemic lymphoma, if any, is useful, as well as performing FISH for *DUSP22* and *TP63* (see molecular findings).

ALCL is negative for keratins, melanoma markers, and germ cell markers (OCT3/4, SALL4). Embryonal carcinoma is strongly positive for CD30, keratin, and germ cell transcription factors and does not express T-cell antigens, ALK, or CD43, which rules out ALCL. Similarly, rhabdoid neoplasms demonstrate loss of INI1 and are negative for CD43 and T-cell markers that are expected markers in ALCL.

**Molecular Findings** The pathogenesis of ALK+ ALCL is related with downstream effects of ALK activation. The *ALK* gene is located in 2p23. *ALK* rearrangements with multiple partners have been described in ALK+ ALCL and they correlate with the subcellular localization of the ALK protein [225]. The most common translocation partner is *NPM* located in 5q35 with the t(2;5)(p23;q35) resulting in the fusion protein ALK-NPM that can be detected in both nucleus and cytoplasm of the neoplastic cells [217–220]. Other gene partners include *TPM3* that codifies for tropomyosin 3 located in chromosome 1, resulting in t(1;2) and ALK protein expression restricted to the cytoplasm, and *CLTC* that codifies for the clathrin heavy chain located in chromosome 17, resulting in t(2;17) and cytoplasmic ALK protein expression with a coarse granular pattern. Multiple other less common gene partners are also known but are out of the scope of this chapter. All these translocations result in ALK activation with downstream activation of multiple signaling pathways, including JAK/STAT and PIK-AKT. As expected, ALK-negative ALCL does not harbor *ALK* translocations. A recent study has shown that ALK-negative ALCL harbors *DUSP22* and *TP63* rearrangements that are found in 30% and 8% of cases, respectively [226]. Cases with *DUSP22* alterations have intermediate prognosis as compared to ALK+ ALCL, while those with *TP63* alterations have a bad prognosis [226]. Cases that are negative for *ALK*, *DUSP22*, and *TP63* rearrangements are known as “triple-negative ALCL.” *TCR* clonality is positive in 90% of ALCLs, however, clonality can be negative in cases with a “null” phenotype.

## Classic Hodgkin Lymphoma (CHL)

**Introduction** CHL is one of the first lymphomas ever described. Originally known as Hodgkin “disease,” this tumor was named after T. Hodgkin who in 1832 described seven cases of a peculiar process that involved the “absorbent glands” (lymph nodes) and the spleen [227]. The eponym was first used by S. Wilks, the successor of Hodgkin at Guy’s Hospital in London, who recognized similar cases to those presented by Hodgkin few decades earlier and who properly acknowledged him as the original author [228]. After the use of the microscope became more widespread, Hodgkin disease was considered to be a form of tuberculosis or a granulomatous process, hence the multiple names used during the 1870s–1890s for this disorder, namely “lymphomatosis granulomatosa”, “lymphadenoma”, “malignant granuloma”, “pseudoleukemia” just to name a few [229]. Although several authors reported the presence of peculiar large cells in Hodgkin disease, it was not until the end of the nineteenth

**Table 8.14** Evolution in the classification of Hodgkin lymphoma

1900–1940s	1944	1966		1994–present
Hodgkin “disease” mostly classified by clinical presentation	Jackson & Parker	Lukes & Butler	Rye	REAL (1994) WHO (2001, 2008, 2017)
Acute Localized Generalized Mediastinal Larval or latent Splenomegalic Osteoperiostitic	Granuloma	Nodular sclerosis (sclerosing granuloma, Smetana and Cohen, 1956) Mixed	Nodular sclerosis Mixed cellularity	Classic CHL <sup>a</sup> Nodular sclerosis Mixed cellularity
“Sarcoma” (Ewing, 1928)	Sarcoma	Diffuse fibrosis Reticular	Lymphocyte depleted	Lymphocyte depleted Lymphocyte-rich <sup>b</sup>
Favorable correlation between amount of lymphocytes and prognosis (Rosenthal, 1936)	Paragranuloma	Lymphocyte and Histiocytic	Nodular lymphocyte predominant	Nodular lymphocyte predominant HL

Abbreviations: *REAL* Revised European and American Lymphoma classification; *WHO* World Health Organization classification; *CHL* classic Hodgkin lymphoma

<sup>a</sup>The adjective “classical” was changed to “classic” in the 2017 WHO classification (revised 4th edition)

<sup>b</sup>This subtype includes prior cases of nodular lymphocyte predominant HL that had worse prognosis and showed immunohistochemical features closer to CHL

century to beginning of the twentieth century when C. Sternberg and D. Reed did a detailed description of these cells that are known today as “Reed-Sternberg” cells [230, 231]. Importantly, D. Reed not only recognized that these peculiar large cells were characteristic of this disorder, but also that Hodgkin disease was not a form of tuberculosis [231]. About nine decades later, the name Hodgkin disease was changed to “Hodgkin lymphoma” when the group of V. Diehl in Germany discovered that Reed-Sternberg cells derived from a germinal center B-cell [232–234].

The evolution in the classification of Hodgkin lymphoma has undergone multiple revisions during the last century (see Table 8.14). To date, Hodgkin lymphoma is divided into classic Hodgkin lymphoma (CHL) and nodular lymphocyte predominant Hodgkin lymphoma. The majority of cases are represented by CHL (>90%) and this category is further subdivided into four morphologic variants: nodular sclerosis CHL, mixed cellularity CHL, lymphocyte-depleted CHL, and lymphocyte-rich CHL. The first two variants are by far the most common (>90% of all CHL cases combined) and relevant to this chapter. About 9000 new cases of CHL occur each year in the United States [235].

**Clinical Features** In general, CHL has a bimodal distribution with a first peak during adolescence and a second one between 40 and 60 years of age [236–238]. However, each subtype has a particular clinical presentation and demographics. Nodular sclerosis CHL is by far the most common variant occurring in the anterior mediastinum (>90% of cases), followed by mixed cellularity CHL occurring in ~10% of cases in the middle or posterior mediastinum [90, 91, 99, 239, 240]. Nodular sclerosis CHL affects individuals between 15 and 35 years of age. This variant is slightly more

common in women and occurs more frequently in developed countries and in individuals from a high socioeconomic status. The prevalence of EBV infection is low (10–20% of cases) and some patients may have an underlying autoimmune disorder. Conversely, mixed cellularity CHL affects older adults, typically men, and is more frequently observed in developing countries, particularly individuals of a lower socioeconomic status. The prevalence of EBV infection is high (>80%) as well as that of HIV infection [195, 241]. Thirty to fifty percent of patients with CHL are asymptomatic and the disease is discovered incidentally [116]. Symptomatic individuals present with fatigue, chest pain, dyspnea, and cough. B-symptoms are seen in 30% of patients, and fever may be cyclic (the so-called Pel-Epstein fever). Additional findings include generalized pruritus preceding diagnosis as well as anecdotal cases of lymph node “pain” after alcohol ingestion. Similar to other mediastinal tumors, nodular sclerosis CHL is typically symptomatic when there is bulky disease (>10 cm) with compression of the great vessels or other mediastinal structures. Superior vena cava syndrome and pleural or pericardial effusion may or may not occur. Abnormal laboratory tests in CHL include leukocytosis with neutrophilia and/or eosinophilia, normocytic normochromic anemia, an elevated erythrocyte sedimentation rate, and elevated lactate dehydrogenase levels.

The Costwolds modified Ann Arbor classification is used to stage CHL and it correlates with survival [242]. Early-stage disease is stratified by the presence/absence of unfavorable factors, namely, bulky mediastinal disease, elevated erythrocyte sedimentation rate, and B-symptoms. CHL is treated with a combined regimen of chemotherapy (adriamycin, bleomycin, vinblastine, and dacarbazine or ABVD) and involved-site radiation therapy. This combined regimen results in cure rates of

>95% in early-stage disease and about 70% in late-stage disease [243]. The presence of unfavorable factors and/or chemotherapy resistance are associated with poor prognosis and early relapse [244]. Recurrent and refractory cases show a positive response with targeted therapies, namely, brentuximab-vedotin (conjugated anti-CD30 antibody) and nivolumab and pembrolizumab (anti-PD1 antibodies) [245–248].

**Pathology** Only reference to nodular sclerosis and mixed cellularity CHL is done here. Large resections of anterior mediastinal lesions are becoming less frequent and sampling is mostly accomplished via a thoroscopic biopsy or an imaging-guided needle biopsy. Lymph node gross specimens involved by nodular sclerosis CHL are described as >1 matted lymph node(s) with rubbery consistency and bands of fibrosis separating tan-white to pale yellow nodules of variable size. Necrosis or suppuration may or may not be seen. When nodular sclerosis CHL involves the thymus, there are usually multiple cysts with well-circumscribed borders [116] that should be sampled extensively to not miss areas of tumor. Lymph nodes involved by mixed cellularity CHL have a homogeneous tan-white to pale yellow surface with or without focal hemorrhage and with no or minimal fibrosis on sectioning.

Microscopically, in nodular sclerosis CHL the lymph node capsule is thickened, and fibrous bands—birefringent under polarized light—extend from the capsule and separate the parenchyma into cellular nodules that contain a mixture

of small lymphocytes, eosinophils, neutrophils, plasma cells, and macrophages with a variable number of Reed-Sternberg cells (Figs. 8.81, 8.82, 8.83, and 8.84). “Classic” Reed-Sternberg cells are usually binucleated and have large eosinophilic or basophilic nucleoli surrounded by a clear halo imparting these cells an “owl’s-eye” appearance. The cytoplasm is abundant and eosinophilic to amphophilic (Fig. 8.85). Variants of Reed-Sternberg cells include Hodgkin cells (monolobated), “lacunar” cells (with artifactual retraction of the cytoplasm leaving an empty space or lacuna), “mummified” cells (with smudged chromatin and glassy eosinophilic cytoplasm), and multinucleated cells with nuclei in a wreath-like configuration (Fig. 8.86). Despite that “lacunar” cells have been reported more frequently in nodular sclerosis CHL and “classic” Reed-Sternberg cells in mixed cellularity CHL, in reality any variant can be seen in any subtype of CHL. However, when Reed-Sternberg cells form solid sheets that are associated with necrosis or an abscess this is called the syncytial variant of CHL (Fig. 8.87). Necrotizing granulomas and microabscesses may or may not be identified, sometimes prominent enough to obscure the recognition of Reed-Sternberg cells (possibly this is why this disorder was thought to be a form of tuberculosis in the past) (Fig. 8.88). When nodular sclerosis CHL involves the thymus, not only there is fibrosis and separation of cellular nodules just as described for nodal disease, but also there are multiple cysts lined by thymic epithelium. Residual Hassall corpuscles may or may not be identified. Mixed cellularity CHL is also composed of variable number of Reed-Sternberg

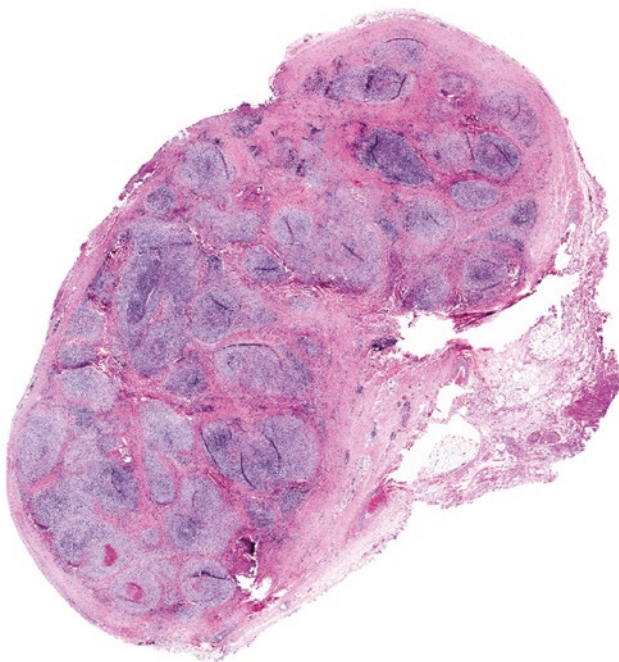


**Fig. 8.81** Nodular sclerosis classic Hodgkin lymphoma. Panoramic view of a lymph node with the characteristic bands of fibrosis separating the lymph node into cellular nodules

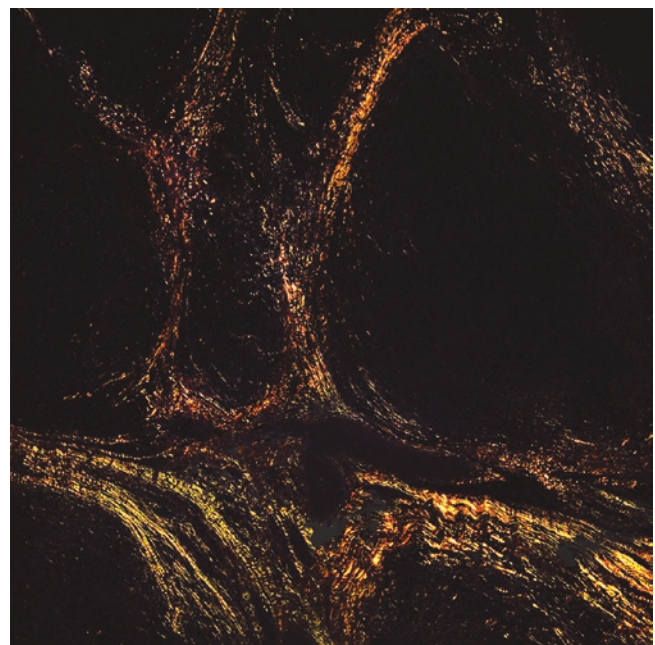


**Fig. 8.82** Nodular sclerosis classic Hodgkin lymphoma. Polarized light microscopy highlights the collagen bands surrounding the cellular nodules

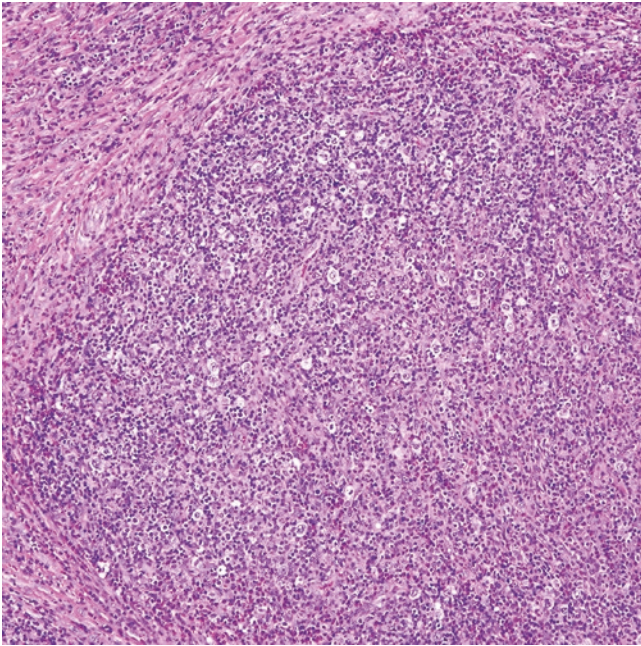


**Fig. 8.83** Nodular sclerosis classic Hodgkin lymphoma. A cellular nodule with a mixed inflammatory background infiltrate and scattered large Reed-Sternberg cells

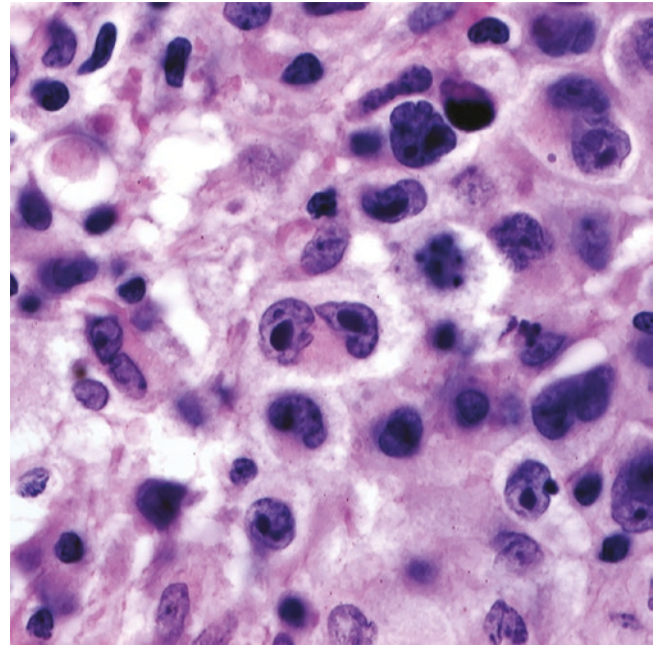


**Fig. 8.85** Classic Reed-Sternberg cells with "owl's eye" appearance

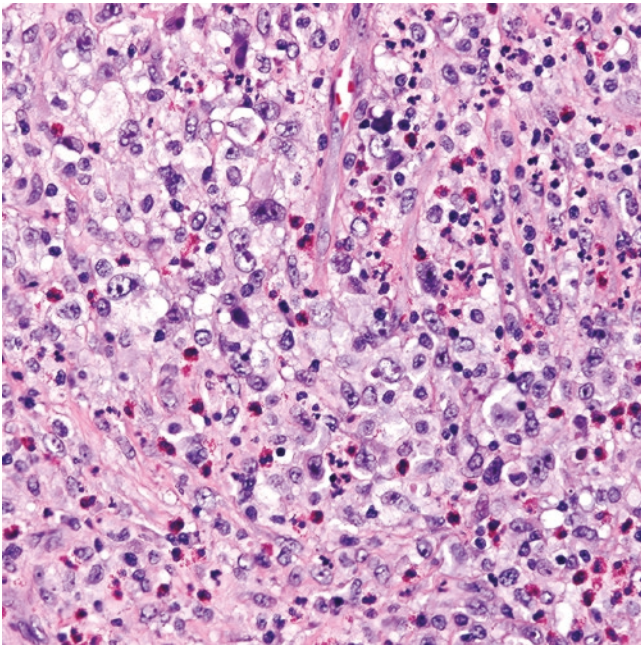


**Fig. 8.84** Polymorphic inflammatory infiltrate of neutrophils, eosinophils, histiocytes, and small lymphocytes and scattered Reed-Sternberg cells

cells in a polymorphic inflammatory background, however, there is no to minimal fibrosis and there is no separation of the tissue into cellular nodules (Fig. 8.89). If there is only partial involvement, mixed cellularity CHL is predominantly located in interfollicular areas.

**Immunohistochemistry and Other Ancillary Studies** The Reed-Sternberg cells, which are the neoplastic component in CHL, are always strongly positive for CD30, variably positive for CD15 (60–70% of cases), positive for MUM1/IRF4 (>90% of cases), weakly positive for PAX5 when compared to background B-cells, and negative for CD45, CD20 (only seen in 10–20% of cases), bcl-6, BOB.1, OCT2, ALK, CD79a, and T-cell markers [249, 250] (Figs. 8.90, 8.91, and 8.92). Only 1–2% of CHL cases may show expression of T-cell markers. CD30 and CD15 decorate Reed-Sternberg cells in a membranous and Golgi (paranuclear dot) pattern, but some cases may show diffuse cytoplasmic labeling (Fig. 8.90). CD15 may be seen only as cytoplasmic granular positivity (Fig. 8.91). Expression of CD30 is required to establish a diagnosis of CHL and when this marker is negative the diagnosis should be reconsidered or exclusion of technical problems should be ruled out (use of B5 fixative, poor fixation, other) [249, 251]. Reed-Sternberg cells are positive for PD-L1 and PD-L2, which justifies treatment with checkpoint inhibitors molecules (see also molecular findings) [125, 252–254]. Just as mentioned above, nodular sclerosis CHL is only occasionally associated with EBV infection whereas in mixed cellularity CHL EBV infection is frequent. Therefore, EBER ISH and/or LMP1 immunohistochemistry are more frequently detected in cases of mixed cellularity than in those of nodular sclerosis [255–257]. Expression of EBER and LMP1 in CHL indicate a type II latency infection (Fig. 8.92).

The non-neoplastic component in CHL shows normal antigen expression. The majority of lymphocytes are T-cells with an increased CD4 to CD8 ratio. CD3 usually highlights

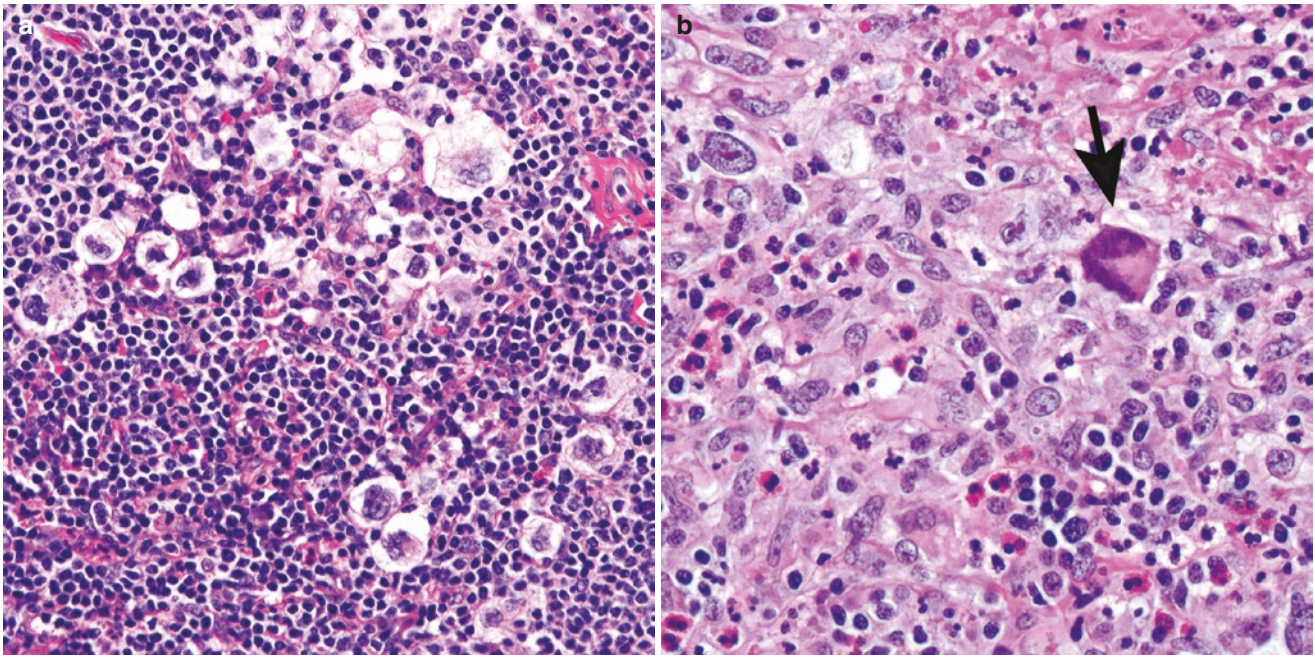


**Fig. 8.86** (a) Reed-Sternberg cells with retraction artifact, called “lacunar” cells. (b) “Mummified” cell (arrow) with smudgy chromatin and glassy eosinophilic cytoplasm

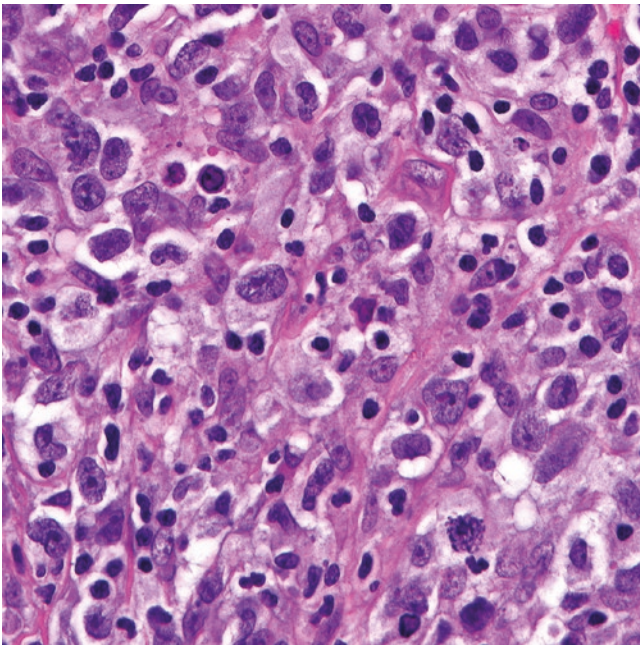


**Fig. 8.87** Syncytial variant of nodular sclerosis classic Hodgkin lymphoma. Sheets of Reed-Sternberg cells with only few scattered small lymphocytes

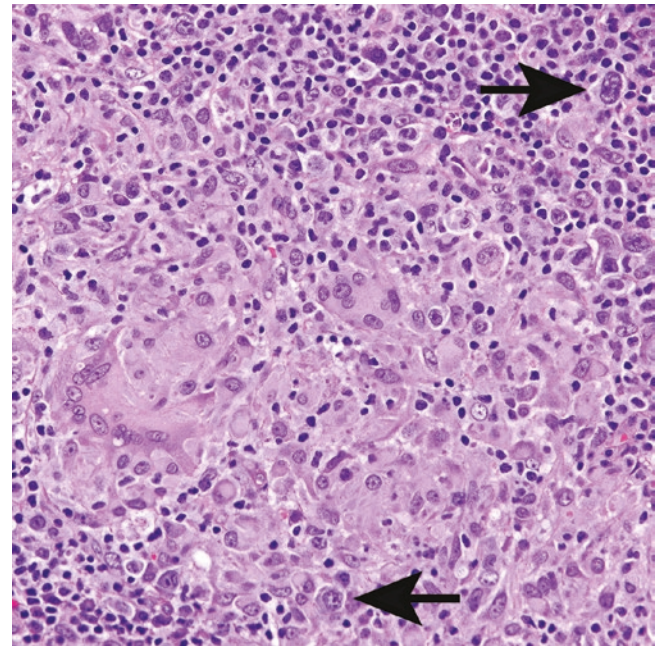


**Fig. 8.88** Prominent granulomatous inflammation can obscure the presence of Reed-Sternberg cells (arrows)

T-cells rimming Reed-Sternberg cells (Fig. 8.92). CD21 shows attenuated or disrupted FDC meshworks. Macrophages are positive for CD68 and/or CD163 and these markers may be useful to better determine the proportion of macrophages [258]. Pan-cytokeratin, p63, p40, or E-cadherin are helpful to delineate residual thymic epithelial structures in cases of

thymic involvement. Flow cytometry is not a helpful tool to diagnose CHL.

**Differential Diagnosis** Despite the characteristic morphology of nodular sclerosis and mixed cellularity CHL, current recommendations point to the use of immunohistochemistry

to exclude other types of B-cell and T-cell lymphomas that can mimic CHL [249, 259]. CHL, particularly those cases of syncytial variant, should be distinguished from DLBCL, M-GZL, PM-LBCL, ALCL, germ cell tumors, atypical thymoma (WHO B3), and metastatic carcinoma or amelanotic melanoma to the mediastinum.

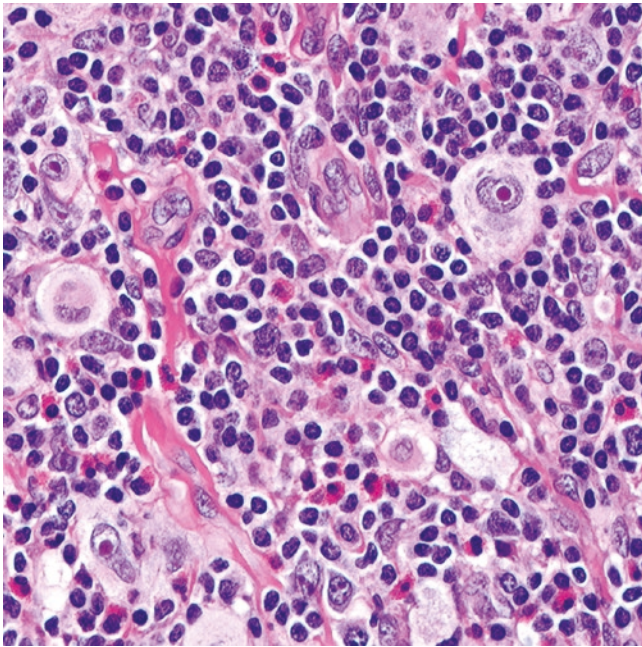


**Fig. 8.89** Mixed cellularity classic Hodgkin lymphoma

As mentioned earlier in other parts of this chapter, mediastinal DLBCL and PM-LBCL demonstrate wide infiltration into mediastinal structures and are composed of sheets of large lymphoma cells that are positive for CD45 and the B-cell markers CD20, CD79a, PAX5 (strong), BOB.1, and OCT2, features that contrast with

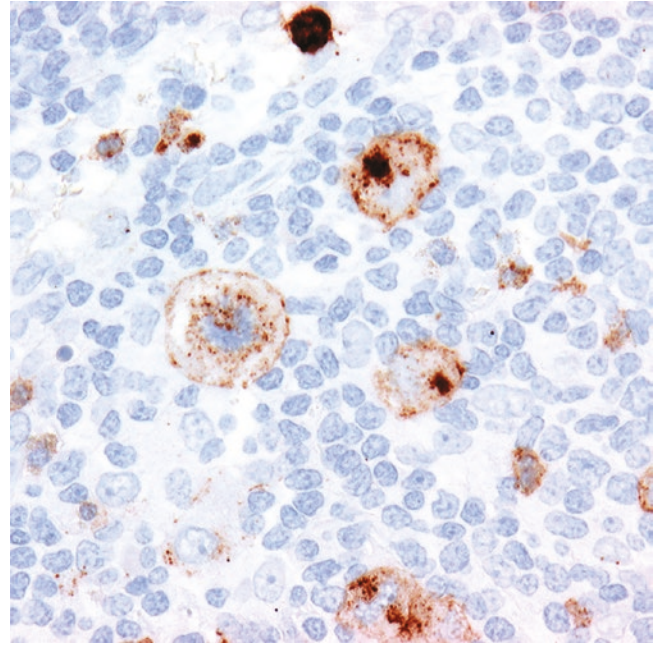


**Fig. 8.91** Membranous and granular cytoplasmic pattern of CD15 in Reed-Sternberg cells along with paranuclear dot pattern

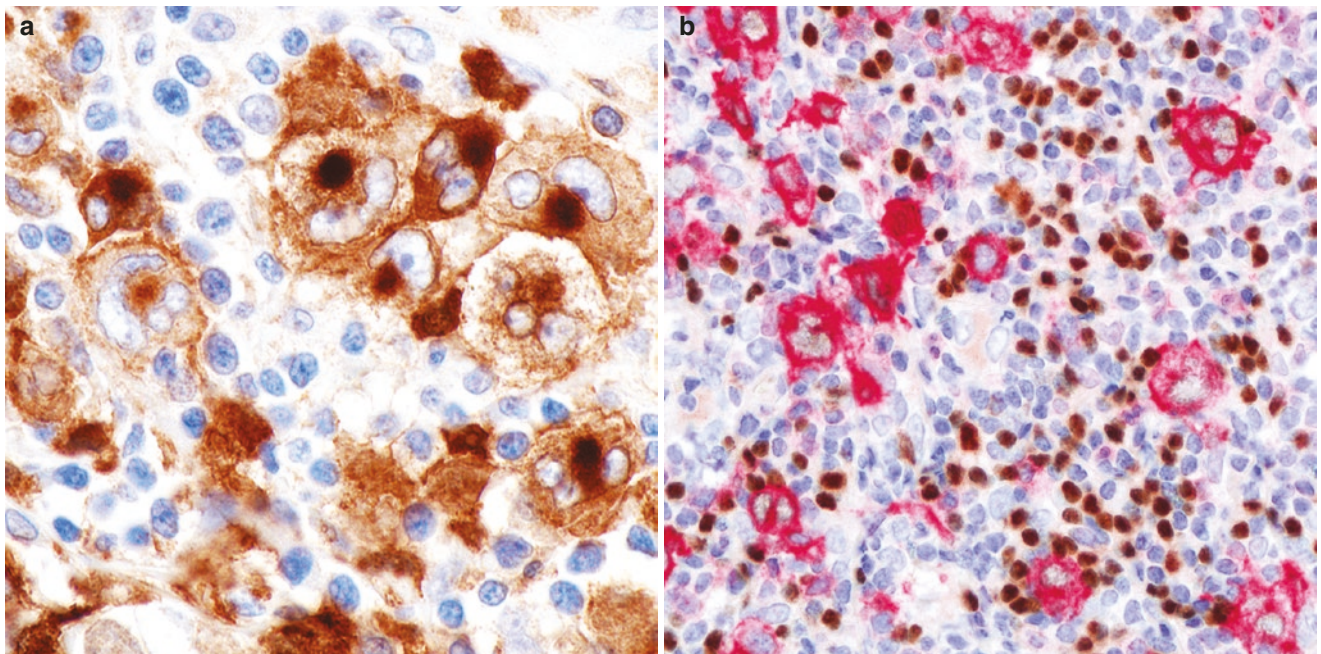


**Fig. 8.90** Reed-Sternberg cells are strongly positive for (a) CD30 and have weak expression of (b) PAX5 when compared to background B-cells (double labeling: CD30-red, alkaline phosphatase; PAX5-brown, peroxidase)

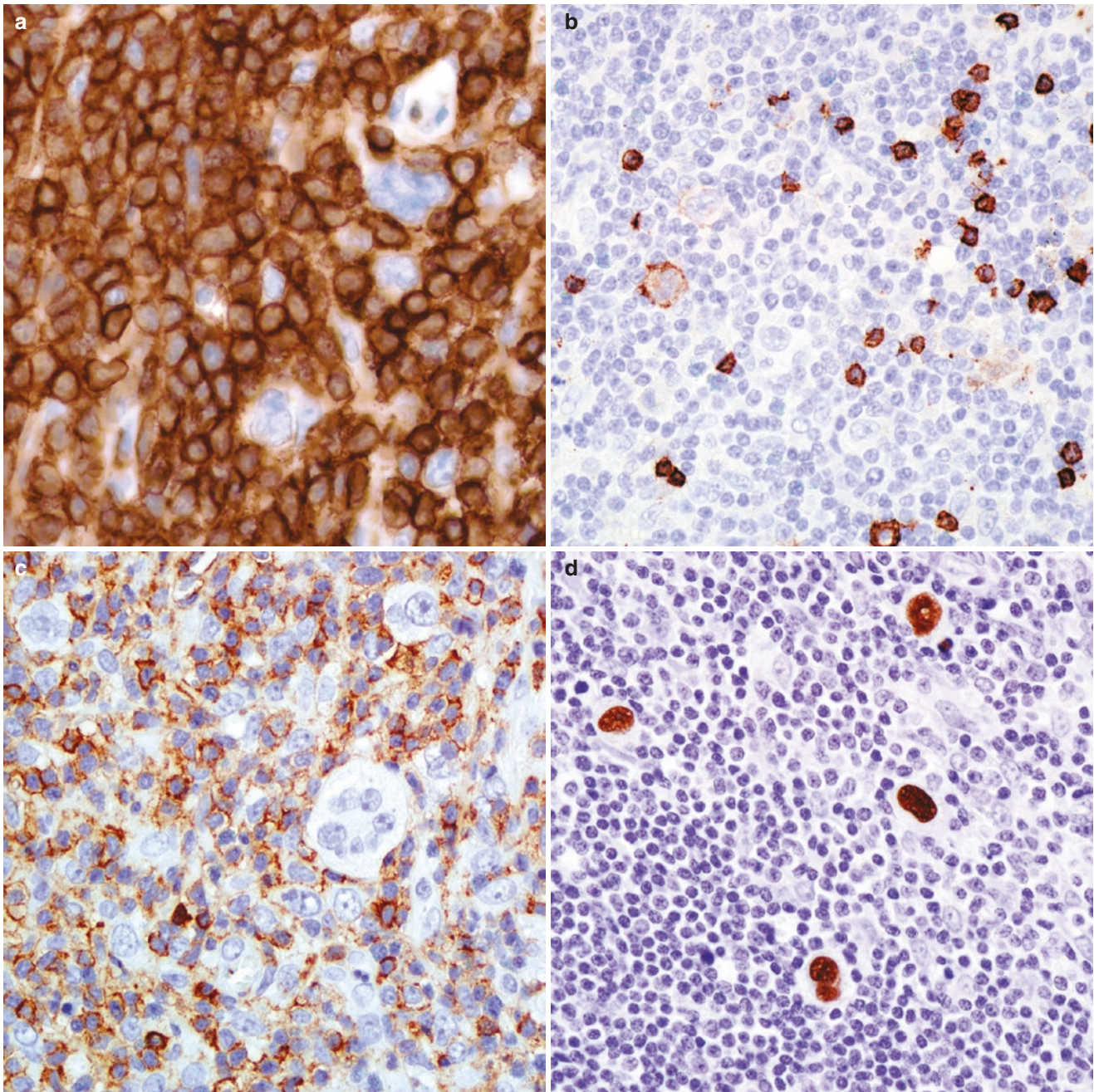


**Fig. 8.92** (a) Reed-Sternberg cells are negative for CD3. There are numerous background T-cells including some around Reed-Sternberg cells. (b) CD20 is negative to weakly positive in Reed-Sternberg cells

as compared to small B-cells. (c) CD45 is negative in Reed-Sternberg cells. (d) Cases of mixed cellularity classic Hodgkin lymphoma are frequently positive for EBER in situ hybridization

CHL even in the syncytial variant. Although PM-LBCL is positive for CD30 in 80–90% of cases, the expression of this marker is only weak and variable. M-GZL may be more difficult to distinguish from CHL since this tumor shares features with PM-LBCL and CHL (see corresponding section). The importance on differentiating CHL from other mediastinal LBCLs lies in the appropriate chemotherapy regimen modality used for each of these diseases (see corresponding sections).

ALCL may mimic the syncytial variant of CHL and to further complicate the issue, there have been rare descriptions of ALCL cases with “Hodgkin-like” pattern. However, ALCL is more common in children—not a typical age for CHL—and only rarely affects the mediastinum [221, 260]. In addition, ALCL is negative for CD15, PAX5, and EBER. If ALK is present, then CHL is excluded [225].

Primary mediastinal germ cell tumors are more common in children and young men and typically present as a bulky medi-

astinal mass [91, 92]. On microscopic examination, “burned out” germ cell tumors (seminoma, embryonal carcinoma, choriocarcinoma, hepatoid yolk sac tumor) can mimic CHL since they feature fibrosis, granulomas, and few scattered large pleomorphic tumor cells [261]. Fortunately, these findings are focal and other areas of the tumor show more classic germ cell tumor histology. However, this may not be the case in a needle biopsy. Immunohistochemical stains for OCT3/4, SALL4,  $\beta$ -hCG, AFP, and pan-cytokeratin are required to confirm the diagnosis of germ cell tumor and exclude CHL. One important consideration is embryonal carcinoma, a tumor that is positive for CD30 and may be confused with the syncytial variant of CHL. However, this tumor tends to form glandular structures and is negative for CD15 and PAX5 while positive for germ cell markers and pancytokeratin.

Thymomas are tumors that involve the anterior mediastinum and by imaging may be difficult to distinguish from nodular sclerosis CHL. Therefore, microscopic examination is needed to confirm the diagnosis. Type B2 and B3 (atypical) thymomas may histologically resemble CHL given the presence of large epithelial cells admixed with abundant lymphocytes but clear-cut Reed-Sternberg cells are not seen. The presence of other features of thymoma, namely, organotypic features, perivascular spaces, and medullary differentiation as well as a positive cytokeratin, p63 and/or p40 in the large cells confirms thymoma and excludes CHL. When nodular sclerosis CHL only partially involves the thymus, additional markers, such as CD15, CD30, PAX5, and pancytokeratin, are required to confirm the nature of the large cells seen.

Metastatic carcinoma or metastatic amelanotic melanoma to the mediastinum may present in middle mediastinal lymph nodes. Few scattered metastatic cells in a lymph node may resemble Reed-Sternberg cells. A prior history of solid malignancy, associated desmoplasia with the tumor cells, the presence of intracellular mucin and glandular formation should point to these possibilities and not CHL. Immunohistochemical markers may be required to exclude or confirm the diagnosis, namely, keratins for carcinoma or melanocytic markers for melanoma. Metastatic nasopharyngeal carcinoma to the mediastinum should not be forgotten, particularly because this tumor is positive for EBER and may resemble CHL if only scattered tumor cells are present in a lymph node. A simple pan-cytokeratin immunostain and negative CD15, CD30, and PAX5 will confirm the diagnosis. The differential diagnosis of mediastinal CHL is summarized in Table 8.15.

**Molecular Findings** Reed-Sternberg cells are germinal center/post germinal center B-cells that have undergone somatic hypermutation with crippled B-cell genes but have escaped the negative selection process [262–264]. Therefore, these cells have a defective B-cell differentiation program and harbor crippling mutations on immunoglobulin expression genes, which explains the decreased expression of CD20, PAX5, and the

**Table 8.15** Differential diagnosis of classic Hodgkin lymphoma (CHL)

Typically an anterior mediastinal mass (if syncytial variant of nodular sclerosis CHL)	
<i>Hematopoietic</i>	
Primary mediastinal (thymic) large B-cell lymphoma	
Mediastinal gray zone lymphoma	
Anaplastic large cell lymphoma	
<i>Non-hematopoietic</i>	
Germinoma (including “burned-out” tumor with associated granulomas and fibrosis)	
Atypical thymoma (WHO B3)	
Metastatic carcinoma or amelanotic melanoma	
Metastatic nasopharyngeal carcinoma (if only scattered tumor cells are present in a lymph node)	

transcription factors OCT2 and BOB.1 [262, 265–267]. Reed-Sternberg cells are resistant to apoptosis by multiple different mechanisms, including canonical and noncanonical activation of the NK- $\kappa$ B pathway and activation of the JAK/STAT pathway [268–270]. Activation of NK- $\kappa$ B is used by Reed-Sternberg cells to attract the supportive microenvironment of inflammatory cells and stromal cells characteristic of this lymphoma. EBV infection also induces NK- $\kappa$ B activation with potential oncogenic results [271]. Some genetic abnormalities in CHL overlap with those of PM-LBCL, including mutations of *SOC1*, a negative regulator in the JAK/STAT pathway [97, 272–274], as well as frequent alterations at 9p24 with overexpression of PD-L1/PD-L2 and JAK2 that result in a suppressive immune response and increased cellular proliferation, respectively [248, 254]. Expression of PD-L1/PD-L2 make antibody therapies against PD-1 an excellent treatment for CHL. Clinical trials using these blocking agents have shown promising results in refractory/relapsed disease [245, 246]. Lastly, it appears that the Reed-Sternberg cell morphology may be related to mechanisms of incomplete cytokinesis and cell re-fusion secondary to mutations in midbody/centromere proteins and to cellular endomitosis without division of the cell nucleus [275].

## Lymphoma Imaging

In general, PET/CT is the modality of choice for staging and restaging mediastinal lymphoma. FDG PET/CT is more accurate than CT for detecting nodal involvement in lymphoma, with a sensitivity and specificity of 94% and 100% compared with 88% and 85%, respectively, for CT alone. FDG PET/CT can effectively identify extranodal disease anywhere within the body with 88% sensitivity and 100% specificity compared with 50 and 90% on CT [276]. Other benefits of FDG PET/CT include the identification of metabolically active disease to guide biopsy as well as in the detection of Richter transformation (conversion of low-grade lymphoma to more aggressive subtypes) [277].

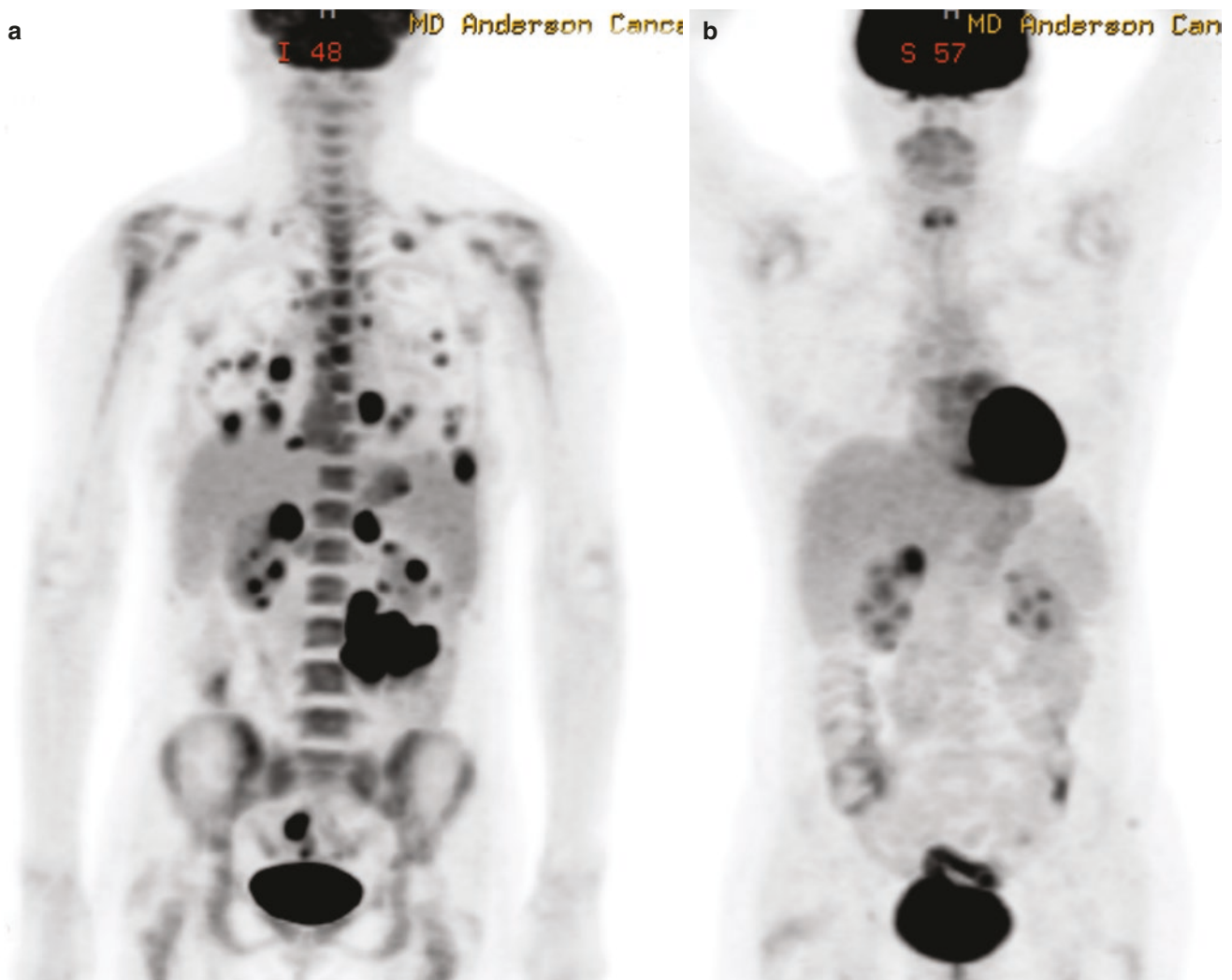


**Fig. 8.93** Response to therapy in diffuse large B cell lymphoma. (a) Whole body PET shows lymphoma involving the lymph nodes above and below the diaphragm, lungs, small, and large bowel. (b) Whole

body PET 6 months later shows complete anatomic and metabolic response. Deauville 5 point score is 1

### Lymphoma Imaging Classification

Classification of lymphoma has undergone numerous revisions over the decades from the classic 1971 Ann Arbor Classification to the current 2014 Lugano Classification. The Lugano Classification informs initial evaluation, staging, prognostic groups, assessment of response, and surveillance. FDG PET/CT is now considered the standard of care imaging evaluation for all FDG avid lymphomas, which include all histological subtypes except lymphocytic leukemia/small lymphocytic lymphoma, lymphoplasmacytic lymphoma/Waldenström's macroglobulinemia, mycosis fungoides, and marginal zone NHLs, unless there is a suspicion for aggressive transformation [278, 279].

Baseline staging PET/CT is recommended to assess baseline tumor FDG avidity/standard uptake value (SUV), sites of nodal involvement, nodal size in each group, local extension, organ involvement, and vascular encasement. It results

in more accurate staging, with stage modifications in as many as 10–30% of patients compared to CT alone [280, 281]. The Lugano Classification also specifies scenarios in which bone marrow biopsies are no longer indicated when PET/CT is positive for marrow involvement [282].

The Lugano Classification recommends utilization of serial interim PET/CT to assess treatment response early during therapy (generally after two to four courses of chemotherapy) and at end of treatment (generally 6–8 weeks following termination of chemotherapy). Response to treatment is classified as complete response, partial response, no response/stable disease, and progressive disease [283]. The 5 point PET scoring system, Deauville criteria, is used to determine response to therapy [(1) No uptake, (2) Uptake equal or less than mediastinum, (3) Uptake greater than mediastinum, but less than liver. (4) Uptake moderately more than liver at any site. (5) Uptake markedly more than liver at any site and new sites of disease.] (Figs. 8.93 and 8.94).

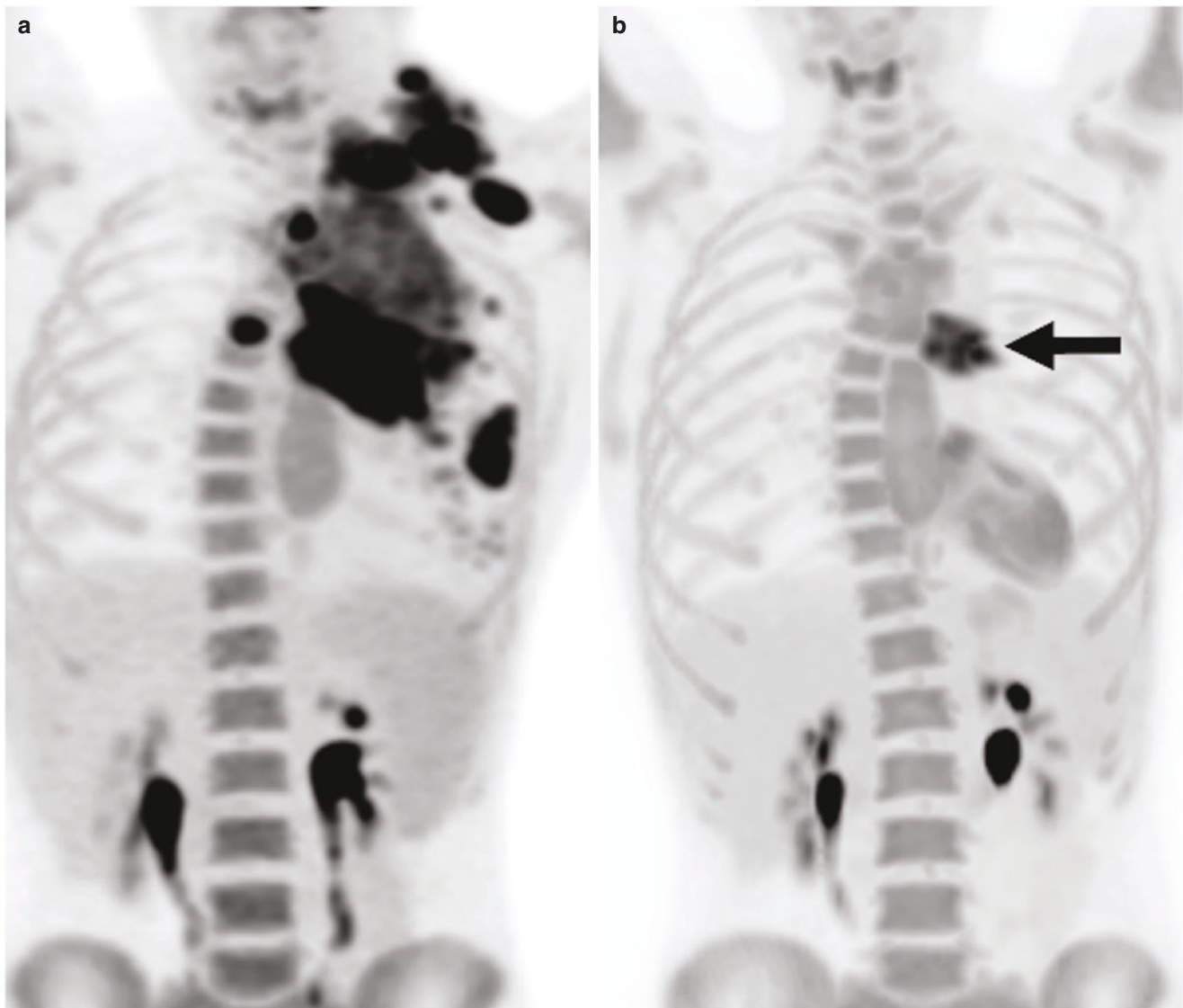


**Fig. 8.94** Response to therapy in non-Hodgkin lymphoma. (a) Whole body PET shows lymphoma involving the lymph nodes above the diaphragm in the mediastinum and left neck, lungs, and thoracic spine. (b)

Whole body PET 6 months later shows partial response with residual mediastinal adenopathy (arrow) showing FDG uptake greater than liver. Deauville 5 point score is 4

By utilizing the Deauville 5 point criteria, complete response is defined as nodal/extranodal uptake with a score of 1–3, no new lesions, and no focal abnormal uptake in the marrow. Partial response is defined as nodal/extranodal uptake with a score of 4–5 but with uptake less than baseline scan, no new lesions, and decreased residual uptake in marrow, if involved on baseline scan. No response/stable disease is defined as nodal/extranodal uptake with a score of 4–5 with no significant change compared with baseline scan, no new lesions, and stable uptake in marrow, if involved on baseline scan. Progressive disease is defined as nodal/extranodal uptake with score of 4–5, increased uptake compared with baseline scan, new focal areas of nodal/extranodal FDG uptake that are consistent with lymphoma and not unrelated pathology, and new areas of marrow uptake that do not appear reactive [282, 283].

### Diffuse Large B Cell Lymphoma

Imaging findings in DLBCL can include extensive disease involving numerous nodal and extranodal locations. Routine chest radiographs are often the initial imaging evaluation as clinically nonspecific “B symptoms” of fever, night sweats, and weight loss are present in 30% of patients [282]. Radiographic findings can include mediastinal widening or mass, hilar masses, as well as pulmonary nodules or areas of consolidation, which can cavitate [284, 285]. Additionally, pleural effusions may be noted [286].

CT with intravenous contrast better demonstrates and delineates nodal and extranodal involvement with often large and locally invasive mediastinal and/or hilar masses.

Pulmonary parenchymal nodules, nodular masses with or without cavitation, and pleural effusions are often visualized [282, 285, 286].

MRI is primarily utilized when DLBCL involves the central or peripheral nervous system.

DLBCL is FDG avid on PET/CT and this modality is useful in diagnosis, staging, and re-assessment. Additionally, PET/CT may detect drug toxicity in lungs following the use of Rituximab, which is a mainstay of DLBCL therapy. In this setting PET/CT demonstrates ground glass opacities with increased FDG uptake, which can alert clinicians to prevent potentially fatal outcomes [282, 287]. Finally, in a meta-analysis of DLBCL patients, PET/CT findings impact prognosis and relapse of disease [288].

### Primary Mediastinal (Thymic) Large B Cell Lymphoma

Imaging findings are largely related to the typical presentation of a rapidly expanding mediastinal mass, with the majority >10 cm at presentation and demonstrating extension into the mediastinum, pericardium, heart, pleura, and chest wall [289, 290].

Routine chest radiographs are often nonspecific, demonstrating large mediastinal and/or hilar masses, pericardial effusions, and pleural effusions.

CT with intravenous contrast reveals masses predominantly involving the prevascular/anterior mediastinum; subcarinal and paravertebral/posterior mediastinal masses occur less frequently [291]. Masses generally have low CT attenuation with variable degrees of cystic degeneration, hemorrhage, and necrosis [292]. Because of often large presenting size and local mass effect, other common CT findings include bowing and narrowing of the trachea, pericardial and pleural effusions, superior vena cava syndrome, and unilateral hemidiaphragm elevation from phrenic nerve compression and dysfunction [293, 294].

The primary role of MRI in PMLBCL is evaluating residual mass after therapy. On T2-weighted images, fibrotic or

sterilized soft tissue shows homogeneous low signal intensity while residual lymphoma shows heterogeneous high signal intensity. High T2 signal intensity can be seen in the setting of residual viable lymphoma, necrosis, and inflammation [295].

PET/CT is utilized for diagnosis, staging, and re-assessment, although response criteria have not been specifically validated in PMLBCL [296]. Additionally, the International Extranodal Lymphoma Study Group-26 prospective study demonstrated that PET/CT can be used prognostically in the setting of PMLBCL to predict progression-free survival and overall survival [297].

### Hodgkin Lymphoma

On routine radiographs HL generally presents as mediastinal widening, which is defined as a mediastinal width >1/3 the intrathoracic diameter, or as a mass with smooth or lobulated borders which may or may not silhouette normal anatomic structures [242, 298].

CT following administration of intravenous contrast media is the imaging modality of choice for evaluation. CT imaging classically demonstrates multiple round, solid, well-circumscribed masses or a bulky solid mass with smooth or lobulated borders in the prevascular/anterior mediastinum (Fig. 8.95). Calcifications and paravertebral/posterior mediastinal location are uncommon. Mediastinal HL tends to not invade adjacent structures or produce great vessel compression; however, larger tumors can displace and compress adjacent anatomic structures as well as invade the chest wall [299, 300].

HL demonstrates high FDG uptake making PET/CT useful in diagnosis, staging, and re-assessment (Fig. 8.96). In particular, post-therapy PET/CT is utilized to distinguish between treatment-related fibrosis and recurrence. Specifically, focal increased FDG uptake on PET/CT in an area of post-treatment soft-tissue is suspicious for residual or recurrent tumor and assists in guiding tissue sampling [301, 302].

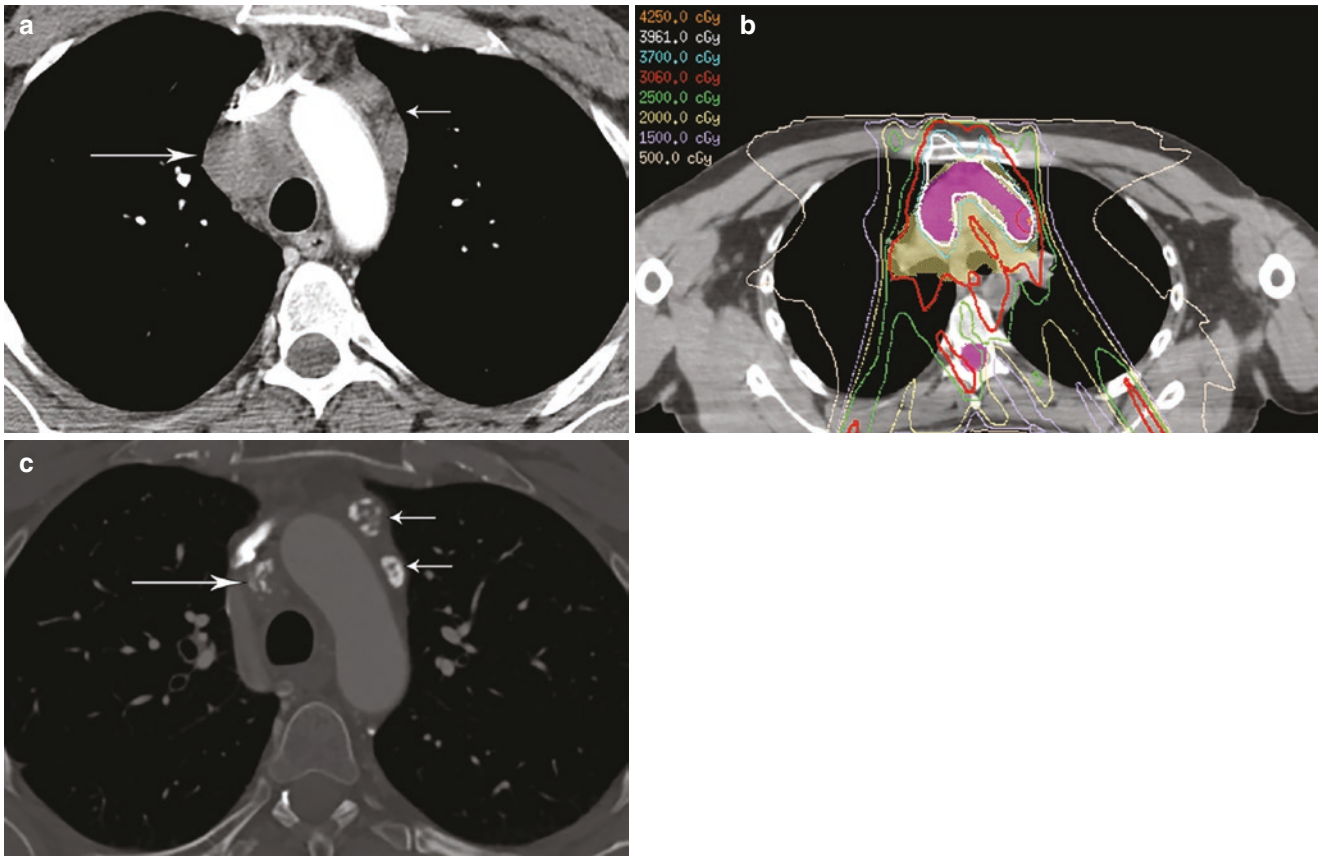


**Fig. 8.95** Hodgkin lymphoma. (a) Contrast-enhanced CT shows mediastinal adenopathy in the right paratracheal (long arrow) and left prevascular (short arrow) space. (b) Radiation treatment plan with isodose curves targeting the anterior mediastinal tumor. (c) Contrast-

enhanced CT with bone window 7 years later shows the nodal disease has decreased in size and shows coarse calcifications in the right paratracheal (long arrow) and left prevascular (short arrows) space

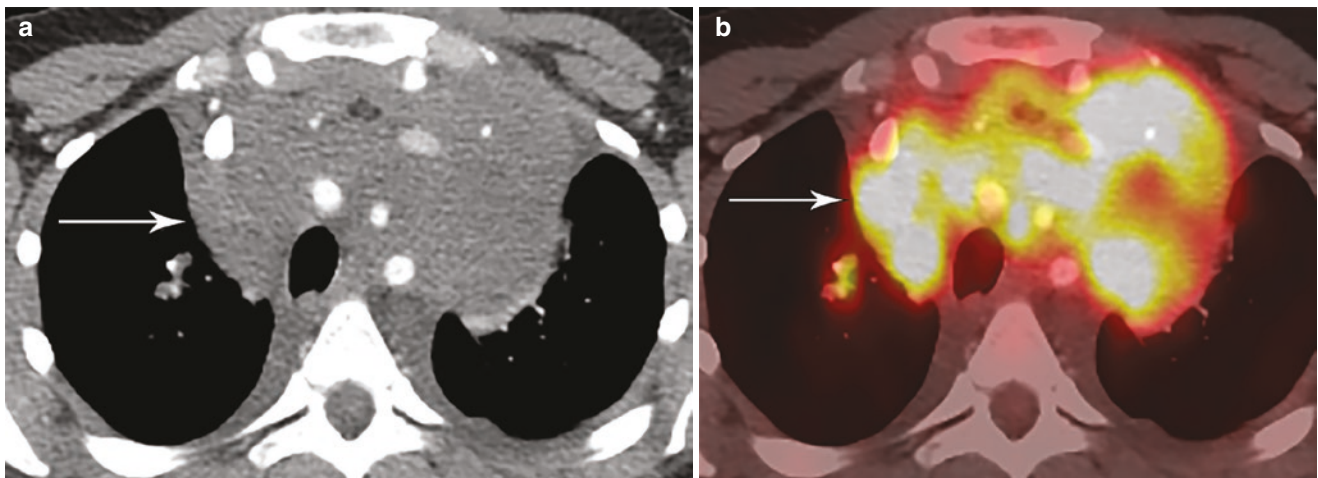


**Fig. 8.96** Hodgkin lymphoma. (a) Contrast-enhanced CT shows large anterior mediastinal mass (arrow) encasing the SVC, left brachiocephalic vein, innominate artery, left common carotid artery, and left sub-

clavian artery. Small pleural effusions are present. (b) PET/CT shows the mass (arrow) is intensely FDG avid

MRI is not routinely used in HL imaging, but overall has similar imaging findings compared with CT. MRI is particularly useful in the setting of potential thymic involvement, however, as chemical shift MRI can readily distinguish between thymic hyperplasia (which can occur after therapy) and residual or recurrent disease in the thymus [303, 304].

## Myeloid Neoplasms: Mediastinal Myeloid Sarcoma

**Introduction** Myeloid sarcoma, also known as chloroma, granulocytic, or monocytic sarcoma, refers to a mass-forming extramedullary neoplasm composed of myeloblasts, monoblasts, or immature myeloid precursors. The incidence of myeloid sarcoma is <10% of all acute myeloid leukemias (AMLs) with monocytic differentiation being more prone to present as extramedullary disease. Primary mediastinal involvement by AML is extremely rare. No particular subtype of AML has a predilection for the mediastinum.

**Clinical Features** Myeloid sarcoma can occur in the mediastinum at all ages but is more frequent in the pediatric population and young adults [305–323]. As with myeloid sarcoma at any other extramedullary site, mediastinal myeloid sarcoma may occur synchronously, antecede or precede the diagnosis of AML. Mediastinal myeloid sarcoma may also be preceded by cytopenias and/or myelodysplasia [315]. The diagnosis may be suspected clinically in a patient who develops a mediastinal mass and has known history of AML, whereas the disease may be an unsuspected diagnosis in a patient who presents with chest pain, respiratory distress, or superior vena cava syndrome and a mediastinal mass is detected on imaging. Myeloid sarcomas may also occur in patients with known chronic myeloid leukemia, which would be classified as the blast phase of this myeloproliferative disorder.

**Pathology** This neoplasm is composed of diffuse sheets of blasts of intermediate to large size with oval, irregular, or cleaved nucleus, vesicular chromatin, prominent nucleolus, and moderate amount of granular eosinophilic cytoplasm (Fig. 8.97). The tumor is widely infiltrative into adjacent tissues. Mitoses are frequent and areas of necrosis may or may not be present. The blasts in monocytic sarcomas are large with reniform to cleaved nucleus and moderate to abundant amphophilic to eosinophilic cytoplasm (Fig. 8.97). Myeloid sarcomas may also be composed preferentially of left-shifted myeloid cells (promyelocytes, myelocytes, metamyelocytes), particularly on those cases arising in the setting of chronic myeloid leukemia.

**Immunohistochemistry and Other Ancillary Studies** Myeloblasts are typically positive for myeloperoxidase, CD34, CD117, CD11c, CD13, CD33, CD43, lysozyme and show weak to variable expression of CD45 (Fig. 8.98). Monocytic sarcomas express CD4, CD14, and CD64 but are usually negative for CD34 and/or CD117. The vascular marker ERG is positive in hematopoietic cells and therefore in myeloid sarcoma [324]. TdT may or may not be expressed by myeloid or monocytic sarcomas and positivity of this marker alone does not support a diagnosis of LBL. Myeloid and monocytic sarcomas are negative for B-cell and T-cell markers, but some cases may show variable expression of T-cell markers and/or CD56. By definition, myeloid or monocytic sarcomas are negative for CD3 and CD19. However, a potential case of myeloid sarcoma developing in a patient having AML with t(8;21) can show strong expression of PAX5. If the diagnosis of AML is already known, a panel of immunohistochemical markers similar to the original leukemic blasts should be used to confirm the diagnosis in a mediastinal lesion.

Flow cytometry is very useful when it is available, but tissue may not always be collected for this test when a mediastinal mass is detected, particularly in cases with no prior history of AML. If fresh tissue or unstained slides are prepared, FISH may be used to detect a particular translocation or a rearrangement of specific AMLs subtypes, namely, AML with t(8;21)(*RUNX1::RUNX1T1*), acute promyelocytic leukemia [t(15;17)(*PML::RARA*)], monocytic sarcoma

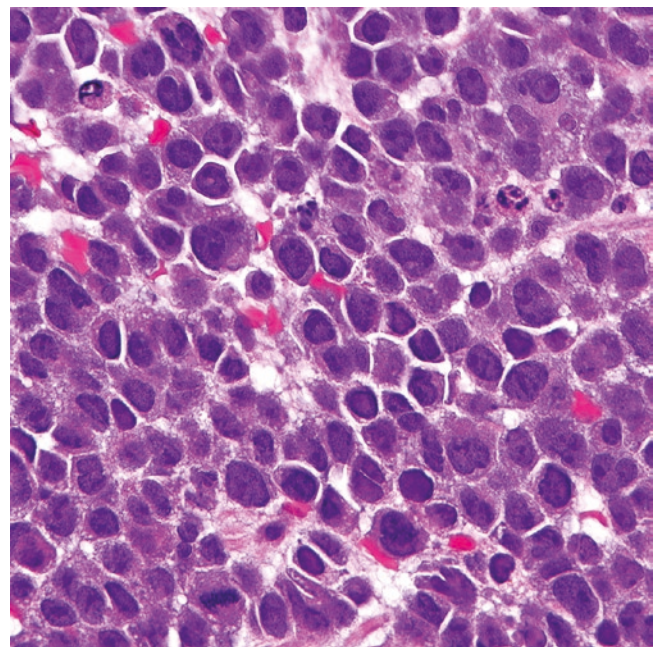


**Fig. 8.97** Myeloid sarcoma is composed of sheets of intermediate to large cells with oval to irregular nuclei, prominent nucleolus, and moderate amount of finely granular cytoplasm

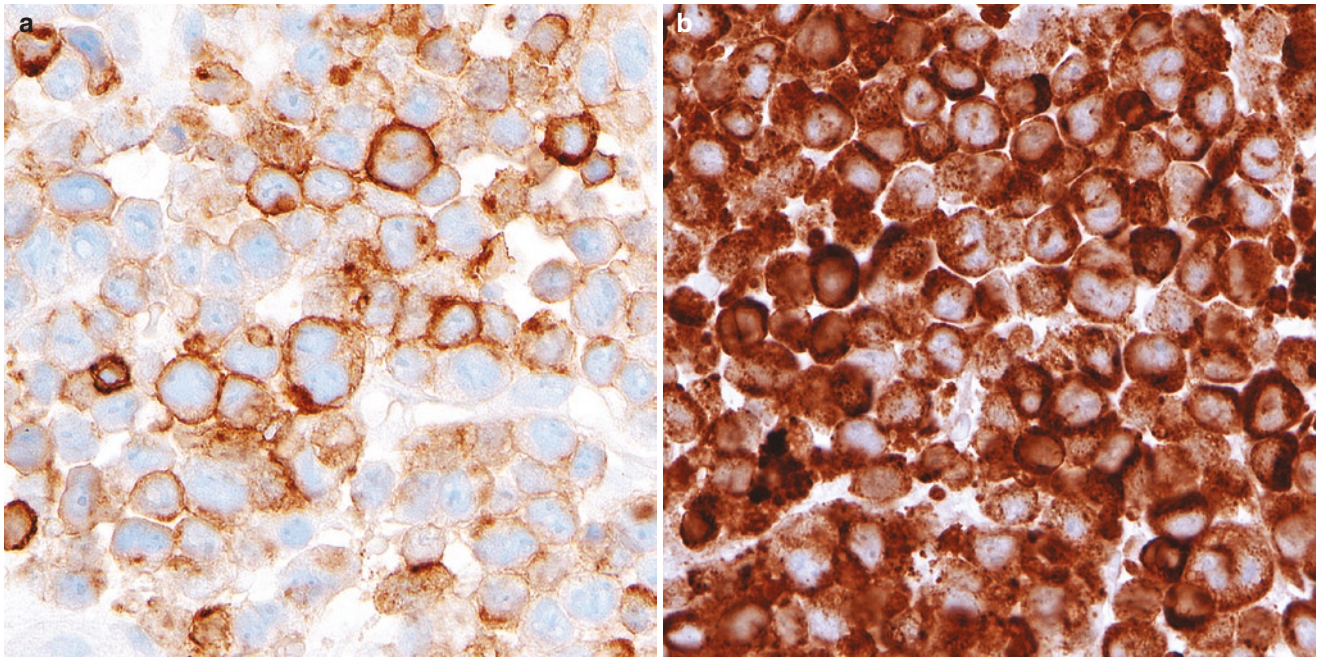


**Fig. 8.98** Myeloid sarcoma with variable immunoreactivity for (a) CD45, and diffuse strong positivity for (b) lysozyme

(*MLL/KMT2A* rearrangement), or a blast phase in chronic myeloid leukemia [ $t(9;22)(BCR::ABL1)$ ]. Next-generation sequencing may help to reclassify difficult cases of myeloid sarcoma that present as a mediastinal mass with no peripheral blood or bone marrow involvement [325]

**Differential Diagnosis** Myeloid sarcoma should be distinguished from LBL, high-grade DLBCL, Burkitt lymphoma, small cell carcinoma, or any small blue round cell tumor primary or metastatic to the mediastinum. Prior clinical history is very important and can point to a prior history of AML or not. Immunohistochemical stains for CD43, CD45, myeloperoxidase, lysozyme, CD34, and/or CD117 support myeloid sarcoma, whereas presence of B-cell markers may suggest B-LBL, Burkitt lymphoma, or any other B-cell lymphoproliferative disorder. T-cell markers, CD34 and/or TdT support T-LBL, whereas keratins and neuroendocrine markers support carcinoma with neuroendocrine differentiation.

**Molecular Studies** Several cytogenetic and molecular alterations are present in AMLs and in myeloid sarcomas. A full description of all these abnormalities is out of the scope of this chapter. If history of a particular AML with recurrent cytogenetic abnormalities is available, cytogenetics, FISH, and/or molecular studies could be performed for further evaluation.

### Other Tumors: Follicular Dendritic Cell (FDC) Sarcoma

**Introduction** The first suggestion of a tumor originating from lymph node dendritic cells was done by K. Lennert in the 1960s [326]. During this same decade, the function, ultrastructural features, and immune-related functions of these dendritic cells were done by Sir G. Nossal, reason why FDCs are also referred to as “Nossal cells” [327, 328]. The recognition of a bona fide tumor with morphologic and ultrastructural characteristics similar to FDCs was done in 1986 by Monda and colleagues [329] and this tumor was referred to as FDC sarcoma. In contrast to other nodal dendritic cells, FDCs and FDC sarcoma do not derive from the bone marrow but from a putative perivascular/pericytic cell precursor [330]. FDC sarcoma may occur in any lymph node or less frequently at an extranodal location.

**Clinical Features** FDC sarcoma is the most common primary sarcoma of lymph nodes in adults [331]. Extranodal disease may occur at any location, with frequent involvement of the head and neck region and the abdomen [329, 332–334]. Mediastinal disease has been described in sporadic cases [335–339]. The majority of FDC sarcomas arise de novo, whereas a subset may develop in patients with a long-

standing history of hyaline vascular Castleman disease. Clinical symptoms include chest pain, cough, or dyspnea and these vary depending on the size and location of the mass. Paraneoplastic pemphigus is a relatively common sign in this tumor. FDC sarcoma does not show a particular site of predilection within the mediastinum [335–339]. Treatment includes surgical resection followed by radiation therapy and chemotherapy, particularly for unresectable cases.

**Pathology** Grossly, FDC sarcoma consists of a tan-white to pink lobulated mass with bulging borders and variable areas of hemorrhage and/or necrosis. Microscopically, the tumor is multilobulated and consists of a proliferation of FDCs with partial or complete effacement of a lymph node. The tumor cells are typically spindle and arranged in short fascicles and whorls (Fig. 8.99), but some cases feature a solid growth, an angiomatoid pattern, abundant myxoid changes, epithelioid morphology, or marked pleomorphism [334, 340, 341]. In those cases with spindle morphology, the tumor cells feature elongated nucleus with thick nuclear membranes, speckled chromatin, one large nucleolus, or multiple small nucleoli (Fig. 8.100). Occasional binucleated cells (the so-called “kissing nuclei” as seen in normal FDCs) may be observed. The cytoplasm is eosinophilic and the cell borders may be clearly defined to ill-defined from area to area. Along with the neoplastic FDCs, these tumors contain variable number of small

mature lymphocytes sprinkled throughout the tumor (Fig. 8.100). Abundant perivascular lymphocytes may be observed in some cases. Mitoses are variable, but in some cases they may be inconspicuous. There are variable areas of hemorrhage and necrosis that may also feature large irregular blood vessels filled with intravascular fibrin. Extranodal FDC sarcoma has an identical morphology. As mentioned previously, a subset of FDC sarcomas arise in the setting of hyaline-vascular Castleman disease (Figs. 8.101 and 8.102), and it is hypothesized that the dysplastic FDCs in hyaline-vascular Castleman disease are the precursors of FDC sarcoma in this context [340]. In addition, FDC sarcomas arising in the setting of hyaline vascular Castleman disease may or may not be accompanied by incidental collections of extrathymic thymocytes that have received the controversial name of indolent T-lymphoblastic proliferations [13].

**Immunohistochemistry and Other Ancillary Studies** This neoplasm is positive for FDC markers, namely, CD21 (C3d receptor 2), CD23 (low affinity IgE receptor), CD35 (C3b/4d receptor 1), as well as clusterin, CXCL13, podoplanin (D2-40), desmoplakin, claudin-1, and the epithelial growth factor receptor (EGFR) [15, 333, 341–343] (Figs. 8.103, 8.104, and 8.105). FDC sarcoma is variably positive for CD68 and S100 and negative for CD45, B- and T-cell markers, keratins, melanoma markers, CD1a, langerin/CD207, CD117, desmin, and

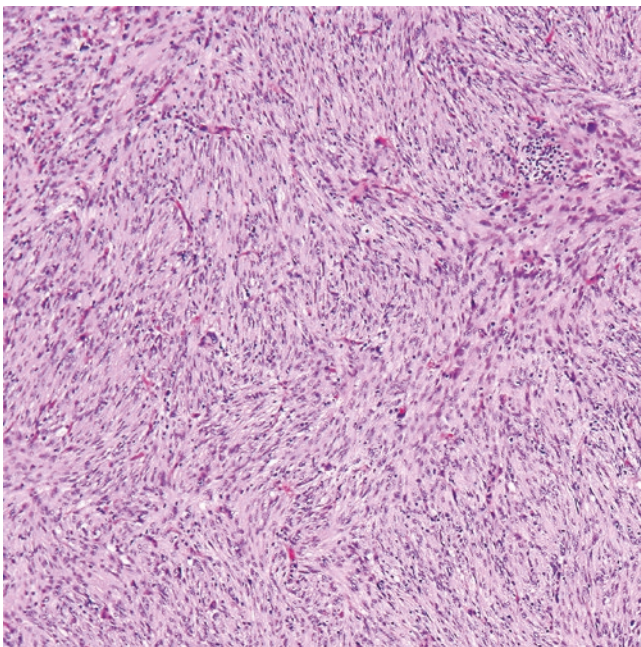


**Fig. 8.99** Follicular dendritic cell sarcoma. The tumor is composed of short fascicles of spindle cells with elongated nucleus and slender eosinophilic cytoplasm. Random pleomorphic cells may or may not be seen (center). Small lymphocytes are scattered throughout the tumor or may form small aggregates (top, right)

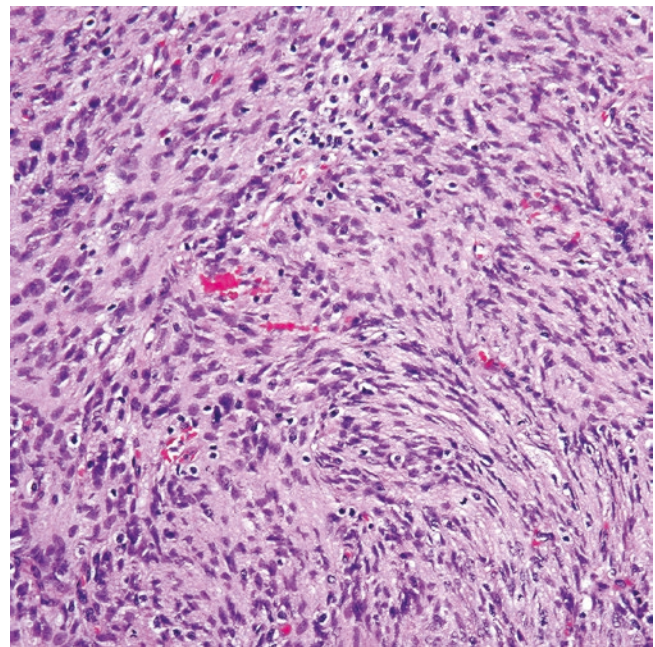


**Fig. 8.100** Follicular dendritic cell sarcoma. The tumor cells are arranged in short fascicles and form vague whorls. Scattered lymphocytes are seen

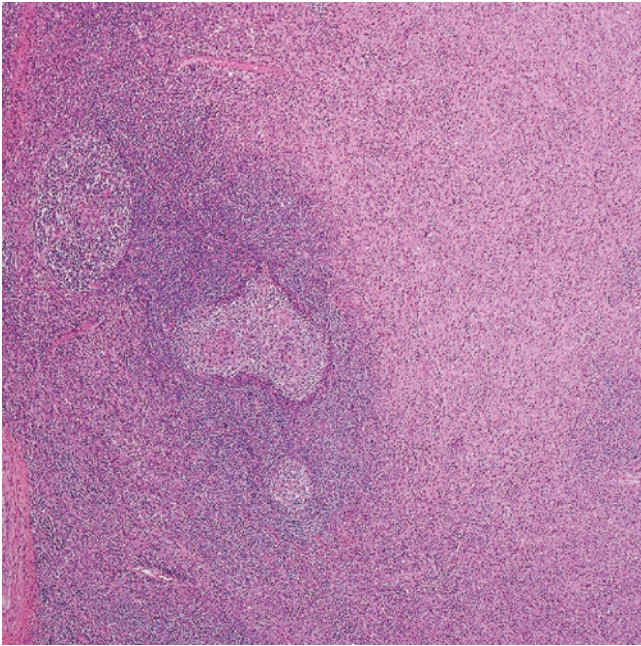


**Fig. 8.101** Follicular dendritic cell sarcoma arising in hyaline vascular Castleman disease. There is replacement of the lymph node by a spindle cell proliferation (right). Residual follicles show features of hyaline vascular Castleman disease, namely, prominent mantle zones, twinning (central follicle), and atrophic germinal center (follicle at the bottom)

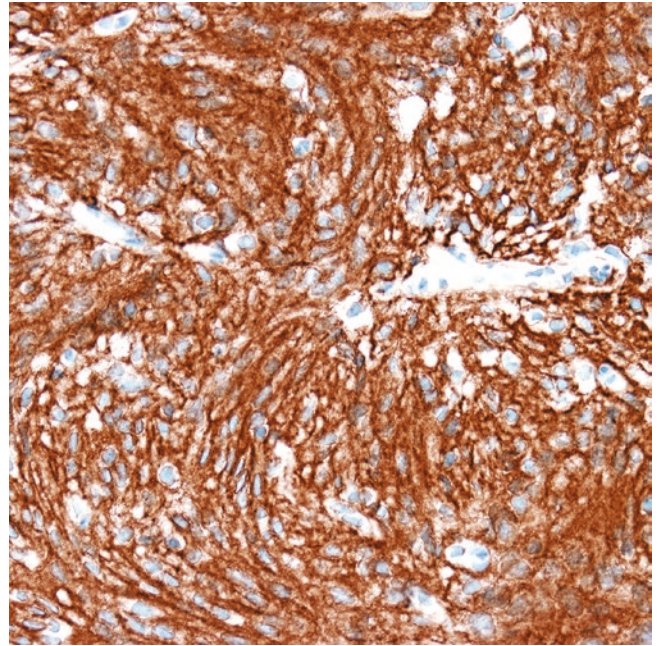


**Fig. 8.103** Follicular dendritic cell sarcoma. Immunohistochemistry for CD21

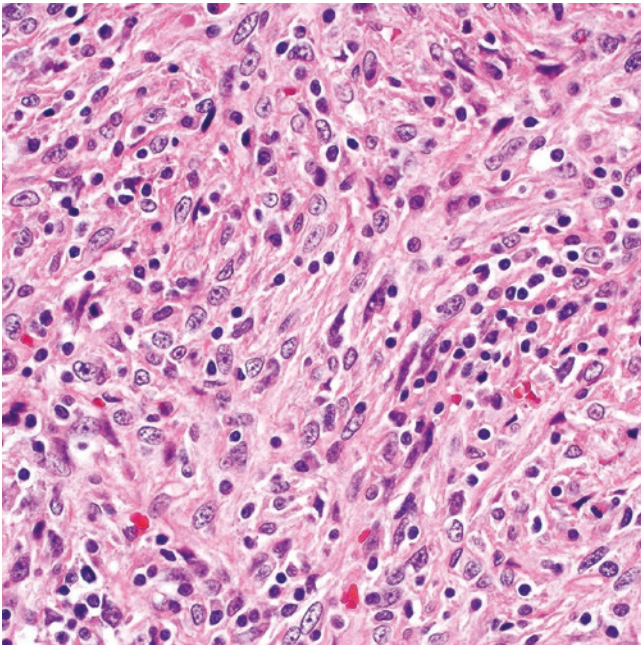


**Fig. 8.102** Follicular dendritic cell sarcoma arising in hyaline vascular Castleman disease. The morphology is strikingly similar to that of a de novo follicular dendritic cell sarcoma, but some cases in this setting may not show marked cytologic atypia

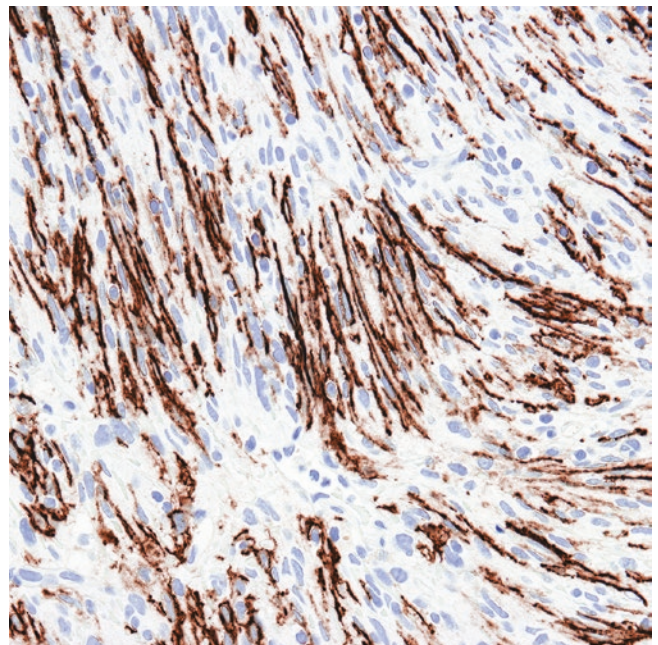


**Fig. 8.104** Follicular dendritic cell sarcoma. Immunohistochemistry for CD23

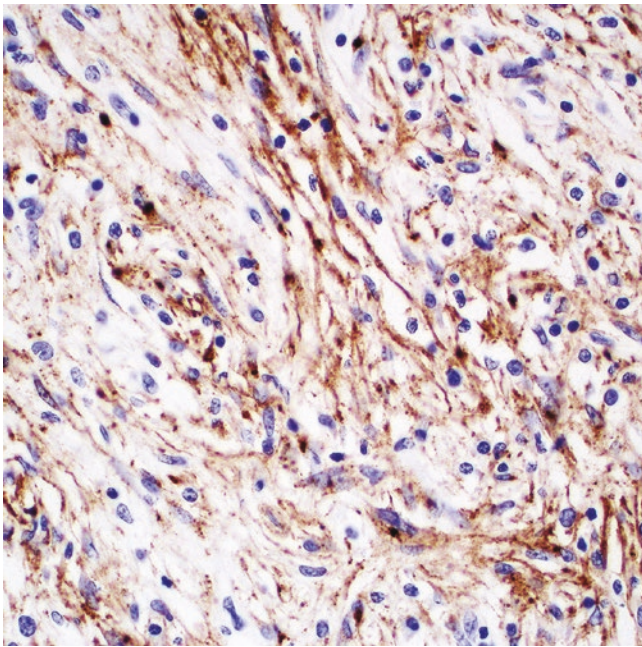


**Fig. 8.105** Follicular dendritic cell sarcoma. Immunohistochemistry for EGFR

EBER ISH. It is not uncommon to have cases of FDC sarcoma that may be positive for only one or few FDCs markers, and in these cases additional FDC markers should be tested. EBER ISH is positive only in the inflammatory pseudotumor variant of this tumor that occurs in the spleen and liver. Extranodal cases and those arising in the setting of hyaline vascular Castleman disease show similar features to the ones previously described. FDC sarcomas are positive for PD-L1 and PD-L2 in about 50% of cases [344], which points to the potential use of immunomodulatory drugs for treatment.

**Differential Diagnosis** Nodal FDC sarcoma should be distinguished from metastatic melanoma, spindle cell carcinoma, Kaposi sarcoma, interdigitating dendritic (reticulum) cell sarcoma, histiocytic sarcoma, and Langerhans cell sarcoma. Depending on the predominant morphology and location within the mediastinum, the differential diagnosis includes spindle cell thymoma, thymic carcinoma, spindle cell carcinoma or melanoma, ectopic meningioma or thymoma, leiomyosarcoma, epithelioid angiosarcoma, or a metastatic gastrointestinal stromal tumor. Immunohistochemistry is mandatory to confirm the expression of FDC markers and rule out all the other entities.

**Molecular Findings** Targeted genomic sequencing has shown that a third of FDC sarcomas in a series of 13 cases feature recurrent loss of function alterations in tumor suppressor genes involved in the negative regulation of NF- $\kappa$ B activation and cell cycle progression [345]. Similarly, another study showed that majority of the tested FDC sarcoma (14 cases) harbor recurrent

alterations in several chromosomes, with the most frequent alteration being 13q, as well as homozygous deletions of *CDKN2A*, *RBI*, *BIRC3*, and *CYLD* [346]. *BRAF V600E* mutation has also been detected in a subset of FDCs but this finding has not been identified in more recent series [347].

## References

1. Scadding JG. The eponymy of sarcoidosis. *J R Soc Med.* 1981;74:147–57.
2. Eishi Y. Etiologic aspect of sarcoidosis as an allergic endogenous infection caused by *Propionibacterium acnes*. *Biomed Res Int.* 2013;2013:935289.
3. Eishi Y. Etiologic link between sarcoidosis and *Propionibacterium acnes*. *Respir Invest.* 2013;51:56–68.
4. Iannuzzi MC, Rybicki BA, Teirstein AS. Sarcoidosis. *N Engl J Med.* 2007;357:2153–65.
5. Narula N, Iannuzzi M. Sarcoidosis: pitfalls and challenging mimickers. *Front Med (Lausanne).* 2020;7:594275.
6. Asano S. Granulomatous lymphadenitis. *J Clin Exp Hematop.* 2012;52:1–16.
7. Fontanilla JM, Barnes A, von Reyn CF. Current diagnosis and management of peripheral tuberculous lymphadenitis. *Clin Infect Dis.* 2011;53:555–62.
8. Crothers JW, Laga AC, Solomon IH. Clinical performance of mycobacterial immunohistochemistry in anatomic pathology specimens. *Am J Clin Pathol.* 2021;155:97–105.
9. Castleman B, Iverson L, Menendez VP. Localized mediastinal lymphnode hyperplasia resembling thymoma. *Cancer.* 1956;9:822–30.
10. Keller AR, Hochholzer L, Castleman B. Hyaline-vascular and plasma-cell types of giant lymph node hyperplasia of the mediastinum and other locations. *Cancer.* 1972;29:670–83.
11. Lin O, Frizzera G. Angiomyoid and follicular dendritic cell proliferative lesions in Castleman's disease of hyaline-vascular type: a study of 10 cases. *Am J Surg Pathol.* 1997;21:1295–306.
12. Ohgami RS, Zhao S, Ohgami JK, et al. TdT+ T-lymphoblastic populations are increased in Castleman disease, in Castleman disease in association with follicular dendritic cell tumors, and in angioimmunoblastic T-cell lymphoma. *Am J Surg Pathol.* 2012;36:1619–28.
13. Ohgami RS, Arber DA, Zehnder JL, Natkunam Y, Warnke RA. Indolent T-lymphoblastic proliferation (iT-LBP): a review of clinical and pathologic features and distinction from malignant T-lymphoblastic lymphoma. *Adv Anat Pathol.* 2013;20:137–40.
14. Nathwani BN, Kansal R, Yiakoumis X, Pangalis GA. Indolent T-lymphoblastic proliferation: a name with specific meaning—reply. *Hum Pathol.* 2015;46:1786–7.
15. Sun X, Chang KC, Abruzzo LV, Lai R, Younes A, Jones D. Epidermal growth factor receptor expression in follicular dendritic cells: a shared feature of follicular dendritic cell sarcoma and Castleman's disease. *Hum Pathol.* 2003;34:835–40.
16. Iwaki N, Fajgenbaum DC, Nabel CS, et al. Clinicopathologic analysis of TAFRO syndrome demonstrates a distinct subtype of HHV-8-negative multicentric Castleman disease. *Am J Hematol.* 2016;91:220–6.
17. Dispenzieri A. POEMS syndrome: 2017 Update on diagnosis, risk stratification, and management. *Am J Hematol.* 2017;92:814–29.
18. Fajgenbaum DC, Uldrick TS, Bagg A, et al. International, evidence-based consensus diagnostic criteria for HHV-8-negative/idiopathic multicentric Castleman disease. *Blood.* 2017;129:1646–57.
19. Cheuk W, Chan JK. Lymphadenopathy of IgG4-related disease: an underdiagnosed and overdiagnosed entity. *Semin Diagn Pathol.* 2012;29:226–34.

20. Dozois RR, Bernatz PE, Woolner LB, Andersen HA. Sclerosing mediastinitis involving major bronchi. *Mayo Clin Proc.* 1968;43:557–69.
21. Afrin LB. Sclerosing mediastinitis and mast cell activation syndrome. *Pathol Res Pract.* 2012;208:181–5.
22. Gorospe L, Ayala-Carbonero AM, Fernandez-Mendez MA, et al. Idiopathic fibrosing mediastinitis: spectrum of imaging findings with emphasis on its association with IgG4-related disease. *Clin Imaging.* 2015;39:993–9.
23. Jain N, Chauhan U, Puri SK, Agrawal S, Garg L. Fibrosing mediastinitis: when to suspect and how to evaluate? *BJR Case Rep.* 2016;2:20150274.
24. Kang DW, Canzian M, Beyruti R, Jatene FB. Sclerosing mediastinitis in the differential diagnosis of mediastinal tumors. *J Bras Pneumol.* 2006;32:78–83.
25. Masunaga A, Ishibashi F, Koh E, Oide T, Sekine Y, Hiroshima K. Possible relationship between fibrosis of IgG4-related thymitis and the profibrotic cytokines, transforming growth factor beta 1, interleukin 1 beta and interferon gamma: a case report. *Diagn Pathol.* 2018;13:6.
26. Peebles RS, Carpenter CT, Dupont WD, Loyd JE. Mediastinal fibrosis is associated with human leukocyte antigen-A2. *Chest.* 2000;117:482–5.
27. D'Agaro T, Bittolo T, Bravin V, et al. NOTCH1 mutational status in chronic lymphocytic leukaemia: clinical relevance of subclonal mutations and mutation types. *Br J Haematol.* 2018;182(4):597–602.
28. Worrell JA, Donnelly EF, Martin JB, Bastarache JA, Loyd JE. Computed tomography and the idiopathic form of proliferative fibrosing mediastinitis. *J Thorac Imaging.* 2007;22:235–40.
29. Lindholm KE, de Groot P, Moran CA. Fibrosing/sclerosing lesions of the mediastinum: a review. *Adv Anat Pathol.* 2019;26(4):235–40.
30. Rossi GM, Emmi G, Corradi D, et al. Idiopathic mediastinal fibrosis: a systemic immune-mediated disorder. A case series and a review of the literature. *Clin Rev Allergy Immunol.* 2017;52:446–59.
31. Chen JL, Osborne BM, Butler JJ. Residual fibrous masses in treated Hodgkin's disease. *Cancer.* 1987;60:407–13.
32. Engleman P, Liebow AA, Gmelich J, Friedman PJ. Pulmonary hyalinizing granuloma. *Am Rev Respir Dis.* 1977;115:997–1008.
33. Flieder DB, Suster S, Moran CA. Idiopathic fibroinflammatory (fibrosing/sclerosing) lesions of the mediastinum: a study of 30 cases with emphasis on morphologic heterogeneity. *Mod Pathol.* 1999;12:257–64.
34. Deshpande V, Zen Y, Chan JK, et al. Consensus statement on the pathology of IgG4-related disease. *Mod Pathol.* 2012;25:1181–92.
35. Coppes-Zantinga A, Egeler RM. The Langerhans cell histiocytosis X files revealed. *Br J Haematol.* 2002;116:3–9.
36. Breathnach AS, Gross M, Basset F, Nezelof C. Freeze-fracture replication of X-granules in cells of cutaneous lesions of histiocytosis-X. *Br J Dermatol.* 1973;89:571–85.
37. Nezelof C, Basset F, Rousseau MF. Histiocytosis X histogenetic arguments for a Langerhans cell origin. *Biomedicine.* 1973;18:365–71.
38. Langerhans P. Ueber die Nerven der Menschlichen Haut. *Virchow Arch [B].* 1868;44:325–37.
39. Birbeck MS, Breathnach AS, Everall JD. An electron microscopy study of basal melanocytes and high-level clear cell (Langerhans cells) in vitiligo. *J Invest Dermatol.* 1961;75:51–64.
40. Willman CL, Busque L, Griffith BB, et al. Langerhans'-cell histiocytosis (histiocytosis X)—a clonal proliferative disease. *N Engl J Med.* 1994;331:154–60.
41. Yu RC, Chu C, Buluwela L, Chu AC. Clonal proliferation of Langerhans cells in Langerhans cell histiocytosis. *Lancet.* 1994;343:767–8.
42. Badalian-Very G, Vergilio JA, Degar BA, et al. Recurrent BRAF mutations in Langerhans cell histiocytosis. *Blood.* 2010;116:1919–23.
43. Capper D, Preusser M, Habel A, et al. Assessment of BRAF V600E mutation status by immunohistochemistry with a mutation-specific monoclonal antibody. *Acta Neuropathol.* 2011;122:11–9.
44. Berres ML, Merad M, Allen CE. Progress in understanding the pathogenesis of Langerhans cell histiocytosis: back to Histiocytosis X? *Br J Haematol.* 2015;169:3–13.
45. Chakraborty R, Hampton OA, Shen X, et al. Mutually exclusive recurrent somatic mutations in MAP2K1 and BRAF support a central role for ERK activation in LCH pathogenesis. *Blood.* 2014;124:3007–15.
46. Nelson DS, van Halteren A, Quispel WT, et al. MAP2K1 and MAP3K1 mutations in Langerhans cell histiocytosis. *Genes Chromosomes Cancer.* 2015;54:361–8.
47. Chakraborty R, Burke TM, Hampton OA, et al. Alternative genetic mechanisms of BRAF activation in Langerhans cell histiocytosis. *Blood.* 2016;128:2533–7.
48. Egeler RM, Katewa S, Leenen PJ, et al. Langerhans cell histiocytosis is a neoplasm and consequently its recurrence is a relapse: In memory of Bob Arceci. *Pediatr Blood Cancer.* 2016;63:1704–12.
49. Emile JF, Ablu O, Fraïtag S, et al. Revised classification of histiocytoses and neoplasms of the macrophage-dendritic cell lineages. *Blood.* 2016;127:2672–81.
50. Haroche J, Charlotte F, Arnaud L, et al. High prevalence of BRAF V600E mutations in Erdheim-Chester disease but not in other non-Langerhans cell histiocytoses. *Blood.* 2012;120:2700–3.
51. Alayed K, Medeiros LJ, Patel KP, et al. BRAF and MAP2K1 mutations in Langerhans cell histiocytosis: a study of 50 cases. *Hum Pathol.* 2016;52:61–7.
52. Nicholson HS, Egeler RM, Nesbit ME. The epidemiology of Langerhans cell histiocytosis. *Hematol Oncol Clin North Am.* 1998;12:379–84.
53. Abramson SJ, Berdon WE, Reilly BJ, Kuhn JP. Cavitation of anterior mediastinal masses in children with histiocytosis-X. Report of four cases with radiographic, pathologic findings and clinical follow up. *Pediatr Radiol.* 1987;17:10–4.
54. Ducassou S, Seyrig F, Thomas C, et al. Thymus and mediastinal node involvement in childhood Langerhans cell histiocytosis: long-term follow-up from the French national cohort. *Pediatr Blood Cancer.* 2013;60:1759–65.
55. Fahrner R, Hokscho B, Gugger M, Schmid RA. Langerhans cell histiocytosis as differential diagnosis of a mediastinal tumor. *Eur J Cardiothorac Surg.* 2008;33:516–7.
56. Khadilkar UN, Rao AT, Sahoo KK, Pai MR. Langerhans cell histiocytosis of mediastinal node. *Indian J Pediatr.* 2008;75:294–6.
57. Mogul M, Hartman G, Donaldson S, et al. Langerhans' cell histiocytosis presenting with the superior vena cava syndrome: a case report. *Med Pediatr Oncol.* 1993;21:456–9.
58. Odagiri K, Nishihira K, Hatekeyama S, Kobayashi K. Anterior mediastinal masses with calcifications on CT in children with histiocytosis-X (Langerhans cell histiocytosis). Report of two cases. *Pediatr Radiol.* 1991;21:550–1.
59. Ablu O, Egeler RM, Weitzman S. Langerhans cell histiocytosis: current concepts and treatments. *Cancer Treat Rev.* 2010;36:354–9.
60. Donadieu J, Bernard F, van Noesel M, et al. Cladribine and cytarabine in refractory multisystem Langerhans cell histiocytosis: results of an international phase 2 study. *Blood.* 2015;126:1415–23.
61. Haroche J, Cohen-Aubart F, Emile JF, et al. Dramatic efficacy of vemurafenib in both multisystemic and refractory Erdheim-Chester disease and Langerhans cell histiocytosis harboring the BRAF V600E mutation. *Blood.* 2013;121:1495–500.
62. Edelweiss M, Medeiros LJ, Suster S, Moran CA. Lymph node involvement by Langerhans cell histiocytosis: a clinicopathologic and immunohistochemical study of 20 cases. *Hum Pathol.* 2007;38:1463–9.
63. Garces S, Yin CC, Miranda RN, et al. Clinical, histopathologic, and immunoarchitectural features of dermatopathic lymphadenopathy: an update. *Mod Pathol.* 2020;33:1104–21.

64. Rosai J, Dorfman RF. Sinus histiocytosis with massive lymphadenopathy. A newly recognized benign clinicopathological entity. *Arch Pathol.* 1969;87:63–70.
65. Foucar E, Rosai J, Dorfman RF. Sinus histiocytosis with massive lymphadenopathy. *Arch Otolaryngol.* 1978;104:687–93.
66. Foucar E, Rosai J, Dorfman RF. Sinus histiocytosis with massive lymphadenopathy. An analysis of 14 deaths occurring in a patient registry. *Cancer.* 1984;54:1834–40.
67. Foucar E, Rosai J, Dorfman RF, Eyman JM. Immunologic abnormalities and their significance in sinus histiocytosis with massive lymphadenopathy. *Am J Clin Pathol.* 1984;82:515–25.
68. Levine PH, Jahan N, Murari P, Manak M, Jaffe ES. Detection of human herpesvirus 6 in tissues involved by sinus histiocytosis with massive lymphadenopathy (Rosai-Dorfman disease). *J Infect Dis.* 1992;166:291–5.
69. Mehraein Y, Wagner M, Remberger K, et al. Parvovirus B19 detected in Rosai-Dorfman disease in nodal and extranodal manifestations. *J Clin Pathol.* 2006;59:1320–6.
70. Ortonne N, Fillet AM, Kosuge H, Bagot M, Frances C, Wechsler J. Cutaneous Destombes-Rosai-Dorfman disease: absence of detection of HHV-6 and HHV-8 in skin. *J Cutan Pathol.* 2002;29:113–8.
71. Tsang WY, Yip TT, Chan JK. The Rosai-Dorfman disease histiocytes are not infected by Epstein-Barr virus. *Histopathology.* 1994;25:88–90.
72. Liu L, Perry AM, Cao W, et al. Relationship between Rosai-Dorfman disease and IgG4-related disease: study of 32 cases. *Am J Clin Pathol.* 2013;140:395–402.
73. Zhang X, Hyjek E, Vardiman J. A subset of Rosai-Dorfman disease exhibits features of IgG4-related disease. *Am J Clin Pathol.* 2013;139:622–32.
74. Menon MP, Evbuomwan MO, Rosai J, Jaffe ES, Pittaluga S. A subset of Rosai-Dorfman disease cases show increased IgG4-positive plasma cells: another red herring or a true association with IgG4-related disease? *Histopathology.* 2014;64:455–9.
75. Marsh WL Jr, McCarrick JP, Harlan DM. Sinus histiocytosis with massive lymphadenopathy. Occurrence in identical twins with retroperitoneal disease. *Arch Pathol Lab Med.* 1988;112:298–301.
76. Morgan NV, Morris MR, Cangul H, et al. Mutations in SLC29A3, encoding an equilibrative nucleoside transporter ENT3, cause a familial histiocytosis syndrome (Faisalabad histiocytosis) and familial Rosai-Dorfman disease. *PLoS Genet.* 2010;6:e1000833.
77. Rossbach HC, Dalence C, Wynn T, Tebbi C. Faisalabad histiocytosis mimics Rosai-Dorfman disease: brothers with lymphadenopathy, intrauterine fractures, short stature, and sensorineural deafness. *Pediatr Blood Cancer.* 2006;47:629–32.
78. Garces S, Medeiros LJ, Patel KP, et al. Mutually exclusive recurrent KRAS and MAP2K1 mutations in Rosai-Dorfman disease. *Mod Pathol.* 2017;30(10):1367–77.
79. Matter MS, Bihl M, Juskevicius D, Tzankov A. Is Rosai-Dorfman disease a reactive process? Detection of a MAP2K1 L115V mutation in a case of Rosai-Dorfman disease. *Virchows Arch.* 2017;471(4):545–7.
80. Jacobsen E, Shanmugam V, Jagannathan J. Rosai-Dorfman disease with activating KRAS mutation—response to Cobimetinib. *N Engl J Med.* 2017;377:2398–9.
81. Costa AL, Silva NO, Motta MP, Athanazio RA, Athanazio DA, Athanazio PR. Soft tissue Rosai-Dorfman disease of the posterior mediastinum. *J Bras Pneumol.* 2009;35:717–20.
82. Cunha BA, Durie N, Selbs E, Perez F. Fever of unknown origin (FUO) due to Rosai-Dorfman disease with mediastinal adenopathy mimicking lymphoma: diagnostic importance of elevated serum ferritin levels and polyclonal gammopathy. *Heart Lung.* 2009;38:83–8.
83. Dalia S, Sagatys E, Sokol L, Kubal T. Rosai-Dorfman disease: tumor biology, clinical features, pathology, and treatment. *Cancer Control.* 2014;21:322–7.
84. Rosai J, Dorfman RF. Sinus histiocytosis with massive lymphadenopathy: a pseudolymphomatous benign disorder. Analysis of 34 cases. *Cancer.* 1972;30:1174–88.
85. Overholtzer M, Brugge JS. The cell biology of cell-in-cell structures. *Nat Rev Mol Cell Biol.* 2008;9:796–809.
86. Rastogi V, Sharma R, Misra SR, Yadav L, Sharma V. Emperipolesis—a review. *J Clin Diagn Res.* 2014;8:ZM01–2.
87. Bonetti F, Chilosi M, Menestrina F, et al. Immunohistological analysis of Rosai-Dorfman histiocytosis. A disease of S-100 + CD1-histiocytes. *Virchows Arch A Pathol Anat Histopathol.* 1987;411:129–35.
88. Emile JF, Charlotte F, Amoura Z, Haroche J. BRAF mutations in Erdheim-Chester disease. *J Clin Oncol.* 2013;31:398.
89. Ozkaya N, Rosenblum MK, Durham BH, et al. The histopathology of Erdheim-Chester disease: a comprehensive review of a molecularly characterized cohort. *Mod Pathol.* 2018;31:581–97.
90. Temes R, Allen N, Chavez T, Crowell R, Key C, Wernly J. Primary mediastinal malignancies in children: report of 22 patients and comparison to 197 adults. *Oncologist.* 2000;5:179–84.
91. Temes R, Chavez T, Mapel D, et al. Primary mediastinal malignancies: findings in 219 patients. *West J Med.* 1999;170:161–6.
92. Macchiarini P, Ostertag H. Uncommon primary mediastinal tumours. *Lancet Oncol.* 2004;5:107–18.
93. Strickler JG, Kurtin PJ. Mediastinal lymphoma. *Semin Diagn Pathol.* 1991;8:2–13.
94. Klapper W, Jaffe E, Gaulard P, et al. Primary mediastinal large B-cell lymphoma. In: Travis W, Brambilla E, Burke A, Marx A, Nicholson A, editors. WHO classification of tumors of the lung, pleura, thymus and heart. 4th ed. Lyon: IARC; 2015. p. 267–9.
95. Cazals-Hatem D, Lepage E, Brice P, et al. Primary mediastinal large B-cell lymphoma. A clinicopathologic study of 141 cases compared with 916 nonmediastinal large B-cell lymphomas, a GELA (“Groupe d’Etude des Lymphomes de l’Adulte”) study. *Am J Surg Pathol.* 1996;20:877–88.
96. Dunleavy K. Primary mediastinal B-cell lymphoma: biology and evolving therapeutic strategies. *Hematol Am Soc Hematol Educ Program.* 2017;2017:298–303.
97. Rosenwald A, Wright G, Leroy K, et al. Molecular diagnosis of primary mediastinal B cell lymphoma identifies a clinically favorable subgroup of diffuse large B cell lymphoma related to Hodgkin lymphoma. *J Exp Med.* 2003;198:851–62.
98. Savage KJ, Al-Rajhi N, Voss N, et al. Favorable outcome of primary mediastinal large B-cell lymphoma in a single institution: the British Columbia experience. *Ann Oncol.* 2006;17:123–30.
99. Lichtenstein AK, Levine A, Taylor CR, et al. Primary mediastinal lymphoma in adults. *Am J Med.* 1980;68:509–14.
100. Miller JB, Variakojis D, Bitran JD, et al. Diffuse histiocytic lymphoma with sclerosis: a clinicopathologic entity frequently causing superior venacaval obstruction. *Cancer.* 1981;47:748–56.
101. Moller P, Lammler B, Eberlein-Gonska M, et al. Primary mediastinal clear cell lymphoma of B-cell type. *Virchows Arch A Pathol Anat Histopathol.* 1986;409:79–92.
102. Moller P, Moldenhauer G, Momburg F, et al. Mediastinal lymphoma of clear cell type is a tumor corresponding to terminal steps of B cell differentiation. *Blood.* 1987;69:1087–95.
103. Nakagawa A, Nakamura S, Koshikawa T, et al. Clinicopathologic study of primary mediastinal non-lymphoblastic non-Hodgkin’s lymphomas among the Japanese. *Acta Pathol Jpn.* 1993;43:44–54.
104. Perrone T, Frizzera G, Rosai J. Mediastinal diffuse large-cell lymphoma with sclerosis. A clinicopathologic study of 60 cases. *Am J Surg Pathol.* 1986;10:176–91.
105. Davis RE, Dorfman RF, Warnke RA. Primary large-cell lymphoma of the thymus: a diffuse B-cell neoplasm presenting as primary mediastinal lymphoma. *Hum Pathol.* 1990;21:1262–8.
106. Lamarre L, Jacobson JO, Aisenberg AC, Harris NL. Primary large cell lymphoma of the mediastinum. A histologic and immunophenotypic study of 29 cases. *Am J Surg Pathol.* 1989;13:730–9.

107. Menestrina F, Chilosi M, Bonetti F, et al. Mediastinal large-cell lymphoma of B-type, with sclerosis: histopathological and immunohistochemical study of eight cases. *Histopathology*. 1986;10:589–600.
108. Yousem SA, Weiss LM, Warnke RA. Primary mediastinal non-Hodgkin's lymphomas: a morphologic and immunologic study of 19 cases. *Am J Clin Pathol*. 1985;83:676–80.
109. Hofmann WJ, Momburg F, Moller P. Thymic medullary cells expressing B lymphocyte antigens. *Hum Pathol*. 1988;19:1280–7.
110. Hofmann WJ, Momburg F, Moller P, Otto HF. Intra- and extra-thymic B cells in physiologic and pathologic conditions. Immunohistochemical study on normal thymus and lymphofollicular hyperplasia of the thymus. *Virchows Arch A Pathol Anat Histopathol*. 1988;412:431–42.
111. Isaacson PG, Norton AJ, Addis BJ. The human thymus contains a novel population of B lymphocytes. *Lancet*. 1987;2:1488–91.
112. Calaminici M, Piper K, Lee AM, Norton AJ. CD23 expression in mediastinal large B-cell lymphomas. *Histopathology*. 2004;45:619–24.
113. Fend F, Nachbaur D, Oberwasserlechner F, Kreczy A, Huber H, Muller-Hermelink HK. Phenotype and topography of human thymic B cells. An immunohistologic study. *Virchows Arch B Cell Pathol Incl Mol Pathol*. 1991;60:381–8.
114. Colby TV, Yousem SA. Pulmonary lymphoid neoplasms. *Semin Diagn Pathol*. 1985;2:183–96.
115. Dunleavy K, Pittaluga S, Maeda LS, et al. Dose-adjusted EPOCH-rituximab therapy in primary mediastinal B-cell lymphoma. *N Engl J Med*. 2013;368:1408–16.
116. Shimosato Y, Mukai K. Atlas of tumor pathology. Tumors of the mediastinum. 3rd ed. Washington: Armed Forces Institute of Pathology; 1995.
117. Pileri SA, Gaidano G, Zinzani PL, et al. Primary mediastinal B-cell lymphoma: high frequency of BCL-6 mutations and consistent expression of the transcription factors OCT-2, BOB.1, and PU.1 in the absence of immunoglobulins. *Am J Pathol*. 2003;162:243–53.
118. de Leval L, Ferry JA, Falini B, Shipp M, Harris NL. Expression of bcl-6 and CD10 in primary mediastinal large B-cell lymphoma: evidence for derivation from germinal center B cells? *Am J Surg Pathol*. 2001;25:1277–82.
119. Hoeller S, Zihler D, Zlobec I, et al. BOB.1, CD79a and cyclin E are the most appropriate markers to discriminate classical Hodgkin's lymphoma from primary mediastinal large B-cell lymphoma. *Histopathology*. 2010;56:217–28.
120. Higgins JP, Warnke RA. CD30 expression is common in mediastinal large B-cell lymphoma. *Am J Clin Pathol*. 1999;112:241–7.
121. Copie-Bergman C, Plonquet A, Alonso MA, et al. MAL expression in lymphoid cells: further evidence for MAL as a distinct molecular marker of primary mediastinal large B-cell lymphomas. *Mod Pathol*. 2002;15:1172–80.
122. Gentry M, Bodo J, Durkin L, Hsi ED. Performance of a commercially available MAL antibody in the diagnosis of primary mediastinal large B-cell lymphoma. *Am J Surg Pathol*. 2017;41:189–94.
123. Bledsoe JR, Redd RA, Hasserjian RP, et al. The immunophenotypic spectrum of primary mediastinal large B-cell lymphoma reveals prognostic biomarkers associated with outcome. *Am J Hematol*. 2016;91:E436–41.
124. Pelland K, Mathews S, Kamath A, et al. Dendritic cell markers and PD-L1 are expressed in mediastinal gray zone lymphoma. *Appl Immunohistochem Mol Morphol*. 2018;26:e101–e6.
125. Tanaka Y, Maeshima AM, Nomoto J, et al. Expression pattern of PD-L1 and PD-L2 in classical Hodgkin lymphoma, primary mediastinal large B-cell lymphoma, and gray zone lymphoma. *Eur J Haematol*. 2018;100:511–7.
126. Shi M, Roemer MG, Chapuy B, et al. Expression of programmed cell death 1 ligand 2 (PD-L2) is a distinguishing feature of primary mediastinal (thymic) large B-cell lymphoma and associated with PDCD1LG2 copy gain. *Am J Surg Pathol*. 2014;38:1715–23.
127. De Mello CA, De Andrade VP, De Lima VC, Carvalho AL, Soares FA. Prognostic impact of MUM1 expression by immunohistochemistry on primary mediastinal large B-cell lymphoma. *Leuk Lymphoma*. 2011;52:1495–503.
128. Lees C, Keane C, Gandhi MK, Gunawardana J. Biology and therapy of primary mediastinal B-cell lymphoma: current status and future directions. *Br J Haematol*. 2019;185:25–41.
129. Guiter C, Dusanter-Fourt I, Copie-Bergman C, et al. Constitutive STAT6 activation in primary mediastinal large B-cell lymphoma. *Blood*. 2004;104:543–9.
130. Menter T, Tzankov A. Genetic alterations of 9p24 in lymphomas and their impact for cancer (immuno-)therapy. *Virchows Arch*. 2019;474:497–509.
131. Mottok A, Woolcock B, Chan FC, et al. Genomic alterations in CIITA are frequent in primary mediastinal large B cell lymphoma and are associated with diminished MHC class II expression. *Cell Rep*. 2015;13:1418–31.
132. Twa DD, Chan FC, Ben-Neriah S, et al. Genomic rearrangements involving programmed death ligands are recurrent in primary mediastinal large B-cell lymphoma. *Blood*. 2014;123:2062–5.
133. Schmitz R, Hansmann ML, Bohle V, et al. TNFAIP3 (A20) is a tumor suppressor gene in Hodgkin lymphoma and primary mediastinal B cell lymphoma. *J Exp Med*. 2009;206:981–9.
134. Mansouri L, Noerenberg D, Young E, et al. Frequent NFKBIE deletions are associated with poor outcome in primary mediastinal B-cell lymphoma. *Blood*. 2016;128:2666–70.
135. Tsang P, Cesarman E, Chadburn A, Liu YF, Knowles DM. Molecular characterization of primary mediastinal B cell lymphoma. *Am J Pathol*. 1996;148:2017–25.
136. Suster S, Moran CA. Pleomorphic large cell lymphomas of the mediastinum. *Am J Surg Pathol*. 1996;20:224–32.
137. Hans CP, Weisenburger DD, Greiner TC, et al. Confirmation of the molecular classification of diffuse large B-cell lymphoma by immunohistochemistry using a tissue microarray. *Blood*. 2004;103:275–82.
138. Klui PM, Harris NL, Stein H, et al. High-grade B-cell lymphoma. In: Swerdlow SH, Campo E, Harris NL, et al., editors. WHO classification of tumors of the hematopoietic and lymphoid tissues. Lyon: IARC; 2017. p. 335–41.
139. Sehn LH, Salles G. Diffuse large B-cell lymphoma. *N Engl J Med*. 2021;384:842–58.
140. Traverse-Glehen A, Pittaluga S, Gaulard P, et al. Mediastinal gray zone lymphoma: the missing link between classic Hodgkin's lymphoma and mediastinal large B-cell lymphoma. *Am J Surg Pathol*. 2005;29:1411–21.
141. García JF, Mollejo M, Fraga M, et al. Large B-cell lymphoma with Hodgkin's features. *Histopathology*. 2005;47:101–10.
142. Jaffe ES, Stein H, Swerdlow SH, Campo E, Pileri SA, Harris NL. B-cell lymphoma, unclassifiable, with features intermediate between diffuse large B-cell lymphoma and classic Hodgkin lymphoma. In: Swerdlow SH, Campo E, Harris NL, et al., editors. WHO classification of tumors of hematopoietic and lymphoid tissues. Lyon: IARC; 2008. p. 267–8.
143. Jaffe ES, Stein H, Swerdlow SH, Campo E, Pileri S, Harris NL. B-cell lymphoma, unclassifiable, with features intermediate between diffuse large B-cell lymphoma and classic Hodgkin lymphoma. In: Swerdlow SH, Campo E, Harris NL, et al., editors. WHO classification of tumors of hematopoietic and lymphoid tissues (revised 4th edition). Lyon: IARC; 2017. p. 342–4.
144. Schurch CM, Federmann B, Quintanilla-Martinez L, Fend F. Tumor heterogeneity in lymphomas: a different breed. *Pathobiology*. 2018;85:130–45.
145. Wilson WH, Pittaluga S, Nicolae A, et al. A prospective study of mediastinal gray-zone lymphoma. *Blood*. 2014;124:1563–9.
146. Evens AM, Kanakry JA, Sehn LH, et al. Gray zone lymphoma with features intermediate between classical Hodgkin lymphoma and diffuse large B-cell lymphoma: characteristics, outcomes, and

- prognostication among a large multicenter cohort. *Am J Hematol*. 2015;90:778–83.
147. Grant C, Dunleavy K, Eberle FC, Pittaluga S, Wilson WH, Jaffe ES. Primary mediastinal large B-cell lymphoma, classic Hodgkin lymphoma presenting in the mediastinum, and mediastinal gray zone lymphoma: what is the oncologist to do? *Curr Hematol Malig Rep*. 2011;6:157–63.
  148. Sarkozy C, Molina T, Ghesquieres H, et al. Mediastinal gray zone lymphoma: clinico-pathological characteristics and outcomes of 99 patients from the Lymphoma Study Association. *Haematologica*. 2017;102:150–9.
  149. Sarkozy C, Copie-Bergmand C, Damotte D, et al. Gray-zone lymphoma between cHL and large B-cell lymphoma: a histopathologic series from the LYSA. *Am J Surg Pathol*. 2019;43(3):341–51.
  150. O'Malley DP, Fedoriw Y, Weiss LM. Distinguishing classical Hodgkin lymphoma, gray zone lymphoma, and large B-cell lymphoma: a proposed scoring system. *Appl Immunohistochem Mol Morphol*. 2016;24:535–40.
  151. Pilichowska M, Pittaluga S, Ferry JA, et al. Clinicopathologic consensus study of gray zone lymphoma with features intermediate between DLBCL and classical HL. *Blood Adv*. 2017;1:2600–9.
  152. Isaacson P, Wright DH. Malignant lymphoma of mucosa-associated lymphoid tissue. A distinctive type of B-cell lymphoma. *Cancer*. 1983;52:1410–6.
  153. Isaacson PG, Chan JK, Tang C, Addis BJ. Low-grade B-cell lymphoma of mucosa-associated lymphoid tissue arising in the thymus. A thymic lymphoma mimicking myoepithelial sialadenitis. *Am J Surg Pathol*. 1990;14:342–51.
  154. Takagi N, Nakamura S, Yamamoto K, et al. Malignant lymphoma of mucosa-associated lymphoid tissue arising in the thymus of a patient with Sjogren's syndrome. A morphologic, phenotypic, and genotypic study. *Cancer*. 1992;69:1347–55.
  155. Weissferdt A, Moran CA. Thymic hyperplasia with lymphoepithelial sialadenitis (LESA)-like features: a clinicopathologic and immunohistochemical study of 4 cases. *Am J Clin Pathol*. 2012;138:816–22.
  156. Porubsky S, Popovic ZV, Badve S, et al. Thymic hyperplasia with lymphoepithelial sialadenitis (LESA)-like features: strong association with lymphomas and non-myasthenic autoimmune diseases. *Cancers (Basel)*. 2021;13.
  157. Go H, Cho HJ, Paik JH, et al. Thymic extranodal marginal zone B-cell lymphoma of mucosa-associated lymphoid tissue: a clinicopathological and genetic analysis of six cases. *Leuk Lymphoma*. 2011;52:2276–83.
  158. Lersbach RB, Pinkus GS, Shahsafaei A, Dorfman DM. Primary marginal zone lymphoma of the thymus. *Am J Clin Pathol*. 2000;113:784–91.
  159. Sakamoto T, Yamashita K, Mizumoto C, et al. MALT lymphoma of the thymus with Sjogren's syndrome: biphasic changes in serological abnormalities over a 4-year period following thymectomy. *Int J Hematol*. 2009;89:709–13.
  160. Shimizu K, Yoshida J, Kakegawa S, et al. Primary thymic mucosa-associated lymphoid tissue lymphoma: diagnostic tips. *J Thorac Oncol*. 2010;5:117–21.
  161. Weissferdt A, Moran CA. Primary MALT-type lymphoma of the thymus: a clinicopathological and immunohistochemical study of six cases. *Lung*. 2011;189:461–6.
  162. Giroux Leprieur E, Antoine M, Gounant V, Copie-Bergman C, Lavole A, Milleron B. [Association between thymic MALT lymphoma and Sjogren's syndrome]. *Rev Pneumol Clin*. 2009;65:108–12.
  163. Kurabayashi A, Iguchi M, Matsumoto M, Hiroi M, Kume M, Furihata M. Thymic mucosa-associated lymphoid tissue lymphoma with immunoglobulin-storing histiocytosis in Sjogren's syndrome. *Pathol Int*. 2010;60:125–30.
  164. Shimizu K, Ishii G, Nagai K, et al. Extranodal marginal zone B-cell lymphoma of mucosa-associated lymphoid tissue (MALT lymphoma) in the thymus: report of four cases. *Jpn J Clin Oncol*. 2005;35:412–6.
  165. Muramatsu T, Tanaka Y, Higure R, Iizuka M, Hata H, Shiono M. Thymic and pulmonary mucosa-associated lymphoid tissue lymphomas. *Ann Thorac Surg*. 2013;95:e69–70.
  166. Nagasaka T, Lai R, Harada T, et al. Coexisting thymic and gastric lymphomas of mucosa-associated lymphoid tissues in a patient with Sjogren syndrome. *Arch Pathol Lab Med*. 2000;124:770–3.
  167. Sunohara M, Hara K, Osamura K, et al. Mucosa associated lymphoid tissue (MALT) lymphoma of the thymus with trisomy 18. *Intern Med*. 2009;48:2025–32.
  168. Yamanaka S, Uekusa T, Tajiri M. [Mucosa-associated lymphoid tissue lymphoma in the thymus with multiple amyloid nodules in the both lungs]. *Kyobu Geka*. 2010;63:392–5.
  169. Balakrishna JP, Jaffe ES. Crystal-storing histiocytosis associated with thymic extranodal marginal zone lymphoma. *Blood*. 2017;130:1683.
  170. Inagaki H, Chan JK, Ng JW, et al. Primary thymic extranodal marginal-zone B-cell lymphoma of mucosa-associated lymphoid tissue type exhibits distinctive clinicopathological and molecular features. *Am J Pathol*. 2002;160:1435–43.
  171. Kominato S, Nakayama T, Sato F, et al. Characterization of chromosomal aberrations in thymic MALT lymphoma. *Pathol Int*. 2012;62:93–8.
  172. Ortonne N, Copie-Bergman C, Remy P, et al. Mucosa-associated lymphoid tissue lymphoma of the thymus: a case report with no evidence of MALT1 rearrangement. *Virchows Arch*. 2005;446:189–93.
  173. Harigae H, Ichinohasama R, Miura I, et al. Primary marginal zone lymphoma of the thymus accompanied by chromosomal anomaly 46,X,dup(X)(p11p22). *Cancer Genet Cytogenet*. 2002;133:142–7.
  174. Momoi A, Nagai K, Isahai N, Sakai T, Ohshima K, Aoki S. Thymic extranodal marginal zone lymphoma of mucosa-associated lymphoid tissue with 8q24 abnormality. *Intern Med*. 2016;55:799–803.
  175. Yoshida M, Okabe M, Eimoto T, et al. Immunoglobulin VH genes in thymic MALT lymphoma are biased toward a restricted repertoire and are frequently unmutated. *J Pathol*. 2006;208:415–22.
  176. Takino H, Li C, Yamada S, et al. Thymic extranodal marginal zone lymphoma of mucosa-associated lymphoid tissue: a gene methylation study. *Leuk Lymphoma*. 2013;54:1742–6.
  177. Ganesh M, Sankar NS, Jagannathan R. Extramedullary plasmacytoma presenting as upper back pain. *J R Soc Promot Health*. 2000;120:262–5.
  178. Jacob JJ, John M, Thomas M, Thomas N, Nair A. Plasmacytoma mimicking mediastinal parathyroid tumour in a patient with primary hyperparathyroidism. *Asian J Surg*. 2007;30:147–50.
  179. Lee SY, Kim JH, Shin JS, et al. A case of extramedullary plasmacytoma arising from the posterior mediastinum. *Korean J Intern Med*. 2005;20:173–6.
  180. Miyazaki T, Kohno S, Sakamoto A, et al. A rare case of extramedullary plasmacytoma in the mediastinum. *Intern Med*. 1992;31:1363–5.
  181. Moran CA, Suster S, Fishback NF, Koss MN. Extramedullary plasmacytomas presenting as mediastinal masses: clinicopathologic study of two cases preceding the onset of multiple myeloma. *Mod Pathol*. 1995;8:257–9.
  182. Raci-Wetherbee E, Dincer HE. IgG myeloma presenting as a large mediastinal mass and pleural effusion. *J Bronchology Interv Pulmonol*. 2012;19:65–7.
  183. Salem KZ, Nishihori T, Kharfan-Dabaja MA, Horna P, Alsina M. Primary plasmacytoma involving mediastinal lymph nodes: A diagnostic mimicry of primary mediastinal lymphoma. *Hematol Oncol Stem Cell Ther*. 2016;9:26–9.
  184. Bink K, Haralambieva E, Kremer M, et al. Primary extramedullary plasmacytoma: similarities with and differences from multi-

- ple myeloma revealed by interphase cytogenetics. *Haematologica*. 2008;93:623–6.
185. Bassan R, Maino E, Cortelazzo S. Lymphoblastic lymphoma: an updated review on biology, diagnosis, and treatment. *Eur J Haematol*. 2016;96:447–60.
  186. Cortelazzo S, Ferreri A, Hoelzer D, Ponzoni M. Lymphoblastic lymphoma. *Crit Rev Oncol Hematol*. 2017;113:304–17.
  187. Maeshima AM, Taniguchi H, Suzuki T, et al. Distribution of malignant lymphomas in the anterior mediastinum: a single-institution study of 76 cases in Japan, 1997–2016. *Int J Hematol*. 2017;106:675–80.
  188. Waldron JA Jr, Dohring EJ, Farber LR. Primary large cell lymphomas of the mediastinum: an analysis of 20 cases. *Semin Diagn Pathol*. 1985;2:281–95.
  189. Boucheix C, Diebold J, Bernadou A, et al. Lymphoblastic lymphoma/leukemia with convoluted nuclei: the question of its relation to the T-cell lineage studied in 13 patients. *Cancer*. 1980;45:1569–77.
  190. Navas Palacios JJ, Valdes MD, Pallares MA, Gomez de Salazar MD, Garcia MA. Lymphoblastic lymphoma/leukemia of T-cell origin: ultrastructural, cytochemical, and immunologic features of ten cases. *Cancer*. 1981;48:1982–91.
  191. Stein H, Petersen N, Gaedicke G, Lennert K, Landbeck G. Lymphoblastic lymphoma of convoluted or acid phosphatase type-a tumor of T precursor cells. *Int J Cancer*. 1976;17:292–5.
  192. Donlon JA, Jaffe ES, Braylan RC. Terminal deoxynucleotidyl transferase activity in malignant lymphomas. *N Engl J Med*. 1977;297:461–4.
  193. Borowitz MJ, Falletta JM. Leukemias and lymphomas of thymic differentiation. *Clin Lab Med*. 1988;8:119–34.
  194. Brazier RM, Keneklis T, Donlon JA, et al. Terminal deoxynucleotidyl transferase in non-Hodgkin's lymphoma. *Am J Clin Pathol*. 1983;80:655–9.
  195. Harris NL, Jaffe ES, Stein H, et al. A revised European-American classification of lymphoid neoplasms: a proposal from the International Lymphoma Study Group. *Blood*. 1994;84:1361–92.
  196. Swerdlow SH, Campo E, Harris NL, et al. WHO classification of tumours of haematopoietic and lymphoid tissues. Lyon: IARC; 2008.
  197. Dong M, Zhang X, Yang Z, et al. Patients over 40 years old with precursor T-cell lymphoblastic lymphoma have different prognostic factors comparing to the youngsters. *Sci Rep*. 2018;8:1088.
  198. Jin X, Zhao HF, Yu Y, et al. Analysis of clinical characteristics and prognostic factors of primary mediastinal T-cell lymphoblastic lymphoma. *Zhongguo Shi Yan Xue Ye Xue Za Zhi*. 2013;21:377–82.
  199. Borowitz MJ, Chan JKC, Bene M-C, Arber DA. T-lymphoblastic leukemia/lymphoma. In: Swerdlow SH, Campo E, Harris NL, et al., editors. WHO classification of tumors of hematopoietic and lymphoid tissue. Revised 4th edition. Lyon: IARC; 2017. p. 209–12.
  200. Abruzzo LV, Jaffe ES, Cotelingam JD, Whang-Peng J, Del Duca V, Jr., Medeiros LJ. T-cell lymphoblastic lymphoma with eosinophilia associated with subsequent myeloid malignancy. *Am J Surg Pathol*. 1992;16:236–45.
  201. Jackson CC, Medeiros LJ, Miranda RN. 8p11 myeloproliferative syndrome: a review. *Hum Pathol*. 2010;41:461–76.
  202. Vega F, Medeiros LJ, Bueso-Ramos CE, Arboleda P, Miranda RN. Hematolymphoid neoplasms associated with rearrangements of PDGFRA, PDGFRB, and FGFR1. *Am J Clin Pathol*. 2015;144:377–92.
  203. Vega F, Medeiros LJ, Davuluri R, Cromwell CC, Alkan S, Abruzzo LV. t(8;13)-positive bilineal lymphomas: report of 6 cases. *Am J Surg Pathol*. 2008;32:14–20.
  204. Jain N, Lamb AV, O'Brien S, et al. Early T-cell precursor acute lymphoblastic leukemia/lymphoma (ETP-ALL/LBL) in adolescents and adults: a high-risk subtype. *Blood*. 2016;127:1863–9.
  205. Chisholm KM, Krishnan C, Heerema-McKenney A, Natkunam Y. Immunohistochemical profile of MYC protein in pediatric small round blue cell tumors. *Pediatr Dev Pathol*. 2017;20:213–23.
  206. Boddu P, Thakral B, Alhurairi A, et al. Distinguishing thymoma from T-lymphoblastic leukaemia/lymphoma: a case-based evaluation. *J Clin Pathol*. 2019;72(3):251–7.
  207. Adam P, Hakrrouch S, Hofmann I, Reidenbach S, Marx A, Strobel P. Thymoma with loss of keratin expression (and giant cells): a potential diagnostic pitfall. *Virchows Arch*. 2014;465:313–20.
  208. Bhaker P, Das A, Rajwanshi A, et al. Precursor T-lymphoblastic lymphoma: Speedy diagnosis in FNA and effusion cytology by morphology, immunochemistry, and flow cytometry. *Cancer Cytopathol*. 2015;123:557–65.
  209. Gorczyca W, Tugulea S, Liu Z, Li X, Wong JY, Weisberger J. Flow cytometry in the diagnosis of mediastinal tumors with emphasis on differentiating thymocytes from precursor T-lymphoblastic lymphoma/leukemia. *Leuk Lymphoma*. 2004;45:529–38.
  210. Ward N, Baqai J, Zehnpfennig A, Fine N, Huang J, Smith MD. Bcl-2 maturation pattern in T-cells distinguishes thymic neoplasm/hyperplasia, T-lymphoblastic lymphoma, and reactive lymph nodes. *Cytometry B Clin Cytom*. 2018;94:444–50.
  211. Siegert E, Weissbach G, Fischer R, Lauterbach I. Non-Hodgkin lymphoma (NHL) as a second neoplasm occurring after neuroblastoma treatment. *Med Pediatr Oncol*. 1998;30:18–21.
  212. Sekimizu M, Sunami S, Nakazawa A, et al. Chromosome abnormalities in advanced stage T-cell lymphoblastic lymphoma of children and adolescents: a report from Japanese Paediatric Leukaemia/Lymphoma Study Group (JPLSG) and review of the literature. *Br J Haematol*. 2011;154:612–7.
  213. Krieger D, Moericke A, Oschlies I, et al. Frequency and clinical relevance of DNA microsatellite alterations of the CDKN2A/B, ATM and p53 gene loci: a comparison between pediatric precursor T-cell lymphoblastic lymphoma and T-cell lymphoblastic leukemia. *Haematologica*. 2010;95:158–62.
  214. Bongiovanni D, Saccomani V, Piovani E. Aberrant signaling pathways in T-cell acute lymphoblastic leukemia. *Int J Mol Sci*. 2017;18.
  215. Baleydiere F, Decouvelaere AV, Bergeron J, et al. T cell receptor genotyping and HOXA/TLX1 expression define three T lymphoblastic lymphoma subsets which might affect clinical outcome. *Clin Cancer Res*. 2008;14:692–700.
  216. Stein H, Mason DY, Gerdes J, et al. The expression of the Hodgkin's disease associated antigen Ki-1 in reactive and neoplastic lymphoid tissue: evidence that Reed-Sternberg cells and histiocytic malignancies are derived from activated lymphoid cells. *Blood*. 1985;66:848–58.
  217. Bullrich F, Morris SW, Hummel M, Pileri S, Stein H, Croce CM. Nucleophosmin (NPM) gene rearrangements in Ki-1-positive lymphomas. *Cancer Res*. 1994;54:2873–7.
  218. Morris SW, Kirstein MN, Valentine MB, et al. Fusion of a kinase gene, ALK, to a nucleolar protein gene, NPM, in non-Hodgkin's lymphoma. *Science*. 1994;263:1281–4.
  219. Shiota M, Fujimoto J, Takenaga M, et al. Diagnosis of t(2;5)(p23;q35)-associated Ki-1 lymphoma with immunohistochemistry. *Blood*. 1994;84:3648–52.
  220. Shiota M, Nakamura S, Ichinohasama R, et al. Anaplastic large cell lymphomas expressing the novel chimeric protein p80NPM/ALK: a distinct clinicopathologic entity. *Blood*. 1995;86:1954–60.
  221. Gonin J, Kadir H, Bensaci S, et al. Primary mediastinal anaplastic alk-1-positive large-cell lymphoma of T/NK-cell type expressing CD20. *Virchows Arch*. 2007;450:355–8.
  222. Sevilla DW, Choi JK, Gong JZ. Mediastinal adenopathy, lung infiltrates, and hemophagocytosis: unusual manifestation of pediatric anaplastic large cell lymphoma: report of two cases. *Am J Clin Pathol*. 2007;127:458–64.

223. Makiguchi N, Ohsaki Y, Fujiuchi S, et al. Ki-1-positive anaplastic large-cell lymphoma with mediastinal involvement. *Nihon Kyobu Shikkan Gakkai Zasshi*. 1997;35:660–4.
224. Kayao J, Tamaru J, Wakita H, et al. Anaplastic large cell lymphoma of the mediastinum diagnosed by transbronchial scratch cytology. A case report. *Acta Cytol*. 2002;46:405–11.
225. Xing X, Feldman AL. Anaplastic large cell lymphomas: ALK positive, ALK negative, and primary cutaneous. *Adv Anat Pathol*. 2015;22:29–49.
226. Parrilla Castellar ER, Jaffe ES, Said JW, et al. ALK-negative anaplastic large cell lymphoma is a genetically heterogeneous disease with widely disparate clinical outcomes. *Blood*. 2014;124:1473–80.
227. Hodgkin T. On some morbid appearances of the absorbent glands and spleen. *Med Chir Trans (London)*. 1832;17:68–114.
228. Wilks S. Cases of enlargement of the lymphatic glands and spleen, (or Hodgkin's disease), with remarks. *Guy's Hospital Rep*. 1865;11:56–67.
229. Ortiz-Hidalgo C. A short history of Hodgkin's disease and Burkitt's lymphoma. *Am J Clin Pathol*. 1994;101:S27–33.
230. Sternberg C. Über eine eigenartige unter dem Bilde der Pseudoleukämie Verlaufende Tuberculose des lymphatischen Apparates. *Ztschz Heilk*. 1898;19:21–90.
231. Reed DM. On the pathological changes in Hodgkin's disease, with especial reference to its relation to tuberculosis. *Johns Hopkins Hosp Rep*. 1902;10:133–96.
232. Kanzler H, Kuppers R, Hansmann ML, Rajewsky K. Hodgkin and Reed-Sternberg cells in Hodgkin's disease represent the outgrowth of a dominant tumor clone derived from (crippled) germinal center B cells. *J Exp Med*. 1996;184:1495–505.
233. Kuppers R, Kanzler H, Hansmann ML, Rajewsky K. Immunoglobulin V genes in Reed-Sternberg cells. *N Engl J Med*. 1996;334:404. Author reply 5–6.
234. Kuppers R, Rajewsky K, Zhao M, et al. Hodgkin disease: Hodgkin and Reed-Sternberg cells picked from histological sections show clonal immunoglobulin gene rearrangements and appear to be derived from B cells at various stages of development. *Proc Natl Acad Sci U S A*. 1994;91:10962–6.
235. Teras LR, DeSantis CE, Cerhan JR, Morton LM, Jemal A, Flowers CR. 2016 US lymphoid malignancy statistics by World Health Organization subtypes. *CA Cancer J Clin*. 2016;66:443–59.
236. Hutchison GB. International symposium on Hodgkin's disease. Session 6. Survival data and prognosis. Criteria of cure: statistical considerations. *Natl Cancer Inst Monogr*. 1973;36:561–5.
237. Shimkin MB. Hodgkin's disease; mortality in the United States, 1921-1951; race, sex and age distribution; comparison with leukemia. *Blood*. 1955;10:1214–27.
238. Shimkin MB, Oppermann KC, Bostick WL, Low-Beer BV. Hodgkin's disease: an analysis of frequency, distribution and mortality at the University of California Hospital 1914-1951. *Ann Intern Med*. 1955;42:136–53.
239. al-Naaman YD, al-Ani MS, al-Omeri MM. Primary mediastinal tumours. *Thorax*. 1974;29:475–81.
240. Benjamin SP, McCormack LJ, Effler DB, Groves LK. Primary lymphatic tumors of the mediastinum. *Cancer*. 1972;30:708–12.
241. Eberle FC, Mani H, Jaffe ES. Histopathology of Hodgkin's lymphoma. *Cancer J*. 2009;15:129–37.
242. Lister TA, Crowther D, Sutcliffe SB, et al. Report of a committee convened to discuss the evaluation and staging of patients with Hodgkin's disease: Cotswolds meeting. *J Clin Oncol*. 1989;7:1630–6.
243. Bonadonna G. Historical review of Hodgkin's disease. *Br J Haematol*. 2000;110:504–11.
244. Diehl V, Thomas RK, Re D. Part II: Hodgkin's lymphoma—diagnosis and treatment. *Lancet Oncol*. 2004;5:19–26.
245. Ansell SM, Lesokhin AM, Borrello I, et al. PD-1 blockade with nivolumab in relapsed or refractory Hodgkin's lymphoma. *N Engl J Med*. 2015;372:311–9.
246. Armand P, Shipp MA, Ribrag V, et al. Programmed death-1 blockade with pembrolizumab in patients with classical Hodgkin lymphoma after brentuximab vedotin failure. *J Clin Oncol*. 2016;34(31):3733–9.
247. Hoppe RT, Advani RH, Ai WZ, et al. Hodgkin lymphoma, version 2.2015. *J Natl Compr Canc Netw*. 2015;13:554–86.
248. Roemer MG, Advani RH, Ligon AH, et al. PD-L1 and PD-L2 genetic alterations define classical Hodgkin lymphoma and predict outcome. *J Clin Oncol*. 2016;34:2690–7.
249. O'Malley DP, Dogan A, Fedoriw Y, Medeiros LJ, Ok CY, Salama ME. American Registry of Pathology Expert Opinions: Immunohistochemical evaluation of classic Hodgkin lymphoma. *Ann Diagn Pathol*. 2019;39:105–10.
250. Carbone A, Ghoghini A, Aldinucci D, Gattei V, Dalla-Favera R, Gaidano G. Expression pattern of MUM1/IRF4 in the spectrum of pathology of Hodgkin's disease. *Br J Haematol*. 2002;117:366–72.
251. Pileri SA, Ascani S, Leoncini L, et al. Hodgkin's lymphoma: the pathologist's viewpoint. *J Clin Pathol*. 2002;55:162–76.
252. Andorsky DJ, Yamada RE, Said J, Pinkus GS, Betting DJ, Timmerman JM. Programmed death ligand 1 is expressed by non-Hodgkin lymphomas and inhibits the activity of tumor-associated T cells. *Clin Cancer Res*. 2011;17:4232–44.
253. Paydas S, Bağır E, Seydaoglu G, Ercolak V, Ergin M. Programmed death-1 (PD-1), programmed death-ligand 1 (PD-L1), and EBV-encoded RNA (EBER) expression in Hodgkin lymphoma. *Ann Hematol*. 2015;94:1545–52.
254. Xie W, Medeiros LJ, Li S, Yin CC, Khoury JD, Xu J. PD-1/PD-L1 pathway and its blockade in patients with classic Hodgkin lymphoma and non-Hodgkin large-cell lymphomas. *Curr Hematol Malig Rep*. 2020;15:372–81.
255. Pallesen G, Hamilton-Dutoit SJ, Rowe M, Young LS. Expression of Epstein-Barr virus latent gene products in tumour cells of Hodgkin's disease. *Lancet*. 1991;337:320–2.
256. Uccini S, Monardo F, Ruco LP, et al. High frequency of Epstein-Barr virus genome in HIV-positive patients with Hodgkin's disease. *Lancet*. 1989;1:1458.
257. Weiss LM, Movahed LA, Warnke RA, Sklar J. Detection of Epstein-Barr viral genomes in Reed-Sternberg cells of Hodgkin's disease. *N Engl J Med*. 1989;320:502–6.
258. Harris JA, Jain S, Ren Q, Zarineh A, Liu C, Ibrahim S. CD163 versus CD68 in tumor associated macrophages of classical Hodgkin lymphoma. *Diagn Pathol*. 2012;7:12.
259. Gomez-Gelvez JC, Smith LB. Reed-Sternberg-like cells in non-Hodgkin lymphomas. *Arch Pathol Lab Med*. 2015;139:1205–10.
260. Etienne B, Guillaud PH, Loire R, Coiffier B, Berger F, Cordier JF. Aggressive primary mediastinal non-Hodgkin's lymphomas: a study of 29 cases. *Eur Respir J*. 1999;13:1133–8.
261. Lam S, Rizkalla K, Hsia CC. Mediastinal choriocarcinoma masquerading as relapsed Hodgkin lymphoma. *Case Rep Oncol*. 2011;4:512–6.
262. Re D, Muschen M, Ahmadi T, et al. Oct-2 and Bob-1 deficiency in Hodgkin and Reed Sternberg cells. *Cancer Res*. 2001;61:2080–4.
263. Thomas RK, Re D, Wolf J, Diehl V. Part I: Hodgkin's lymphoma—molecular biology of Hodgkin and Reed-Sternberg cells. *Lancet Oncol*. 2004;5:11–8.
264. Schwering I, Bräuninger A, Klein U, et al. Loss of the B-lineage-specific gene expression program in Hodgkin and Reed-Sternberg cells of Hodgkin lymphoma. *Blood*. 2003;101:1505–12.
265. Chan WC. The Reed-Sternberg cell in classical Hodgkin's disease. *Hematol Oncol*. 2001;19:1–17.
266. Kuppers R, Hansmann ML. The Hodgkin and Reed/Sternberg cell. *Int J Biochem Cell Biol*. 2005;37:511–7.

267. Stein HS, Hummel M. Hodgkin's disease: biology and origin of Hodgkin and Reed-Sternberg cells. *Cancer Treat Rev*. 1999;25:161–8.
268. Hinz M, Lemke P, Anagnostopoulos I, et al. Nuclear factor kappaB-dependent gene expression profiling of Hodgkin's disease tumor cells, pathogenetic significance, and link to constitutive signal transducer and activator of transcription 5a activity. *J Exp Med*. 2002;196:605–17.
269. Hinz M, Löser P, Mathas S, Krappmann D, Dörken B, Scheidereit C. Constitutive NF-kappaB maintains high expression of a characteristic gene network, including CD40, CD86, and a set of antiapoptotic genes in Hodgkin/Reed-Sternberg cells. *Blood*. 2001;97:2798–807.
270. Skinnider BF, Elia AJ, Gascoyne RD, et al. Signal transducer and activator of transcription 6 is frequently activated in Hodgkin and Reed-Sternberg cells of Hodgkin lymphoma. *Blood*. 2002;99:618–26.
271. Farrell K, Jarrett RF. The molecular pathogenesis of Hodgkin lymphoma. *Histopathology*. 2011;58:15–25.
272. Weniger MA, Melzner I, Menz CK, et al. Mutations of the tumor suppressor gene SOCS-1 in classical Hodgkin lymphoma are frequent and associated with nuclear phospho-STAT5 accumulation. *Oncogene*. 2006;25:2679–84.
273. Savage KJ, Monti S, Kutok JL, et al. The molecular signature of mediastinal large B-cell lymphoma differs from that of other diffuse large B-cell lymphomas and shares features with classical Hodgkin lymphoma. *Blood*. 2003;102:3871–9.
274. Gunawardana J, Chan FC, Telenius A, et al. Recurrent somatic mutations of PTPN1 in primary mediastinal B cell lymphoma and Hodgkin lymphoma. *Nat Genet*. 2014;46:329–35.
275. Rengstl B, Rieger MA, Newrzela S. On the origin of giant cells in Hodgkin lymphoma. *Commun Integr Biol*. 2014;7:e28602.
276. Schaefer NG, Hany TF, Taverna C, et al. Non-Hodgkin lymphoma and Hodgkin disease: coregistered FDG PET and CT at staging and restaging—do we need contrast-enhanced CT? *Radiology*. 2004;232:823–9.
277. Bruzzi JF, Macapinlac H, Tsimberidou AM, et al. Detection of Richter's transformation of chronic lymphocytic leukemia by PET/CT. *J Nucl Med*. 2006;47:1267–73.
278. Cheson BD, Pfistner B, Juweid ME, et al. Revised response criteria for malignant lymphoma. *J Clin Oncol*. 2007;25:579–86.
279. Barrington SF, Mikhael NG, Kostakoglu L, et al. Role of imaging in the staging and response assessment of lymphoma: consensus of the International Conference on Malignant Lymphomas Imaging Working Group. *J Clin Oncol*. 2014;32:3048–58.
280. Cheson BD. Role of functional imaging in the management of lymphoma. *J Clin Oncol*. 2011;29:1844–54.
281. Cheson BD. Staging and response assessment in lymphomas: the new Lugano classification. *Chin Clin Oncol*. 2015;4.
282. Shah HJ, Keraliya AR, Jagannathan JP, Tirumani SH, Lele VR, DiPiro PJ. Diffuse large B-cell lymphoma in the era of precision oncology: how imaging is helpful. *Korean J Radiol*. 2017;18:54–70.
283. Cheson BD, Fisher RI, Barrington SF, et al. Recommendations for initial evaluation, staging, and response assessment of Hodgkin and non-Hodgkin lymphoma: the Lugano classification. *J Clin Oncol*. 2014;32:3059–68.
284. Hare SS, Souza CA, Bain G, et al. The radiological spectrum of pulmonary lymphoproliferative disease. *Br J Radiol*. 2012;85:848–64.
285. William J, Variakojis D, Yeldandi A, Raparia K. Lymphoproliferative neoplasms of the lung: a review. *Arch Pathol Lab Med*. 2013;137:382–91.
286. Cadranel J, Wislez M, Antoine M. Primary pulmonary lymphoma. *Eur Respir J*. 2002;20:750–62.
287. van der Kolk LE, Grillo-Lopez AJ, Baars JW, Hack CE, van Oers MH. Complement activation plays a key role in the side-effects of rituximab treatment. *Br J Haematol*. 2001;115:807–11.
288. Sauter CS, Matasar MJ, Meikle J, et al. Prognostic value of FDG-PET prior to autologous stem cell transplantation for relapsed and refractory diffuse large B-cell lymphoma. *Blood*. 2015;125:2579–81.
289. Broccoli A, Zinzani PL. The unique biology and treatment of primary mediastinal B-cell lymphoma. *Best Pract Res Clin Haematol*. 2018;31:241–50.
290. Jacobson JO, Aisenberg AC, Lamarre L, et al. Mediastinal large cell lymphoma. An uncommon subset of adult lymphoma curable with combined modality therapy. *Cancer*. 1988;62:1893–8.
291. Pfau D, Smith DA, Beck R, et al. Primary mediastinal large B-cell lymphoma: a review for radiologists. *AJR Am J Roentgenol*. 2019;213:W194–210.
292. Kocurek A, Malkowski B, Giza A, Jurczak W. Primary mediastinal B-cell lymphoma—metabolic and anatomical features in 18FDG-PET/CT and response to therapy. *Contemp Oncol (Pozn)*. 2016;20:297–301.
293. Lekovic D, Miljic P, Mihaljevic B. Increased risk of venous thromboembolism in patients with primary mediastinal large B-cell lymphoma. *Thromb Res*. 2010;126:477–80.
294. Shaffer K, Smith D, Kirn D, et al. Primary mediastinal large-B-cell lymphoma: radiologic findings at presentation. *AJR Am J Roentgenol*. 1996;167:425–30.
295. Hill M, Cunningham D, MacVicar D, et al. Role of magnetic resonance imaging in predicting relapse in residual masses after treatment of lymphoma. *J Clin Oncol*. 1993;11:2273–8.
296. Barrington SF, Kluge R. FDG PET for therapy monitoring in Hodgkin and non-Hodgkin lymphomas. *Eur J Nucl Med Mol Imaging*. 2017;44:97–110.
297. Martelli M, Ceriani L, Zucca E, et al. [18F]fluorodeoxyglucose positron emission tomography predicts survival after chemioimmunotherapy for primary mediastinal large B-cell lymphoma: results of the International Extranodal Lymphoma Study Group IELSG-26 Study. *J Clin Oncol*. 2014;32:1769–75.
298. Strollo DC, Rosado de Christenson ML, Jett JR. Primary mediastinal tumors. Part 1: tumors of the anterior mediastinum. *Chest*. 1997;112:511–22.
299. Pina-Oviedo S, Moran CA. Primary mediastinal classical Hodgkin lymphoma. *Adv Anat Pathol*. 2016;23:285–309.
300. Tateishi U, Muller NL, Johkoh T, et al. Primary mediastinal lymphoma: characteristic features of the various histological subtypes on CT. *J Comput Assist Tomogr*. 2004;28:782–9.
301. Rios A, Torres J, Roca MJ, Galindo PJ, Alonso JL, Parrilla P. [Primary thymic lymphomas]. *Rev Clin Esp*. 2006;206:326–31.
302. Tsang RW, Hodgson DC, Crump M. Hodgkin's lymphoma. *Curr Probl Cancer*. 2006;30:107–58.
303. Inaoka T, Takahashi K, Mineta M, et al. Thymic hyperplasia and thymus gland tumors: differentiation with chemical shift MR imaging. *Radiology*. 2007;243:869–76.
304. Takahashi K, Inaoka T, Murakami N, et al. Characterization of the normal and hyperplastic thymus on chemical-shift MR imaging. *AJR Am J Roentgenol*. 2003;180:1265–9.
305. D'Angio M, Paesano P, Quattrocchi L, et al. Mediastinal isolated myeloid sarcoma: a single-institution experience. *Leuk Lymphoma*. 2015;56:539–41.
306. Gogia A, Sharma A, Chopra A, Kumar R. Mediastinal granulocytic sarcoma: poor risk AML? *J Indian Med Assoc*. 2013;111:562.
307. Howell DL, Abramowsky CR. Granulocytic sarcoma presenting as a large mediastinal mass with acute spinal cord compression in a non-leukemic child. *Pediatr Blood Cancer*. 2005;44:527.
308. Lee JM, Song HN, Kang Y, et al. Isolated mediastinal myeloid sarcoma successfully treated with chemoradiotherapy followed by unrelated allogeneic stem cell transplantation. *Intern Med*. 2011;50:3003–7.

309. Lee MJ, Grogan L, Meehan S, Breatnach E. Pleural granulocytic sarcoma: CT characteristics. *Clin Radiol*. 1991;43:57–9.
310. Liu HW, Wong KL, Chan TY, Lau CC, Liang R. Superior vena cava syndrome: a rare presenting feature of acute myeloid leukemia. *Acta Haematol*. 1988;79:213–6.
311. Makis W, Hickeson M, Derbeykan V. Myeloid sarcoma presenting as an anterior mediastinal mass invading the pericardium: Serial Imaging With F-18 FDG PET/CT. *Clin Nucl Med*. 2010;35:706–9.
312. McCluggage WG, Boyd HK, Jones FG, Mayne EE, Bharucha H. Mediastinal granulocytic sarcoma: a report of two cases. *Arch Pathol Lab Med*. 1998;122:545–7.
313. Naesens L, Devos H, Nolle F, Michaux L, Selleslag D. Mediastinal myeloid sarcoma with TP53 mutation preceding acute myeloid leukemia with a PICALM-MLLT10 fusion gene. *Acta Haematol*. 2018;140:97–104.
314. Ramasamy K, Lim Z, Pagliuca A, Devereux S, Ho AY, Mufti GJ. Acute myeloid leukaemia presenting with mediastinal myeloid sarcoma: report of three cases and review of literature. *Leuk Lymphoma*. 2007;48:290–4.
315. Ravandi-Kashani F, Cortes J, Giles FJ. Myelodysplasia presenting as granulocytic sarcoma of mediastinum causing superior vena cava syndrome. *Leuk Lymphoma*. 2000;36:631–7.
316. Rege K, Powles R, Norton J, et al. An unusual presentation of acute myeloid leukaemia with pericardial and pleural effusions due to granulocytic sarcoma. *Leuk Lymphoma*. 1993;11:305–7.
317. Sahu KK, Tyagi R, Law AD, et al. Myeloid sarcoma: an unusual case of mediastinal mass and malignant pleural effusion with review of literature. *Indian J Hematol Blood Transfus*. 2015;31:466–71.
318. Suemitsu R, Fukuyama S, Ondo K, Ueda H. Resection of mediastinal granulocytic sarcoma triggered the rapid progression of acute myeloid leukemia. *Ann Thorac Cardiovasc Surg*. 2008;14:181–3.
319. Takahashi H, Koh K, Kato M, Kishimoto H, Oguma E, Hanada R. Acute myeloid leukemia with mediastinal myeloid sarcoma refractory to acute myeloid leukemia therapy but responsive to L-asparaginase. *Int J Hematol*. 2012;96:136–40.
320. Toback A, Hasbrouck DJ, Blaustein J, Ershler WB. Granulocytic sarcoma of the anterior mediastinum. *Am J Med Sci*. 1985;290:206–8.
321. Tsai MH, Yang CP, Chung HT, Shih LY. Acute myeloid leukemia in a young girl presenting with mediastinal granulocytic sarcoma invading pericardium and causing superior vena cava syndrome. *J Pediatr Hematol Oncol*. 2009;31:980–2.
322. Tufekci O, Yilmaz S, Erdem M, Baysal B, Oren H. Isolated mediastinal myeloid sarcoma after NPM1 positive acute myeloid leukemia. *Turk J Haematol*. 2019;36(4):285–6.
323. Wong WS, Loong F, Ooi GC, Tse TC, Chim CS. Primary granulocytic sarcoma of the mediastinum. *Leuk Lymphoma*. 2004;45:1931–3.
324. Miettinen M, Wang ZF, Paetau A, et al. ERG transcription factor as an immunohistochemical marker for vascular endothelial tumors and prostatic carcinoma. *Am J Surg Pathol*. 2011;35:432–41.
325. Fang L, Cui Y, Mi Y, et al. Somatic ASXL1 p.R693X mutation identified by next generation sequencing in isolated myeloid sarcoma involving the mediastinum. *Curr Med Res Opin*. 2020;36:1003–7.
326. Heesters BA, Myers RC, Carroll MC. Follicular dendritic cells: dynamic antigen libraries. *Nat Rev Immunol*. 2014;14:495–504.
327. Nossal GJ, Ada GL, Austin CM. Antigens in immunity. Iv. cellular localization of 125-I- and 131-I-labelled flagella in lymph nodes. *Aust J Exp Biol Med Sci*. 1964;42:311–30.
328. Nossal GJ, Abbot A, Mitchell J, Lummus Z. Antigens in immunity. XV. Ultrastructural features of antigen capture in primary and secondary lymphoid follicles. *J Exp Med*. 1968;127:277–90.
329. Monda L, Warnke R, Rosai J. A primary lymph node malignancy with features suggestive of dendritic reticulum cell differentiation. A report of 4 cases. *Am J Pathol*. 1986;122:562–72.
330. Aguzzi A, Kranich J, Krautler NJ. Follicular dendritic cells: origin, phenotype, and function in health and disease. *Trends Immunol*. 2014;35:105–13.
331. Perkins SM, Shinohara ET. Interdigitating and follicular dendritic cell sarcomas: a SEER analysis. *Am J Clin Oncol*. 2013;36:395–8.
332. Chan JK, Fletcher CD, Nayler SJ, Cooper K. Follicular dendritic cell sarcoma. Clinicopathologic analysis of 17 cases suggesting a malignant potential higher than currently recognized. *Cancer*. 1997;79:294–313.
333. Chan JKC. Proliferative lesions of follicular dendritic cells: an overview, including a detailed account of follicular dendritic cell sarcoma, a neoplasm with many faces and uncommon etiologic associations. *Adv Anat Pathol*. 1997;4:387–411.
334. Perez-Ordóñez B, Erlandson RA, Rosai J. Follicular dendritic cell tumor: report of 13 additional cases of a distinctive entity. *Am J Surg Pathol*. 1996;20:944–55.
335. Hu J, Dong D, Jiang Z, Hu H. Clinicopathological characteristics of mediastinal follicular dendritic cell sarcoma: report of three cases. *J Cardiothorac Surg*. 2016;11:56.
336. Lee BE, Korst RJ, Taskin M. Right pneumonectomy for resection of a posterior mediastinal follicular dendritic cell sarcoma arising from Castleman's disease. *Ann Thorac Surg*. 2014;97:e101–3.
337. Purkait S, Mallick S, Joshi PP, et al. Retroperitoneal and mediastinal follicular dendritic cell sarcoma: report of 3 cases with review of literature. *Hematol Oncol*. 2017;35:374–9.
338. Viola P, Vroobel KM, Devaraj A, et al. Follicular dendritic cell tumour/sarcoma: a commonly misdiagnosed tumour in the thorax. *Histopathology*. 2016;69:752–61.
339. Wu YL, Wu F, Xu CP, et al. Mediastinal follicular dendritic cell sarcoma: a rare, potentially under-recognized, and often misdiagnosed disease. *Diagn Pathol*. 2019;14:5.
340. Chan AC, Chan KW, Chan JK, Au WY, Ho WK, Ng WM. Development of follicular dendritic cell sarcoma in hyaline-vascular Castleman's disease of the nasopharynx: tracing its evolution by sequential biopsies. *Histopathology*. 2001;38:510–8.
341. Facchetti F, Lorenzi L. Follicular dendritic cells and related sarcoma. *Semin Diagn Pathol*. 2016;33:262–76.
342. Vermi W, Lonardi S, Bosisio D, et al. Identification of CXCL13 as a new marker for follicular dendritic cell sarcoma. *J Pathol*. 2008;216:356–64.
343. Xie Q, Chen L, Fu K, et al. Podoplanin (d2-40): a new immunohistochemical marker for reactive follicular dendritic cells and follicular dendritic cell sarcomas. *Int J Clin Exp Pathol*. 2008;1:276–84.
344. Xu J, Sun HH, Fletcher CD, et al. Expression of programmed cell death 1 ligands (PD-L1 and PD-L2) in histiocytic and dendritic cell disorders. *Am J Surg Pathol*. 2016;40:443–53.
345. Griffin GK, Sholl LM, Lindeman NI, Fletcher CD, Hornick JL. Targeted genomic sequencing of follicular dendritic cell sarcoma reveals recurrent alterations in NF-kappaB regulatory genes. *Mod Pathol*. 2016;29:67–74.
346. Andersen EF, Paxton CN, O'Malley DP, et al. Genomic analysis of follicular dendritic cell sarcoma by molecular inversion probe array reveals tumor suppressor-driven biology. *Mod Pathol*. 2017;30(9):1321–34.
347. Go H, Jeon YK, Huh J, et al. Frequent detection of BRAF(V600E) mutations in histiocytic and dendritic cell neoplasms. *Histopathology*. 2014;65:261–72.